# University of Hawaii at Manoa

# INSTRUMENTATION AND MONITORING OF SAND PLUGGING AND BRIDGE SCOUR AT SELECTED STREAMS IN HAWAII

## FINAL REPORT


**PRINCIPAL INVESTIGATOR:**

**Michelle H. Teng, Ph.D., P.E.**
**Associate Professor**

**CO – PRINCIPAL INVESTIGATOR:**

**Edmond D.H. Cheng, Ph.D.**
**Professor Emeritus**



**PREPARED IN COOPERATION WITH:**

**State of Hawaii, Department of Transportation, Highway Division**
**and U.S. Department of Transportation, Federal Highway Administration**

**Honolulu, Hawaii**
**May 13, 2013**

**Technical Report Documentation Page**

| 1. Report No. | 2. Government Accession No. | 3. Recipient's Catalog No. |
|---|---|---|
| HWY-L-2000-05 | | |

| 4. Title and Subtitle | 5. Report Date |
|---|---|
| **Instrumentation and Monitoring of Sand Plugging and Bridge Scour at Selected Streams in Hawaii** | May 13, 2013 |
| | 6. Performing Organization Code |

| 7. Author(s) | 8. Performing Organization Report No. |
|---|---|
| Gavin Masaki, Michelle H. Teng, & Edmond D.H. Cheng | |

| 9. Performing Organization Name and Address | 10. Work Unit No. (TRAIS) |
|---|---|
| Department of Civil and Environmental Engineering<br>University of Hawaii at Manoa<br>2540 Dole St. Holmes Hall 383, Honolulu, HI 96822 | 11. Contract or Grant No.<br>46509 |

| 12. Sponsoring Agency Name and Address | 13. Type of Report and Period Covered |
|---|---|
| Hawaii Department of Transportation<br>Highways Division<br>869 Punchbowl St., Honolulu, HI 96813 | FINAL<br>05/00 – 12/06 |
| | 14. Sponsoring Agency Code |

15. Supplementary Notes

Prepared in cooperation with the U.S. Department of Transportation, Federal Highway Administration

16. Abstract

In this project, we investigated two practical problems in highway design and maintenance, namely the sand-plugging of highway culverts and flood-induced bridge scour.

In coastal states like Hawaii, our highway culverts are frequently clogged by sand carried onshore by ocean tides. The sand plugging of a culvert reduces the drainage capacity of the culvert and may cause serious water backup and flooding of the nearby communities during a storm. The objective of the present study is to achieve a better understanding of sand-plugging and develop potential engineering solutions to mitigate the problem. This was done through field survey, laboratory experiments, and numerical computations. Specifically, the criteria to assess whether an existing culvert can self-clean of the sand blockage during a storm are developed and demonstrated for two specific culverts – the Punaluu and Hauula culverts – in windward Oahu.

For flood induced bridge scour, our main objective is to install sensors on selected bridges on Oahu to collect data on scour depth during flood events. These field data can be used to compare with the predicted scour depth based on the HEC-18 scour design manual. The goal is to examine whether the existing prediction equations can provide accurate scour depth calculations for streams and bridges in Hawaii. In this study, we installed sensors on two bridges on Oahu. Scour depth data during one flood event were recorded. These data were compared with the predicted scour depth using the HEC-18 equations and the HEC-RAS computer software. It was found that the existing HEC-18 equations over-predicted the scour depth by a large margin and need improvement.

| 17. Key Words | 18. Distribution Statement |
|---|---|
| bridge scour, sand-plugged culverts, magnetic sliding collars, sonar sensors, detention pond, highway overtopping. | No restriction. This document is available to the public from the sponsoring agency at the website http://www.cflhd.gov. |

| 19. Security Classif. (of this report) | 20. Security Classif. (of this page) | 21. No. of Pages | 22. Price |
|---|---|---|---|
| Unclassified | Unclassified | 225 | |

**Form DOT F 1700.7 (8-72)** **Reproduction of completed page authorized**

## ACKNOWLEDGEMENT AND DISCLAIMER

The authors are very grateful for the funding and support provided by the Hawaii Department of Transportation (HDOT) and the Federal Highway Administration (FHWA). The authors would like to thank Mr. Casey Abe, the Director of the HDOT Research Program, Mr. Curtis Matsuda, the section chief of HDOT's Hydraulic Design Section and Mr. Steve Ege, the HDOT fiscal manager for funding and sponsoring this project.

Gavin Masaki's MS thesis and Mr. Michael Kamaka's MS Plan B report form a great part of this research report. We are also indebted to other former research assistants in helping us to carry out the project. These assistants include Mr. Mathew Fujioka, Mr. Michael Miyagi, Mr. Jianping Johnny Liu, Mr. Tsung I Liao, Dr. Edison Gica, Dr. Hongqiang John Zhou, and Mr. Mason Suga. Without their help and support in field survey of sand-plugged culverts, laboratory experiments, and in sensor installation on two bridges on Oahu, we would not have been able to carry out the project. The assistance from our technicians Mr. Miles Wagner and Mr. Andrew Oshita are also gratefully acknowledged.

The authors would like to thank HDOT Hydraulic Design Section Chief Mr. Curtis Matsuda and FHWA Hawaii representative Mr. Domingo Galicinao for reviewing this report and providing their very helpful comments and suggestions.

---



---

## TABLE OF CONTENTS

# PART I STUDY ON FLOOD-INDUCED BRIDGE SCOUR

# CHAPTER 1 INTRODUCTION

## 1.1 Technical Background

In 1987 the failure of an interstate highway bridge over Schoharie Creek in New York focused engineers' attention on scour. This failure resulted in the Federal Highways Administration (FHWA) requiring that all new bridges be designed to resist major damage due to scour for a 100-year flood and existing bridges be evaluated to still stand after 500-year flood with no live load. In addition scour monitoring was added to each state's bridge inspection program.

Scour is the erosion or removal of streambed or bank material from bridge foundations and abutments due to flowing water. The loss of bed material reduces the effectiveness of the bridge foundation. The most common cause of bridge failures is from floods scouring bed material from around bridge foundations (Richardson et al, 2001, Arneson et al 2012). Materials scour at different rates; for example, granular sized soil scours faster while cohesive soil is more resistant. Scour can be classified as live-bed scour or clear water scour. Live bed scour occurs when there is sediment in the upstream flow while clear water scour occurs when the bed material upstream is not moving. Typically scour at low flow conditions is clear-water scour and scour at high flow conditions is live-bed scour.

There are three components of scour: contraction scour, local scour at piers and abutments, and long-term aggradation and degradation of the riverbed (Figure 1-1). Contraction scour is the removal of material from the riverbed across the width of the channel. Contraction scour is caused by the contraction of flow area by bridges. The reduced flow area will increase the average velocity and bed shear stress, which increases the erosive forces in the contracted area. Contraction scour is usually cyclic in nature where scour occurs on the rising limb of the

flood and refills on the receding limb. Local scour is the scour in the riverbed that is localized at a pier, abutment, embankment or any other flow obstructions. When water passes around a pier, a horseshoe vortex forms upstream of the pier, which removes the soil from the base of the pier. As the scour hole deepens, the strength of the horseshoe vortex decreases until equilibrium is reached. Aggradation and degradation are long-term streambed elevation changes due to natural or man-made causes (Richardson et al, 2001). Aggradation is the deposit of material on the streambed and degradation is the removal of material on the streambed by the flow of the river over time.

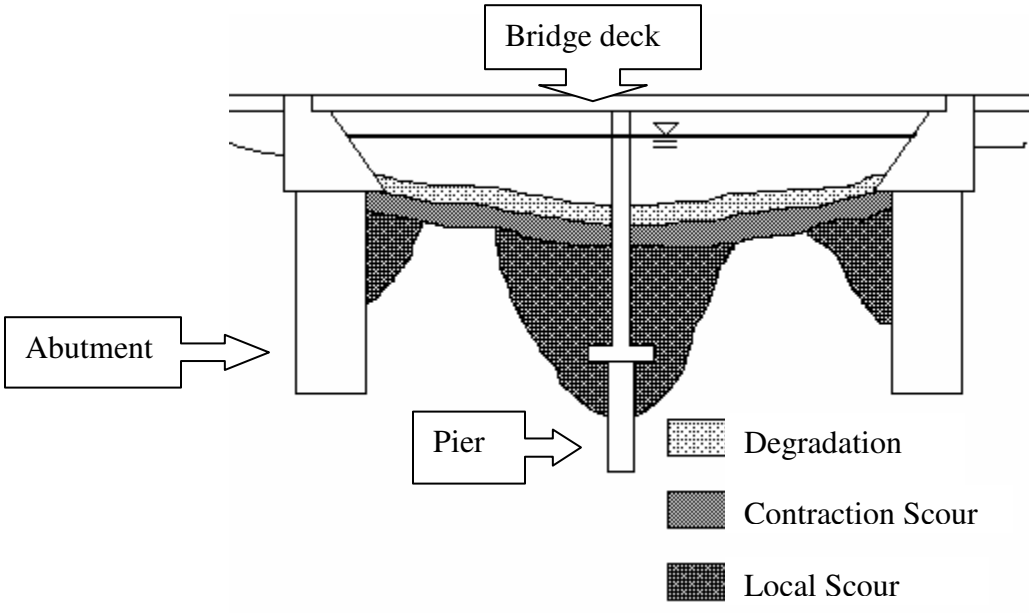


**Figure 1-1:** Components of Scour

To alleviate the potential damage caused by scour, engineers can design the bridge span to be continuous, and to account for hydraulic forces such as buoyancy, drag, and debris impact. Bottom of footing/pile cap should be designed below the total scour depth or on solid rock. The bridge piers should be aligned with the direction of the flow and round in shape when possible. Engineers should design sloping abutments (instead of vertical wall abutments) and use riprap to

protect the embankments upstream and downstream of the abutment. Relief bridges, guide banks, ripraps, and river training should be used in order to reduce the intensity of scour through the bridge. More information on designing scour resistant bridges can be found in FHWA Hydraulic Engineering Circular 18, 20, and 23.

Most existing older bridges were not designed for scour and may have unknown foundations. Since replacing each of the bridges would be expensive, the bridges must be evaluated to consider if the bridge is "scour critical". A scour critical bridge is defined as a bridge with abutment or pier foundations which are unstable due to: (1) observed scour at the bridge site or, (2) scour potential as determined by scour evaluation study (Richardson et al, 2001). As of May 8, 2013, there are 14 bridges that were identified by the State Department of Transportation as scour critical on Oahu (Table 1-1).

**Table 1-1:** Scour critical bridges on Oahu

| | FEATURE CARRIED | FEATURE CROSSED | STRUCTURAL NO |
|---|---|---|---|
| 1. | Kamehameha Highway | Hakipuu Stream Bridge | 3000830303252 |
| 2. | Kamehameha Highway | Kaalaea Stream | 3000830303575 |
| 3. | Likelike Highway OB | Kalihi Stream | 3000630400166 |
| 4. | Farrington Highway | Kaukonahua Stream | 3009300501748 |
| 5. | Kamehameha Highway | Koloa Stream | 3000830301970 |
| 6. | Kamehameha Highway | Lauhulu Stream | 3000830300339 |
| 7. | South King Street | Manoa-Palolo Stream | 3000H10202513 |
| 8. | Old Waialae Road | Manoa-Palolo Stream | 3000H11202486 |
| 9. | H-1 Lunalilo Freeway | Manoa-Palolo Stream | 3000H10202512 |
| 10. | Kamehameha Highway | North Punaluu Stream | 3000830302412 |
| 11. | Kamehameha Highway | Paumalu Stream | 3000830300869 |
| 12. | Kamehameha Highway | Waialua Stream Twin A | 3000830300041 |
| 13. | Kamehameha Highway | Waialua Stream Twin B | 3000830300043 |
| 14. | Kamehameha Highway | Waimea River | 3000830300573 |

This project was funded by HDOT to investigate the problem of scour on coastal bridges in Hawaii. In the project fixed scour instruments were mounted on Kaelepulu Bridge spanning across Kaelepulu stream near Kailua Beach Park, and on Kahaluu Bridge spanning across Kahaluu stream near Kahaluu Beach Park. The scour instruments used are the magnetic sliding collar with telemetry, sonar scour tracker with telemetry, as well as the portable sonar scour tracker, and a sounding reel. These instruments were developed by FHWA and AASHTO (American Association of State Highway and Transportation Officials) funded projects on the continental United States and have been tested in several states on the U.S. mainland.

The instruments used in this project are based on fairly new technology including remote control of data logging and automatic data recording. This was the first time that the state-of-the-art instrumentation was used to monitor scour in the State of Hawaii, which has unique weather conditions, and stream and soil characteristics. One of the objectives of the project is to determine if the scour equipment is suitable for use in Hawaii's environment. The installation of the instruments on selected bridges on Oahu will help the State Department of Transportation to develop a future scour monitoring program for larger bridges on Kauai and the Big Island, which may face more serious flood threats. Before this project, there was no instrumentation or monitoring program for measuring bridge scour in the State of Hawaii.

The field data obtained from scour monitoring can provide a necessary database for validating the existing empirical formulas for predicting scour depth used in bridge design. The empirical equations for estimating scour depth have been developed by different research groups on the US mainland. These equations are based on laboratory experiments using homogeneous bed materials and have been verified only by limited field studies conducted on the U.S. mainland and have not been verified for bridges and streams in Hawaii, which differs in

watershed and stream characteristics. If the field data are collected in Hawaii, they can be used to help validate the existing scour equations for application in Hawaii. If significant discrepancies between the predicted and measured scour depth are observed then the empirical parameters in the predictive equations can be adjusted so that the equations are specifically applicable to Hawaii's streams. This will lead to more accurate predictions of bridge scour and better design of safer bridges in Hawaii.

## 1.2 Literature Review

After the fatal collapse of Interstate I-90 over Schoharie Creek in New York, the FHWA released Technical Advisory 5140.20 in 1988 (later revised in 1991 as Technical Advisory 5140.23). This technical advisory gives guidelines and recommendations for implementing a scour monitoring program and a plan of action regarding scour critical bridges. Also the technical advisory provides guidelines on how to design new bridges to resist scour and how to evaluate existing bridges to determine if they are scour critical.

The FHWA published coding guide Report No. FHWA-PD-96-001 (last revised in 1995) to evaluate the condition of bridges for recording in the National Bridge Inventory Database. Items related to scour are item No. 60, 61, 71, and 113. Item 60 refers to the condition of the substructure such as piers, abutments, and footings for damage such as cracking, settlement, and scour. Item 61 refers to the condition of the channel and channel protection for bridges such as scour countermeasures (rip-rap, spurs). Item 71 refers to the chance of overtopping and the impact due to the closure of the bridge. Item 113 refers to the susceptibility of current bridges to scour.

Scour monitoring instrumentation was developed by the National Cooperative Highway Research Program (NCHRP) project 21-3, and the results were published in reports 396, 397A and 397B. Report 396 (Lagasse et al., 1997) evaluated and tested (in a laboratory flume and field) different scour monitoring devices such as sounding rods, magnetic sliding collar, and sonar. Report 397A (Shall, et al., 1997) gives background information, installation instructions, fabrication details, and operation manuals on scour monitor. Report 397B (Shall, et al., 1997) gives background information, installation instructions, fabrication details, and operation manuals for sliding magnetic collar. Demonstration project 97 (FHWA-SA-96-036) published in 1998 by the FHWA demonstrated the installation and application of different types of scour devices published in NCHRP 396.

The FHWA steps to evaluating bridge scour and stream instability for new and existing bridges are presented in three FHWA manuals: HEC-20 FHWA-NHI-01-002 (Lagasse, et al., 2001), HEC 18 FHWA-NHI-01-001 (Richardson, et al., 2001, Arneson et al 2012), and HEC 23 FHWA-NHI-01-003 (Lagasse, et al., 2001). HEC-20 introduces a three level procedure to analyze stream stability and potential future response of the stream. HEC-18 presents in detail to help engineers implement the recommendations in FHWA Tech Advisory 5140.23. In addition, HEC-18 presents the equations for determining the depths of different types of scour, and design recommendations for new bridges to resist scour. HEC-23 introduces and provides guides to design scour countermeasures such as spurs, riprap, and other commonly used countermeasures. HEC-23 also identifies which countermeasure to use for a particular scour and stream instability problem.

The equations used to calculate the maximum depth of contraction scour were based on results from two papers published by Laursen in 1960 and 1963 in the Journal of Hydraulic

Engineering. The equation for critical velocity, i.e. the velocity necessary to move a particle of size D50, was derived from Laursen's equation for clear-water scour. These equations were obtained from approximate analysis and laboratory experiments using flumes.

The clear-water and live-bed pier scour equations were developed by Colorado State University and first published in 1966 by the Bureau of Public Roads. FHWA Tech Advisory 5140.20 recommends using the CSU equations for pier scour design. Johnson and Torrico (1994) "Scour around wide piers in shallow water" developed equations for wide piers for the Transportation Research Board. Jones in 2000 "Local scour around complex pier geometries" in the Proceedings of the ASCE 2000 Joint Conference on Water Resources Planning and Management developed procedures to determine scour for complex piers (such as a pier with a pile cap and pile group). Research on scour from debris on piers was reported in HEC-20 and by Melville and Dongol in 1992 in the Journal of Hydraulic Engineering.

The live-bed and clear-water abutment scour equations were developed by Froehlich, which were presented to the Transportation Research Board in 1989 "Abutment Scour Prediction". These equations were based on dimensional and regression analysis of 170 live-bed scour measurements of laboratory data. Few field measurements are available and most research on abutment scour is based on laboratory experiments. Alternate equations were developed by Strum in 1999 and published in FHWA report FHWA-RD-99-156 and by Chang in 1999 who published "The Maryland State Highway Administration ABSCOUR Program".

To analyze bridge crossing at tidal waterways, a three level analysis was developed and presented in HEC-20 and HEC-18. In 1973, Neil in his paper, "Guide to Bridge Hydraulics", developed a multi-step procedure for evaluating scour at unconstricted waterway. Scour evaluation procedures for constricted waterways were devolved by Van de Kreeke in 1967 in

"Water-Level Fluctuations and Flow in Tidal Inlets" and Brunn in 1990 in "Tidal Inlets on Alluvial Shores".

The computer programs used by the FHWA to analyze scour are WSPRO and HEC-RAS. Both programs analyze 1-D flow computations to determine water surface profiles and flow through bridges. These computer programs obtain the hydraulic variables necessary to use the scour equations presented in HEC-18. WSPRO (Water-Surface Profile computations) was developed by the U.S. Geological Survey for the FHWA in 1988. HEC-RAS (Hydrologic Engineering Center River Analysis System) was developed by the U.S. Army Corps of Engineers in 1964 as the computer program HEC-2. Both programs are free to download: WSPRO can be downloaded at the FHWA website at http://www.fhwa.dot.gov/, while HEC-RAS can be downloaded at the USACOE Hydraulic Engineering Center's website at http://www.hec.usace.army.mil/.

Most of the equations presented in HEC-18 are based on scour of sand and gravels not cohesive soil. Although the depth of maximum scour is the same as cohesive soils scour, the rate of the scour development is very different (cohesive may take days while non-cohesive may take hours to scour).

While research on bridge scour on the US mainland and other parts of the world has been very active for the recent two decades, research in this area in Hawaii has been very limited. This HDOT funded project is among the first research efforts to study bridge scour in Hawaii. The questions of interest to the HDOT and local engineers include:

1. Does Hawaii have serious flood and scour risk?
2. The existing scour equations are mostly based on laboratory experiments using homogeneous sand. Are the equations valid and accurate for application to actual

streams/bridges in Hawaii? Both local and mainland engineers' current consensus is that the existing empirical equations may over-predict the scour depth by a large margin. This overestimate may increase the difficulty and cost of designing and building new bridges. There is a desire to validate and improve the scour equations for more accurate and realistic estimates.

3. In order to validate the scour equations, field data on scour depth during floods are needed. Before this project, there was no scour-monitoring program existing in Hawaii. One of the questions related to scour monitoring is "whether the instruments developed for US mainland bridges are suitable for use in Hawaii".

### 1.3 Objectives of the Study

This study focuses on analyzing the risk of flood and bridge scour in Hawaii by examining selected typical watersheds and bridges on Oahu as case studies. The study includes two main parts, namely hydrological analysis of rainfall and streamflow, and prediction and monitoring of bridge scour.

The specific objectives are to:

1. Perform statistical analysis of rainfall data for rain gaging stations on Oahu based on the most updated and complete data records;
2. Predict stream flows for 10, 50, 100-year floods for selected watersheds on Oahu by applying three different methods;
3. Determine the validity of the three methods for predicting streamflow in Hawaii by comparing predicted results with field data measured by stream gages;

4. Predict scour depths for existing bridges on Oahu under 100-year flood by using HEC-RAS computer software to analyze the risk of these bridges due to scour;
5. Conduct a sensitivity study to evaluate the quantitative effect of different factors (such as particle size, pier width, and flow angle) on bridge scour;
6. Compare different methodologies for predicting contraction scour for multilayered stratified streambeds;
7. Install and evaluate two different types of scour sensors for monitoring bridge scour in Hawaii;
8. Evaluate the validity of the existing scour prediction equations by comparing predicted results with the measured results during a flood event at Kaelepulu Bridge in this study.

# CHAPTER 2 HYDROLOGICAL ANALYSIS

In order to predict the scour risk for bridges, engineers must first determine the flow discharge of flood events of different return frequencies. In this chapter, statistical analysis of rainfall data acquired from the National Weather Service for different watersheds on Oahu is presented. From the rainfall analysis, the streamflow of floods of different frequencies can be determined using three methods such as the City and County of Honolulu Method, regression equations, and the TR-55 method.

In this study, the rainfall records (updated in year 2002) are analyzed and applied to predict stream flow of flood of different return periods. The results are compared with existing rainfall maps (produced in the 1980s) in order to evaluate the validity and accuracy of the existing hydrologic analysis results that are currently used by design engineers in Hawaii. The results from this chapter help to better understand the severity of floods on Oahu and the potential risk of bridge scour due to the floods. In addition, since three methods are used in this study to predict the stream discharge based on the rainfall analysis, a comparative study among the three methods was conducted to determine which one is better suited for application in Hawaii.

## 2.1 Rainfall Frequency Analysis

Flow discharge of streams is an important parameter in engineering design of hydraulic structures such as bridges and culverts. To determine the appropriate flow rates, the flood results for different frequencies and reoccurrence intervals need to be estimated. The first step is to perform a frequency analysis of past rainfall data from rain gaging stations located in selected watersheds that contribute to the streamflow. If past rainfall data is not available, frequency

analysis of rainfall can be estimated using rainfall charts from the State of Hawaii Department of Land and Natural Resources "Rainfall Frequency Study for Oahu" Report R-73. One of the objectives of this section is to compare Report R-73 with the new frequency analysis of updated historical rainfall and determine if Report R-73 is still valid despite being published in 1984.

### 2.1.1 Theoretical Background

Frequency analysis is used to analyze the historical data from stream and rain gaging stations. The data is fitted into different distribution curves to predict the return period for a storm of a particular magnitude. The first step in rainfall frequency analysis is to obtain the maximum annual daily rainfall data for the selected rain gaging station. This means that for each year, the daily rainfall is examined and only the peak daily rainfall is selected for use in that year.

#### 2.1.1.1 Rainfall Data Adjustment (For Rainfall Analysis Only)

The type of rain gaging station used to record the daily rainfall must be determined for frequency analysis of the rainfall. There are two types of rain gaging stations: (1) autographic (recording) and (2) standard (non-recording). Autographic rain gaging stations record the rainfall at 15-minitue and 1-hour intervals. Standard rain gaging stations record the rainfall at fixed 24-hour intervals such as for example from 6:00 am today to 6:00 am the next day. Since rainfall is a random event, rainfall may overlap one of the intervals. This means that the standard rain gage will record a portion of the rainfall on one day and the rest of the rainfall on the next day. As a result the true daily rainfall will not be reflected in the record. Research from Weiss (1964)

found that the true daily rainfall total would exceed the rainfall total from a standard rain gage by a factor of 1.143.

#### 2.1.1.2 Distribution Characteristics

The next step is to calculate the three parameters that describe the data set, which are the mean, variance, and skewness. The mean is the average value of the data, which is obtained by summing the values of the data and dividing it by the number of data.

$$\bar{x} = \frac{1}{n}\sum_{i=1}^{n} x_i \qquad (2\text{-}1)$$

where:

$\bar{x}$ = Mean

n = Number of data (events)

x = The data of number i

i = 1,2,3……n

The average spread of the distribution about the mean is called the variance. Of importance is the square root of the variance or the standard deviation. The variance is given by:

$$s^2 = \frac{1}{n-1}\sum_{i=1}^{n} (x_i - \bar{x})^2 \qquad (2\text{-}2)$$

where:

$s^2$ = Variance

s = Standard deviation

The symmetry of a distribution is called the skewness. A symmetrical frequency distribution about the mean would have a skewness coefficient of zero ($C_s = 0$). A positive skewness coefficient ($C_s > 0$) has a distribution that leans to the left of the mean. A negative skewness coefficient ($C_s < 0$) has a distribution that leans to the right of the mean.

$$a = \frac{n}{(n-1)(n-2)} \sum_{i=1}^{n} (x_i - \bar{x})^3 \tag{2-3}$$

$$C_s = \frac{a}{s^3} \tag{2-4}$$

where:

a = Skewness

$C_s$ = Coefficient of skewness

#### 2.1.1.3 Streamflow Weighted Skewness Coefficient (Streamflow Analysis Only)

In addition to calculating the skewness coefficient for the data from the gaging stations, the US Water Resources Council (USWRC) developed generalized skew coefficients for the annual maximum streamflow for various locations around the United States. This was developed since $C_s$ is sensitive to the amount and the magnitudes of the data. For Hawaii the USWRC determined the generalized skew coefficient to be $C_g$ =-0.05 (Viessman, et al., 1996). The USWRC recommended method is to use a weighted skewness coefficient that involves both $C_s$ and $C_g$.

$$C_w = \frac{MSG_g * C_g + MSG_s * C_s}{MSG_g + MSG_s} \tag{2-5}$$

$$MSG = 10^{(A - B[\log(n/10)])} \tag{2-6}$$

$$A_w = -0.33 + 0.08|C| \text{ for } |C| \le 0.90 \quad (2\text{-}7)$$

$$A_w = -0.52 + 0.30|C| \text{ for } |C| > 0.90 \quad (2\text{-}8)$$

$$B_w = 0.94 - 0.26|C| \text{ for } |C| \le 1.50 \quad (2\text{-}9)$$

$$B_w = 0.55 \text{ for } |C| > 1.50 \quad (2\text{-}10)$$

where:

$C_w$ = Weighted skewness coefficient (for streamflow frequency analysis only)

$C_s$ = Coefficient of skewness from the data

$C_g$ = Generalized skewness coefficient equal to -0.05 for Hawaii

$A_w$ = Weighted skewness coefficient frequency factor

$B_w$ = Weighted skewness coefficient frequency factor

$MSG_s$ = Mean-square error for skewness coefficient

$MSG_g$ = Mean-square error for generalized skewness coefficient

#### 2.1.1.4 Return Period and Exceedance Probability

The next step in hydrologic frequency analysis involves sorting and ranking the data in descending order where the data with maximum value is given the rank of one and the data with the minimum value is given the rank of n (total number of data). For each ranked data it is important to calculate the return period and exceedance probability. The return period (5, 10, 25 years) is the time interval in between storms of a particular magnitude. The exceedance probability (20%, 10%, 4%) is the inverse of the return period or the probability of a storm of a particular magnitude that would be exceeded in a given year. An example of ranked rainfall data

is shown in Table 2-1 for Kalihi Reservoir rain gaging station number 777 (this is a rainfall table of selected years).

$$T = \frac{n+1}{m} \tag{2-11}$$

$$EP = \frac{m}{n+1} = \frac{1}{T} \tag{2-12}$$

where:

T = Return period, years

EP = Exceedance probability

n = Number of data (events)

m = The rank of descending data where 1 equals the data with the largest value.

**Table 2-1:** Selected ranked rainfall data for Kalihi Reservoir State #777

| Rank | Year | Maximum Annual Daily Rainfall (in) | Return Period (years) | Exceedance Probability |
|---|---|---|---|---|
| 1 | 1950 | 16.74 | 16.00 | 0.06 |
| 2 | 1951 | 16.53 | 8.00 | 0.13 |
| 3 | 1955 | 8.72 | 5.33 | 0.19 |
| 4 | 1942 | 8.24 | 4.00 | 0.25 |
| 5 | 1954 | 7.94 | 3.20 | 0.31 |
| 6 | 1949 | 6.72 | 2.67 | 0.38 |
| 7 | 1952 | 5.75 | 2.29 | 0.44 |
| 8 | 1957 | 3.92 | 2.00 | 0.50 |
| 9 | 1953 | 3.56 | 1.78 | 0.56 |
| 10 | 1956 | 3.52 | 1.60 | 0.63 |

**Table 2-1** (Continued): Ranked rainfall data for Kalihi Reservoir

| | | | | |
|---|---|---|---|---|
| 11 | 1946 | 3.26 | 1.45 | 0.69 |
| 12 | 1958 | 3.25 | 1.33 | 0.75 |
| 13 | 1945 | 3.18 | 1.23 | 0.81 |
| 14 | 1944 | 2.26 | 1.14 | 0.88 |
| 15 | 1943 | 2.24 | 1.07 | 0.94 |

### 2.1.1.5 Probability Distribution

The next step is to "fit" the ranked data into a distribution curve. An example of a distribution curve can be represented by plotting the rainfall data from Table 2-1. The probability of the rainfall landing within a certain interval is equal to the frequency of the rainfall divided by the total years of record (Table 2-2 summarizes the outcome). Notice that the sum of probabilities is equal to 1. If a histogram were plotted with probability on the y-axis and rainfall of the x-axis it would be called a probability distribution (Figure 2-1) and the equation describing the curve is called the probability density function (PDF).

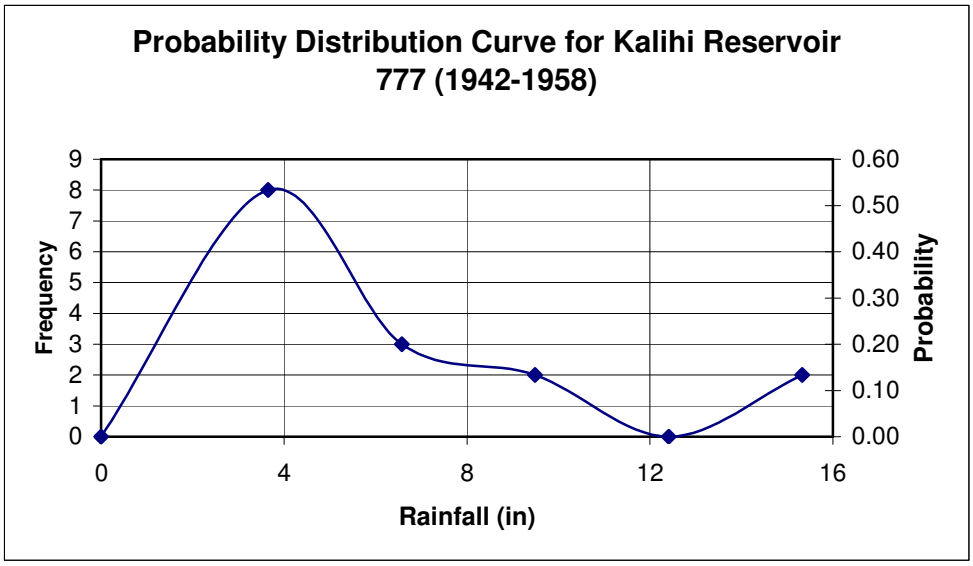


**Figure 2-1:** Probability distribution curve for Kalihi Reservoir maximum annual rainfall

**Table 2-2:** Histogram analysis for Kalihi Reservoir

| Interval Number | Rainfall Interval (in) | Frequency | Probability | Cumulative Probability |
|---|---|---|---|---|
| 1 | 2.19-5.11 | 8 | 0.533 | 0.533 |
| 2 | 5.11-8.03 | 3 | 0.200 | 0.733 |
| 3 | 8.03-10.95 | 2 | 0.133 | 0.866 |
| 4 | 10.95-13.87 | 0 | 0.000 | 0.866 |
| 5 | 13.87-16.79 | 2 | 0.133 | 1.000 |

Another way to describe probability would be the cumulative distribution function (Figure 2-2). Cumulative distribution function is the equation describing the area underneath the probability distribution curve. The cumulative distribution is the probability of the rainfall value not exceeding a certain amount. This is obtained by summing the probabilities up to that value (shown in Table 2-2). Cumulative distribution function plots have been widely used in analyzing hydrologic data to determine the return period and the exceedance probability of a storm. The two distributions used in this report are the Gumbel Extreme Value and Log Pearson Type III distribution.

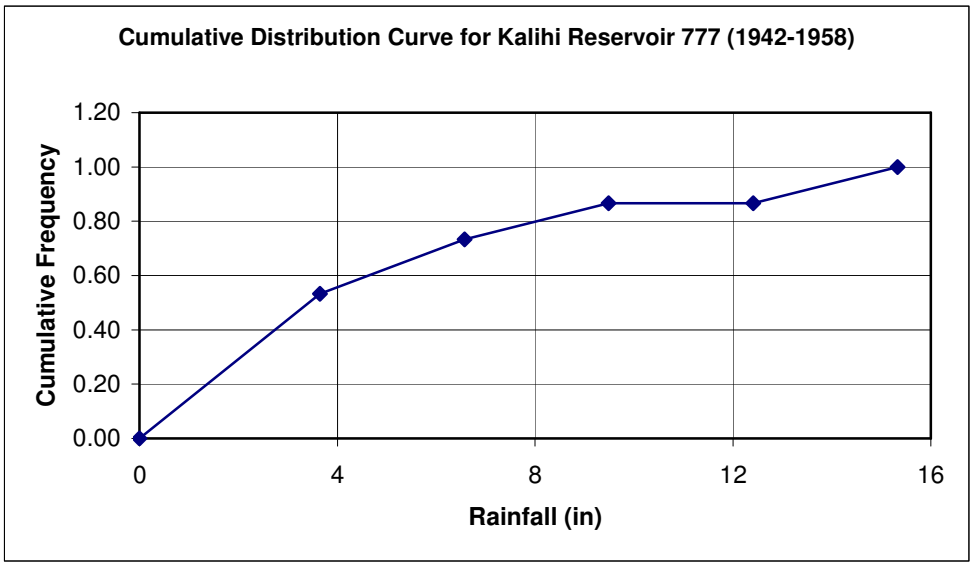


**Figure 2-2:** Cumulative distribution curve for Kalihi Reservoir maximum annual rainfall

### 2.1.1.6 Gumbel Distribution

There are three types of extreme value distributions (Gumbel, Frechet, and Weibull). Gumbel Distribution is a type I extreme value distribution that is used to describe the distribution of the largest or smallest value in a data set. For example the analysis of the distribution of the largest values can be used for flood flow analysis and the distribution of the smallest values can be used for drought analysis. The general equation for the Gumbel Extreme distribution curve is:

$$F(x) = \bar{x} + K_g s \tag{2-13}$$

$$K_g = (-0.45 - 0.78 \ln \ln \frac{T}{T-1}) \tag{2-14}$$

where:

F(x) = Gumbel cumulative distribution function

$\bar{x}$ = Mean

$K_g$ = Gumbel frequency factor (Table 2-3)

s = Standard deviation

n = Number of data (events)

The Gumbel distribution is plotted on Gumbel paper where return period is on the x-axis and rainfall is on the y-axis. Gumbel paper is available at USGS offices or can be downloaded at ftp://sorrel.humboldt.edu/pub/geodept/graphpaper/gumbel.pdf. The Gumbel distribution can also be plotted on a spreadsheet application such as Excel using the reduced variate W where $W = -\ln \ln \frac{T}{T-1}$ (Table 2-4). When using excel, plot rainfall frequency on the y-axis and reduced variate W on the x-axis.

**Table 2-3:** Frequency factor $K_g$ for Gumbel distribution (USACOE, 1993)

| n | Exceedance Probability (%) | | | | | | | |
|---|---|---|---|---|---|---|---|---|
| | 50 | 20 | 10 | 5 | 4 | 2 | 1.33 | 1 |
| | Return Period (Years) | | | | | | | |
| | 2 | 5 | 10 | 20 | 25 | 50 | 75 | 100 |
| 15 | -0.143 | 0.967 | 1.703 | 2.410 | 2.632 | 3.321 | 3.721 | 4.005 |
| 20 | -0.147 | 0.919 | 1.625 | 2.302 | 2.517 | 3.179 | 3.563 | 3.936 |
| 25 | -0.151 | 0.888 | 1.575 | 2.235 | 2.444 | 3.088 | 3.463 | 3.729 |
| 30 | -0.153 | 0.866 | 1.541 | 2.188 | 2.393 | 3.026 | 3.393 | 3.653 |
| 40 | -0.155 | 0.838 | 1.495 | 2.126 | 2.326 | 2.943 | 3.301 | 3.554 |
| 50 | -0.157 | 0.820 | 1.466 | 2.086 | 2.283 | 2.889 | 3.241 | 3.491 |
| 60 | -0.158 | 0.807 | 1.446 | 2.059 | 2.253 | 2.852 | 3.200 | 3.446 |
| 70 | -0.159 | 0.797 | 1.430 | 2.038 | 2.230 | 2.824 | 3.169 | 3.413 |
| 75 | -0.159 | 0.794 | 1.423 | 2.029 | 2.220 | 2.812 | 3.155 | 3.400 |
| 100 | -0.160 | 0.779 | 1.401 | 1.998 | 2.187 | 2.770 | 3.109 | 3.349 |

**Table 2-4:** Relationship between return period and reduced variate

| Return Period | Exceedance Probability | Reduce Variate |
|---|---|---|
| 1.01 | 0.990 | -1.529 |
| 2 | 0.500 | 0.367 |
| 5 | 0.200 | 1.500 |
| 10 | 0.100 | 2.250 |
| 25 | 0.040 | 3.199 |
| 50 | 0.020 | 3.902 |
| 75 | 0.013 | 4.313 |
| 100 | 0.010 | 4.600 |

### 2.1.1.7 Log Pearson Type III Distribution

The second distribution used in hydrologic frequency analysis is the Log-Pearson Type III distribution. Log Pearson Type III distribution is a three parameter (mean, standard deviation, and skewness coefficient) gamma distribution. This distribution has been adopted as the method

for flood frequency analysis for government agencies since the stream data frequently fits the distribution. For this distribution the mean, standard deviation, and skewness coefficient of the logged data must be calculated. The general equation for the Log-Pearson Type III distribution is:

$$\log F(x) = \bar{y} + K_L s_y \tag{2-15}$$

$$K_L = \frac{2}{C_y}\{[(z - \frac{C_y}{6})\frac{C_y}{6} + 1]^3 - 1\} \tag{2-16}$$

where:

F(x) = Log Pearson III cumulative distribution function

$\bar{y}$ = Mean value of the logged data

$s_y$ = Standard deviation of the logged data

$C_y$ = Skewness coefficient of the logged data

z = Standard normal deviate for a return period T

$K_L$ = Log Pearson III frequency factors (Table 2-5)

The Log-Pearson III distribution is plotted on log-probability paper where exceedance probability is plotted on a probability scale on the x-axis while rainfall frequency is plotted on a logarithmic scale on the y-axis. Log Pearson III distribution probability graph paper is commercially available and be downloaded at ftp://sorrel.humboldt.edu/pub/geodept/graphpaper/2_cycle_log_probability_bw.pdf. Log Pearson III distribution can also be plotted on Excel by setting the y-axis to a logarithmic scale and using the expected normal value on the x-axis. The exceedance probability can be converted into the expected normal value using the NORMSINV functions in Excel (Table 2-6). For streamflow

analysis it is recommended to compare the Log-Pearson III plot to another Log Pearson III plot using the weighted skewness coefficient $C_w$ by substituting $C_w$ for $C_s$.

**Table 2-5:** Frequency factor $K_L$ for Log Pearson Type III (Viessman, et al., 1996)

| $C_y$ | Exceedance Probability (%) | | | | | | | |
|---|---|---|---|---|---|---|---|---|
| | 99 | 90 | 50 | 20 | 10 | 4 | 2 | 1 |
| | Return Period (Years) | | | | | | | |
| | 1.01 | 1.11 | 2 | 5 | 10 | 25 | 50 | 100 |
| 1.00 | -1.588 | -1.128 | -0.164 | 0.758 | 1.340 | 2.043 | 2.542 | 2.542 |
| 0.80 | -1.733 | -1.166 | -0.132 | 0.780 | 1.336 | 1.993 | 2.453 | 2.453 |
| 0.60 | -1.880 | -1.200 | -0.099 | 0.800 | 1.328 | 1.939 | 2.359 | 2.755 |
| 0.40 | -2.029 | -1.231 | -0.066 | 0.816 | 1.317 | 1.880 | 2.261 | 2.615 |
| 0.20 | -2.178 | -1.258 | -0.033 | 0.830 | 1.301 | 1.818 | 2.159 | 2.472 |
| 0 | -2.326 | -1.282 | 0 | 0.842 | 1.282 | 1.751 | 2.054 | 2.326 |
| -0.20 | -2.472 | -1.301 | 0.033 | 0.850 | 1.258 | 1.680 | 1.945 | 2.178 |
| -0.40 | -2.615 | -1.317 | 0.066 | 0.855 | 1.231 | 1.606 | 1.834 | 2.029 |
| -0.60 | -2.755 | -1.328 | 0.099 | 0.857 | 1.200 | 1..528 | 1.720 | 1.880 |
| -0.80 | -2.891 | -1.336 | 0.132 | 0.856 | 1.166 | 1.448 | 1.606 | 1.733 |
| -1.00 | -3.022 | -1.340 | 0.164 | 0.852 | 1.128 | 1.366 | 1.492 | 1.588 |

**Table 2-6:** Relationship between return period and expected normal value

| Return Period | Exceedance Probability | Expected Normal Value |
|---|---|---|
| 1.01 | 0.990 | -2.326 |
| 2 | 0.500 | 0 |
| 5 | 0.200 | 0.842 |
| 10 | 0.100 | 1.282 |
| 25 | 0.040 | 1.751 |
| 50 | 0.020 | 2.054 |
| 75 | 0.013 | 2.216 |
| 100 | 0.010 | 2.326 |

#### 2.1.1.8 Rainfall Partial Duration Series (For Rainfall Analysis Only)

The frequency analysis of maximum daily annual rainfall is called annual series while the analysis of all high daily rainfall above a given magnitude is called partial duration series. Partial duration series takes into account that there might be several heavy rainfall days in a year, which would not be included in the maximum daily annual rainfall for that specific year but would exceed the maximum in another year. To account for partial duration series adjust the return period values by the factors in Table 2-7. For return period greater than 10-years no adjustment is necessary (U.S. Weather Bureau, 1962). These factors were based on the frequency analysis of 50 rain-gaging stations across the mainland United States. The rainfall frequency analysis used to make the rainfall maps in Technical Paper 43 and Report R-73 (refer to section 2.1.2) use partial duration series.

**Table 2-7:** Conversion factors for adjusting annual series to partial duration series (U.S. Weather Bureau, 1962)

| Return Period | Conversion Factor |
|---|---|
| 2 | 1.14 |
| 5 | 1.04 |
| 10 | 1.01 |
| 20 | 1.00 |

#### 2.1.1.9 Error Limits

The final step in hydrologic frequency analysis is to decide which distribution to use. The method which hydrologists prefer is to use confidence intervals of 5% and 95%. This means that there is a 5% probability the data is greater than the 5% confidence interval and a 5% probability the data is less than the 95% confidence interval for a given return period. The two confidence

intervals define a range where the data probably will fall between the two confidence intervals 90% of the time. The confidence intervals are plotted of the same graph as the distribution curve (Gumbel or Log Pearson III). The distribution that best fits the data the best would have the data fall between the two confidence intervals. For the Gumbel distribution use equations 2-17 and 2-18 for Log Pearson Type III use equations 2-19 and 2-20.

$$x_U = \bar{x} + sK_c \tag{2-17}$$

$$x_L = \bar{x} - sK_c \tag{2-18}$$

$$x_U = 10^{\bar{y}+s_y * K_c} \tag{2-19}$$

$$x_L = 10^{\bar{y}+s_y * K_c} \tag{2-20}$$

where:

$x_U$ = Upper limit confidence limits (5% confidence interval)

$x_L$ = Lower limit confidence limits (95% confidence interval)

$K_c$ = Confidence interval frequency factors for error limits (Table 2-8)

**Table 2-8:** Frequency factors $K_c$ for error limits (Viessman, et al., 1996)

| n | Exceedance Probability at 5% Confidence Interval (%) | | | | | | |
|---|---|---|---|---|---|---|---|
| | 99.9 | 99 | 90 | 50 | 10 | 1 | 0.1 |
| 5 | 1.22 | 1.00 | 0.76 | 0.95 | 2.12 | 3.41 | 4.41 |
| 10 | 0.94 | 0.76 | 0.57 | 0.58 | 1.07 | 1.65 | 2.11 |
| 15 | 0.80 | 0.65 | 0.48 | 0.46 | 0.79 | 1.19 | 1.52 |
| 20 | 0.71 | 0.58 | 0.42 | 0.39 | 0.64 | 0.97 | 1.23 |
| 30 | 0.60 | 0.49 | 0.35 | 0.31 | 0.50 | 0.74 | 0.93 |
| 40 | 0.53 | 0.43 | 0.31 | 0.27 | 0.42 | 0.61 | 0.77 |
| 50 | 0.49 | 0.39 | 0.28 | 0.24 | 0.36 | 0.54 | 0.67 |

**Table 2-8 (Continued):** Frequency factors $K_c$ for error limits (Viessman, et al., 1996)

| | | | | | | | |
|---|---|---|---|---|---|---|---|
| 70 | 0.42 | 0.34 | 0.24 | 0.20 | 0.30 | 0.44 | 0.55 |
| 100 | 0.37 | 0.29 | 0.21 | 0.17 | 0.25 | 0.36 | 0.45 |
| n | 0.1 | 1 | 10 | 50 | 90 | 99 | 99.9 |
| | Exceedance Probability at 95% Confidence Interval (%) | | | | | | |

### 2.1.2 Rainfall Database Used

Rainfall data used in this report were obtained from three sources. The first source is from the National Weather Service web page at http://cdo.ncdc.noaa.gov. The National Weather Service (NWS) keeps records for 15-minute, hourly, and daily rainfall for various rain gaging stations on Oahu. For an inventory of rainfall stations in Hawaii including start/finish dates, type of record (daily, hourly, etc), and location please refer to the Hawaii State Climatologist website at http://lumahai.soest.hawaii.edu/Hsco/stn.htm.

The second source is the Technical Paper 43 (TP-43): Rainfall Frequency Atlas of the Hawaiian Islands published by the U.S. Department of Commerce. Published in 1962, TP-43 uses rain data from 287 rainfall gaging stations in the state and performed frequency analysis to obtain rainfall maps of the state. Report TP-43 encompasses rainfall maps for durations of 30-minute, 1, 2, 3, 6, 12, and 24-hours and return periods of 1, 2, 5, 10, 25, 50, and 100 years for the entire state.

The third source is Report R-73: Rainfall Frequency Study for Oahu published by the Hawaii State Department of Land and Natural Resources and US Army Corps of Engineers in 1984. Report R-73 presents updated rainfall maps for the island of Oahu. Frequency analysis was performed on 96 rainfall gaging stations using Gumbel Extreme Value distribution. Report R-73 includes rainfall maps for durations of 30-minute, 1, 6, and 24-hour return periods of 2, 10, 50,

and 100-years for the island of Oahu. Report R-73 is the most recent rainfall analysis for Oahu and the results are also used in the City and County of Honolulu Storm Drainage Standards (2000). Selected rainfall maps of Oahu are presented in Figure 2-3

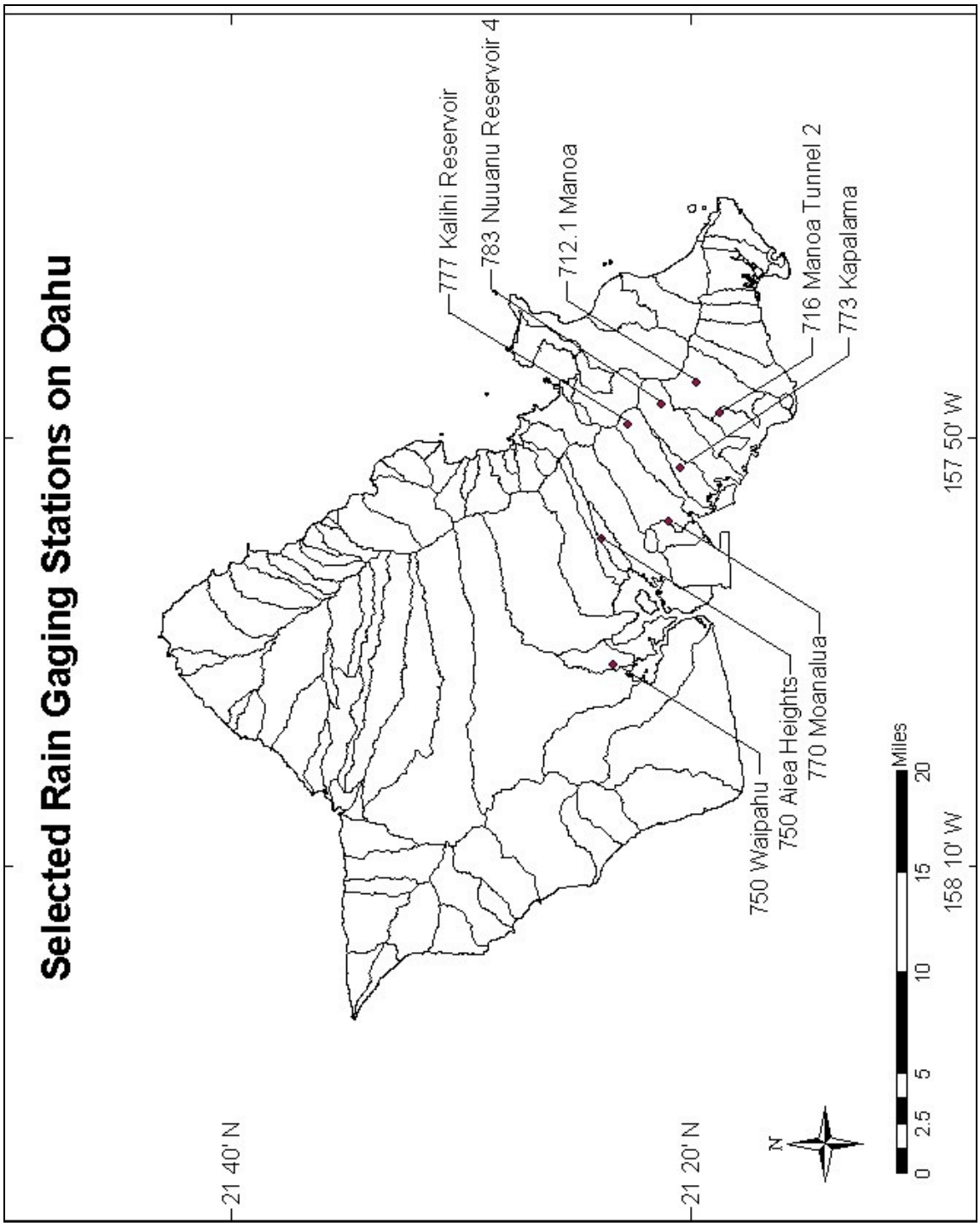


**Figure 2-3:** Selected rain gaging stations on Oahu

### 2.1.3 Rainfall Frequency Results

The maximum annual 24-hour rainfall data was obtained from the National Weather Service website for the rain gaging stations shown in Table 2-9. The data were analyzed using the frequency analysis procedures in section 2.1.1. The data were then fitted into the Gumbel and Log-Pearson III distribution with the purpose of determining the magnitude of a rainfall intensity of a certain return period. The frequency analysis of the NWS data was plotted and compared to the data from TP-43 and R-73 rainfall maps for return periods of 2, 10, 50, and 100-years for rainfall durations of 24-hours.

**Table 2-9:** Selected rain gaging stations in the present study

| Rain Station Location | Station Number | Agency | Type of Rain Gage | Resolution of Data | Years of record |
|---|---|---|---|---|---|
| Aiea Heights | 764.6 | NWS | Standard | Daily | 21 |
| Kalihi Reservoir | 777 | NWS | Recording | Daily | 52 |
| Kapalama | 773 | NWS | Standard | Daily | 72 |
| Manoa | 712.1 | NWS | Standard | Daily | 84 |
| Manoa Tunnel 2 | 716 | NWS | Recording | Daily | 57 |
| Moanalua | 770 | NWS | Standard | Daily | 83 |
| Nuuanu Reservoir 4 | 783 | NWS | Standard | Daily | 83 |
| Waipahu | 750 | NWS | Standard | Daily | 73 |

From the rainfall distributions plots (Masaki 2004), rainfall data from Aiea Heights, Moanalua, and Nuuanu Reservoir 4 were found to fit into the Gumbel distribution while the rest of the rain gaging stations were found to fit into the Log Pearson III distribution. The distribution was chosen based on if more of the data rest between the 5% and 95% interval limits for that specific distribution than the other distribution. If data rest between the confidence intervals for

both distributions, the distributions were chosen based on if the data followed the specific distribution.

The following two figures show sample plots of rainfall distribution based on Gumbel and log Pearson III probability distributions. For the complete plots for all the watersheds studied, please refer to Masaki (2004).

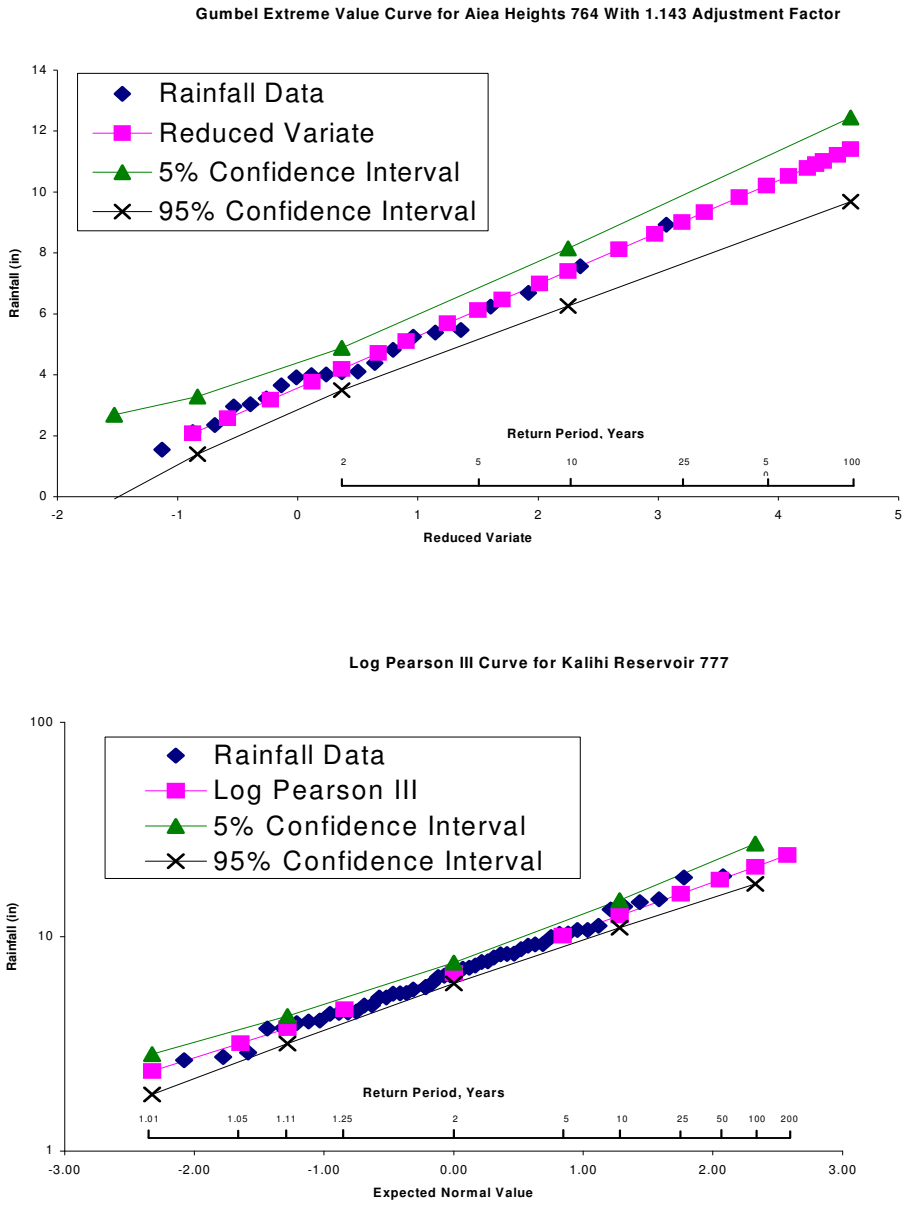


**Figure 2-5:** Sample plots of rainfall analysis based on Gumbel and Log Pearson III

Tables 2-10 thru 2-17 present the data from the frequency analysis versus the rain data analysis from R-73 and TP-43. From the tables, most of the present data matches the data from the R-73 except for Moanalua, and Waipahu rain gaging stations. Differences in the Moanalua and Waipahu rain gaging stations can be due to large amounts of missing daily rainfall data from the NWS website. Small differences are due to the difficulty in locating the location of the rain gaging stations on the rainfall maps.

From tables 2-10 thru 2-17 R-73 can be relied upon to obtain rainfall intensities but daily rainfall records should be checked for heavy daily rainfall and proximity to nearby rain gages before relying on results of report R-73. Recent heavy rainfall will alter the return period for rainfall intensities. Proximity of rain gage stations is the concentration of rain gages on rainfall maps, which affects the accuracy of the lines on the rainfall maps. Honolulu has the highest concentration of rain gages while Waipahu and the Ewa plain has a low concentration of rain gages. If heavy rainfall and far proximity is observed, then frequency analysis from section 2.1.1 should be performed on the rainfall data.

From these tables it is important to notice that for some watersheds, there is a relatively large difference (e.g., 20-30%) between the analysis of the present data compared to the analysis done in TP-43. For example if the engineers rely on TP-43 for design of hydraulic structures then the rainfall might be underestimated and might result in flood damage in some areas.

**Table 2-10:** Gumbel distribution results for Aiea Heights vs. R-73 and TP-43

| Aiea Heights 764.6 | | | | | |
|---|---|---|---|---|---|
| T | Present | R-73 | Difference | TP-43 | Difference |
| 2-yr | 4.77” | 5.25” | -9% | 5” | -5% |
| 10-yr | 7.48” | 8.25” | -9% | 10” | -25% |
| 50-yr | 10.21” | 11.75” | -13% | 13” | -21% |
| 100-yr | 11.40” | 13” | -12% | 14” | -19% |

**Table 2-11:** Log Pearson III distribution results for Kalihi Reservoir vs. R-73 and TP-43

| Kalihi Reservoir 777 | | | | | |
|---|---|---|---|---|---|
| T | Present | R-73 | Difference | TP-43 | Difference |
| 2yr | 7.69” | 8” | -4% | 6” | 28% |
| 10-yr | 12.67” | 12” | 6% | 11” | 15% |
| 50-yr | 18.42” | 17” | 8% | 16” | 15% |
| 100-yr | 21.14” | 19.25” | 10% | 18” | 17% |

**Table 2-12:** Log Pearson III distribution results for Kapalama vs. R-73 and TP-43

| Kapalama 773 | | | | | |
|---|---|---|---|---|---|
| T | Present | R-73 | Difference | TP-43 | Difference |
| 2-yr | 4.14” | 4.75” | -13% | 6” | -31% |
| 10-yr | 8.04” | 8.5” | -5% | 10” | -20% |
| 50-yr | 12.54” | 11.25” | 11% | 13.75” | -9% |
| 100-yr | 14.67” | 13.25” | 11% | 15.75” | -7% |

**Table 2-13:** Log Pearson III distribution results for Manoa vs. R-73 and TP-43

| Manoa 712.1 | | | | | |
|---|---|---|---|---|---|
| T | Present | R-73 | Difference | TP-43 | Difference |
| 2-yr | 4.77” | 5” | -5% | 5” | -5% |
| 10-yr | 8.04” | 8” | 0% | 8.5” | -5% |
| 50-yr | 11.86” | 10.5” | 13% | 12” | -1% |
| 100-yr | 13.68” | 12.75” | 7% | 13” | 5% |

**Table 2-14:** Log Pearson III distribution results for Manoa Tunnel 2 vs. R-73 and TP-43

| Manoa Tunnel 2 716 | | | | | |
|---|---|---|---|---|---|
| T | Present | R-73 | Difference | TP-43 | Difference |
| 2-yr | 7.86” | 8.25” | -5% | 7” | 12% |
| 10-yr | 11.34” | 12” | -5% | 11.5” | -1% |
| 50-yr | 15.49” | 16” | -3% | 14” | 11% |
| 100-yr | 17.45” | 17” | 3% | 16” | 9% |

**Table 2-15:** Gumbel distribution results for Moanalua vs. R-73 and TP-43

| Moanalua 770 | | | | | |
|---|---|---|---|---|---|
| T | Present | R-73 | Difference | TP-43 | Difference |
| 2-yr | 4.27” | 4.5” | -5% | 5.5” | -22% |
| 10-yr | 7.32” | 7.75” | -6% | 10” | -27% |
| 50-yr | 10.31” | 8” | 29% | 13.75” | -25% |
| 100-yr | 11.60” | 11.75” | -1% | 16” | -28% |

**Table 2-16:** Gumbel distribution results for Nuuanu Reservoir 4 vs. R-73 and TP-43

| Nuuanu Reservoir 4 783 | | | | | |
|---|---|---|---|---|---|
| T | Present | R-73 | Difference | TP-43 | Difference |
| 2-yr | 7.88” | 7.75” | 2% | 6” | 31% |
| 10-yr | 11.86” | 12” | -1% | 11” | 8% |
| 50-yr | 15.96” | 15.75” | 1% | 16” | 0% |
| 100-yr | 17.75” | 17.75” | 0% | 18” | -1% |

**Table 2-17:** Log Pearson III distribution results for Waipahu vs. R-73 and TP-43

| Waipahu 750 | | | | | |
|---|---|---|---|---|---|
| T | Present | R-73 | Difference | TP-43 | Difference |
| 2-yr | 3.37” | 4” | -16% | 4.25” | -21% |
| 10-yr | 8.08” | 7.5” | 8% | 8” | 1% |
| 50-yr | 13.36” | 10.5” | 27% | 11” | 21% |
| 100-yr | 15.77” | 12.5” | 26% | 13” | 21% |

Our results show that the rainfall statistics presented in TP-43 (1962) are significantly different from the results using the updated rainfall data (2002). On the other hand, the difference between the current results and that from R-73 (1984) is relatively small. This indicates that the rainfall analysis should be updated every 40 years or more often.

## 2.2 Prediction of Stream Discharge

The main objective of this section is to predict flow discharge for 10-year, 20-year, 50-year and 100-year as well as 500-year flood for representative streams on Oahu. The goal is to better understand the potential severity of floods on Oahu. In addition, the validity of several existing methods for predicting stream flow from rainfall data is further examined in order to determine the most suitable method for application in Hawaii. This is done by applying three different methods to estimate the flow discharge for a gaged stream and then comparing the results with the recorded streamflow data from the gage. Once the method is determined, it can be used to predict flood discharge for the streams of interest in a study for scour prediction.

For gauged streams, return periods for floods of a certain discharge can be obtained by using hydrologic frequency analysis from section 2.1.1 on historical discharge data from USGS (U.S. Geological Survey) stream gaging stations. For ungaged streams, the State of Hawaii Department of Transportation recommends using the following methods to estimate streamflow: the rational method, the City and County of Honolulu method, USGS regional flood frequency regression equations, and the National Resources Conservation Service (NRCS) Technical Release 55 (TR-55).

### 2.2.1 The Rational Method

The rational method is the most commonly used method to determine peak flow at an ungaged site for small watersheds with drainage areas less than 100 acres. The rational formula is given as:

$$Q = CIA \tag{2-21}$$

where:

Q = Peak discharge, $ft^3/s$

C = Runoff coefficient: a dimensionless number related to the drainage land use, rainfall intensity, and soil type

I = Rainfall intensity, in/hr for a rainfall duration equal to the time of concentration

$T_c$ = Time of concentration: the time it takes for water from the most remote part of the drainage area to reach the outlet, hr

A = Drainage area, acres

The rational formula assumes that the rainfall is uniform over the watershed area and storm duration. Also the peak rainfall occurs when the storm duration equals to the time of concentration when every area of the watershed contributes to runoff. In addition, the rational formula assumes that the return period of particular rainfall intensity will give the peak flow for that return period. For more information regarding the rational method please refer to the City and County of Honolulu Rules Relating to Storm Drainage Standards (2000).

### 2.2.2 The City and County of Honolulu Method

This method for determining streamflow uses Plate 6 from the City and County of Honolulu Rules Relating to Storm Drainage Standards (2000). Plate 6 (attached on next page) was developed by the USGS using the Log-Pearson Type III distribution analysis of 74 stream gaging stations on Oahu. The results were regionalized into three different groups and multi-regression techniques were used to obtain the design curves. The design curves are based on the 100-year flood return period and relate peak discharge to drainage area. The State Department of

Transportation recommends that this method be used for checking the results of the other streamflow estimation techniques only.

The following figure is Plate 6 from the storm drainage standard of the City and County of Honolulu:

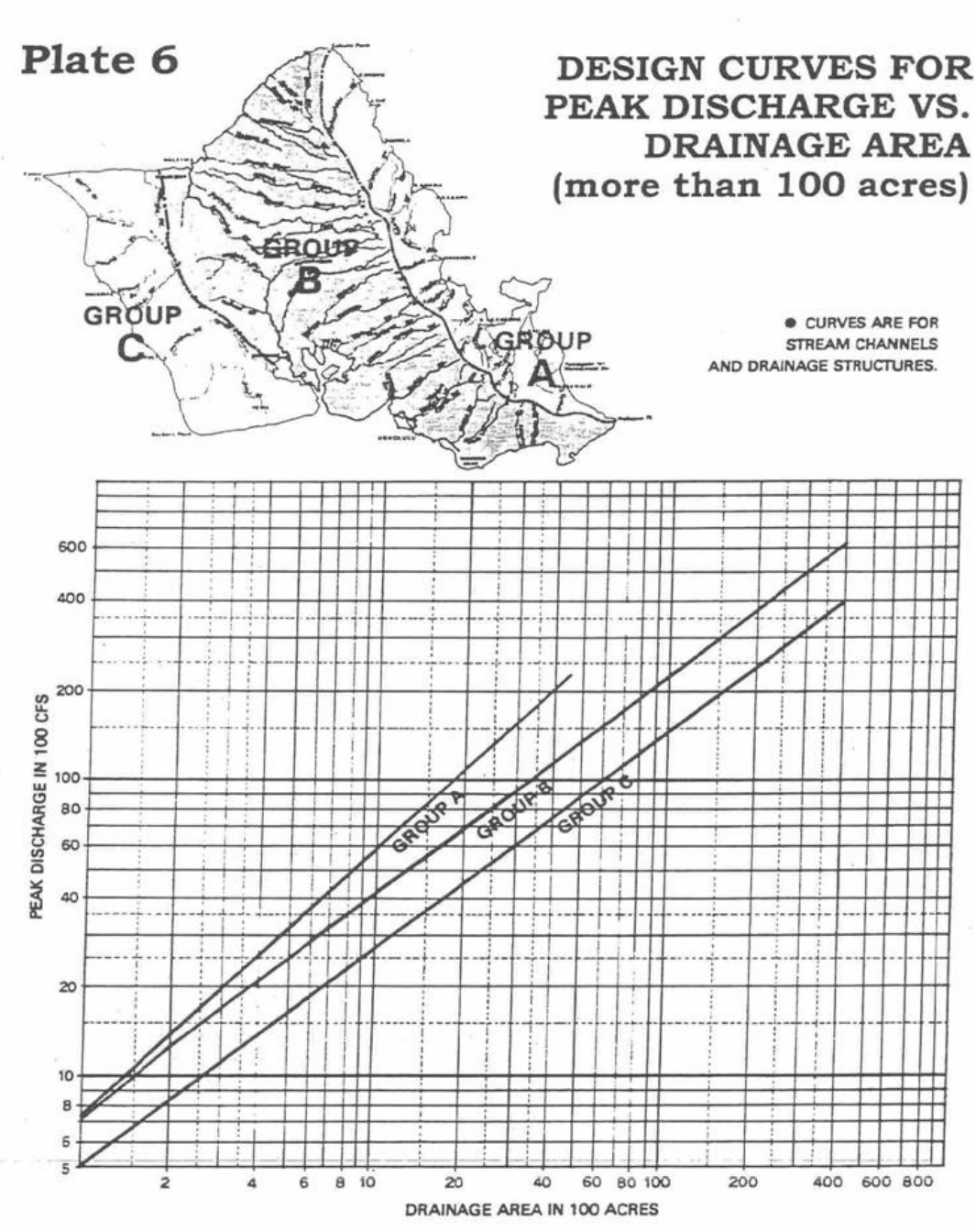


**Figure 2-5:** Plate 6 from the storm drainage standards of the City and County of Honolulu

### 2.2.3 USGS National Flood Frequency Regression Equations

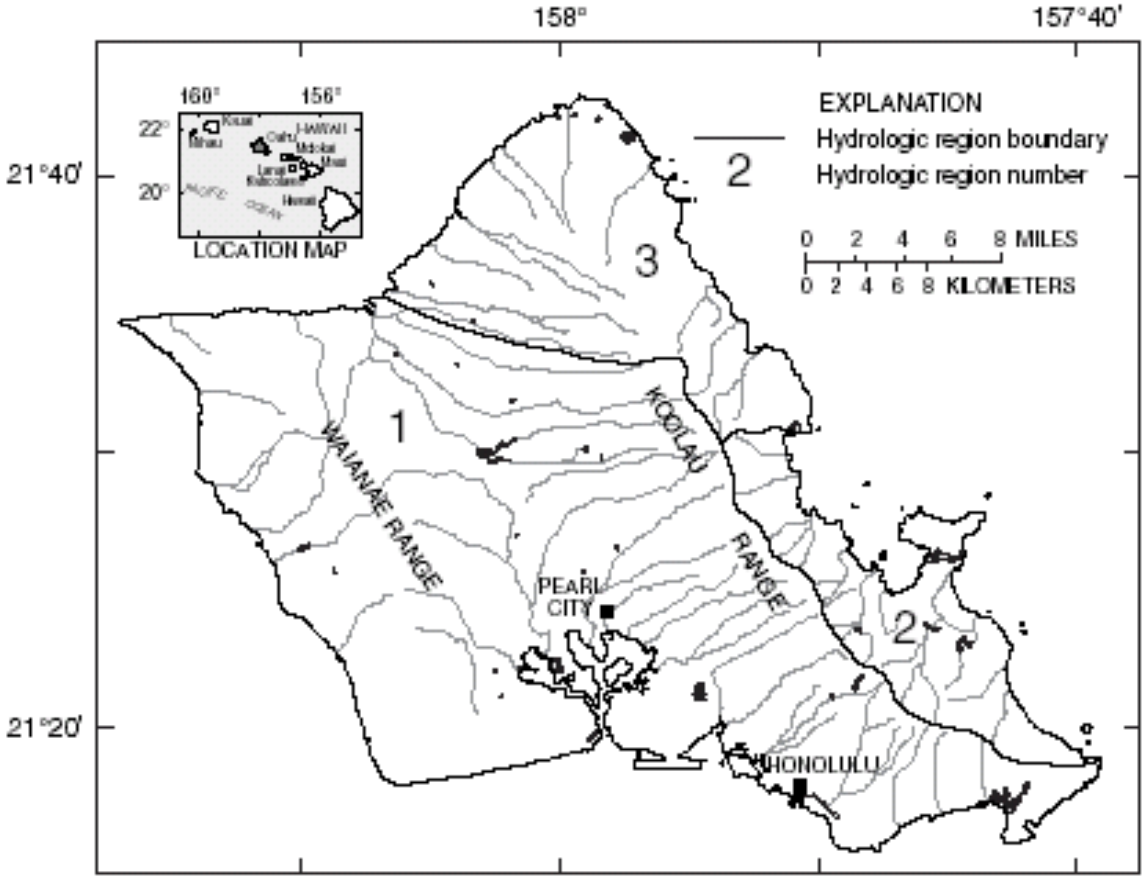


**Figure 2-6:** USGS hydrologic regions on Oahu (Wong, 1994)

Another method used to determine peak flow is the regional regression formulas developed by the USGS in cooperation with the City and County of Honolulu. These formulas were based on the Log-Pearson Type III distribution analysis of 79-gaged streams on the island of Oahu. Multi-regression analysis was performed on the results of the frequency analysis to obtain regression formulas for ungaged streams. These formulas determine peak flow for return intervals from 2 to 100 years and are based on streamflow data through 1998. The variables used in the equation are in terms of basin characteristics and rainfall intensity. The island of Oahu is divided into three hydrologic areas with different regression equations. Region 1 consists of

Honolulu, central Oahu, and leeward Oahu. Region 2 consists of windward Oahu and region 3 consists of north Oahu (Figures 2-6). The regression equations are listed in Table 2-18.

**Table 2-18:** USGS regression equations (USGS, 2000)

| Regression Equations | Standard Error (%) | Equivalent Years of Record (EQ) |
|---|---|---|
| Regression equations for streams in Region 1: Leeward Oahu | | |
| $Q2 = 3.26 * (DA^{0.634}) * (P_m^{1.08}) * 1.115$ | 43 | 4.2 |
| $Q5 = 25.8 * (DA^{0.642}) * (P_m^{0.773}) * 1.069$ | 40 | 5.8 |
| $Q10 = 73.5 * (DA^{0.646}) * (P_m^{0.621}) * 1.052$ | 39 | 8.2 |
| $Q25 = 217 * (DA^{0.646}) * (P_m^{0.464}) * 1.040$ | 38 | 11.4 |
| $Q50 = 425 * (DA^{0.645}) * (P_m^{0.368}) * 1.037$ | 38 | 13.7 |
| $Q100 = 758 * (DA^{0.643}) * (P_m^{0.286}) * 1.040$ | 39 | 15.8 |
| Regression equations for streams in Region 2: Windward Oahu | | |
| $Q2 = 525 * (DA^{0.704}) * 1.165$ | 62 | 2.5 |
| $Q5 = 1140 * (DA^{0.748}) * 1.138$ | 58 | 3.9 |
| $Q10 = 1700 * (DA^{0.763}) * 1.129$ | 54 | 5.7 |
| $Q25 = 2580 * (DA^{0.773}) * 1.124$ | 52 | 8.6 |
| $Q50 = 3360 * (DA^{0.776}) * 1.125$ | 51 | 11.0 |

**Table 2-18 (Continued):** USGS regression equations (USGS, 2000)

| | | |
|---|---|---|
| $Q100 = 4250 * (DA^{0.777}) * 1.133$ | 50 | 13.6 |
| Regression equations for streams in Region 3: North Oahu | | |
| $Q2 = 0.00356 * (DA^{0.870}) * (P224^{5.85}) * 1.036$ | 45 | 3.6 |
| $Q5 = 0.151 * (DA^{0.836}) * (P224^{4.30})$ | 34 | 8.3 |
| $Q10 = 1.76 * (DA^{0.805}) * (P224^{3.24})$ | 34 | 10.2 |
| $Q25 = 24.8 * (DA^{0.777}) * (P224^{2.10})$ | 38 | 10.7 |
| $Q50 = 125 * (DA^{0.765}) * (P224^{1.39})$ | 43 | 10.5 |
| $Q100 = 500 * (DA^{0.758}) * (P224^{0.792}) * 1.011$ | 48 | 10.1 |

where:

DA= Drainage area, $mi^2$

$P_m$ = Median annual rainfall, in

P224 = 2-year 24-hour rainfall intensity, in

These equations were recently updated in 2010, however, since this study was carried out during the period of 2000 – 2006, the results presented in this report were based on the regressions equations of 2000.

#### 2.2.3.1 Using USGS Regression Equations for Gauged Sites

For gaged stations 2 methods are available to determine peak discharge, one from the regression equations and the other from the frequency analysis of the stream data. A weighting method was developed to improve the peak flow estimate by combining the results of the two methods. The weights are based on the equivalent years of record for the regression equation and the length of gaged record from the frequency analysis. The weighted equation for peak discharge at gaged sites is:

$$Q_{tw} = \frac{Q_{tg}(N) + Q_{tr}(EQ)}{(N + EQ)} \tag{2-22}$$

where:

$Q_{tw}$= Weighted average peak discharge at gaged location, $ft^3/s$

$Q_{tg}$ = Discharge from frequency analysis, $ft^3/s$

$Q_{tr}$ = Regression estimate for gaged location, $ft^3/s$ (Table 2-18)

N = Number of years of gaged record used to compute $Q_{tg}$

EQ = Equivalent years of record (Table 2-18)

### 2.2.3.2 Using USGS Regression Equations for Ungaged Sites

The purpose of dividing Oahu into hydrological regions was to use the regression equations (based on gaged stream stations) for ungaged sites in the same region. Equations in table 2-18 can be used for the ungaged sites, but if the ungaged site lies on the same stream as the gaged site the equations can be used. The equation uses an adjustment factor ($C_u$) that incorporates both the peak flow estimates of the regression formulas and the estimates from frequency analysis of the gaged record. The restriction to using this equation is that if the drainage area is above 150% or below 50% of a nearby gaged station then no adjustment factor is applied to the regression equation for the gaged site ($C_u$=1).

$$Q_{tu} = C_u(Q_{ru}) \tag{2-23}$$

$$C_u = R - \frac{2\left|DA_g - DA_u\right|}{DA_g}(R-1) \tag{2-24}$$

where:

$Q_{tu}$ = Peak discharge for the ungaged site, $ft^3/s$

$C_u$ = Adjustment factor

$Q_{ru}$ = Regression estimate for ungaged site, $ft^3/s$ (Table 2-18)

R = Ratio of weighted discharge for a gaged site to the regression estimate for a gaged site

$= \frac{Q_{tw}}{Q_{tr}}$, $ft^3/s$

$DA_g$ = The drainage area of the gaged site, $mi^2$

$DA_u$ = The drainage area of the ungaged site, $mi^2$

#### 2.2.3.3 Limitations to the USGS Regression Equations

Limitations to using the regression equations include that the equation can only be used if the watershed characteristics (DA, $P_m$, P224, and years of record) fall within parameters used in its development (Table 2-19). For example the regression equations require that the urban cover for the particular watershed be less than 36%. If the watershed characteristics fall outside the parameters then the error for the equations will increase. More information regarding the use of regression equations can be found in Wong (1994).

**Table 2-19:** Range of values used in the USGS regression equations (Wong, 1994)

| Watershed Characteristics | Region 1 | Region 2 | Region 3 |
|---|---|---|---|
| Drainage Area, DA ($mi^2$) | 0.60-45.7 | 0.03-5.34 | 1.11-13.5 |
| Median Annual Rainfall, P (in) | 29-239 | 52-146 | 66-197 |
| 2-year 24-hour rainfall intensity, P224, in. | 4.72-8.78 | 5.62-9.10 | 5.21-9.04 |
| Urban Cover, UC (%) | 0-32 | 0-36 | 0 |
| Years of Record | 11-72 | 13-49 | 21-35 |

### 2.2.4 National Resources Conservation Service TR-55 Method

The last method used for determining flow at an ungaged site is the Department of Agriculture (USDA) National Resources Conservation Service (NRCS) Technical Release 55 (TR-55). TR-55 relates peak flow to drainage area, land use, soil type, and rainfall distribution type. TR-55 was first published in 1975 by the Soil Conservation Service (now NCRS) to provide a simplified procedure for estimating runoff and peak discharges on small urban and urbanizing watersheds. The TR-55 model begins with rain falling uniformly on an area over a specified time distribution. Using the runoff curve numbers (CN), the rainfall is converted into runoff. Runoff is then converted to peak flow using hydrograph and routing procedures. There

are two methods for computing peak flow using TR-55: the graphical peak discharge method and the tabular hydrograph method. Both these methods are derived from the TR-20 computer program output. TR-20, Computer Program for Project Formulation Hydrology, is a computer program written in FORTRAN that develops flood hydrographs from runoff and routes the flow through stream channels and reservoirs (SCS, 1992).

#### 2.2.4.1 SCS Runoff Depth Equation

TR-55 separates rainfall into three components: direct runoff, retention, and initial abstraction. The first step in the TR-55 analysis is to calculate each of the different rainfall components. The equation was based on the relationship between accumulated rainfall and accumulated runoff derived by SCS from experimental plots for numerous soils and vegetative cover conditions The following equations is used to estimate direct runoff from 24- hour or 1-day storm rainfall:

$$Q_r = \frac{(P - 0.2S)^2}{(P + 0.8S)} \tag{2-25}$$

$$S = \frac{1000}{CN} - 10 \tag{2-26}$$

$$I_a = 0.2S \tag{2-27}$$

where:

$Q_r$ = Depth of runoff, in

P = Rainfall, in

S = Maximum potential retention, in

$I_A$ = Initial abstraction, in

CN = NRCS runoff curve number

The NRCS curve number (CN) is based on the soil type, land use, treatment, and hydrologic condition. The soil type is classified into hydrologic soil groups to indicate the minimum rate of infiltration obtained for bare soil after prolong wetting (NRCS, 1986). The hydrologic soil groups are labeled as A, B, C, and D where group A has the highest infiltration rate and lowest runoff while group D has the lowest infiltration and highest runoff (Table 2-20). Soil type maps can be obtained from USDA soil surveys and GIS software such as ArcView. Land use represents the cover type of the watershed such as residential district or a farmland. Land use can be obtained using land use maps from GIS software based on government databases. Treatment is only used when the land use of the watershed is classified as agricultural. Treatment suggests how the agricultural land is farmed such as contoured, terraced, or bare soil. Hydrologic condition represents how much of the land use is covered by plants. If the watershed requires more than one CN then a weighted average is used.

For urban areas there is a certain degree of imperviousness that must be considered when determining the curve number. For example does the water drain into a storm drain or to a pervious area, which will infiltrate the soil. To determine the CN use a weighted approach was developed where impervious areas have a CN of 98 and pervious areas have a CN equal to a pasture in good hydrologic condition or 39, 61, 74, and 80 for soil hydrologic groups A, B, C, and D. If runoff from an urban area drains directly to a drainage system such as a canal or storm drain, use equation 2-27. If runoff from an urban area drains into a pervious area, use equation 2-28. Refer to Appendix Section E.1 for the average percent of impervious areas for urban and residential districts.

$$CN_c = CN_p + \left(\frac{P_{imp}}{100}\right)\left(98 - CN_p\right) \qquad (2\text{-}28)$$

$$CN_c = CN_p + \left(\frac{P_{imp}}{100}\right)\left(98 - CN_p\right)\left(1 - 0.5R_{imp}\right) \text{ for } P_{imp} \leq 30\% \qquad (2\text{-}29)$$

where:

$CN_c$ = Composite runoff curve number

$CN_p$ = Pervious runoff curve number

$P_{imp}$ = Percent imperviousness

$R_{imp}$ = Ratio of unconnected impervious area to total impervious area

Limitations in determining rainfall runoff include the following. The equations above cannot be used to calculate runoff from snow or rain from frozen ground. The CN procedure should not be used when runoff is less than 0.5 in and if the weighed CN is less then 40. The SCS runoff procedures apply only to direct surface runoff not other factors that contribute to runoff such as subsurface flow or high ground water levels. The runoff curve number equation does not account for rainfall duration or intensity. The equation for initial abstraction was based on data from agricultural conditions, as a result for urban areas a significant initial loss may not take place.

**Table 2-20**: Soil characteristics for each soil hydrologic group (McCuen et al., 2002) and (NRCS, 1986).

| Soil Hydrologic Group | Soil Characteristics |
|---|---|
| A | Deep well drained sand and gravel, deep loess; aggregated silts, high rate of water transmission (greater than 0.30 in/hr). |
| B | Moderately deep moderately drained soils, Shallow loess, sandy loam, moderate rate of water transmission (0.15-0.30 in/hr) |
| C | Clay loams, shallow sandy loams, soils high is clay, soils low in organic content, low rate of water transmission (0.05-0.15 in/hr). |
| D | Soils that swell significantly when wet, heavy plastic clays, very low rate of water transmission (0-0.05 in/hr) |

### 2.2.4.2 Time of Concentration

The next step is to calculate the time of concentration ($T_c$) and travel time ($T_t$), where $T_t$ is the time it takes water to travel from one part of a subbasin to another, while $T_c$ is the time water travels from the furthest part of the basin to the outlet. Travel time is based on surface roughness, slope, channel shape, and flow patterns. There are three different types of travel times: sheet, shallow concentrated, and open channel flow.

Sheet flow is defined as flow over plane surfaces (NRCS, 1986). Sheet flow usually exists in the upper reaches of the hydraulic flow path such as in the headwater of streams. Sheet flow should be used for flow lengths less than 300 feet. The travel time equation for sheet flow is calculated using Manning's kinematic solution given as:

$$T_t = \frac{0.007(n_m L)^{0.8}}{(P_2)^{0.5} s_L^{0.4}} \tag{2-30}$$

where:

$n_m$ = Manning's roughness coefficient (Table 2-22)

L = Flow length, ft

$P_2$ = 2-year, 24-hour rainfall, in

$s_L$ = Slope of hydraulic grade line/land slope, ft/ft

After short distances flow is concentrated in rills and then gullies of increasing proportions (McCuen et al., 2002). This type of flow is called shallow concentrated flow, which begins after a maximum 300 feet of sheet flow. The travel time equation for shallow concentrated flow is given as:

$$T_t = \frac{L}{3600 * V} \tag{2-31}$$

$$V = 33ks_L^{0.5} \quad (2\text{-}32)$$

Where:

L = Flow length, ft

V = Average velocity, ft/s

k = Intercept coefficient (Table 2-21)

$s_L$ = Slope of hydraulic grade line/land slope, ft/ft

Open channels are assumed to begin where surveyed cross section information has been obtained, where channels are visible on aerial photographs, or where blue lines (indicating streams) appear on the USGS quadrangle sheets. (NRCS, 1986) The equation to calculate travel time for open channel is the same as shallow concentrated flow. Manning's equation is used to determine the average velocity.

$$V = \frac{1.49r^{2/3}s_c^{1/2}}{n_m} \quad (2\text{-}33)$$

where:

V = Average velocity, ft/s

r = Hydraulic radius, ft

$s_c$ = Channel slope, ft/ft

$n_m$ = Manning's roughness coefficient (Table 2-22)

Limitations in calculating travel time and time of concentration include that the minimum $T_c$ is 0.1 hour. In addition Manning's kinematic solution for sheet flow should not be used for

flow lengths longer than 300 feet. In watersheds with storm sewers, the sewers generally handle only a small portion of the peak flow and rest travels by streets and lawns to the outlet.

**Table 2-21:** Intercept coefficients for shallow concentrated flow (McCuen et al, 2002)

| k | Land Cover/Flow Regime |
|---|---|
| 0.076 | Forest with heavy ground litter; hay meadow (overland flow) |
| 0.152 | Trash fallow or minimum tillage cultivation; contour or strip cropped; woodland (overland flow). |
| 0.213 | Short-grassed pastures (overland flow). |
| 0.274 | Cultivated straight rows (overland flow). |
| 0.305 | Nearby bare and untilled (overland flow); alluvial fans in western mountain regions. |
| 0.457 | Grassed waterways (shallow concentrated flow) |
| 0.491 | Unpaved (shallow concentrated flow) |
| 0.619 | Paved area (shallow concentrated flow); small upland gullies. |

**Table 2-22:** Manning's roughness coefficient for sheet flow (McCuen et al., 2002)

| n | Surface Description |
|---|---|
| 0.011 | Smooth surfaces (concrete, asphalt, gravel, or bare soil) |
| 0.014 | Brick with cement mortar and food wood |
| 0.015 | Cast iron and vitrified clay |
| 0.024 | Corrugated metal pipe and cement rubble surface |
| 0.05 | Fallow (no residue) |
| 0.06 | Cultivated soils: Residue cover =20% |
| 0.17 | Cultivated soils: Residue cover >20% |
| 0.13 | Cultivated soils: Natural |
| 0.15 | Grass: Short grass prairie |
| 0.24 | Grass: Dense grasses |
| 0.41 | Grass: Bermuda grass |
| 0.13 | Grass: Range (natural) |
| 0.40 | Woods: Light underbrush |
| 0.80 | Woods: Dense underbrush |

Because of all the limitations and variables involved in calculating $T_c$, one may question the $T_c$ calculations and the subsequent peak flow results formulated. According to the TR-20 computer program, which is the basis of the TR-55 method, out of the five main input parameters (drainage area, curve number, time of concentration, run-off depth, and rainfall distribution type) variations in $T_c$ will affect the peak discharge the least. A 10% variation in $T_c$ will affect the peak discharge by 4-5% while a 10% variation in CN will affect the peak discharge by 23-28% (see Table 2-23). Table 2-23 was formed from a TR-20 analysis of a watershed with the following characteristics DA=1.2 $mi^2$ CN=75, $T_c$=0.33 hours, runoff depth=5.2 in, and rainfall type 2. Four of the watershed characteristics were held constant while one was varied by 10%. The peak discharge was determined and compared to the original value.

**Table 2-23:** Sensitivity of input parameters for TR-20 analysis (SCS, 1992)

| Variable | Variation | Value | Peak Discharge |
|---|---|---|---|
| Drainage Area | 100% | 1.20 $mi^2$ | 2128 (100%) |
| | 90% | 1.08 $mi^2$ | 1915 (90%) |
| | 110% | 1.32 $mi^2$ | 2341 (110%) |
| Curve Number | 100% | 75 | 2128 (100%) |
| | 90% | 68 | 1628 (77%) |
| | 110% | 83 | 2733 (128%) |
| Time of Concentration | 100% | 0.33 hours | 2128 (100%) |
| | 90% | 0.30 hours | 2224 (105% |
| | 110% | 0.36 hours | 2050 (96%) |
| Runoff Depth | 100% | 5.20 in | 2128 (100%) |
| | 90% | 4.68 in | 1794 (84% |
| | 110% | 5.72 in | 2480 (117% |
| Rainfall Type (See Sect. 2.2.3.1) and Fig. 2.5) | ---------- | Type 2 | 2128 (100%) |
| | ---------- | Type 1 | 1069 (50%) |
| | ---------- | Type 1A | 436 (20%) |
| | ---------- | Type 3 | 1543 (73%) |

### 2.2.4.3 Synthetic Rainfall Distributions

An important parameter for the graphical peak discharge method is the rainfall distribution type. Rainfall distribution types were developed since some rainfall models require that a variation of rain with time as input rather than a rainfall amount for a particular return period. The National Weather Service developed dimensionless rainfall distribution types for the United States from Rainfall Frequency Atlases Technical Papers. There are four different rainfall distributions (Figure 2-7): type I, type IA, type II and type III. An example of how the distributions work is by showing that peak rainfall depth occurs at 8-hours for rain distributions I and IA while for II and III the peak occurs at 12-hours (Figure 2-8). For more information refer to NRCS TR-55 manual (1986).

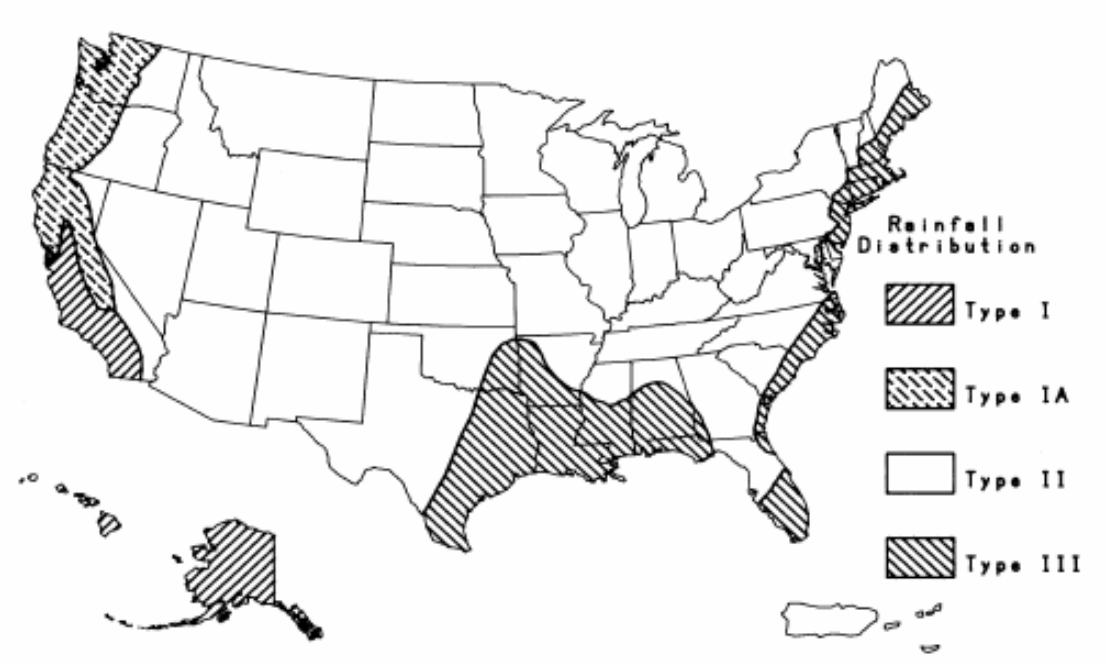


**Figure 2-7:** Approximate geographic boundaries for NCRS (SCS) rainfall distributions (NCRS, 1986)

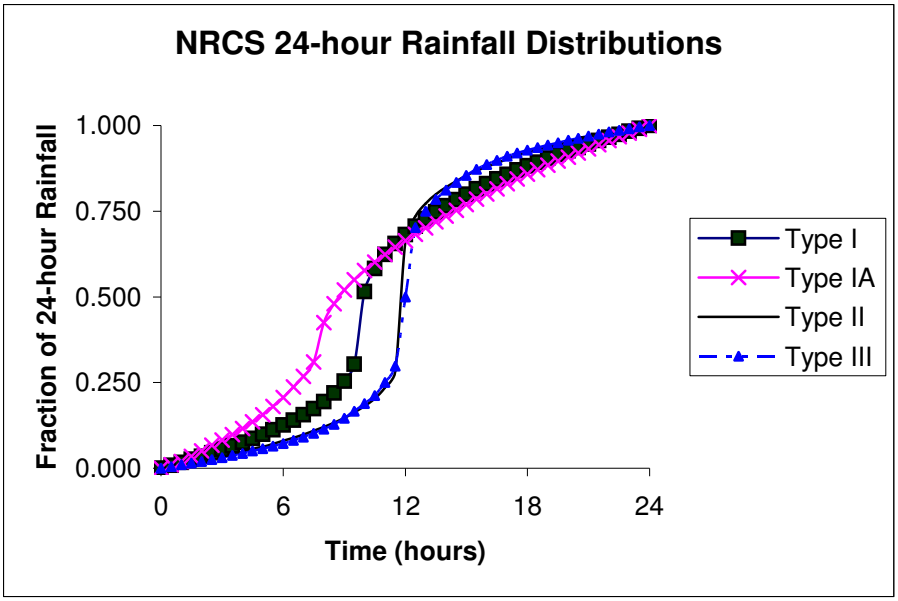


**Figure 2-8:** NCRS Rainfall distribution types (McCuen et al, 2002)

### 2.2.4.4 Graphical Peak Discharge Method

The final step in the TR-55 analysis is to determine the peak flow. The graphical peak discharge method is one of the methods used by TR-55 to calculate the peak flow (the outer being the tabular hydrograph method). Graphical peak discharge method was developed from hydrograph analysis using the TR-20 computer program. This method only provides the peak discharge of the watershed. If the watershed is complex or a hydrograph is needed use the tabular hydrograph method (section 2.2.4.5) or TR-20 computer program. The graphical peak discharge method is given as:

$$q_p = q_u A_m Q_r F_p \tag{2-34}$$

$$q_u = 10^{C_0 + C_1 \log t_c + C_2 [\log(t_c)]^2} \tag{2-35}$$

where:

$q_p$ = Peak discharge, cfs

$q_u$ = Unit peak discharge, csm/in

$A_m$ = Drainage area, $mi^2$

$Q_r$ = Depth of runoff, in

$F_p$ = Pond and swamp adjustment factor (Table 2-23)

$C_0$ = Regression coefficients for various $I_a/P$ ratios (Table 2-22)

$C_1$ = Regression coefficients for various $I_a/P$ ratios (Table 2-22)

$C_2$ = Regression coefficients for various $I_a/P$ ratios (Table 2-22)

Limitations to the graphical peak discharge method include that the watershed CN must be homogenous and greater than 40. The watershed must have only one main stream or two streams with similar time of concentration. In addition TR-55 cannot method cannot perform valley or reservoir routing. The Fp adjustment factor can only be applied for ponds and swamps not in the flow path used to calculate $T_c$. If Ia/P > 0.5 use 0.5 and if Ia/P < 0.1 use 0.1. Using Ia/P factors greater than 0.5 and less than 0.1 will affect the accuracy of the results. Minimum $T_c$ is 0.1 hours and the maximum $T_c$ is 10 hours.

**Table 2-24:** C coefficients for unit peak discharge for rainfall distribution type I (NRCS, 1986)

| $I_a/P$ | $C_0$ | $C_1$ | $C_2$ |
|---|---|---|---|
| 0.10 | 2.30550 | -0.51429 | -0.11750 |
| 0.20 | 2.23537 | -0.50387 | -0.08929 |
| 0.25 | 2.18219 | -0.48488 | -0.06589 |
| 0.30 | 2.10624 | -0.45695 | -0.02835 |
| 0.35 | 2.00303 | -0.40769 | 0.01983 |
| 0.40 | 1.87733 | -0.32274 | 0.05754 |
| 0.45 | 1.76312 | -0.15644 | 0.00453 |
| 0.50 | 1.67889 | -0.06930 | 0.0 |

**Table 2-25:** Pond and swamp adjustment factor (NRCS, 1986)

| Percentage of Pond and Swamp Area | Fp |
|---|---|
| 0 | 1.00 |
| 0.2 | 0.97 |
| 1.0 | 0.87 |
| 3.0 | 0.75 |
| 5.0 | 0.72 |

### 2.2.4.5 Tabular Hydrograph Method

The tabular hydrograph method is used if a hydrograph is needed or watershed subdivision is required. This method approximates the results of the TR-20 computer program. This method is able to develop partial runoff hydrographs anywhere in the watershed by subdividing the watershed and using the following equation:

$$q = q_t A_m Q \tag{2-36}$$

where:

q = Hydrograph coordinate at hydrograph time t, cfs

$q_t$ = Tabular hydrograph unit discharge from Appendix E, csm/in

$A_m$ = Drainage area of individual subarea, $mi^2$

Q = Runoff, in

The procedure in obtaining the hydrograph begins with first subdividing the watershed into homogeneous subareas. Next obtain all subarea characteristics detailed in section 2.2.4.1 such as curve number, runoff, and drainage area. Subsequently calculate $T_t$ and $T_c$ of each subarea as described in section 2.2.4.2. Also compute the sum of the travel time each subarea through the watershed to the point needing the hydrograph. Next find the variable $q_t$ for different

hydrograph times from tabular hydrograph unit discharges tables, which is a function of $T_t$, $T_c$, Ia/P, and rainfall distribution type of the subarea. Finally solve equation 2-36 for each subarea and sum variable q for each hydrograph time to obtain the composite hydrograph.

Limitations to the tabular hydrograph method include that the travel time must be less than 3 hours and the time of concentration be less than 2 hours. The drainage areas of the subareas must not differ by a factor of five or more. In addition this method should not be used if a more accurate time of peak discharge is required than one obtained through the tabular method. Also the tabular method only gives a portion of the hydrograph, use another method if the entire hydrograph is needed. If the watershed exhibits characteristics beyond the capabilities of the TR-55 method, use the TR-20 computer program (http://www.wcc.nrcs.usda.gov/hydro/hydro-tools-models-tr20.html). For more information and tables regarding the TR-55 method please refer to the USDA Technical Release 55.

### 2.2.5 Selected Watersheds

Watershed characteristics (Table 2-26) were determined using Watershed Modeling System (WMS) computer program. WMS, developed by the Environmental Modeling Research Laboratory at Brigham Young University, extracts input data from computerized maps for hydrologic models such as TR-55, rational method, and regression equations. Computerized maps include digital raster graphics (DRG) and digital elevation models (DEM), which can be downloaded at http://data.geocomm.com/catalog/index.html. Digital raster graphics are scanned USGS topographic quadrangle maps, and referenced to the earth surfaces using Universal Transverse Mercator (UTM) coordinate system. Digital elevation models are a digital form of the quadrangle which contain x, y, and elevation coordinates for a portion of the earth's surface.

WMS overlays DEM and DRG and uses TOPAZ software to obtain flow directions and accumulations. Topographic Parameterization Software or TOPAZ, developed by the USDA, analyzes landscape topography from DEM's to identify and measure topographic features, define surface drainage, subdivide watersheds along drainage divides, quantify the drainage network, and calculate representative subcatchment parameters (USDA 99). With the flow directions and accumulations, WMS can delineate watersheds and compute the basin characteristics. For more information about WMS, visit http://www.aquaveo.com/wms.

Watershed characteristics are also available from the USGS, but if an engineer needed watershed information for a location upstream of a stream gaging station or for a stream without a stream gaging station, the USGS would not have the information. The engineer would then have to use a cumbersome and error prone process to define the watershed using topographic maps. Defining the watershed boundaries using WMS is fast and fairly accurate when compared to the USGS watershed characteristics. In this study all streamflow analysis using the Rational, City and County of Honolulu, USGS Regression, and TR-55 method used the watershed characteristics from the WMS analysis.

**Table 2-26:** Selected watersheds (from WMS analysis)

| Stream Name | USGS Site Number | Years of Record | Drainage Area ($mi^2$) | Flow Slope (ft/ft) | Flow Length (ft) |
|---|---|---|---|---|---|
| Kalihi | 16229000 | 82 | 2.44 | 0.490 | 14846 |
| Kaluanui | 16304200 | 33 | 1.10 | 0.500 | 17497 |
| Makaha | 16211600 | 40 | 2.39 | 0.570 | 18069 |
| Opaeula | 16345000 | 40 | 2.93 | 0.090 | 59188 |
| Punaluu | 16303000 | 46 | 2.53 | 0.500 | 16231 |
| Waiakeakua | 16240500 | 81 | 1.06 | 0.730 | 9261 |
| Waiawa | 16216000 | 47 | 26.40 | 0.140 | 64825 |
| Waikane | 16294900 | 40 | 2.35 | 0.550 | 15797 |
| Waikele | 16213000 | 47 | 45.70 | 0.080 | 113280 |

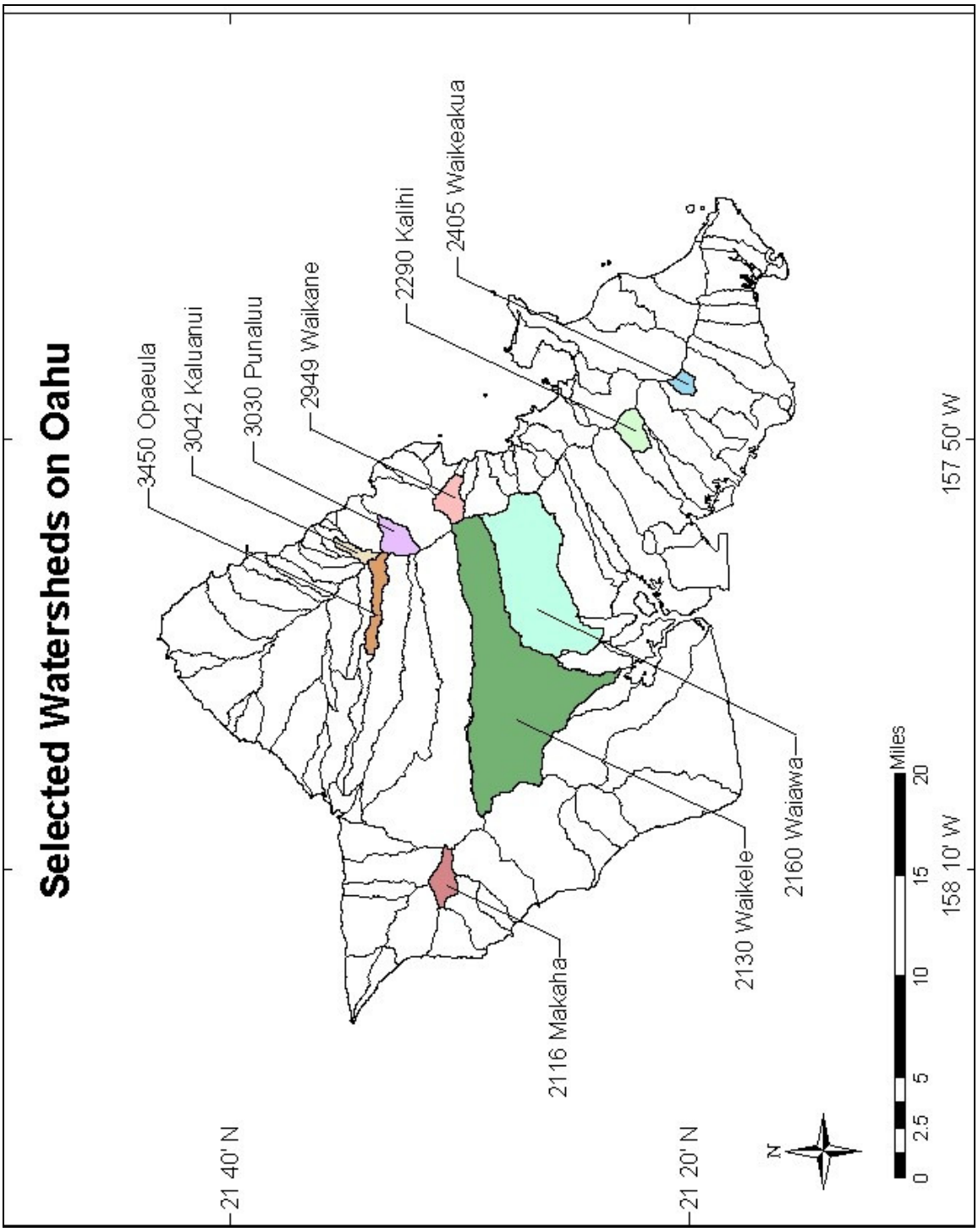


**Figure 2-9:** Selected watersheds on Oahu

### 2.2.6 Discharge Prediction Results

The rational, City and County of Honolulu, USGS regression, and NCRS TR-55 method were applied in this study to perform hydrological analysis on stream flow discharge for several watersheds with existing stream gaging stations for flood return periods of 10, 50, and 100 years (Tables 2-27 to 2-31). The results were compared with frequency analysis of the stream gaging station records in order to verify the validity of the stream flow predicting methods.

**Table 2-27:** Streamflow results using the rational method

| Stream Name | 10-Year Storm (cfs) | 50-Year Storm (cfs) | 100-Year Storm (cfs) |
|---|---|---|---|
| Kalihi | 2869.44 | 4099.20 | 4919.04 |
| Kaluanui | 844.80 | 1182.72 | 1351.68 |
| Makaha | 1468.42 | 2019.07 | 2202.62 |
| Opaeula | Not Applicable | | |
| Punaluu | 2428.80 | 3036.00 | 4048.00 |
| Waiakeakua | 1411.07 | 2062.34 | 2518.22 |
| Waiawa | Not Applicable | | |
| Waikane | 1955.20 | 2820.00 | 3384.00 |
| Waikele | Not Applicable | | |

**Table 2-28:** Streamflow results using City and County of Honolulu Plate 6

| Stream Name | 100-Year Storm (cfs) |
|---|---|
| Kalihi | 5800 |
| Kaluanui | 4400 |
| Makaha | 3700 |
| Opaeula | 6500 |
| Punaluu | 8800 |
| Waiakeakua | 2000 |
| Waiawa | 32500 |
| Waikane | 8500 |
| Waikele | 50000 |

Note: The City and County of Honolulu Method only have design curves for a 100-year storm.

**Table 2-29:** Streamflow results using USGS regression equations

| Stream Name | 10-Year Storm (cfs) | 50-Year Storm (cfs) | 100-Year Storm (cfs) |
|---|---|---|---|
| Kalihi | 2689.85 | 4562.18 | 5500.98 |
| Kaluanui | 1416.00 | 2295.08 | 2736.51 |
| Makaha | 1743.56 | 3509.42 | 4473.18 |
| Opaeula | 3262.35 | 4952.78 | 5815.49 |
| Punaluu | 3886.82 | 5020.31 | 5589.90 |
| Waiakeakua | 1495.53 | 2589.22 | 3147.29 |
| Waiawa | 10976.01 | 19599.01 | 23933.74 |
| Waikane | 3683.56 | 7335.68 | 9352.73 |
| Waikele | 12889.63 | 24892.97 | 31152.19 |

**Table 2-30:** Streamflow results using TR-55

| Stream Name | 10-Year Storm (cfs) | 50-Year Storm (cfs) | 100-Year Storm (cfs) |
|---|---|---|---|
| Kalihi | 5283 | 7657 | 9418 |
| Kaluanui | 2934 | 3979 | 4684 |
| Makaha | 2686 | 4887 | 6077 |
| Opaeula | 3436 | 5364 | 6072 |
| Punaluu | 5766 | 8865 | 10145 |
| Waiakeakua | 2863 | 4235 | 4935 |
| Waiawa | 19571 | 35948 | 42857 |
| Waikane | 5158 | 7853 | 9237 |
| Waikele | 17398 | 26312 | 33504 |

### 2.2.7 Comparison with Measured Discharge Data

The historical stream gage data were obtained from the USGS website at http://waterdata.usgs.gov/nwis/sw up to the year 1999. The USGS provides daily, monthly, and annual streamflow for 94 stream gaging stations on Oahu. For more information of stream gaging stations currently in use please refer to the USGS Water Data Report HI-99-1 at http://wwwdhihnl.wr.usgs.gov/pubs/wdr-hi-99-1/index.html. With the stream gaging data a

hydrological frequency analysis were performed to obtain 10-year, 50-year, and 100-year storm flow (Table 2-31).

**Table 2-31:** Results of hydrologic frequency analysis based on measured data from selected stream gaging stations

| Stream Name | Frequency Analysis Method | 10-Year Storm (cfs) | 50-Year Storm (cfs) | 100-Year Storm (cfs) |
|---|---|---|---|---|
| Kalihi | Log Pearson | 4155.37 | 7457.22 | 9053.96 |
| Kaluanui | Log Pearson | 1789.83 | 2783.73 | 3223.06 |
| Makaha | Log Pearson | 999.08 | 1938.42 | 2415.19 |
| Opaeula | Weighted Skew | 3619.01 | 5126.69 | 5754.63 |
| Punaluu | Log Pearson | 3808.82 | 5685.17 | 6512.40 |
| Waiakeakua | Log Pearson | 1166.98 | 2229.76 | 2859.32 |
| Waiawa | Log Pearson | 19965.89 | 29276.29 | 32935.40 |
| Waikane | Weighted Skew | 5938.32 | 9325.43 | 10761.17 |
| Waikele | Log Pearson | 9218.98 | 16824.42 | 20632.26 |

### 2.2.8 Discussions

When one compares the streamflow results from the TR-55 analysis and USGS regression methods with the results predicted directly from the Log-Pearson III frequency analysis of the stream gaging stations records, one can see that the results vary between watersheds. Figures 2-10 thru 2-16 present a comparison between the Log Pearson frequency analysis and the Plate 6, Regression, and TR-55 methods for 10-year, 50-year, and 100-year storm. Figure 2-10 shows that Plate 6 varies an average of 31% greater than the Log-Pearson analysis for a 100-year flood of the 9 streams. Figures 2-11 thru 2-13 show that the USGS Regression equation average 7% less for a 100-year flood, 14% less for a 50-year flood, and 29% less for a 10-year flood than the Log-Pearson analysis of the 9 streams. Figures 2-14 thru 2-16

show that the TR-55 method average 35% greater for a 100-year flood, 28% greater of a 50-year flood, and 14% greater for a 10-year flood than the Log-Pearson analysis of the 9 streams. From these results for the streamflow predictions based on the USGS regression equation (Table 2-29), match closer to the Log Pearson III frequency analysis of the recorded data than the TR-55 method and Plate 6. The reason for this better agreement is that the regression equations are based directly on the Log-Pearson Type III frequency analysis of the maximum annual streamflow records for 79 stream gage stations on Oahu while the TR-55 method predicts streamflow indirectly based on rainfall and hydrological parameters.

However, engineers should not immediately dismiss the streamflow prediction from the TR-55 analysis for a variety of reasons. For instance the TR-55 analysis input parameters include hydrologic variables that require an experienced engineer to administer properly (very subjective). As a result the TR-55 streamflow prediction will differ from each person who administers this method. For instance one of the parameters involved in the TR-55 method is the SCS curve numbers. This is an important parameter since Table 2-23 displays that a 10% increase in the SCS curve number will increase the flow by 28%. The SCS curve number is dependent on the watershed's hydrologic soil group and land use. Soil hydrologic group is simple to determine from ArcView that has a shapefile that conveniently displays the soil type, which can be converted to the hydrological group. The land use is difficult to establish since the ArcView shapefiles define the land use cover types as either agricultural, conservation, or urban. To obtain an exact curve number, an extensive land use survey with aerial photographs is required, which is beyond the extent of this research project. Therefore for this project all agricultural land was defined as straight row crops in poor condition, conservation land was defined as woods in good condition, and urban districts were defined as ¼ acre residential area.

However, with sufficient information (very difficult), an experienced engineer would be able to make more accurate predictions using the TR-55 method.

The other methods mentioned in this chapter are the rational method and the City and County of Honolulu Method. These two methods are quick techniques to obtain the streamflow and require little hydrologic knowledge. According to the HDOT, these methods should only be used to check the results from the SCS and USGS regression methods. The rational method should be used for small watersheds (less than 100 acres) and the accuracy decreases as the watershed drainage area increases. The results of the rational method in Table 2-27 do not compare well to the Log Pearson III results in Table 2-31. From the results the rational method underestimates the actual flow, which may be dangerous if one relies solely on this analysis for an ungaged drainage area. Since the watershed analyzed in this chapter are over 100 acres the City and County of Honolulu suggest using Plate 6 in the Rules Relating to Storm Drainage Standard. When comparing the City and County of Honolulu Method in Table 2-28 to the Log Pearson Results in Table 2-31, the 100-year streamflow data compare favorably. This method is similar to the USGS regression equations where Oahu is split into hydrologic areas and that the curve (equation) is based on Log-Pearson III results of existing streamflow records. The City and County of Honolulu Method only uses drainage area as an input parameter while the regression equation require more hydrological input parameters such as median rainfall, 2-year 24-hour rainfall, and drainage area. Although this method is quicker to use than the regression equations, the disadvantage is that a large watershed with low rainfall totals such as Waikele will have overestimated flows. Fortunately for Oahu there are not many watersheds with the size of Waikele hence this method is a quick way to check the TR-55 analysis of an ungaged watershed.

### 2.2.9 Prediction for 500-Year Flood Flow

In FHWA Technical Advisory T5140.23 "Evaluating Scour at Bridges", it states that existing bridges must be analyzed for the risk of failure from scour during both 100-year and 500-year flood flows. Since in most cases, there are no streamflow records that are 500 years long, the FHWA advises that a factor of 1.7 be applied to the 100-year flood flow to predict the 500-year flood flow. However, thus far, the validity of this factor for application in Hawaii has not been examined or established. In this section, the Log-Pearson analysis of the nine streams with flow records was extended past 100 years to obtain the predicted flow rate for 500 years. The 500-year flow rate result was then divided by the 100-year data and the resulting ratio was compared with the FHWA- recommended 1.7 adjustment factor (Table 2-32). From the results, the 1.7 adjustment factor seems to be the upper limit for the ratio between the 500-year and the 100-year flood flows in Hawaii. Therefore the 1.7 adjustment factor will give a conservative estimate of the 500-year flood in Hawaii.

**Table 2-32:** 500-year flood flow

| Stream Name | 100-Year Storm (cfs) | 500-Year Storm (cfs) | Ratio | % Diff |
|---|---|---|---|---|
| Kalihi | 9054 | 13166 | 1.45 | 14.46% |
| Kaluanui | 3223 | 4277 | 1.33 | 21.94% |
| Makaha | 2415 | 3692 | 1.53 | 10.07% |
| Opaeula | 5755 | 7405 | 1.29 | 24.31% |
| Punaluu | 6512 | 8510 | 1.31 | 23.13% |
| Waiakeakua | 2859 | 4889 | 1.71 | 0.59% |
| Waiawa | 32935 | 40742 | 1.24 | 27.23% |
| Waikane | 10761 | 14011 | 1.30 | 23.41% |
| Waikele | 20632 | 30839 | 1.49 | 12.08% |

This method of determining the 500-year flood flow is unreliable since the streamflow records for the selected watersheds range between 33 and 82 years as compared to 500 years. The Log-Pearson III method is acceptable for estimating the 100-year flood flow but the more curve is extended (from 100-years to 500-years) the less accurate the results become. Since there are no measured streamflow records for a 500-year time frame, this remains one of the alternative methods to predict the 500-year flood flow. Many government agencies such as the Federal Emergency Management Agency uses the Log Pearson III curve of the available streamflow records to predict the 500-year flood flow.

## 2.2 Discussions

In Chapter 2, the hydrology of Hawaii watersheds was analyzed first with the frequency analysis of selected rainfall and streamflow data. The rainfall analysis was compared to State of Hawaii Oahu rainfall maps from DLNR R-73 and little variation was found. However a large variation was found between the rainfall analysis and the rainfall maps from TP-43. The TP-43 consists of older rainfall maps using rainfall data up to the 1960's. DLNR R-73, published in 1984, is basically an updated version of TP-43 for Oahu that includes over 20-years worth of data per rain station in addition to the rainfall records used by TP-43. It should be noted that R-73 is only for Oahu and the neighbor islands rely on the older TP-43 for their drainage standards. The neighbor islands need to update the rainfall maps to provide proper drainage and ensure against any flooding.

The streamflow analysis was compared to three methods of obtaining the flood flow without the benefit of streamflow record. Of the 3 methods, the USGS Regression Equations matched the field data the closest. In addition the streamflow frequency analysis was extended

from a flood return period of 100-year to a flood return period of 500-years by using the Log-Pearson analysis. The 500-year flood flow was compared to the 100-year flood flow and the ratio was found to be 1.7 or less, thus confirming the nationwide assumption that the 500-year flood flow is equal to 1.7 times the 100-year flood flow.

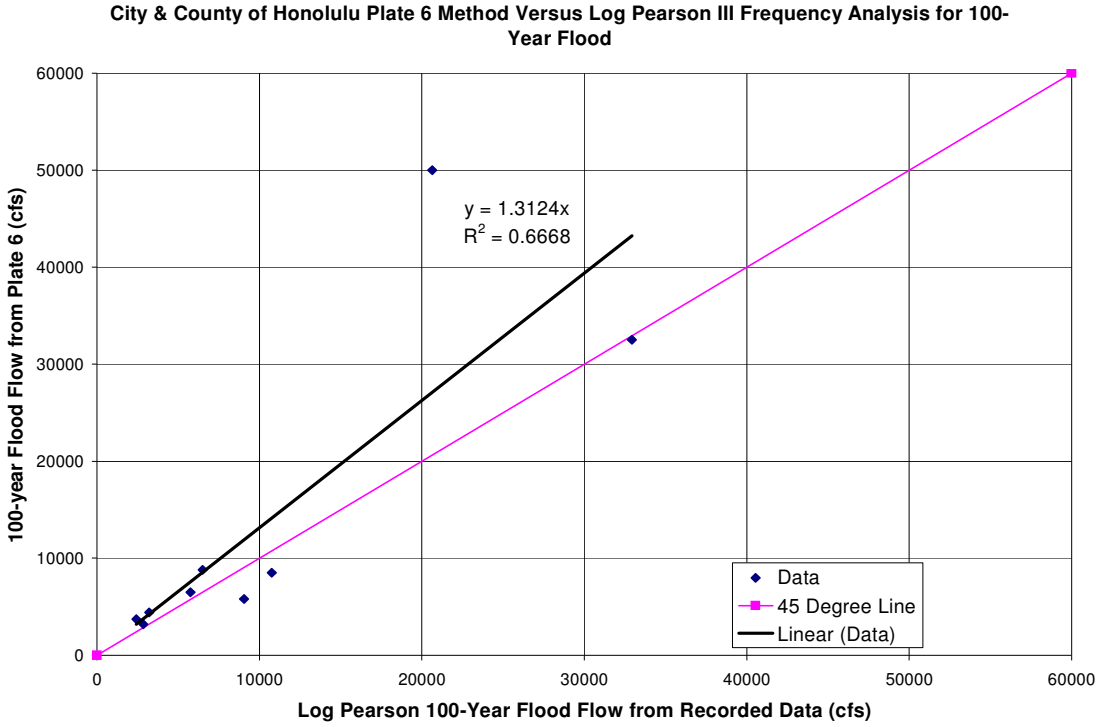


**Figure 2-10:** 100-year flood comparison between Plate 6 and Log Pearson

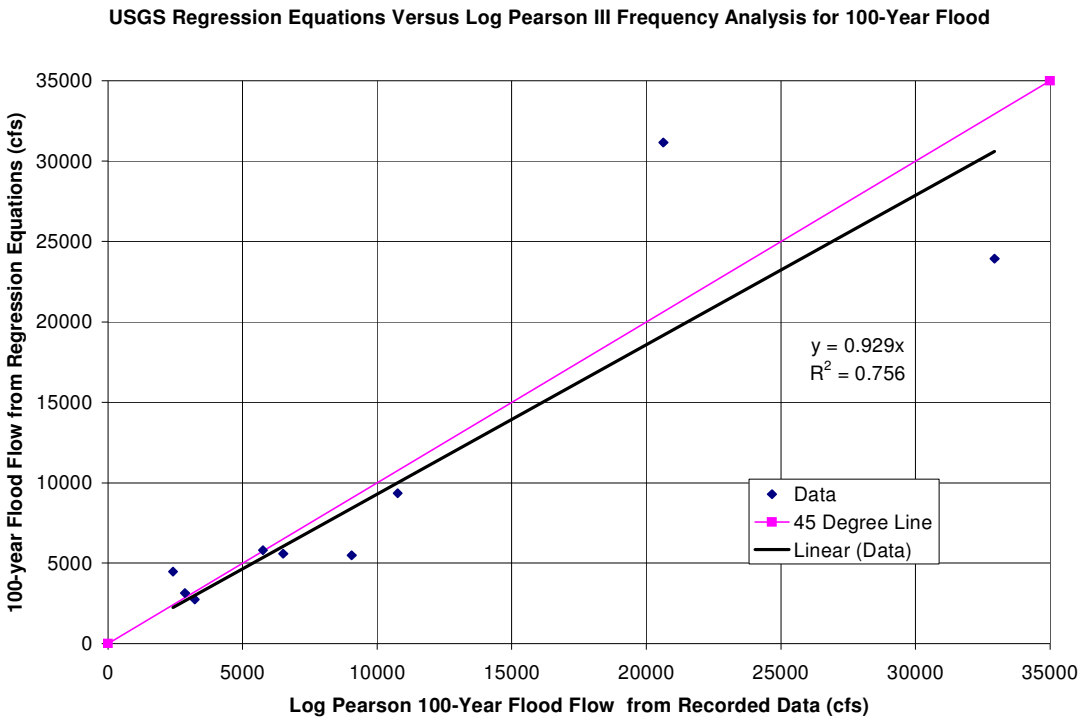


**Figure 2-11:** 100-year flood comparison between Regression and Log Pearson

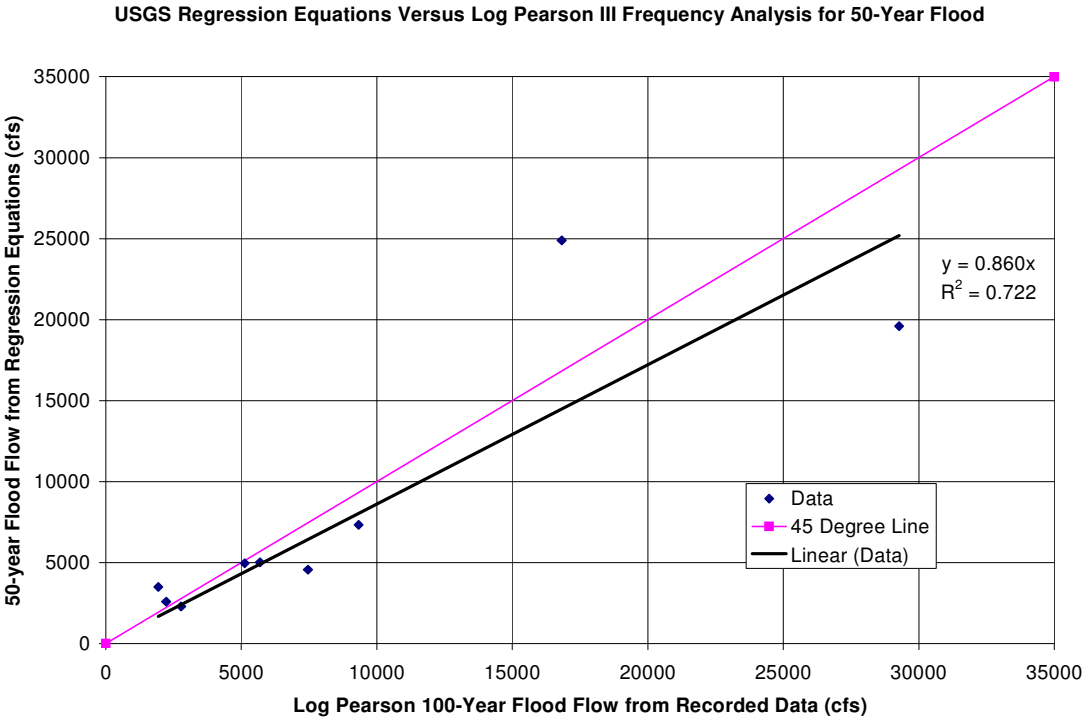


**Figure 2-12:** 50-year flood comparison between Regression and Log Pearson

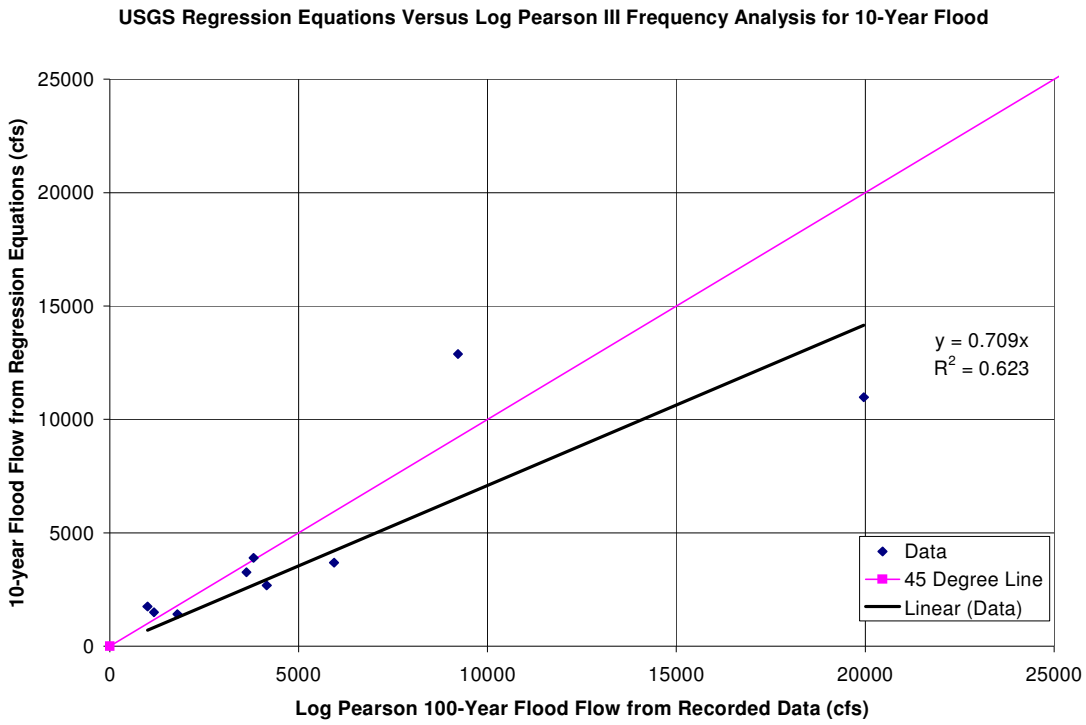


**Figure 2-13:** 10-year flood comparison between Regression and Log Pearson

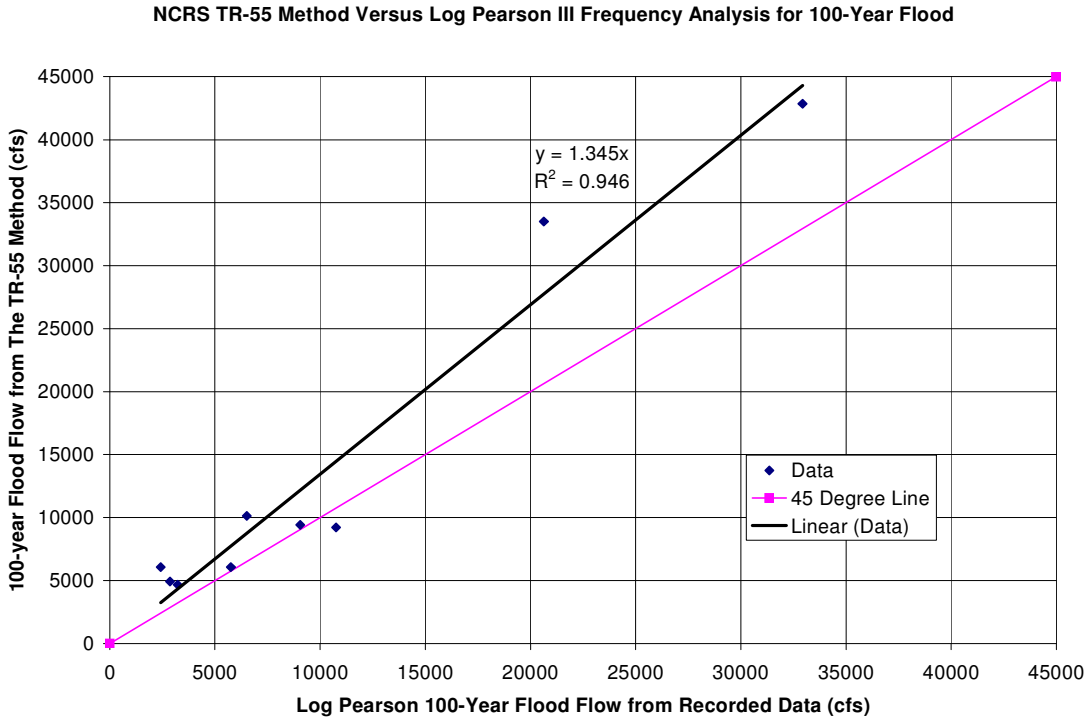


**Figure 2-14:** 100-year flood comparison between TR-55 and Log Pearson

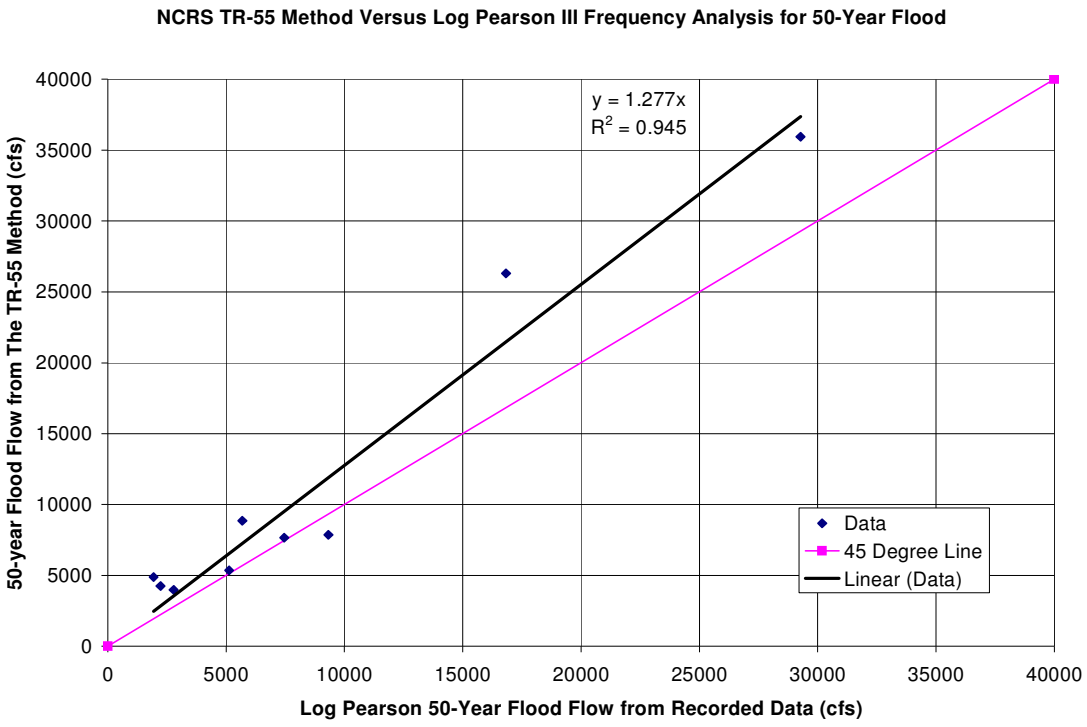


**Figure 2-15:** 50-year flood comparison between TR-55 and Log Pearson

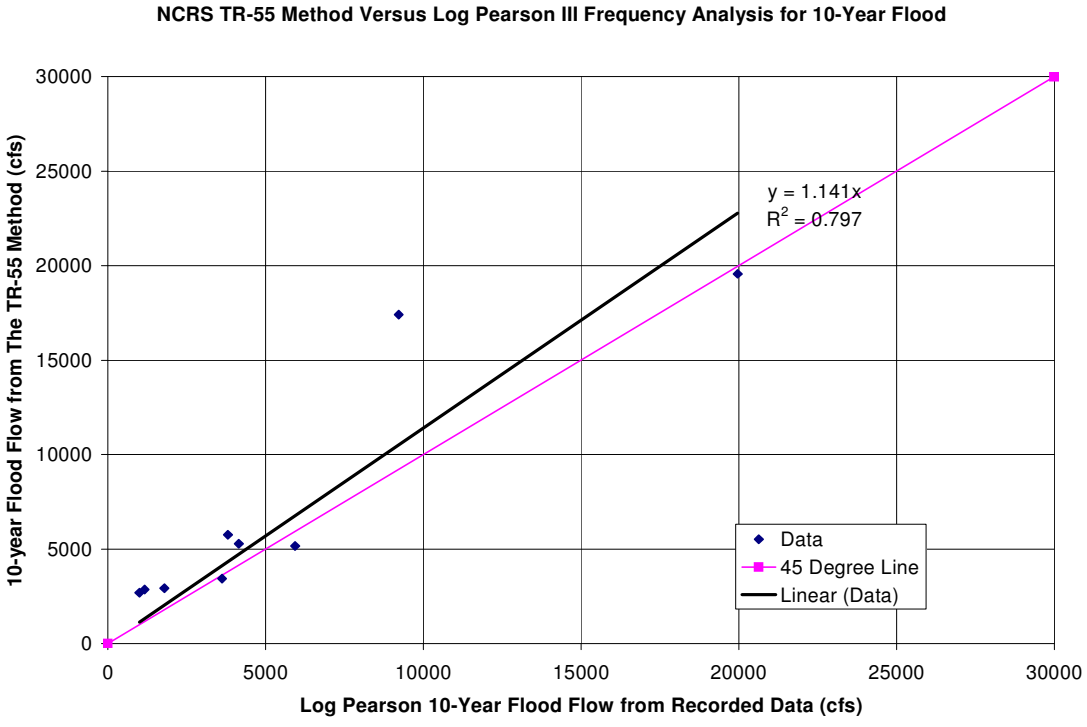


**Figure 2-16:** 10-year flood comparison between TR-55 and Log Pearson

# CHAPTER 3 BRIDGE SCOUR PREDICTION AND ANALYSIS

In this chapter the equations and methods for calculating the total depth of scour are described and applied to calculate the scour at two selected bridges on Oahu. One objective is to determine the susceptibility of existing bridges on Oahu to scour and to examine which type of scour is dominant. The results will reveal the effect of different hydraulic variables on the scour depth. The other objective is to validate the existing scour equations by comparing the predicted scour depth with the measured data during a storm at Kaelepulu Bridge.

## 3.1 Methodology

The methods for calculating the depth of scour are presented in this section beginning with the introduction of the scour equations developed in the FHWA Hydraulic Engineering Circular 18 (HEC-18) which includes the equations for contraction scour, local scour at the pier, and local scour at the abutment. This section concludes with the discussion of how the input parameters for the HEC-18 formulas are ascertained using the U.S. Army Corps of Engineers HEC-RAS computer software.

### 3.1.1 Critical Velocity Calculations

Before calculating the scour depth, the engineer must determine if the flow upstream of the bridge is transporting sediment. This is necessary to verify if the scour is under clear-water versus live-bed conditions. The velocity that transports the sediment of a particular diameter size D is called the critical velocity $V_c$. Laursen derived this formula in 1963 based on the clear water contraction scour equation and is given by the equation below.

$$V_C = K_U y^{1/6} D^{1/3} \quad (3\text{-}1)$$

where:

$V_C$ = Critical velocity above which bed material of size D and smaller will be transported, m/s (ft/s)

y = Average depth of flow upstream of bridge, m (ft)

D = Particle size for $V_c$, m (ft)

$K_U$ = 6.19 S.I. units

11.17 English units

### 3.1.2 Live-Bed Contraction Scour

The narrowing of the flow area that increases the water velocity causes contraction scour. The addition of a bridge to a stream usually narrows the flow area and therefore causes contraction scour at the bridge (Figures 3-1 and 3-2). There are two types of contraction scour, live-bed and clear-water.

If the velocity upstream of the bridge is greater than the critical velocity for particle size $D_{50}$ (particle size in a mixture of which 50% is finer), then the scour can be described as live-bed contraction scour. Live-bed contraction occurs when there is sediment in the flow upstream into the bridge section. The scour will increase under live-bed conditions until there is equilibrium in the sediment transported in and out of the bridge section. The depth of scour under live-bed conditions was developed by Laursen in 1960 and is given below:

$$\frac{Y_2}{Y_1} = \left(\frac{Q_2}{Q_1}\right)^{(6/7)} \left(\frac{W_1}{W_2}\right)^{K1} \quad (3\text{-}2)$$

$$Y_S = Y_2 - Y_0 \quad (3\text{-}3)$$

where:

$Y_1$ = Average depth in the upstream main channel, m (ft)

$Y_2$ = Average depth in the contracted section, m (ft)

$Y_0$ = Existing depth in the contracted section before scour, m (ft)

$Q_1$ = Flow in upstream channel transporting sediment, $m^3/s$ ($ft^3/s$)

$Q_2$ = Flow in contracted channel, $m^3/s$ ($ft^3/s$)

$W_1$ = Bottom width of the upstream main channel, m (ft)

$W_2$ = Bottom width of the main channel in the contracted section less pier width, m (ft)

$K_1$ = Exponent determined in the table below

$Y_s$ = Scour depth, m (ft)

**Table 3-1:** Live-bed contraction scour $K_1$ exponent (Richardson et al., 2001)

| $V_S/\omega$ | $K_1$ | Mode of Bed Material Transport |
|---|---|---|
| <0.50 | 0.59 | Mostly contact bed material discharge |
| 0.50 to 2.0 | 0.64 | Some suspended bed material discharge |
| >2.0 | 0.69 | Mostly suspended bed material discharge |

$V_S$ = $(\tau_O/\rho)^{1/2} = (gY_1S_1)^{1/2}$, shear velocity in the upstream section, m/s (ft/s)

$\omega$ = Fall velocity of bed material based on $D_{50}$, m/s (ft/s)

g = Acceleration of gravity, $9.81 m/s^2$ ($32.2 ft/s^2$)

$S_1$ = Slope of energy grade line of main channel, m/m (ft/ft)

$\tau_O$ = Shear stress on the streambed, $N/m^2$ ($lb/ft^2$)

$\rho$ = Density of water, $1000 kg/m^3$ ($1.94 slugs/ft^3$)

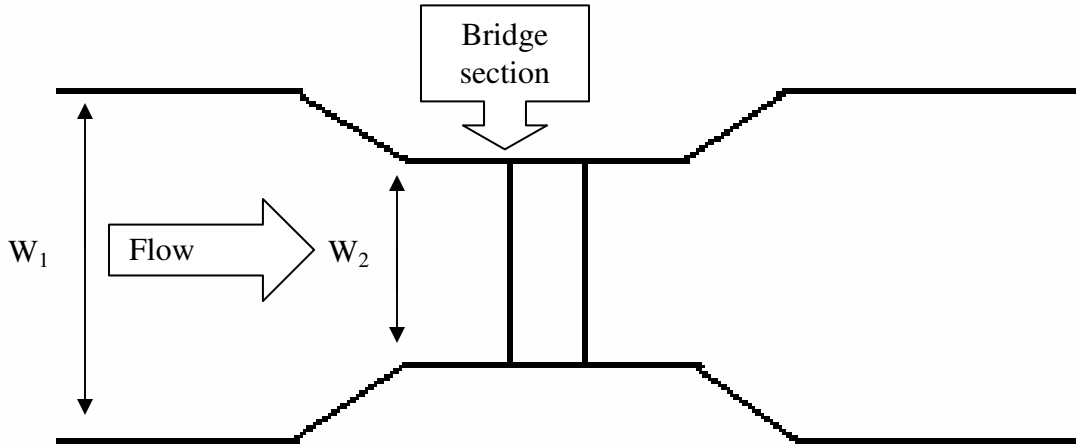


**Figure 3-1:** Bridge over contracted area of the river

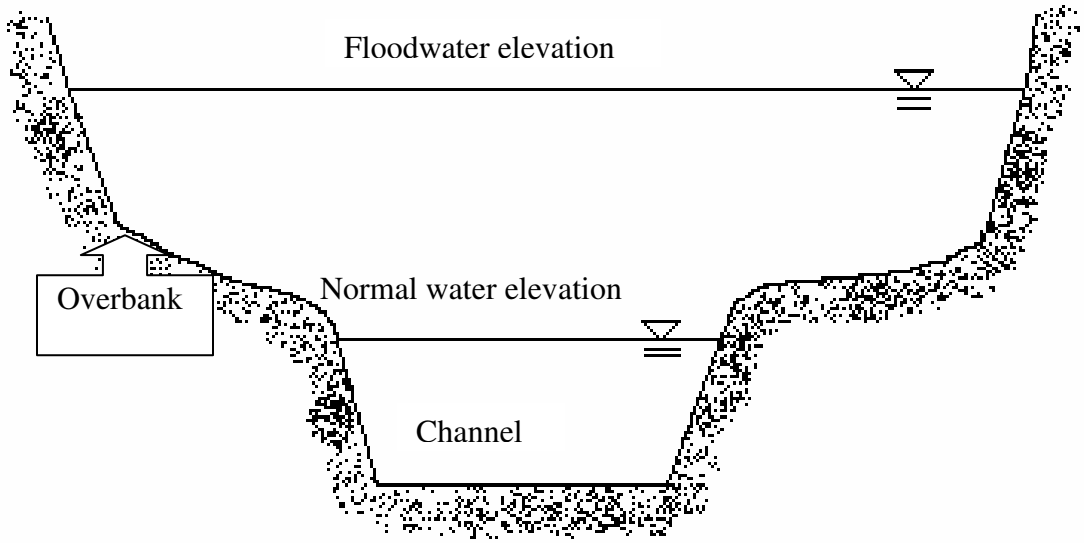


**Figure 3-2:** Cross-section of a river

### 3.1.3 Clear-Water Contraction Scour

If the velocity upstream of the bridge is less than the critical velocity for $D_{50}$ then the scour can be described as clear water contraction scour. In other words, there is no bed material transport from the upstream reach into the downstream reach, or the material being transported in the upstream reach is transported through the downstream reach mostly in suspension and at less than capacity of the flow (Richardson et al., 2001, Arneson et al 2012)). The scour depth reaches equilibrium, when the average bed shear stress is less than that required for incipient motion of the bed material. The equation for scour depth under clear-water conditions (Laursen 1963) is given below:

$$Y_2 = \left( \frac{Q^2 K_U}{D_M{}^{2/3} W^2} \right)^{(3/7)} \tag{3-4}$$

$$Y_S = Y_2 - Y_0 \tag{3-5}$$

where:

$Y_2$ = Average depth of contracted section after contraction scour, m (ft)

Q = Discharge through the bridge or on the overbank at the bridge associated with the width W, $m^3/s$ ($ft^3/s$)

$D_M$ = Diameter of the smallest non-transportable particle in the bed material ($1.25D_{50}$) in the contracted section, m (ft)

$D_{50}$ = Particle size in a mixture of which 50 percent are smaller, m (ft)

W = Bottom width of the contracted section less pier widths, m (ft)

$Y_0$ = Existing depth in the contracted section before scour, m (ft)

$Y_s$ = Scour depth, m (ft)

$K_U$ = 0.025 S.I. units

0.0077 English units

### 3.1.4 Local Scour at Piers

Local scour is due to a different mechanism from contraction scour. Local scour is usually caused by the vortex generated by the backup and acceleration of water upstream from the bridge pier. For estimating maximum local scour at bridge piers, the CSU (Colorado State University) equation is used. Hydraulic Engineering Circular 18 recommends that the CSU equation be used for both clear-water and live-bed scour conditions. The specific equation is given as follows:

$$\frac{Y_S}{Y_1} = 2.0 K_1 K_2 K_3 K_4 \left(\frac{a}{Y_1}\right)^{0.65} Fr_1^{0.43} \qquad (3\text{-}6)$$

where:

$Y_S$ = Scour depth, m (ft)

$Y_1$ = Flow depth directly upstream of the pier, m (ft)

$K_1$ = Correction factor for pier nose shape (Table 3-2)

$K_2$ = Correction factor for angle of flow attack (Table 3-3)

= $(\text{Cos } \theta + L/a \text{ Sin } \theta)^{0.65}$ where if $L/a > 12$ then $L/a = 12$.

$\theta$ = Skew angle of flow

For $\theta > 5^O$ $K_1 = 1.0$

$K_3$ = Correction factor for bed condition (Table 3-4)

a = Pier width, m (ft) (Figure 3-3)

L = Length of pier, m (ft)

$Fr_1$ = Froude number directly upstream of the pier = $V_1/(gY_1)^{1/2}$

$V_1$ = Mean velocity directly upstream of the pier, m/s (ft/s)

g = Acceleration of gravity, 9.81m/s$^2$ (32.2 ft/s$^2$)

$K_4$ = Correction factor for armoring of bed material size

= 1 if $D_{50} < 2$mm or $D_{95} < 20$mm

Minimum $K_4$ factor is 0.4

$$K_4 = 0.4(V_R)^{0.15} \tag{3-7}$$

$$V_R = \frac{V_1 - V_{icD50}}{V_{cD50} - V_{icD95}} > 0 \tag{3-8}$$

$$V_{icDx} = 0.645(\frac{D_x}{a})^{0.053} V_{cDx} \tag{3-9}$$

$$V_{cDx} = K_u y_1 D_x^{1/3} \tag{3-10}$$

where:

$V_{icDx}$= approach velocity (m/s or ft/sec) required to initiate scour at the pier for the grain size Dx (m or ft)

$V_{cDx}$= critical velocity (m/s or ft/s) for incipient motion for the grain size Dx (m or ft)

$y_1$ = Depth of flow just upstream of the pier, excluding local scour, m (ft)

$V_1$ = Velocity of the approach flow just upstream of the pier, m/s (ft/s)

$D_x$ = Grain size for which x percent of the bed material is finer, m (ft)

$K_u$ = 6.19 SI Units

$K_u$ = 11.17 English Units

**Table 3-2:** Pier scour $K_1$ factor for pier nose shape (Richardson et al., 2001)

| Shape of Pier Nose | $K_1$ |
|---|---|
| Square Nose | 1.1 |
| Round Nose | 1.0 |
| Circular Cylinders | 1.0 |
| Group of Cylinders | 1.0 |
| Sharp Nose | 0.9 |

**Table 3-3:** Pier scour $K_2$ factor for angle of attack of flow (Richardson et al., 2001)

| θ | L/a = 4 | L/a =8 | L/a =12 |
|---|---|---|---|
| 0 | 1.0 | 1.0 | 1.0 |
| 15 | 1.5 | 2.0 | 2.5 |
| 30 | 2.0 | 2.75 | 3.5 |
| 45 | 2.3 | 3.3 | 4.3 |
| 90 | 2.5 | 3.9 | 5.0 |

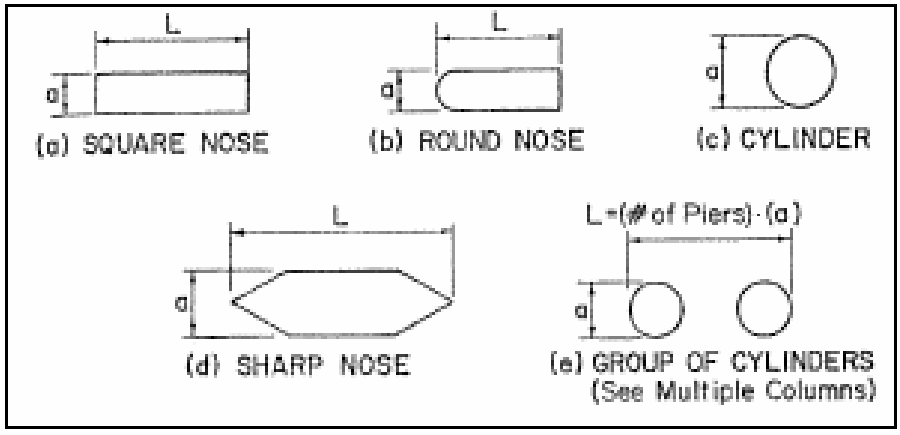


**Figure 3-3:** Common pier shapes (Richardson et al., 2001)

**Table 3-4:** Pier scour $K_3$ factor for bed condition (Richardson et al., 2001)

| Bed Condition | Dune Height, m | $K_3$ |
|---|---|---|
| Clear-Water Scour | N/A | 1.1 |
| Plane bed and Antidune flow | N/A | 1.1 |
| Small Dunes | $3 > H \geq 0.6$ | 1.1 |
| Medium Dunes | $9 > H \geq 3$ | 1.2 to 1.1 |
| Large Dunes | $H \geq 9$ | 1.3 |

### 3.1.5 Local Scour at Abutments

The final scour equation is Froehlich's 1989 equation for live-bed local scour at the abutments. Researchers believe that clear water scour equations underestimate scour at the abutment. Since there are insufficient field data, HEC-18 recommends that Froehlich's equation be also used for clear-water conditions to be on the safe side. Froehlich's equation for predicting local abutment scour is given as:

$$\frac{Y_S}{Y_A} = 2.27 K_1 K_2 \left( \frac{L'}{Y_A} \right)^{0.43} Fr^{0.61} + 1 \qquad (3\text{-}11)$$

where:

$K_1$ = Coefficient for the abutment shape (Table 3-5 and Figure 3-4)

$K_2$ = Coefficient for angle of embankment to flow, $(\theta/90)^{0.13}$ (Figure 3-5)

= $\theta < 90^o$ if embankment points downstream

= $\theta > 90^o$ if embankment points upstream

$L'$ = Length of active flow obstructed by the embankment, m (ft)

Fr = Froude Number of flow upstream of the abutment, $V_E/(gY_A)^{1/2}$

g = Acceleration of gravity, 9.81m/s$^2$ (32.2 ft/s$^2$)

$V_E$ = $Q_E/A_E$, m/s (ft/s)

$Q_E$ = Flow obstructed by the abutment and approach embankment, m$^3$/s (ft$^3$/s)

$A_E$ = Flow area if the approach cross-section obstructed by the embankment, m$^2$ (ft$^2$)

L = Length of embankment projected normal to flow, m (ft)

$Y_A$ = Average depth of flow on the floodplain, m (ft)

$Y_S$ = Scour depth, m (ft)

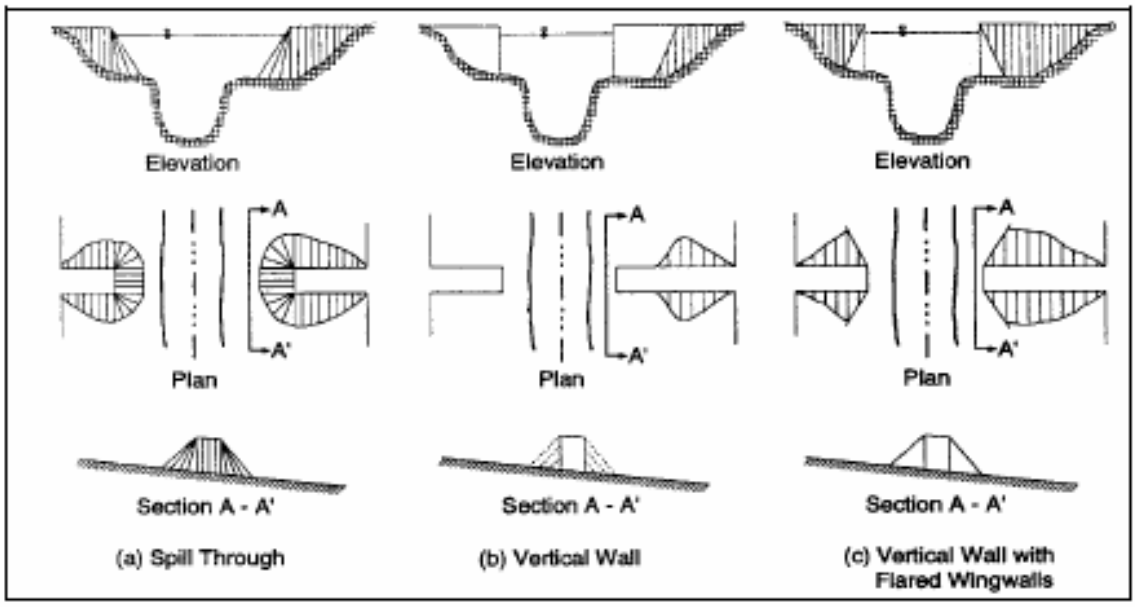


**Figure 3-4:** Abutment shapes (Richardson et al., 2001)

**Table 3-5:** Abutment shape coefficient (Richardson et al., 2001)

| Description | $K_1$ |
|---|---|
| Vertical-wall abutment | 1.00 |
| Vertical-wall abutment with wing walls | 0.82 |
| Spill-through abutment | 0.55 |

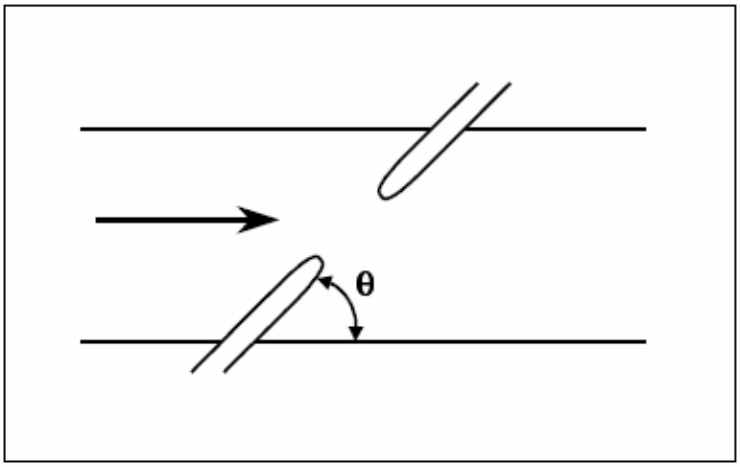


**Figure 3-5:** Orientation of embankment angle, θ, to the flow (Richardson et al., 2001)

### 3.1.6 HEC-RAS

The U.S. Army Corps of Engineers Hydraulic Engineering Center's River Analysis System (HEC-RAS) is a computer program that models river flows based on one-dimensional continuity and energy equations to determine water surface profiles for both steady and unsteady flows. HEC-RAS can handle a full range of river reaches and hydraulic structures such as bridges, culverts, and weirs. The program has a graphical interface to input the data and to display the results, making the program user friendly. HEC-RAS is used in this chapter to model the flow through a bridge and determine the hydraulic parameters needed for the HEC-18 scour calculations such as $Y_1$ (flow depth directly upstream of the pier for local pier scour).

To determine bridge scour through HEC-RAS, the user must first input geometric data and boundary conditions in order to perform a steady flow simulation. The geometric data is the outline of the stream system including the length of the reaches, the cross-sectional geometry of the stream, and any hydraulic structure data (such as bridge and culvert cross-sections). The outline of the stream system can be obtained by studying USGS quadrangle maps or digital elevation maps of the area (section 2.2.5). The stream cross-section and hydraulic structure data are from bridge blue prints available from the State Department of Transportation Design Branch in Kapolei or the City and County of Honolulu first floor of the Municipal Building. For accurate results the user should include several stream cross-sections both upstream (to evaluate the long term effects of the bridge on the water surface profile upstream) and downstream (such that any user-defined downstream boundary condition does not affect the hydraulic results inside and just upstream of the bridge) from the bridge (USACOE, 1998).

Boundary conditions are needed to establish the starting water surface at one particular location, which is required by HEC-RAS to begin the steady flow simulation. The user must

input any flow change locations and the corresponding flow rates. The flow rates can be determined from FEMA FIS (Federal Emergency Management Agency Flood Insurance Study), and for scour calculations the design flow rates are associated with return periods of 100 and 500 years. The user must also input the water surface elevation for each of the flow change locations. The water surface elevations are available from the FEMA FIRM (Flood Insurance Rate Maps) and FEMA FIS, both of which can purchased from the FEMA Flood Map Store Website at http://store.msc.fema.gov/.

The next step is to perform the steady flow simulation using the flow distribution option. This option allows the user to specify the locations where the program will calculate flow distributions. With this option the user can divide the cross-section into subsections so the flow can be calculated for the left and right overbanks in addition to the main channel. As a result the user can obtain additional hydraulic information so a complete mapping of the scour across the cross section can be obtained. The user should request the flow distribution output for the cross-section at the bridge, just upstream of the bridge, and far upstream of the bridge.

After running the steady flow simulation HEC-RAS will have computed all the hydraulic variables needed to compute scour. HEC-RAS has a convenient window, called the Hydraulic Design Function Window, which lists the hydraulic variables automatically after performing the steady simulation. The user only needs to enter which scour equations HEC-RAS should use and some of the non-hydraulic variables such as $D_{50}$, skew angle, and the correction factors (Table 3-6). After inputting these variables HEC-RAS will compute the different types of scour (contraction, pier, and abutment) and present the total scour with a graphical picture of the bridge cross-section depicting the scour results. More information including additional documentation,

tutorials and free software, can be found at the U.S. Army Corps of Engineers Hydraulic Engineering Center's Website at http://www.hec.usace.army.mil/.

**Table 3-6:** Flow chart of HEC-RAS input parameters

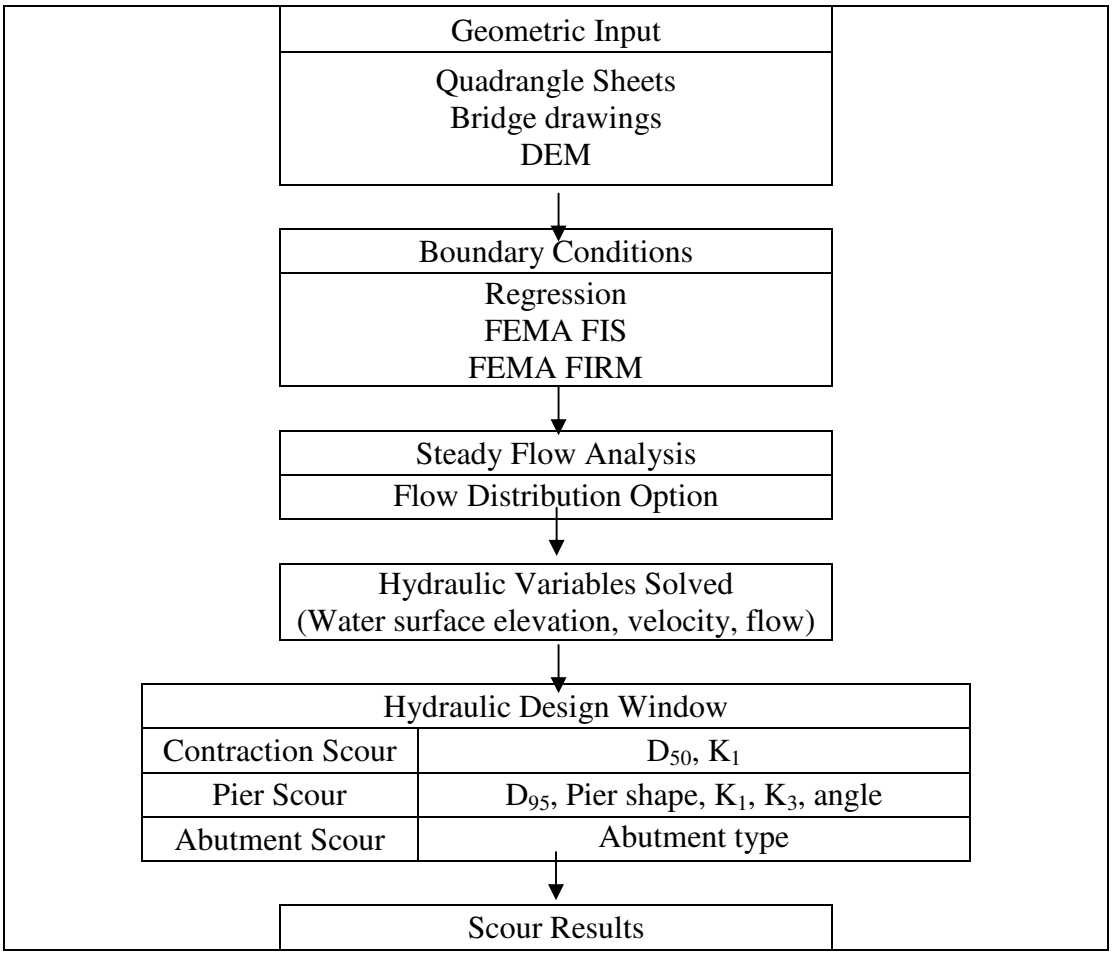

## 3.2 Prediction of Scour Depth for Selected Bridges on Oahu


**Figure 3-6:** Locations of bridges studied

The objective of this section is to analyze two bridges for maximum scour depth during a 100-year flood event using HEC-RAS. This section will also perform a sensitivity analysis of HEC-RAS input parameters in order to examine how the parameters affect the total depth of scour on the two bridges. The two bridges evaluated in this study are Kaelepulu Bridge and Kahaluu Bridge (Figure 3-6), which are both located on the windward coast of Oahu. These bridges were chosen because they are located in flood prone areas and they are currently monitored with scour sensors (Chapter 4) in this project. The active sonar scour tracker was installed on Kahaluu Bridge while the sliding magnetic collar scour tracker was installed at Kaelepulu Bridge.

### 3.2.1 Kaelepulu Bridge

Kaelepulu Bridge is located at Kailua Beach Park on Kawailoa Road in Kailua, Hawaii. The bridge spans over Kaelepulu Stream, which runs from Kaelepulu Pond (Enchanted Lakes) and drains into Kailua Bay. The reinforced concrete bridge is approximately 200 feet long and supported on nine reinforced concrete piers. The bridge is maintained and managed by the City and County of Honolulu Department of Facilities Maintenance. This bridge was chosen since it is located in a populous area and experienced both flood and serious sand plugging problems. Several times during the year the sand plugging prevents water in Kaelepulu Stream from reaching the ocean and requires city maintenance crews to routinely dredge the stream opening. This presents a problem since heavy rains might cause the overtopping of Kaelepulu Bridge and flooding the area around the bridge. Figure 3-7 shows a picture of Kaelepulu Bridge.

**Figure 3-7:** Kaelepulu Bridge

### 3.2.1.1 Input Parameters

The geometric input parameters for Kaelepulu Bridge were obtained from highway maps dated 1960 from the City and County of Honolulu, on-site investigations in the present study, topographic maps, and FEMA FIS. Unfortunately the 1960 plans are for the extension of Kaelepulu Bridge rather than the original bridge. The plans for the original bridge are very old, difficult to read, and the City and County of Honolulu only has the original bridge plans on microfilm not on vellum or any other media that can be reproduced by a blue print company.

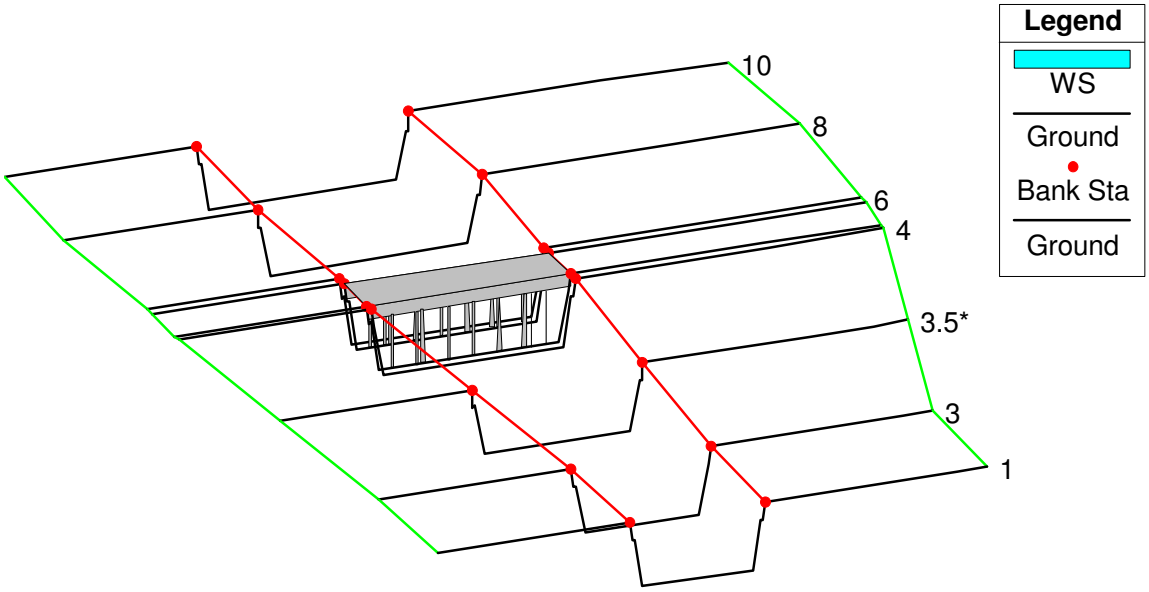


**Figure 3-8:** Kaelepulu Bridge geometric input in HEC-RAS

Site investigations revealed that the north and south abutments of the bridge does not protrude into the flow path, thus abutment scour will not be a factor. The upstream and downstream cross sections were determined from USGS 7.5-minute topographic maps (1:24,000 metric scale or 1 centimeter = 0.25 kilometers) and FEMA FIS. Seven cross-sections were used (Figure 3-8), the first is 188 ft upstream of the bridge (cross-section 10), the second 97 ft

upstream of the bridge (cross-section 8), the third 3 ft upstream of the bridge (cross-section 6), the forth 3 ft downstream of the bridge (cross-section 4), another 111.5 ft downstream of the bridge (cross-section 3.5*), the next 220 ft downstream of the bridge (cross-section 3), and the last 294 ft downstream of the bridge (cross-section 1).

The next step in the analysis is to specify the 100-year flow and the required boundary condition for the HEC-RAS analysis. The boundary condition needed is the water surface elevation under a particular flow rate at the farthest downstream cross-section (Figure 3-8 cross-section 1). Data on this boundary condition were found from the rating curves in the FEMA FIRM maps. A rating curve is a function of water surface elevation (stage) versus flow rate, which can be developed by a USGS stream gage station. Unfortunately the stream gages for both bridges are miles upstream from the location of the bridge. Therefore the boundary condition of the water surface elevation versus flow rate at the downstream section of the bridge needs to be determined though proper routing. Since this analysis has been done by FEMA, this project directly adopts the result of the 100-year flow and the water surface elevation from the FEMA study.

From the FEMA FIRM (Masaki 2004, Appendix F Figure F-1) the water surface elevation during a 100-year flood is about 2 ft (from Mean Sea Level) at the bridge (to obtain a water surface elevation of 2 ft at the bridge, the water surface elevation at station 1 was adjusted through trial and error until HEC-RAS analysis showed a water surface elevation of 2 ft at the bridge). Figure G-2 in Masaki 2004 presents the FEMA FIS flow curve for Kaelepulu Stream, which is about 10800 cfs. The 100-year flow was developed using updated data from a previous flood insurance study from the Federal Insurance Administration Report “Kailua Flood Insurance Study (Type 10)” dated 1971.

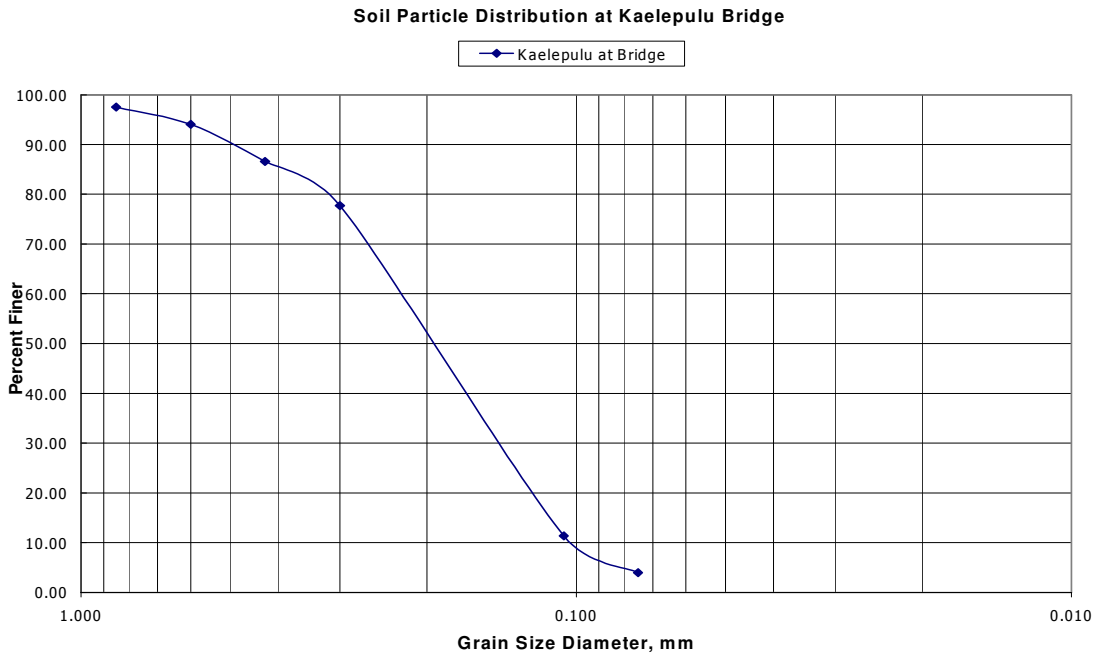


**Figure 3-9:** Kaelepulu Bridge streambed gradation curve

After the HEC-RAS analysis was performed, the scour input variables were entered in the HEC-RAS Hydraulic Design Data Window. The parameters for contraction scour are grain size diameter $D_{50}$ and the contraction scour constant $K_1$. In the present study, grain size diameter $D_{50}$ was tested from soil samples taken from the streambed surface using particle size sieve analysis (ASTM D422) and found to be 0.19 mm (Figure 3-9). Contraction scour constant $K_1$ was automatically solved by the computer when $D_{50}$ was obtained. For local scour at piers the parameters needed were determined from the bridge plans and on-site investigations of the bridge, which include pier shape (pier scour constant $K_1$), pier width, pier length, angle of flow to the pier (pier scour constant $K_2$), bed condition (pier scour constant $K_3$), and grain size diameter $D_{95}$ (pier scour constant $K_4$).

Site investigations revealed that Kaelepulu Bridge is supported on two different types of piers with one being squared faced (supporting the bridge extension) and the other sharp-faced

piers (supporting the original bridge). The HEC-RAS analysis consisted of two parts, one where the entire bridge was assumed to have square piers and one where the entire bridge was assumed to have sharp piers. The square-faced piers ($K_1$=1.1) are 1 ft wide and 29 ft long that is aligned to the flow ($K_2$=1.0). The sharp-faced piers ($K_1$=0.9) are 3 ft wide and 33 ft long that is aligned 25 degrees to the flow ($K_2$=3.0). Local pier scour constants $K_1$ and $K_2$ differ because of pier geometry, while constants $K_2$ and $K_4$ are the same since they rely on bed material rather than pier geometry. The streambed was observed to have a slight aggradation problem with medium sand dunes beneath the bridge ($K_3$=1.1). Grain size diameter $D_{95}$ was found to be 0.50 mm ($K_4$=1.0). Here the surface particle size was used to obtain the most conservative estimate ($K_4$=1.0) as many practicing engineers currently do. Since the abutments do not appear to intrude into the flow area, no abutment parameters are required.

#### 3.2.1.2 Simulation Result

After the hydraulic variables were entered, the total depth of scour was calculated through HEC-RAS and a Hydraulic Design Data report was printed. Figure 3-10 shows the cross-sectional view of Kaelepulu Bridge during the HEC-RAS analysis of the 100-year flood flow obtained from FEMA FIS.

The cross-sectional scour plot of Kaelepulu Bridge (Figure 3-10) shows significant scour at the piers (Figure 3-10). Also below is an excerpt from the Hydraulic Design Data Report that shows the different types of scour. HEC-RAS calculated the scour at Kaelepulu Bridge to be 17.96 ft at the sharp-faced piers, 3.22 ft at the square-faced piers, and 2.60 ft of contraction scour across the width of the bridge streambed. This computes to a total scour of 20.56 ft at the sharp-

faced piers and 5.82 ft at the square-faced piers. From Figure 3-10, a 100-year flood will not overtop Kaelepulu Bridge under the conditions stated in Section 3.2.1.1.

Kaelepulu Bridge consists of two different pier formations, square piers at the end of the bridge and sharp-faced piers at the middle. The square piers, built during the extension of the original bridge, are aligned to the flow and have total scour of 5.82 ft under a 100-year flood. The bridge plans show two different foundation designs for the square piers, one on spread footings 5 ft below the streambed and the other on piles that extend 16 ft below the streambed. Engineers must do a foundation study to determine the foundation type below the square-face pier since the undermining of the foundation will occur if pier is supported on a spread footing. The sharp-faced pier is aligned 25 degrees to the flow and HEC-RAS calculated the total scour at the piers to be 20.56 ft. The sharp-faced piers are in danger of undermining since the bridge plans show the pier on spread footings where the bottom sits 1 to 5 ft below the streambed. Engineers must install scour countermeasures before a serious flood undermines the bridge foundations and collapse the bridge. Kaelepulu Bridge also suffers from a serious aggradation problem where the streambed needs to be dredged several times during the year.

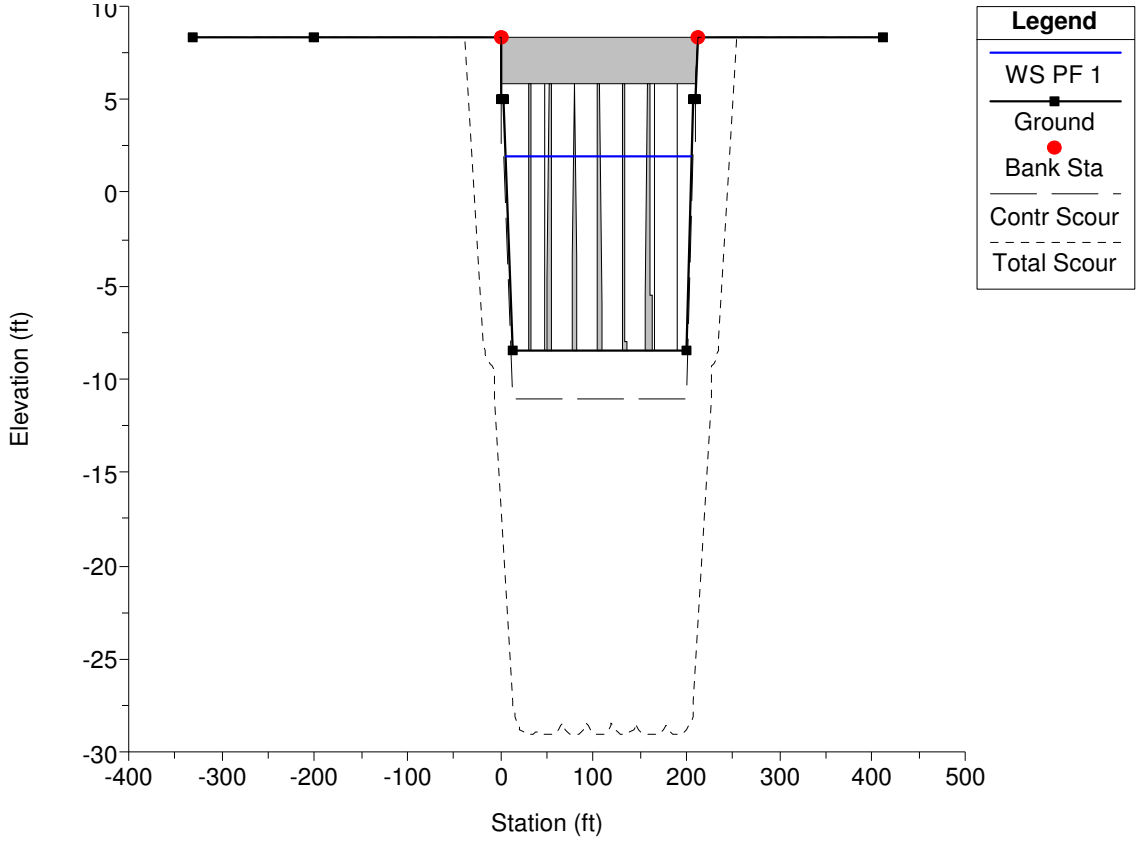


**Figure 3-10:** Cross-section of Kaelepulu Bridge (sharp-faced piers) during 100-year flood

```
Hydraulic Design Data
Contraction Scour
     Scour Depth Ys (ft):                2.60
     Critical Velocity (ft/s):           1.38
     Equation:                           Live

Pier Scour (Sharp Piers)
     All piers have the same scour depth
     Scour Depth Ys (ft):                17.96
     Equation:                           CSU equation

Pier Scour (Square Piers)
     All piers have the same scour depth
     Scour Depth Ys (ft):                3.22
     Equation:                           CSU equation

Combined Scour Depths
```

```
Pier Scour + Contraction Scour (ft): (Sharp Piers)
     Channel:       20.56

Pier Scour + Contraction Scour (ft): (Square Piers)
     Channel:       5.82
```

#### 3.2.1.3 Error Analysis

Possible sources of errors include that the streambed elevation estimated in FEMA FIS is at -8.5 ft MSL throughout stream reach. Realistically Kaelepulu Bridge suffers from a serious aggradation problem where on-site investigations revealed that the streambed elevation is at about mean sea level near the center of the bridge. FEMA FIS displayed a water surface elevation of 2 ft MSL, thus a water depth of 10.5 ft at the bridge during a 100-year flood. Assuming the streambed elevation at 0 ft, the water surface elevation during a 100-year flood would be 10.5 ft MSL. With the bridge deck elevation at 8.57 ft, the bridge will be over-topped and significant flooding will occur. If adjustments are made to the streambed elevations (running HEC-RAS with the streambed at 0 ft rather than –10.5 ft MSL) then the FEMA FIRM water surface elevation and flow rates can not be used since they were made specifically for the condition that the streambed elevation is at –8.5 ft.

In addition the Kailua abutment is covered by sand. Site investigations revealed that the condition of the sand plugging near the Kailua abutment is very severe since the two square pier groups are not visible. Due to the sand plugging problem and dredging, it is difficult to describe a constant cross-sectional profile accurately, and therefore there are significant errors in the scour prediction as averaged cross-sectional profiles were used.

Furthermore when GEOLABS installed the sliding magnetic collar at Kaelepulu Bridge, they had to drill through the streambed. After the installation the drill crew bought out the drill

and displayed hard coral rocks beneath the sand layer that was collected in the drill shaft (Figure 3-18). The HEC-RAS analysis does not take the coral rock layer into account that varies between a few feet and 7 ft below the streambed. With the coral rock, the bridge would not experience the 20.56 ft of scour at the sharp-faced piers calculated by HEC-RAS.

Figure 3-10 displays a large magnitude of local scour at the abutments, but field studies show that the abutment does not protrude into the flow area and therefore local scour at the abutment does not exist. The abutment scour computed in HEC-RAS is an error and this result shows that field studies of the bridges must be performed in order to rule out some forms of erroneous scour. If perhaps the abutment did protrude into the flow area, the abutments are armored with concrete that can resist the flood flow. Currently HEC-RAS is based on the FHWA HEC-18 equations, which do not take into account the property of different streambed material near the abutments. It only considers the abutment geometry and flow conditions.

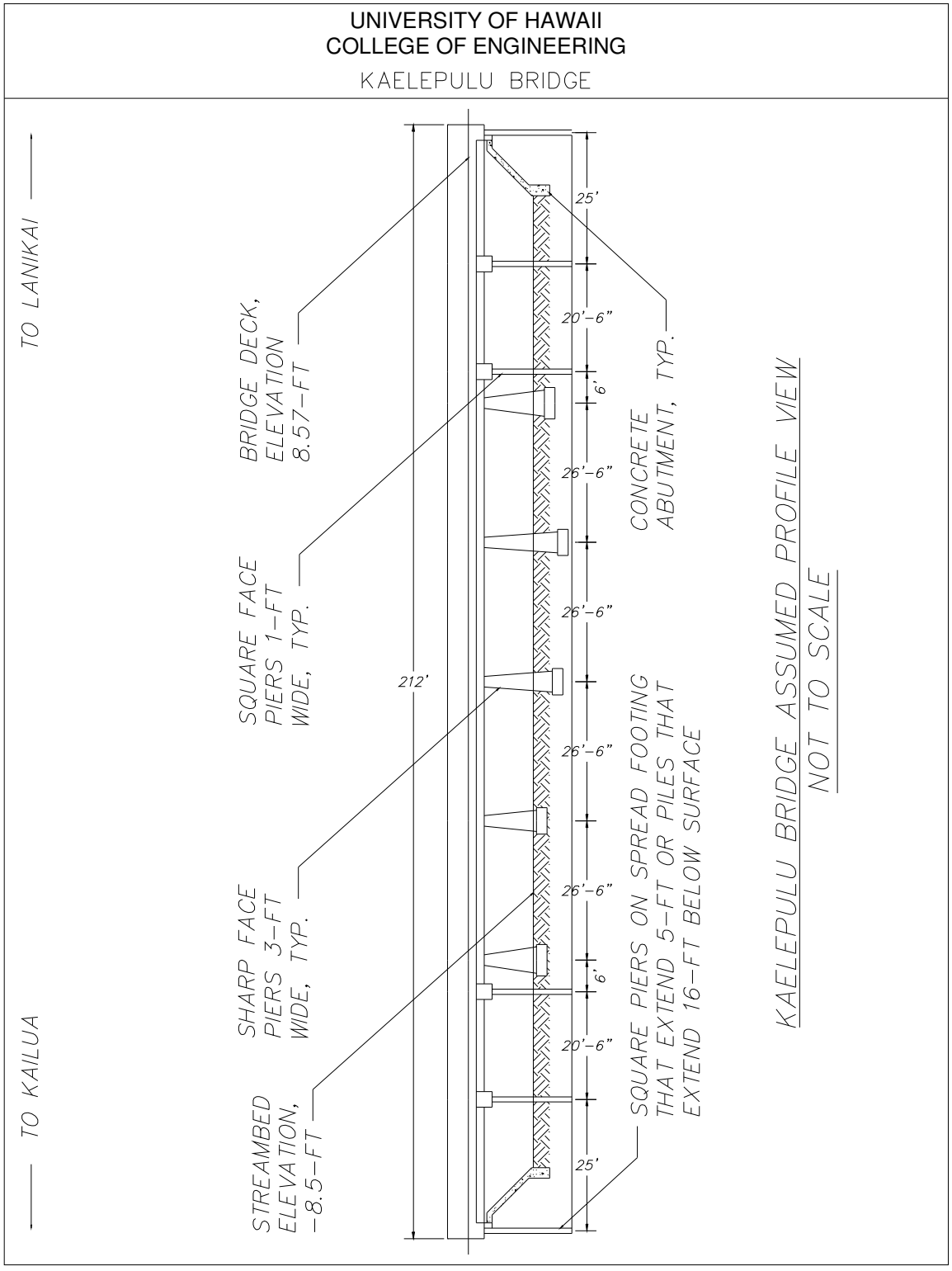


**Figure 3-11:** Profile of Kaelepulu Bridge used in HEC-RAS analysis

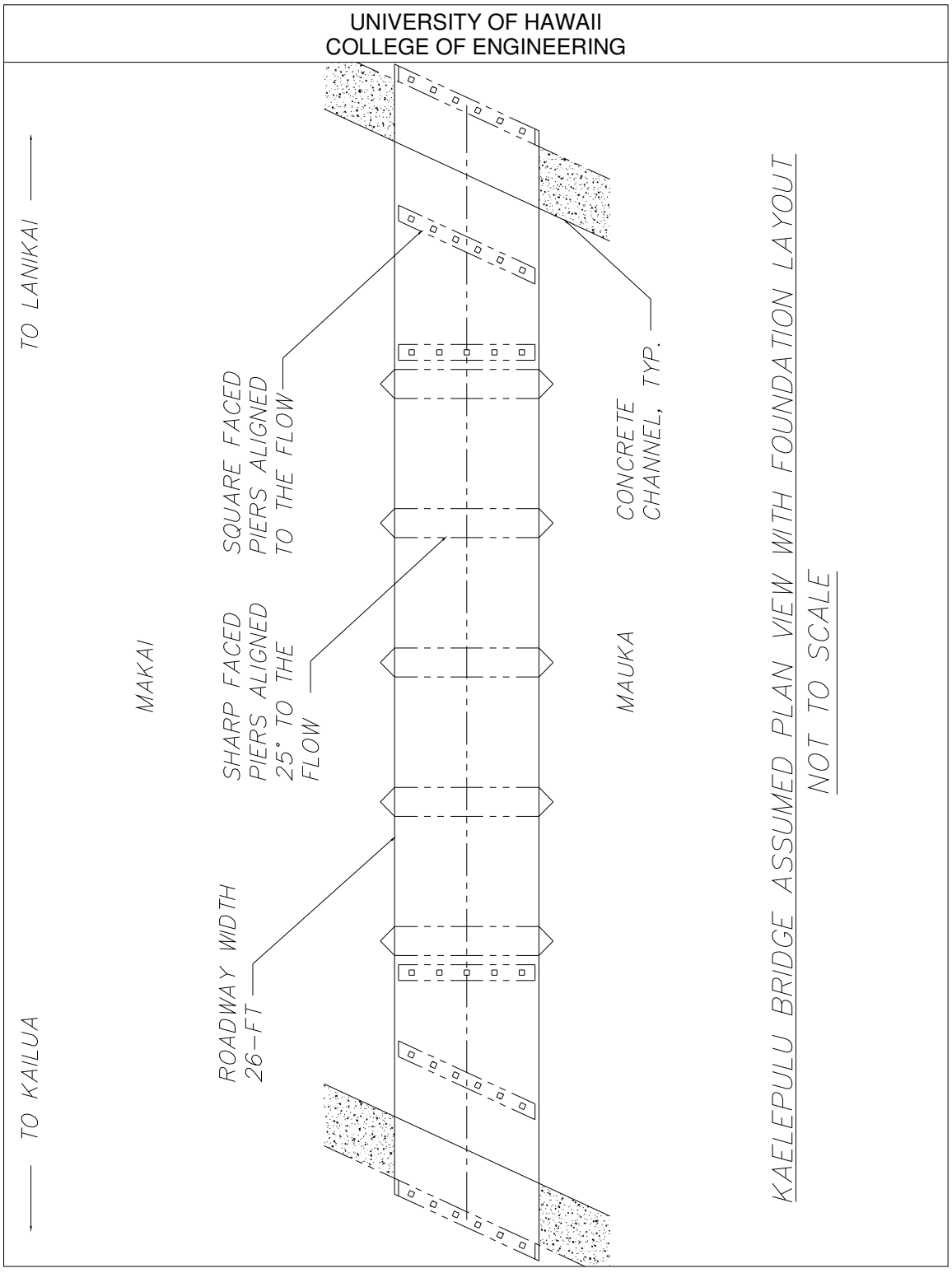


**Figure 3-12:** Plan view of Kaelepulu Bridge used in HEC-RAS analysis

### 3.2.2 Kahaluu Bridge

Kahaluu Bridge (Figure 3-13) is located near the intersection of Kahekili and Kamehameha Highway in Kaneohe, Hawaii. The bridge spans over Kahaluu Stream and is approximately 318 ft long. The bridge deck is supported on AASHTO girders, which are then supported on two piers and two abutments. The piers are supported by pile footings embedded in the streambed. Rock walls support the abutment, which run along both stream banks and prevents the stream from eroding the embankment. The stream width is almost equal to the bridge length and the stream is approximately 5 to 6 ft deep at the center. Water flows continuously throughout the year and drains into the ocean near Kahaluu Park. This bridge was selected in this study due to the large flow rate of Kahaluu Stream and the project team's familiarity with the hydrology of this stream. This bridge is maintained and managed by the State of Hawaii Department of Transportation.

**Figure 3-13:** Kahaluu Bridge

### 3.2.2.1 Input Parameters

The geometric input parameters for Kaelepulu Bridge were obtained from highway maps dated 1977 from the HDOT Design Branch in Kapolei, on-site investigations, topographic maps, and FEMA FIS. Site investigations revealed that the north and south abutments of the bridge do not protrude into the flow path, thus abutment scour will not be a factor. The upstream and downstream cross sections were determined from topographic maps and FEMA FIS. Six major cross-sections were used (Figure 3-14), the first 1111 ft upstream of the bridge (cross-section 10), the second 679 ft upstream of the bridge (cross-section 8), the third 250 ft upstream of the bridge (cross-section 7), the next 10 ft upstream of the bridge (cross-section 5), another 10 ft downstream of the bridge (cross-section 4), and the last 488 ft downstream of the bridge (cross-section 1).

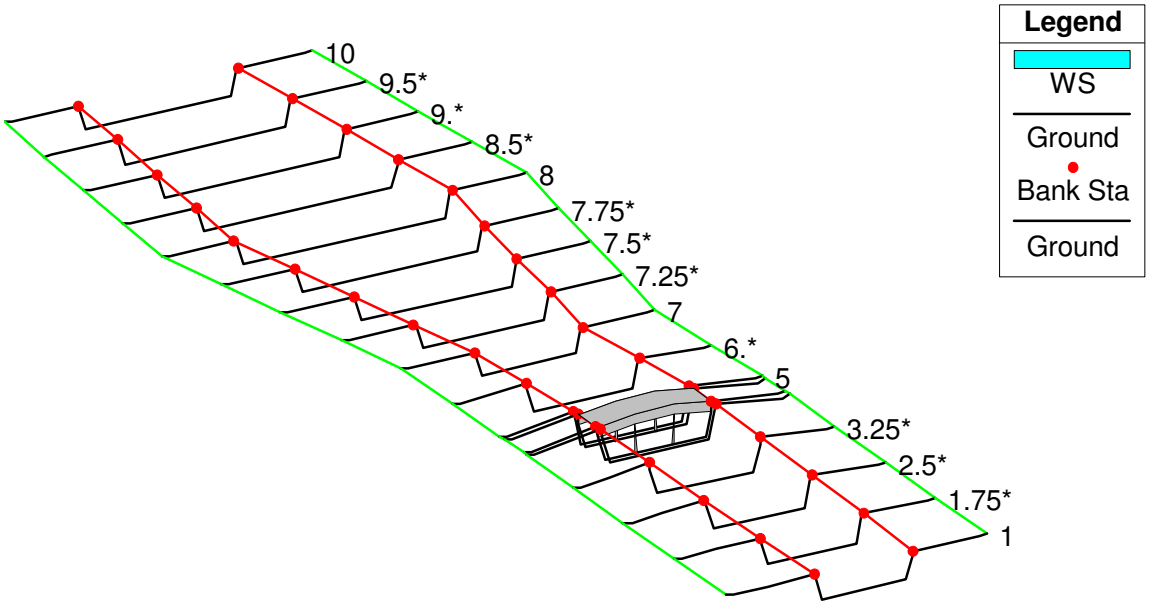


**Figure 3-14:** Kahaluu Bridge geometric input in HEC-RAS

The other cross-sections (noted with an asterisk) are cross-sections that were interpolated from the six major cross-sections. The stream cross-sections between 10 and 8 (8.5*, 9*, 9.5*) are spaced 108 ft apart from the center. The stream cross-sections between 8 and 7 (7.25*, 7.5*, 7.75*) are spaced 107 ft apart from the center. The stream cross-sections between 4 and 1 (3.25*, 2.5*, 1.75*) are spaced 123 ft apart from the center. The stream cross-section between 7 and 5 (cross-section 6*) are spaced 113 ft apart from the center. The reason for using many cross-sections was to reduce the amount of errors during the HEC-RAS analysis and to account for the large width changes of the upstream cross-section. The upstream section of the bridge is a reservoir that collects the water from three tributaries, while the downstream section of the bridge is a channel that drains into the ocean.

The next step in the analysis was to specify the 100-year flow and the required boundary conditions for the HEC-RAS analysis. From the FEMA FIRM the water surface elevation during a 100-year flood is 4 ft (from Mean Sea Level) at the bridge. The FEMA FIS predicted flow rate for Kahaluu Stream is about 24900 cfs. The 100-year flow was developed in the FEMA study using the frequency analysis of stream gage records for the three upstream tributaries (Ahiumanu, Kahaluu, and Waihee). With the boundary conditions and flow rate complete, the HEC-RAS analysis is ready to be performed.

After the HEC-RAS analysis was performed, the scour input variables were entered in the HEC-RAS Hydraulic Design Data Window. The parameters for contraction scour are grain size diameter $D_{50}$ and the contraction scour constant $K_1$. No soil samples from Kahaluu streambed were taken back to UH for sieve analysis but field observations of the streambed material indicated that the soil is cohesive silt thus the grain size diameter $D_{50}$ was assumed to be a conservative value of 0.05 mm, which will allow for the greatest contraction scour. Contraction

scour constant $K_1$ was automatically solved by the computer when $D_{50}$ was inputted. For local scour at piers the parameters needed were determined from the bridge plans and on-site investigations of the bridge, which include pier shape (pier scour constant $K_1$), pier width, pier length, angle of flow to the pier (pier scour constant $K_2$), bed condition (pier scour constant $K_3$), and grain size diameter $D_{95}$ (pier scour constant $K_4$).

Site investigations revealed that Kahaluu Bridge has round faced piers ($K_1$=1.0), which are 5.5 ft wide and 44 ft long that is aligned to the flow ($K_2$=1.0). The streambed was observed to have a plane bed condition beneath the bridge ($K_3$=1.1). Grain size diameter $D_{95}$ was assumed to be a conservative 0.52 mm ($K_4$=1). The parameter $K_4$ is a factor that accounts for the property of the streambed and would decrease the depth of total scour if armoring units were present, thus $K_4$=1 is a conservative estimate. This estimate is more accurate for Kahaluu Bridge than for Kaelepulu Bridge because at the Kahaluu Bridge site, the streambed material is mostly mud and sand over a deep depth. Since the abutments do not appear to intrude into the flow area, no abutment parameters are required.

#### 3.2.2.2 Simulation Result

After the hydraulic variables were entered, the total depth of scour was calculated through HEC-RAS and a Hydraulic Design Data report was printed. Figure 3-15 shows the cross-sectional view of Kahaluu Bridge during the HEC-RAS analysis of the 100-year flood flow of 24900 cfs with a water surface elevation of 4 ft (from Mean Sea Level) at the bridge. From the cross-sectional scour plot, Kahaluu Bridge shows significant scour at the piers. Below is an excerpt from the Hydraulic Design Data Report that displays the different types of scour. HEC-RAS calculated the scour at Kahaluu Bridge to be 12.18 ft at the two piers and 0.29 ft of

contraction scour across the width of the bridge streambed. This computes to a total scour of 12.47 ft at the piers. From Figure 3-15, a 100-year flood will not overtop Kahaluu Bridge, thus the road may be opened to traffic during a storm assuming that the foundation is still safe, though some flooding upstream may occur. Although Kahaluu Bridge is supported by piles that extend beyond the total depth of scour, the pier scour depth will reach under the pile cap and expose the pile group. For Kahaluu Bridge, engineers should study the foundation to check if the loss of ground cover will affect the bearing capacity of the piles. For this bridge there is no evidence of long-term degradation scour.

```
Hydraulic Design Data
Contraction Scour
     Scour Depth Ys (ft):                0.29
     Critical Velocity (ft/s):           0.75
     Equation:                           Live

Pier Scour
     All piers have the same scour depth
     Scour Depth Ys (ft):                12.18
     Equation:                           CSU equation

Combined Scour Depths

     Pier Scour + Contraction Scour (ft):
          Channel:       12.47
```

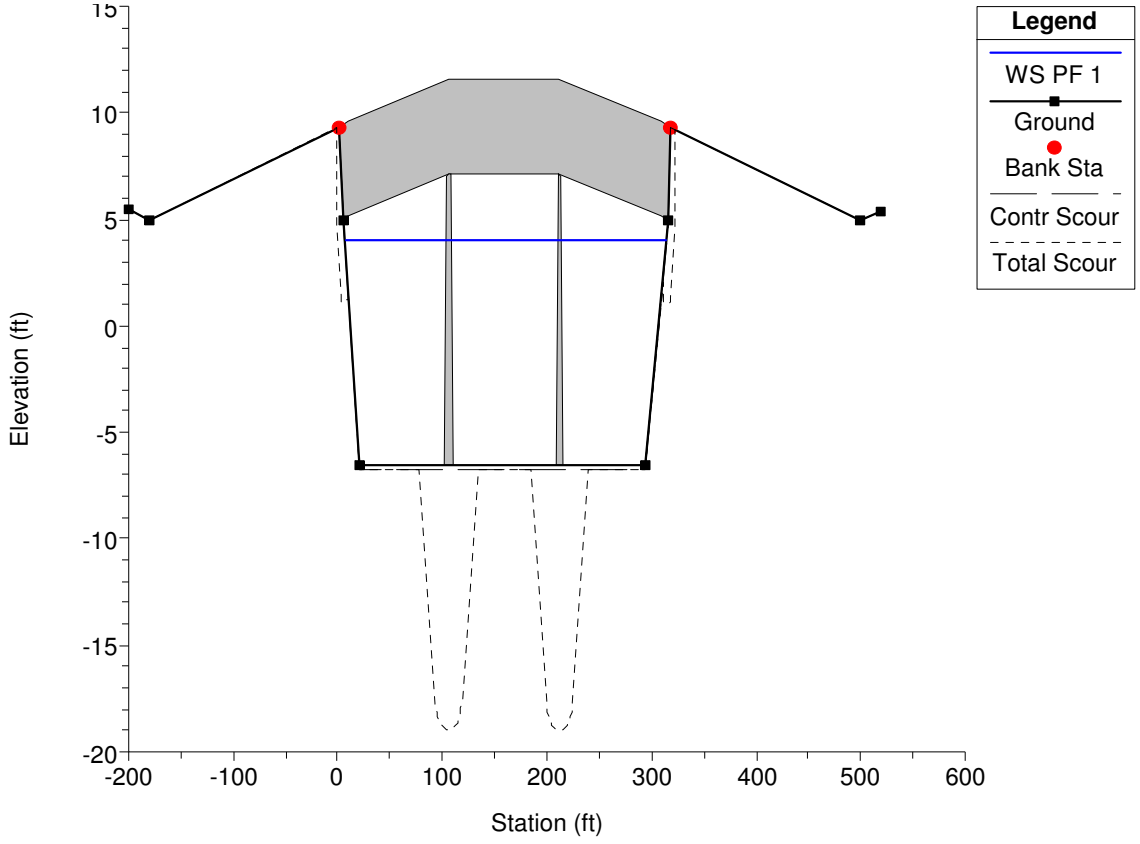


**Figure 3-15:** Cross-section of Kahaluu Bridge during 100-year flood

### 3.2.2.3 Error Analysis

Possible sources of errors include that no updated surveying was performed on the upstream and downstream cross-sections in this present study. The width and distances between cross-sections were from USGS Topographic Maps and the streambed depth was from FEMA FIS. The basic outline of the cross-sections was assumed to be similar to the outline of the streambed at the bridge. Detailed surveying would improve the accuracy of the scour results. Figure 3-15 displays some local scour at the abutments, but field studies show that the abutment does not protrude into the flow area and therefore local scour at the abutment does not exist. The abutment scour computed in HEC-RAS is an error and this situation shows that field studies of

the bridges must be performed in order to rule out some forms of scour. If perhaps the abutment did protrude into the flow area, the abutments are armored with large boulders that can resist the flood flow. Currently HEC-RAS is based on the FHWA HEC-18 equations, which do not take into account the property of different streambed material near the abutments. It only considers the abutment geometry and flow conditions.

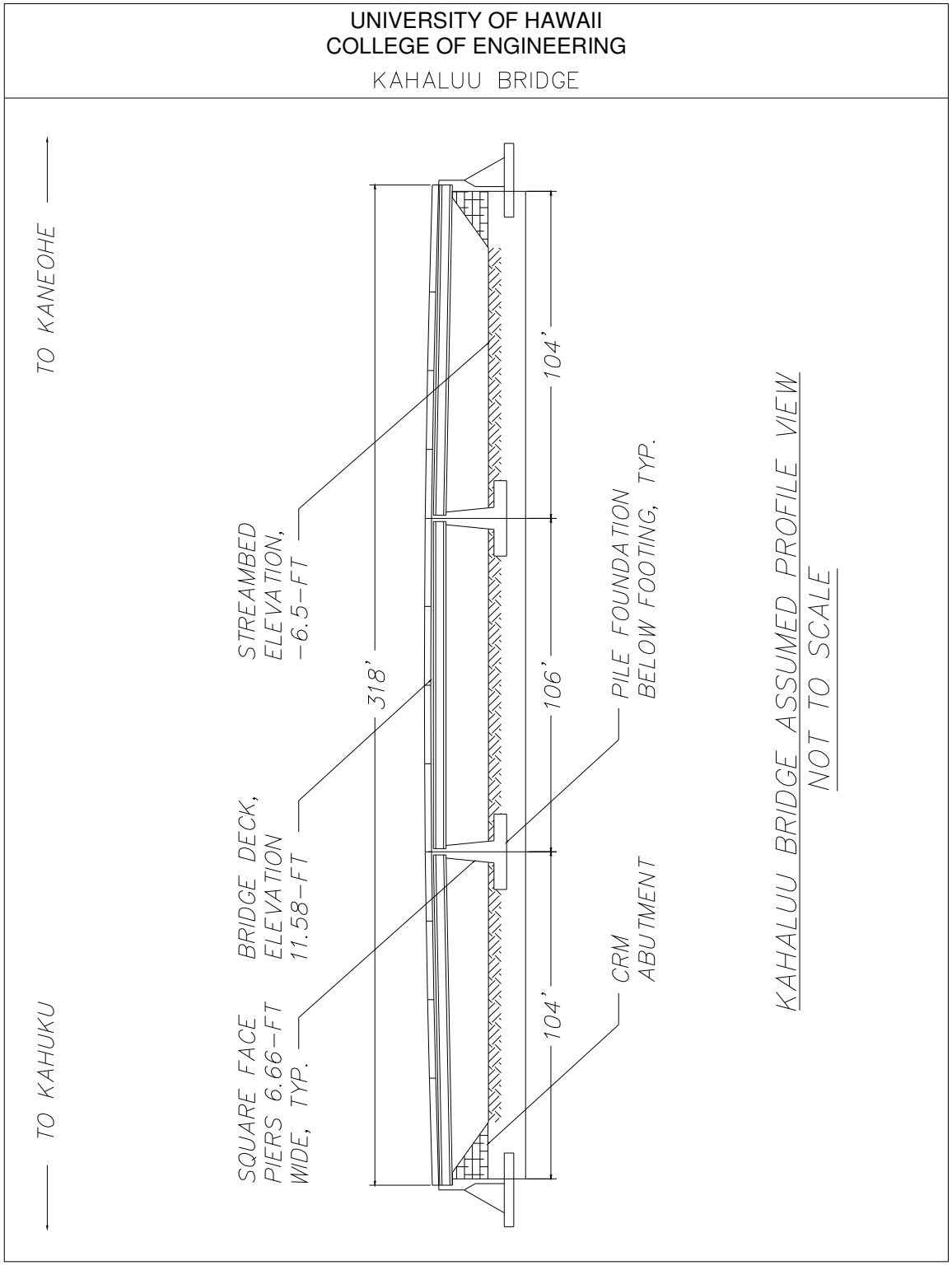


**Figure 3-16:** Profile of Kahaluu Bridge used in HEC-RAS analysis

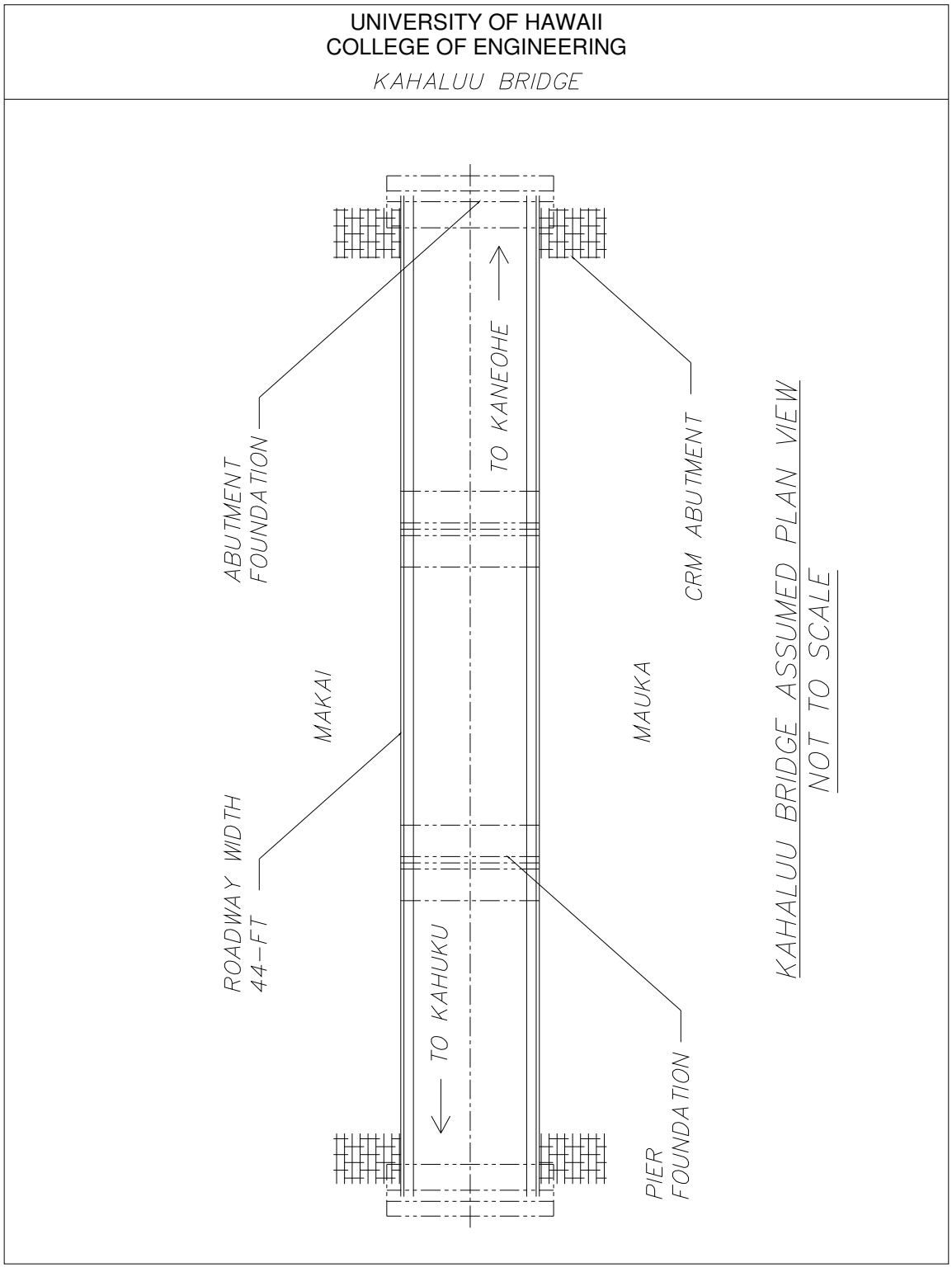


**Figure 3-17:** Plan view of Kahaluu Bridge used in HEC-RAS analysis

### 3.2.3 Discussions

From Table 3-7, the dominant scour found is the local scour at piers for the two bridges. Local scour contributes more than contraction scour because the cross-sectional area of the selected bridges is almost the same as the flow approach area, thus little contraction of the flow occurs. Local scour at the piers was dominant for Kaelepulu and Kahaluu Bridge based on HEC-18 equations. Local scour at the abutment was assumed to be zero since the abutments for Kaelepulu and Kahaluu are set back from the flow area.

**Table 3-7:** Input parameters and results for HEC-RAS analysis

| | Kaelepulu Bridge | Kaelepulu Bridge | Kahaluu Bridge |
|---|---|---|---|
| 100 yr Flow | 10800 cfs | 10800 cfs | 24900 cfs |
| Water Surface Elevation for 100-Year Flow at Bridge | 2 ft | 2 ft | 4 ft |
| $D_{50}$ | 0.19 mm<br>0.00062 ft | 0.19 mm<br>0.00062 ft | 0.05 mm Assumed |
| Pier Width a | 3 ft | 1 ft | 6.66 ft |
| Pier Length L | 33 ft | 29 ft | 44 ft |
| Pier Nose Shape | Sharp | Square | Round Nose |
| Pier Scour $K_1$ | 0.9 | 1.1 | 1.0 |
| Flow Angle | 25 Degrees | 0 Degrees | 0 Degrees |
| Pier Scour $K_2$ | 3.0 | 1.0 | 1.0 |
| Bed Condition | Medium Dunes | Medium Dunes | Plane Bed |
| Pier Scour $K_3$ | 1.1 | 1.1 | 1.1 |
| $D_{95}$ | 0.50 mm<br>0.0016 ft | 0.50 mm<br>0.0016 ft | 0.52 mm Assumed |
| Pier Scour $K_4$ | 1.0 | 1.0 | 1.0 |
| 100-year Contraction Scour | 2.60 ft | 2.60 ft | 0.29 ft |
| 100-year Pier Scour | 17.96 ft | 3.22 ft | 12.18 ft |
| 100-year Total Scour | 20.56 ft | 5.82 ft | 12.47 ft |

Studying the 100-year flood scour results, one can predict that Kahaluu Bridge most likely will not fail during a 100-year flood since the HEC-RAS results show that the bridge would not be overtopped during flood and the foundation is on piles that extend beyond the 12.47 ft pier scour. For Kahaluu Bridge, engineers should study the foundation to check if the loss of ground cover significantly will affect the bearing capacity of the piles. For Kahaluu Bridge there is no evidence of long-term degradation.

Kaelepulu Bridge consists of two different pier formations, square piers at the end of the bridge and sharp-faced piers at the middle. The square piers, built during the extension of the original bridge, are aligned to the flow and have a total scour of 5.82 ft. The bridge plans show two different foundation designs for the square piers, one on spread footings 5 ft below the streambed and the other on piles 16 ft below the streambed. Engineers must do a foundation study to determine the foundation type below the square-face pier since the undermining of the foundation will occur if pier sits on a spread footing. The sharp-faced pier is aligned 25 degrees to the flow and HEC-RAS calculated the total scour at the piers to be 20.56 ft. The sharp-faced piers are in danger of undermining since the bridge plans show the pier on spread footings where the bottom sits 1 to 5 ft below the streambed. In the future engineers must install scour countermeasures before a serious flood undermines the bridge foundations and collapse the bridge. Kaelepulu Bridge also suffers from a serious aggradation problem where the streambed is dredged several times during the year.

Tables 3-8 and 3-9 present a scour sensitivity analysis of the bridge input parameters to determine which parameter will have the largest effect on scour. The four bridge results and input parameters listed in Table 3-7 were used and the three major parameters tested were $D_{50}$ particle size, pier width, flow angle, and flow rate. To accomplish this, one parameter was

adjusted by the values listed in Table 3-8 while the other two parameters were kept constant during the HEC-RAS analysis. Grain size diameter $D_{50}$ and pier width was adjusted by 20%, while the flow angle was increased to 2 and 4 degrees. The results of these HEC-RAS analyses are presented in Table 3-9.

**Table 3-8:** Input parameters for HEC-RAS sensitivity scour analysis

| Variable | Variation | Kahaluu Bridge | Kaelepulu Bridge |
|---|---|---|---|
| $D_{50}$ (mm) | 100% | 0.05 | 0.19 |
| | 80% | 0.04 | 0.152 |
| | 120% | 0.06 | 0.228 |
| Pier Width a (ft) | 100% | 6.6 | 3 |
| | 90% | 5.94 | 2.7 |
| | 110% | 7.26 | 3.3 |
| Flow Angle | +0 Degrees | 0 degrees | 25 degrees |
| | +2 Degrees | 2 Degrees | 27 degrees |
| | +4 Degrees | 4 Degrees | 29 degrees |

**Table 3-9:** Sensitivity results for HEC-RAS scour analysis

| | | Calculated Total Scour (ft) | |
|---|---|---|---|
| Variable | Variation | Kahaluu Bridge | Kaelepulu Bridge |
| $D_{50}$ | 100% | 12.47 | 20.56 |
| | 80% | 12.47 | 20.56 |
| | 120% | 12.47 | 20.56 |
| Pier Width a | 100% | 12.47 | 20.56 |
| | 90% | 11.59 | 20.32 |
| | 110% | 13.17 | 20.63 |
| Flow Angle | +0 Degrees | 12.53 | 20.56 |
| | +2 Degrees | 13.81 | 21.34 |
| | +4 Degrees | 15.15 | 22.06 |

Table 3-8 and 3-9 shows that adjusting the grain size diameter by 20% will not have an effect on the scour results based on the current scour equations. In addition, smaller pier width

will decrease the depth of scour. The most significant parameter is the angle of the flood flow into the bridge. For instance, by adjusting the angle by 2 degrees the depth of scour increases by a foot. Comparing the sharp-faced pier with an angle of 25 degrees to the flow and the square-nosed pier, which is aligned with the flow at Kaelepulu Bridge in Table 3-7, one can see that the square nose pier scour depth is about 14 ft less than the sharp-faced pier, which further underlines the significance of the flow angle. Other input factors such as pier nose shape and bed condition were left out since changing these will only increase/decrease the scour values slightly by those listed in Table 3-2 and 3-4. For instance changing from a round nose pier ($K_1$=1.0) to a square nose ($K_1$=1.1) will increase the pier scour depth by a factor of 1.1.

It is important to state that all simulations and analysis presented so far are based on existing empirical scour equations, which have not been fully validated in Hawaii or on the mainland. For local pier scour, the equations were developed through laboratory experiments using homogenous sand, and more or less ignore the effect of actual streambed material properties in the field. During the installation of the scour monitoring instrumentation at Kaelepulu Bridge in this project, boring samples were obtained by hammering into the streambed. The samples as shown in Figure 3-18 revealed that the streambed material at this bridge site consists of a layer of sand near the surface while hard coral layer about –7 ft in elevations MSL. These coral rocks serve as a natural armoring unit and are unlikely to be scoured significantly during a flood, However, this type of actual streambed condition is not considered in the current design, instead engineers use the particle size $D_{50}$ at the streambed surface as the input parameter to determine the factor $K_4$ in equation 3-6 and obtain the most conservative scour condition. Obviously, the current practice can easily over-predict the local scour by a large margin at a bridge site such as Kaelepulu.

**Figure 3-18:** Boring samples (hard coral rocks) at 7-10 ft depth at Kaelepulu Bridge

## 3.3 Multilayered Streambed Analysis

Boring logs of the scour critical bridges on Oahu show multiple layers of soil within a depth that may become scoured away during a flood. HEC-18 scour equations (CSU and Laursen's) assume streambeds of uniform sand and do not deal with multilayered and cohesive streambeds. Cohesive soil streambeds are common on Oahu and the analysis of cohesive soil scour is relatively new. In addition, the HEC-RAS computer simulation cannot simulate scour in multilayered streambeds. This section will present a new method developed in this study for analyzing multilayer streambed scour.

### 3.3.1 Boring Logs of Scour Critical Bridges

Figures 3-25 to 3-30 display selected boring logs from bridges deemed scour critical by the HDOT on Oahu (refer to Figure 1-2 for a map displaying the bridges location) plus Kaelepulu Bridge and Kahaluu Bridge (bridges where the scour monitoring instrumentation are installed on). These boring logs were performed by consulting engineers and reproduced on the bridge blueprints, which are available from the HDOT Design Branch in Kapolei. Each bridge has multiple boring locations but Figures 3-25 to 3-30 display the boring log typical of that bridge. Although the boring logs are representative of the bridge, each bridge has log characteristics that differ in each location such as missing layers and different layer depths. Many of the borings were drilled until hard lava rock or mud rock was hit up to depths of 100 ft below the surface. Most of the boring logs indicate there are multiple layers of soil mostly consisting of sand near the surface, while a few of the bridges have a top layer of cohesive material (silts and clays) located at a depth that may become scoured away during a flood. The boring logs are relatively old and are missing information such as the standard penetration test

and classification of the soil layers according to the Unified Soil Classification System. Despite these shortfalls the soil description are satisfactory and give an idea of the characteristics of the different soil layers for scour analysis.

### 3.3.2 Review of HEC-18 Equations for Scour in Multilayered Streambeds

Before describing procedures for calculating scour of stratified streambeds, it is important to review the common scour depth equations. Per the CSU local scour formulas presented in Section 3.1.4, local scour is mainly dependent on the bridge geometric features (skew angle to flow, shape/width/length of pier) and approach velocity rather than particle size. For local scour, streambeds consisting of sand have little effect on scour, but larger particles will delay the time that maximum scour occurs. Even larger bed material that can withstand hydraulic forces will armor the scour hole and limit the effects of scour. The CSU equations were derived from laboratory experiments using homogenous layers of fine sand with no consideration for multilayered streambeds. The CSU local scour equations are basically live-bed scour equations in sand beds.

For contraction scour based on Laursen's scour equations, multilayered soil may be important in the determination of critical velocity $V_c$ (the minimum velocity required to move a particle of diameter $D_{50}$ and smaller). If the velocity upstream of the bridge is greater than the critical velocity, sediment is transported in the flow and the contraction scour that results is called live-bed scour. If the velocity upstream of the bridge is less than the critical velocity then no sediment is transported with the flow and the contraction scour is called clear-water scour. Both Laursen's contraction scour equations are a function of geometry and particle size, which can affect the results of multilayer scour analysis.

FHWA HEC-18 provides notes that may help analyze scour in the multilayered streambed conditions. Since live-bed contraction scour is limited if coarse material armor the streambed, HEC-18 recommends calculating both clear-water and live-bed equations and using the smallest depth of scour calculated. Another note states that for layered bed material the depth of scour can be determined by using the clear water scour equation sequentially with successive $D_{50}$ of the bed material layer (Richardson et al., 2001). An alternative method is to assume a homogenous soil layer throughout the streambed depth and use the layer with the finest $D_{50}$ to obtain the most conservative scour depth.

Similar to the CSU local scour equations, Laursen's equations were obtained based on laboratory flume experiments using sand as bed material. However, the HDOT boring logs indicate that there are many instances where large bed material layer such as boulders, gravels, and coral are near the surface, which will armor the streambed and slow down the scour. Large bed size material that may armor the streambed against scour is known as riprap and is a common scour counter measure.

The greatest depth of scour has been found on bridges with streambeds consisting of sand and silts. The problem of scour exists with streambeds of coarse and fine-grained bed material although deeper scour holes occur in streambeds with sandy material than stream with coarse and cohesive beds. Therefore the knowledge of bed sediment at a bridge is important to determine the susceptibility of scour or armoring potential.

### 3.3.3 HEC-RAS Simulation of Multilayer Soil Scour

In this study, HEC-RAS was used to calculate contraction scour for stratified streambed using a layered approach. This method is demonstrated by studying a bridge with three different layers of soil and the effects of stratified soil have on bridge scour. Since HEC-RAS cannot model bridge scour with multiple layer of soil directly, an indirect approach is proposed. Figure 3-19 shows a generic bridge with a streambed consisting of three layers of soil with different $D_{50}$.

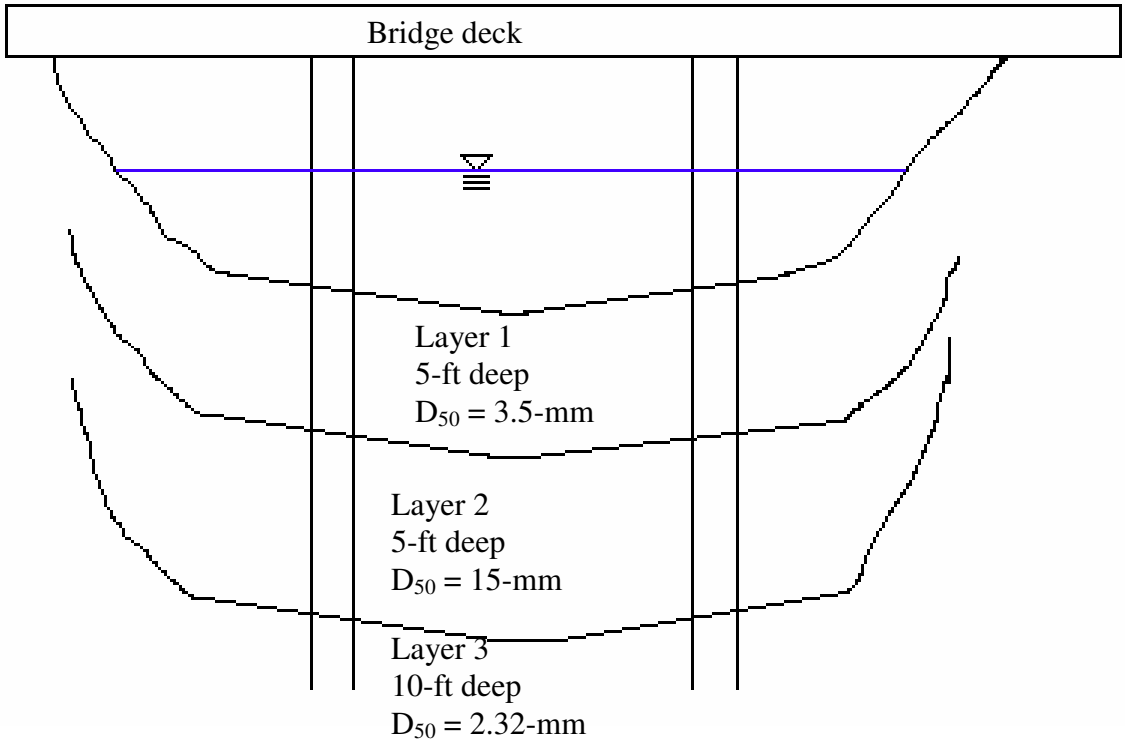


**Figure 3-19:** Generic bridge with multi-layered streambed.

The HEC-RAS scour analysis for a bridge with a stratified streambed such as the bridge in Figure 3-19 would be to first run the HEC-RAS simulation for the bridge assuming the entire streambed consisted of layer 1 with $D_{50}$ = 3.5 mm. If HEC-RAS determines the contraction scour to be less than the depth of layer 1 then that scour is the final contraction scour. If HEC-RAS

determined the contraction scour to be deeper than layer 1, then remove layer 1 from the cross-sectional geometry of the bridge streambed and rerun HEC-RAS using the $D_{50}$ from layer 2. Repeat the previous steps until the scour depth is less than layer X depth. This analysis was compared to a simulation with one uniform layer consisting of the smallest $D_{50}$ and an average $D_{50}$ used in the multiple layer simulation. Since the bridges studied in this report have small contraction scour results, 2 generic bridges were used.

The first bridge (Figure 3-20 and Figure 3-21) is an example bridge from the HEC-RAS program called Bridge Scour - Chapter 11. The bridge is approximately 3000 ft long and 50 ft wide and is supported by six 5-foot wide piers. The bridge opening is approximately 635 ft wide and the flow rate through the bridge is 30000 cfs. The generic river that the bridge spans over is approximately 2200 ft wide at the bridge. HEC-RAS modeled the river with 9 cross-sections that vary from 300 to 1000 ft apart.

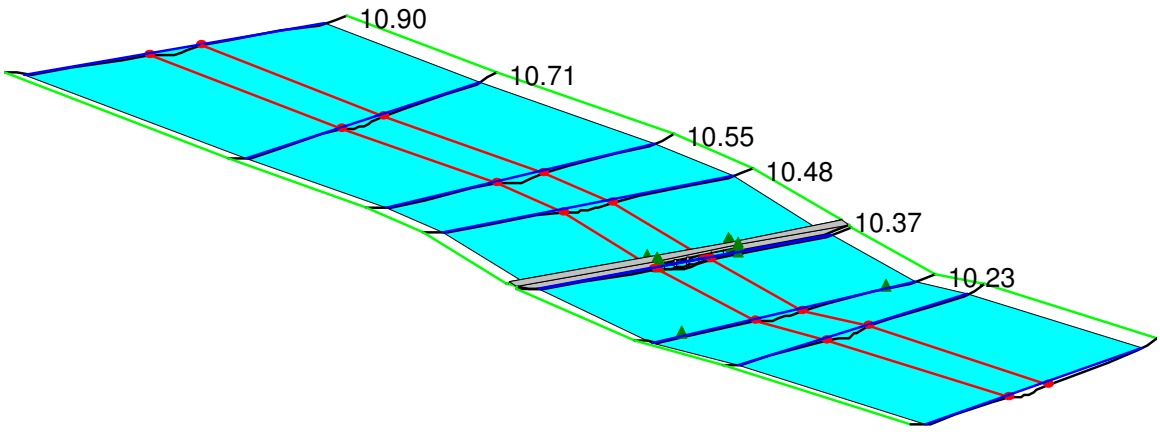


**Figure 3-20:** Isometric view of river showing location of river cross-sections

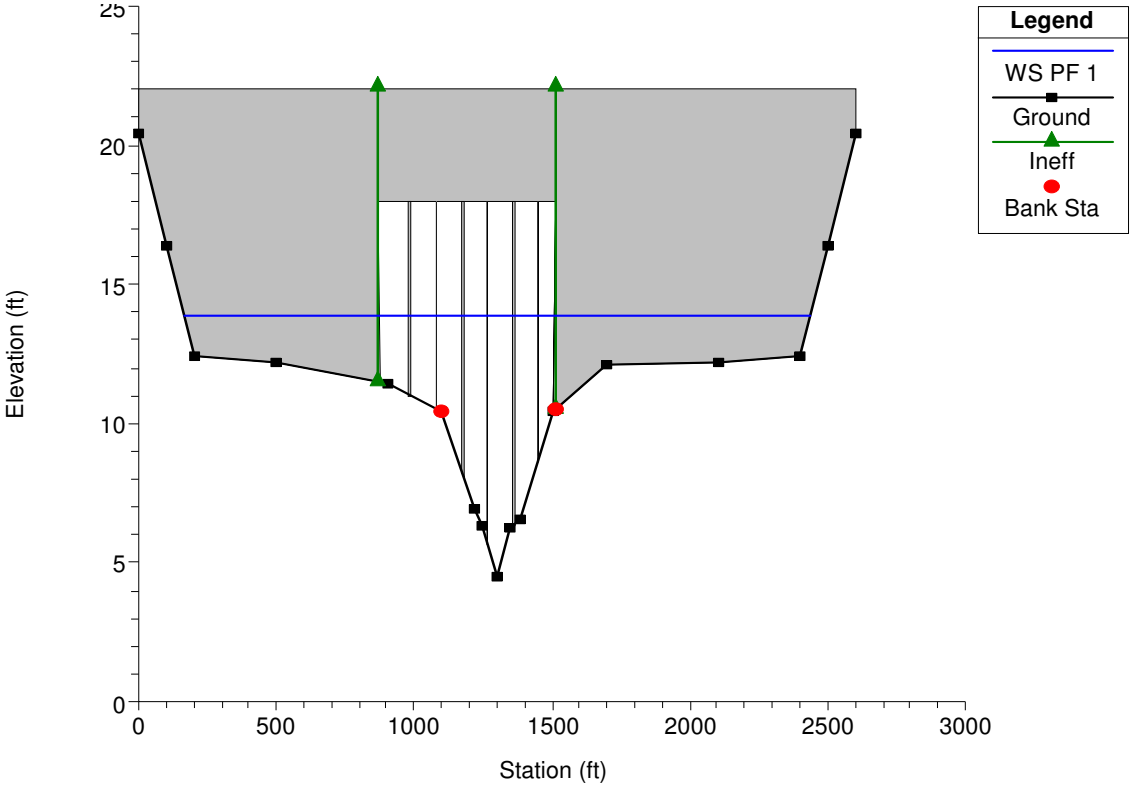


**Figure 3-21:** Cross-section of generic bridge 1

The first layer of soil was assumed to have the $D_{50}$ of 20 mm (0.066 ft) with a layer depth of 2.19 ft below the streambed. The second layer of soil was assumed to have the $D_{50}$ of 15 mm (0.049 ft) with a layer depth of 0.41 ft below layer 1. The last layer was assumed to have the $D_{50}$ of 2.01 mm (0.0066 ft) with an infinite layer depth below layer 2. The first uniform single layer simulation was assumed to have the smallest $D_{50}$ of 2.01 mm to obtain the most conservative answer. The second uniform single layer simulation was assumed to have the average $D_{50}$ of the three layers that was 12.34 mm. The flow rate applied to all simulations at this bridge was 30,000 cfs.

**Table 3-10:** HEC-RAS results of multilayered contraction scour for bridge 1

| | Multiple Layer | One Layer ($D_{50}$ = 2.01 mm) | Average Layer ($D_{50}$ = 12.34 mm) |
|---|---|---|---|
| First Layer | 2.19 ft | 6.65 ft | 3.58 ft |
| Second Layer | 0.41 ft | | |
| Third Layer | 0.00 ft | | |
| Total Contraction Scour | 2.60 ft | 6.65 ft | 3.58 ft |

The second bridge is a generic bridge (Figure 3-22 and Figure 3-23) created by the research project team. The bridge is approximately 430 ft long and 50 ft wide and is supported by two 2-foot wide piers. The bridge opening is approximately 150 ft wide and the flow rate through the bridge is 25000 cfs. The generic river that the bridge spans over is approximately 454.37 ft at the bridge. HEC-RAS modeled the river with 6 cross-sections that vary from 100 to 400 ft apart.

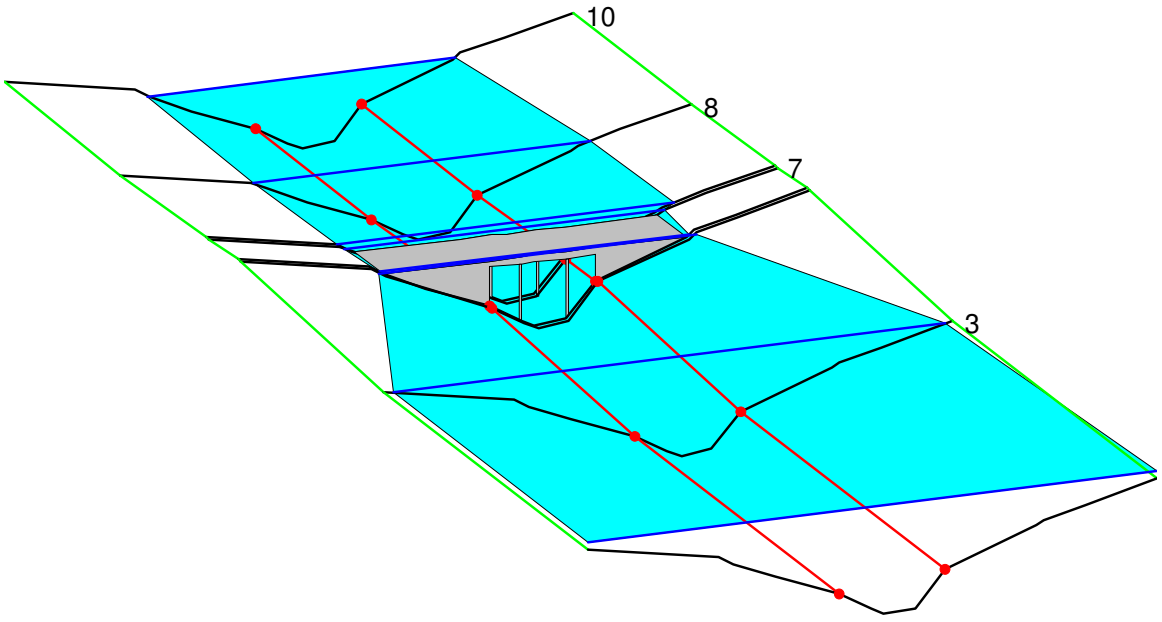


**Figure 3-22:** Isometric view of river showing location of river cross-sections

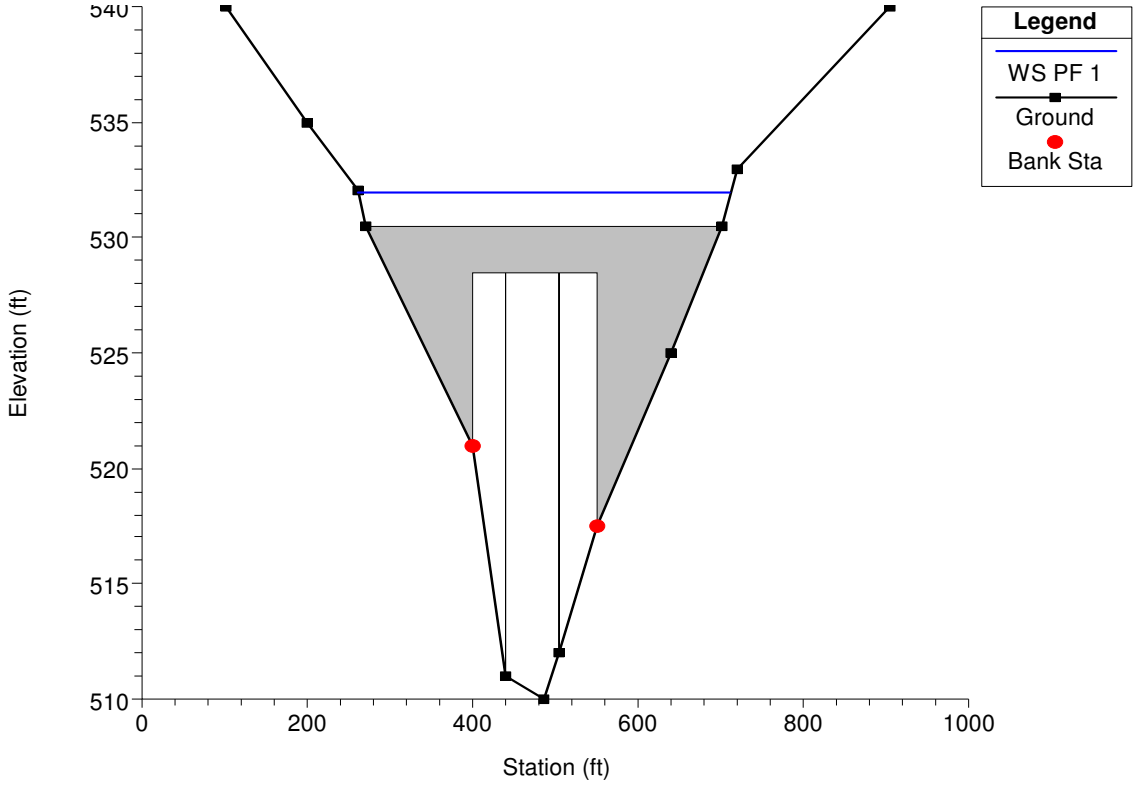


**Figure 3-23:** Cross-section of generic bridge 2

The first layer of soil was assumed to have the $D_{50}$ of 30 mm (0.098 ft) with a layer depth of 1.46 ft below the streambed. The second layer of soil was assumed to have the $D_{50}$ of 20 mm (0.066 ft) with a layer depth of 2.39 ft below layer 1. The last layer was assumed to have the $D_{50}$ of 2.32 mm (0.0076 ft) with an infinite depth below layer 2. The first uniform single layer simulation was assumed to have the smallest $D_{50}$ of 2.32 mm to obtain the most conservative scour depth. The second uniform single layer simulation was assumed to have the average $D_{50}$ of the three layers that was 17.44 mm. The flow rate applied to all simulations at this bridge was 25,000 cfs. Please refer to Appendix Section F.4 for the HEC-RAS output and Table 3-11 for a summary of the simulation.

**Table 3-11:** HEC-RAS results of multilayered contraction scour for bridge 2

| | Multiple Layer | One Layer ($D_{50}$ = 2.32 mm) | Average Layer ($D_{50}$ = 17.44 mm) |
|---|---|---|---|
| First Layer | 1.46 ft | 6.19 ft | 4.42 ft |
| Second Layer | 2.39 ft | | |
| Third Layer | 1.91 ft | | |
| Total Contraction Scour | 5.76 ft | 6.19 ft | 4.42 ft |

From the results in Tables 3-10 and 3-11 one can surmise that layered soil has a smaller scour depth than a soil with a single uniform layer of soil if the smallest size is assumed throughout the depth of the streambed. In addition the one-layer soil approach over-estimates the scour depth thus increasing the cost of new bridge construction. Current practice assumes one uniform layer of soil instead of a realistic view of layered soil. The average layer approach varies between both bridges but in both cases the average layer scour gives scour depths less than the conservative one layer approach. For these two examples HEC-RAS was preformed assuming the streambed becomes finer with depth since this scenario would produce a deeper contraction scour then if the streambed becomes coarser with depth. The reason is that as contraction scour progresses into the streambed the cross-sectional flow area increases and the flow velocity decreases. As the loss of velocity through the bridge occurs, the flow's ability to scour coarser materials decreases until equilibrium is reached.

The results from this study indicate that by using a multi-layer approach, the predicted scour depth is consistently smaller than using a one-layer approach. As more and more studies (Mueller and Wagner 2005, Zhang et al 2013 among others) have shown that the HEC-18 equations tend to over-estimate scour depth, we would like to recommend that when possible,

both a multi-layer and one-layer method should be used to estimate the scour depth. The two results should be compared and analyzed. An average of the two may provide a more accurate yet still safe estimate of the scour depth compared with using a one-layer approach alone.

### 3.3.4 Scour in Cohesive Soils

Since both the CSU local scour and Laursen's contraction scour equations were derived from sandy material and some of the boring logs indicate a layer of cohesive bed material near the surface, one must look at the scour effects of cohesive material. FHWA HEC-18 gives no guidelines on how to determine scour in cohesive material although it is believed that in sandy and cohesive soils the maximum depth of scour will be the same but not at the same rate. Since scour in cohesive soil erodes slower than in sand it is important to know the rate at which it achieves maximum scour so construction cost can be reduced.

According to the Unified Soil Classification, cohesive soils are usually soils that have particles that can pass through a number 200 sieve (grain size diameter less than 0.075mm) and usually consist of silts and clays. Unlike coarse-grained material (sand gravels), cohesive soils are classified by their consistency (solid, plastic, liquid) with varying moisture contents (Atterburg Limits) while sand are classified by their grain size diameter. Cohesive soils have particles that stick together when wet and have properties that are dependent upon the amount of water.

For local scour for circular pier in cohesive soils Briaud et al (1999), using the SRICOS method, published a recent study in 1999. The SRICOS (Scour Rate In COhesive Soil) consists of testing bridge soil samples in an EFA (Erosion Function Apparatus). Basically the EFA

consists of the soil sample being pushed into a Plexiglas tube 1 mm at a time with flowing water at a constant velocity (Figure 3-24). The time required to erode the sample is recorded and the erosion rate with the shear strength of the water exerted on the soil is calculated. The shear strength and the erosion rate is plotted on a graph and the maximum depth of scour can be determined using equations. Finally the method was compared to 42 laboratory flume experiments where the laboratory measurements have a small scatter around the results predicted by SRICOS. Some disadvantages in using the SRICOS method are that the method is site specific for that particular bridge only, and the equations can only be applied to local scour at circular piers.

The SRICOS method was also used to predict local scour at multilayered streambeds and floods with random velocity time history. The research was performed by most of the same professionals (Briaud et al) and published in 2001. The SRICOS method was run for multilayer cases where there is a hard layer over a soft soil and vise-versa. The SRICOS method was run for one method first (soft soil) then the other (hard soil) to obtain the scour versus time plot for each condition. Then the scour versus time plots for each condition is transposed on each other to obtain the scour versus time plot for the whole multilayered condition. This method was tested against 8 case histories of bridges in Texas and the results were favorable.

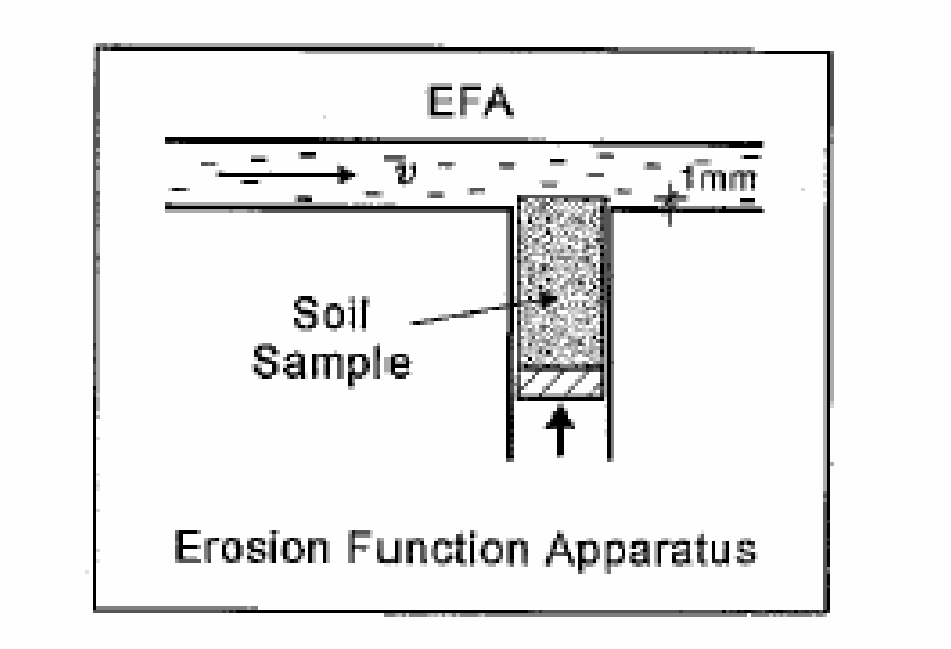


**Figure 3-24:** Erosion function apparatus for the SCIROS method

### 3.3.5 Future Studies in Multilayer Soil Scour

Since there is little research done on multilayered soil, more future studies are needed. Sand and gravel can be used in future experimental studies as bed material since sand and gravel are easily segregated into layers by particle size diameter and can be recovered for additional testing. Cohesive material is difficult to segregate into layers (cohesive soils as segregated by Atterburg Limits) and complicated to recover after an experimental run. The sand diameter should be segregated into layers by using sieves. The velocity required to move the sand particles to simulate live-bed scour conditions can be calculated using the critical velocity equation. A design of an experimental setup for future bridge study scour is shown in Figure 3-31. Using the energy equation around the flume, the horsepower required for the pump can be calculated for the setup.

One must carefully choose the depth of water flowing through the flume since the depth is proportional to the maximum depth of scour according to the HEC-18 equations. The decision on the width of the flume must be studied since with a smaller width, the water flowing against sides of the flume will cause some interference with the test. The different layers of sand and gravel can be dyed a different color to differentiate the layer and see how deep the scour penetrates each layer. Some type of catch basin and filter is needed at the end of the flume to prevent the sand from entering the pump. The pump must be carefully chosen to generate the required water depth, width, and velocity. Therefore more than one pump may be necessary. The flume can be set up to simulate both local and contraction scour.

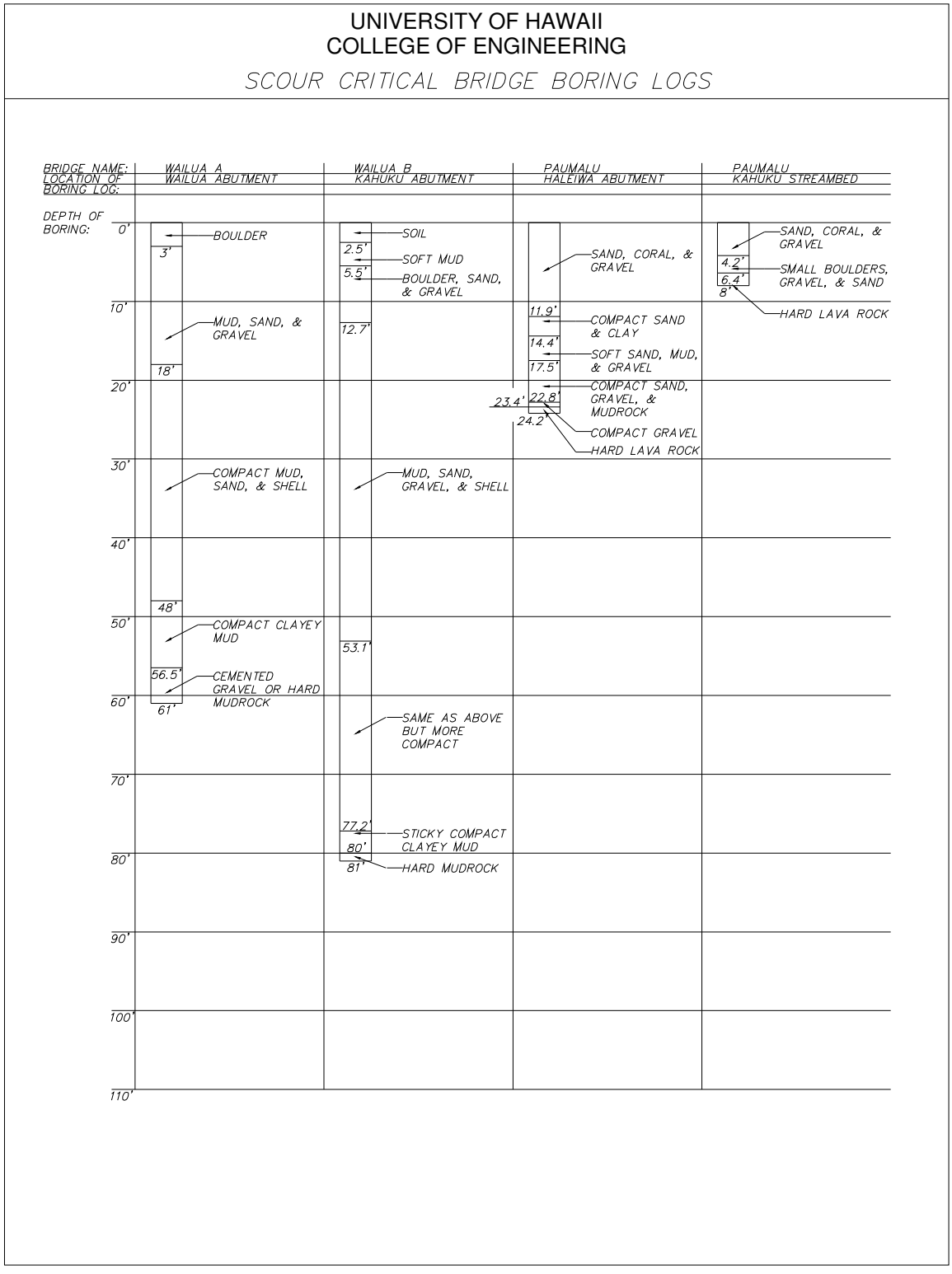


**Figure 3-25:** Boring logs of scour critical bridges

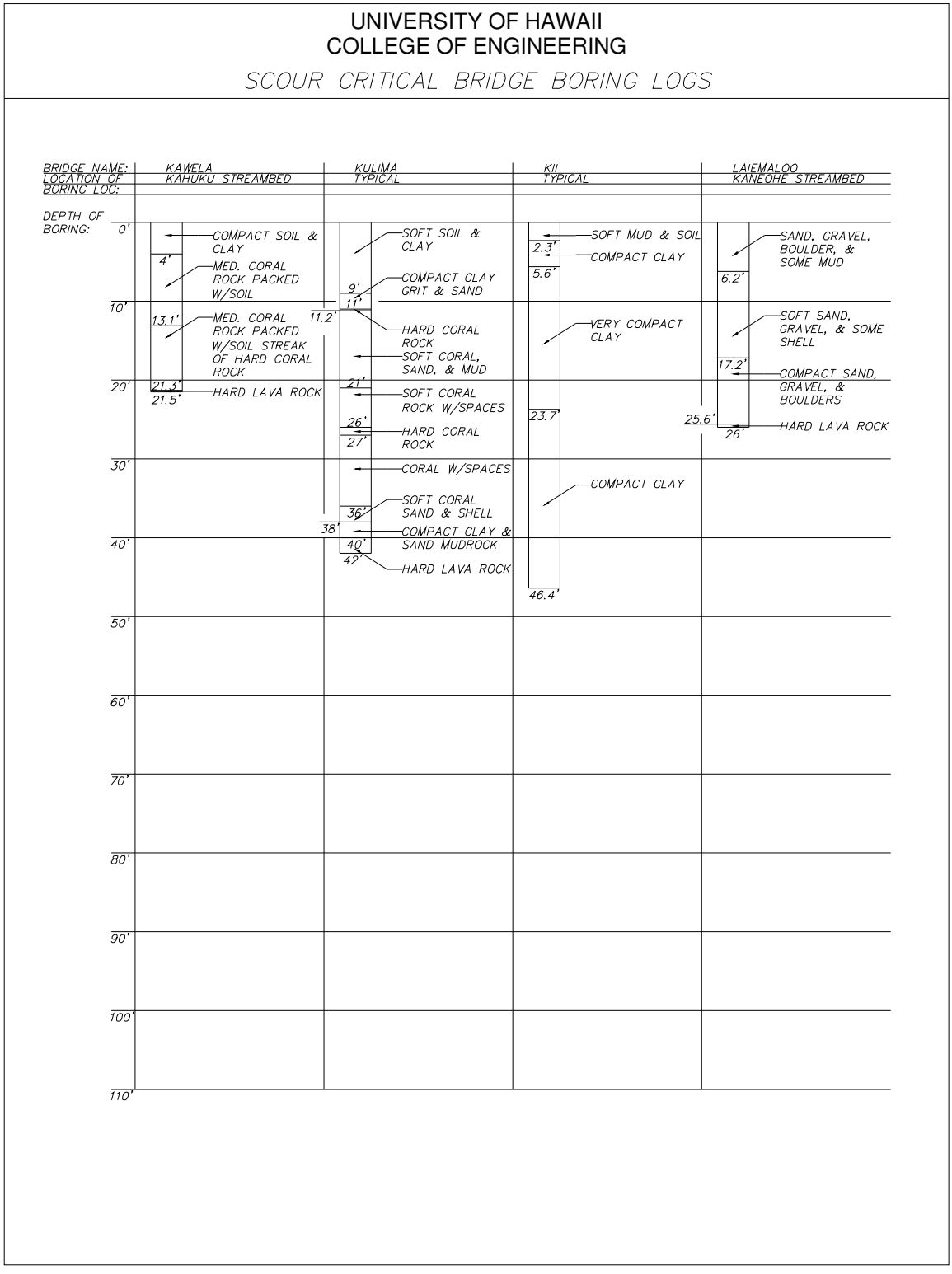


**Figure 3-26:** Boring logs of scour critical bridges

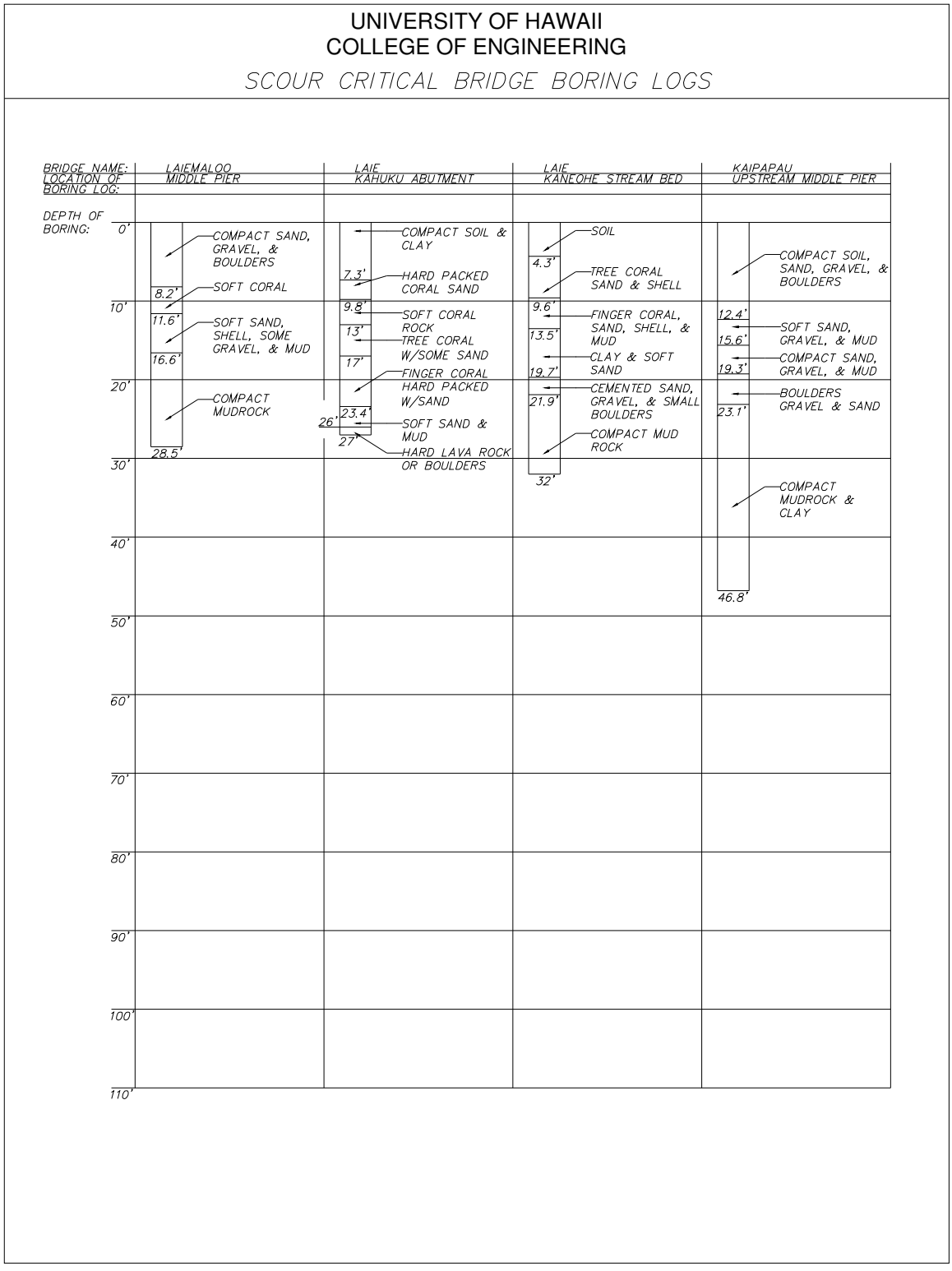


**Figure 3-27:** Boring logs of scour critical bridges

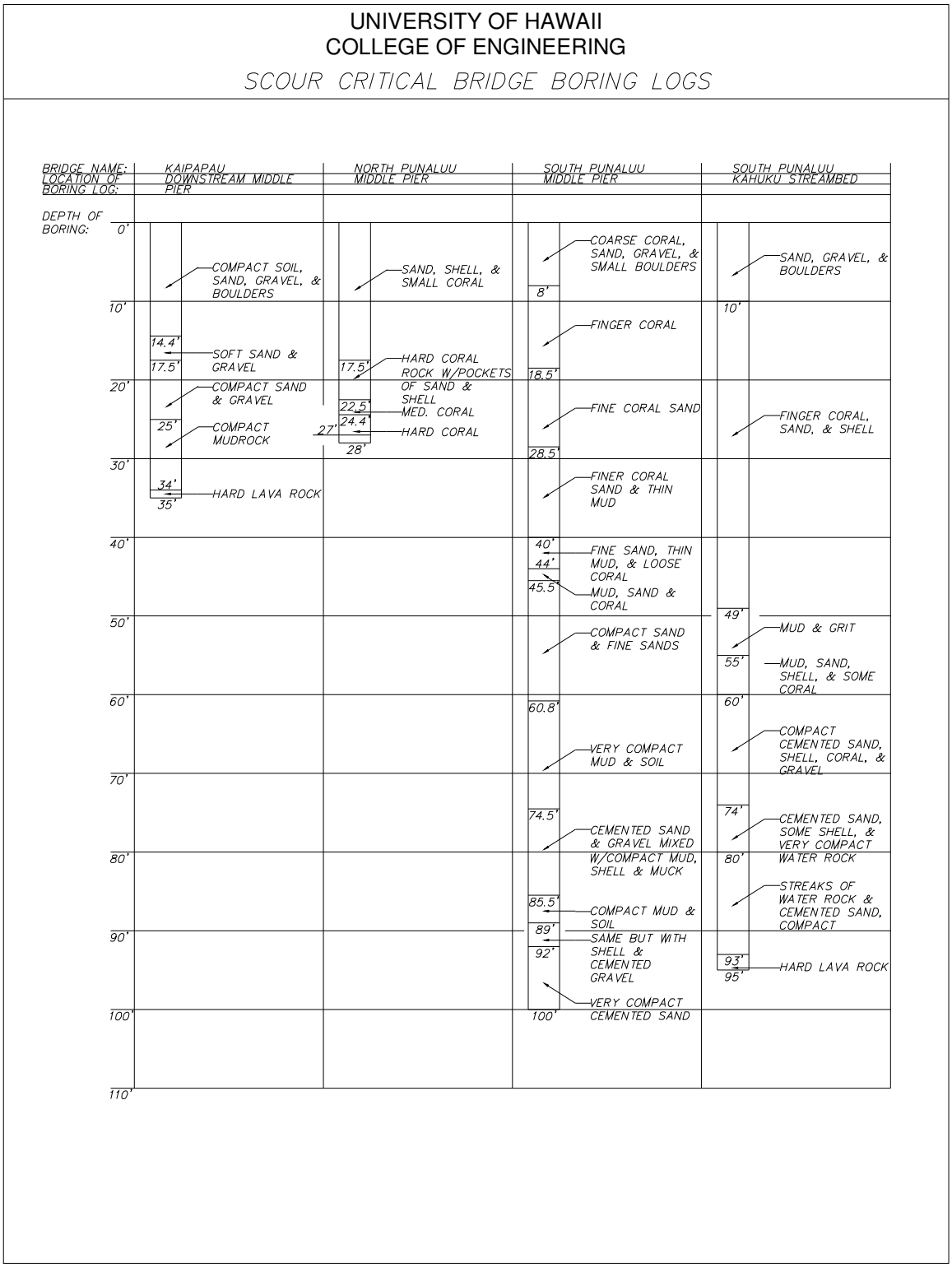


**Figure 3-28:** Boring logs of scour critical bridges

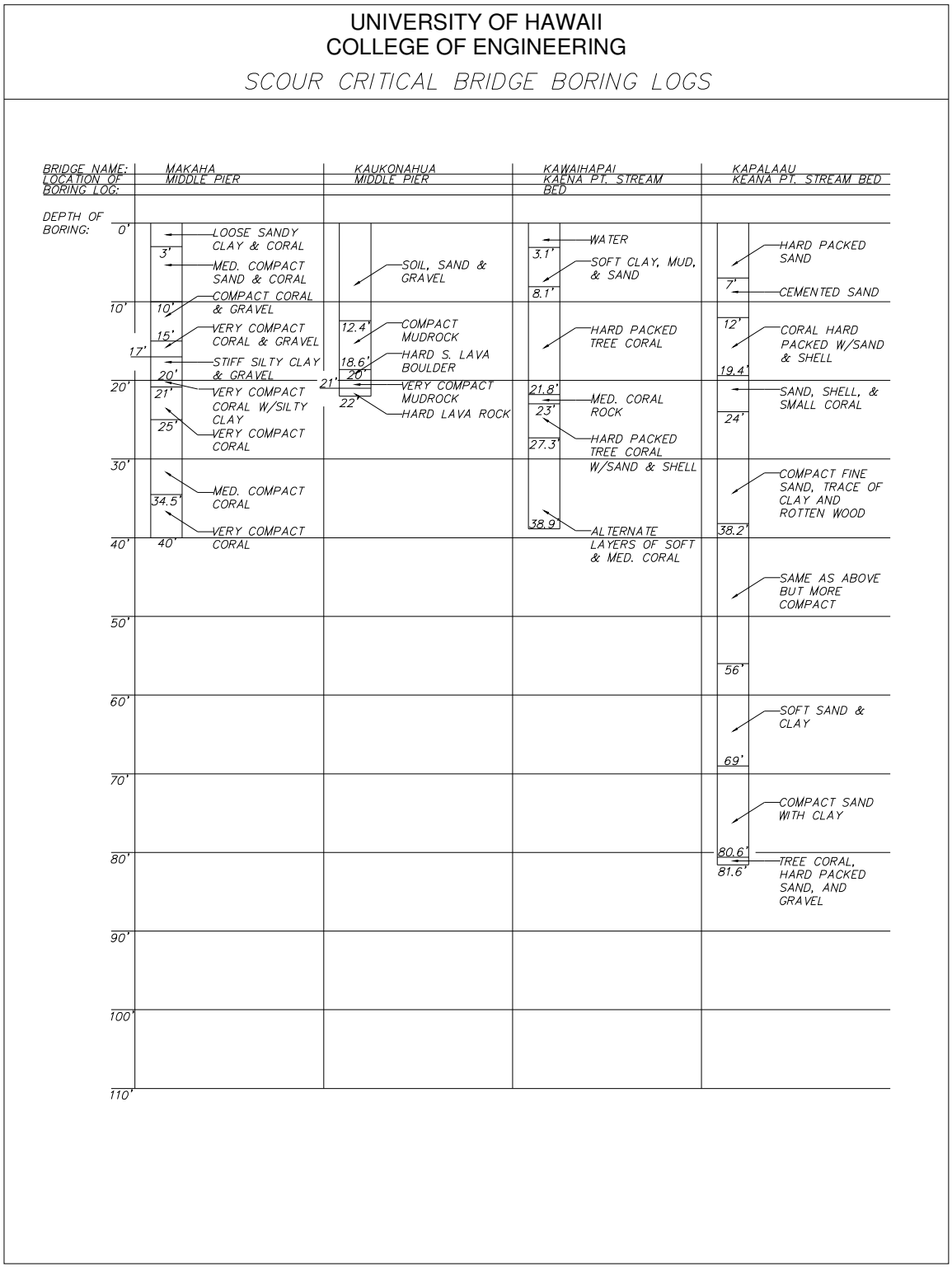


**Figure 3-29:** Boring logs of scour critical bridges

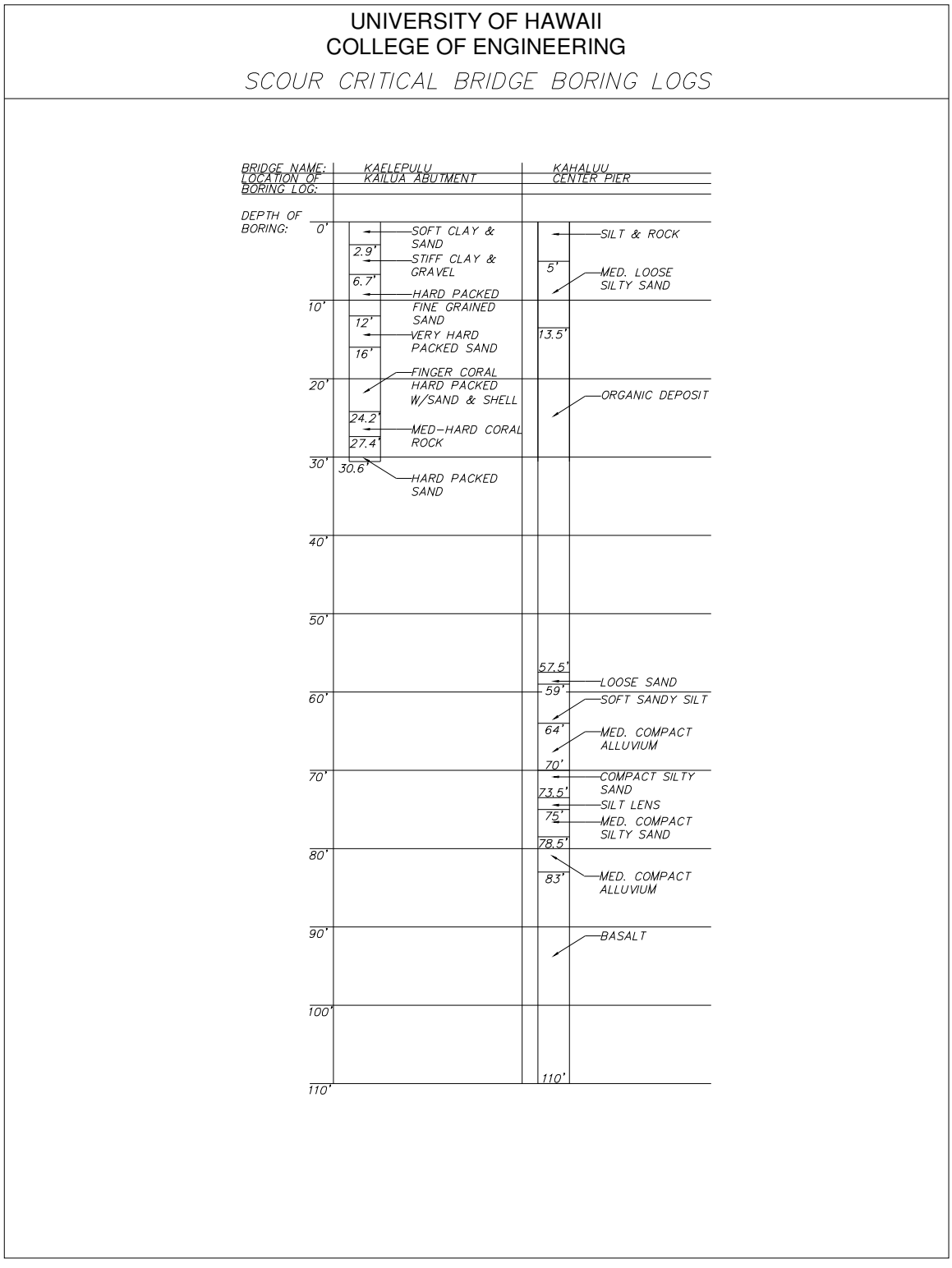


**Figure 3-30:** Boring logs of Kaelepulu and Kahaluu bridges

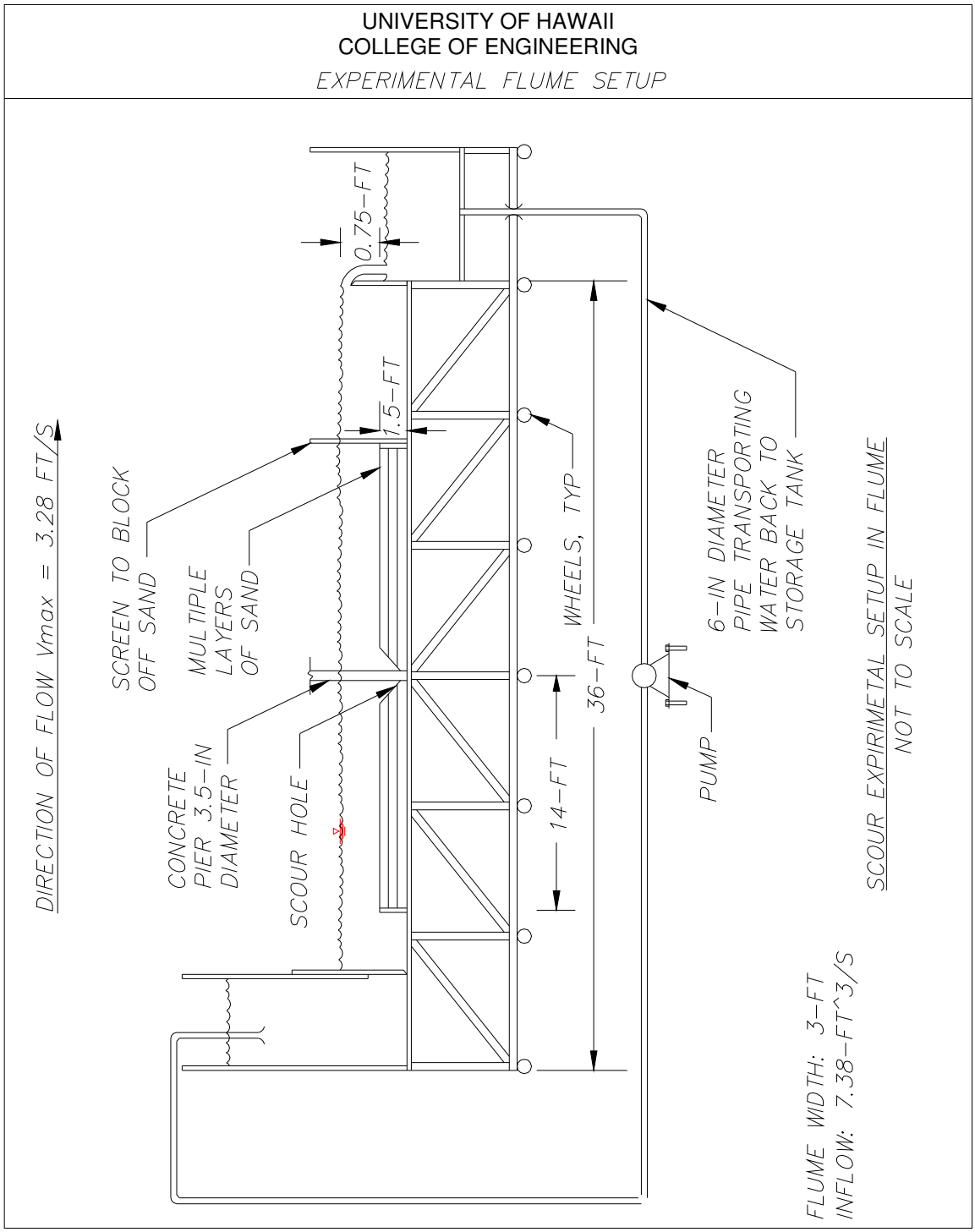


**Figure 3-31:** Experimental flume setup for multilayered scour

# CHAPTER 4 INSTRUMENTATION FOR MONITORING BRIDGE SCOUR

This chapter describes the different types of scour monitoring instruments installed on the selected bridges with discussions on the advantages and limitations of the instrumentation. Instrumentation installation will be described along with scour monitoring procedures. Finally, this chapter concludes with evaluations and recommendations on the instrumentation for applications to coastal bridges.

## 4.1 Description of Scour Measuring Devices

Instrumentation is an important part of monitoring scour at bridges. There are two types of instrumentation: fixed and portable. Fixed instrumentation, which includes the sliding magnetic collar and the active sonar scour monitor, are monitoring devices fixed on the bridge pointing at a certain location of the streambed. Portable instrumentation, which includes the portable sonar monitor and the sounding reel, are monitoring devices that can be moved to different locations to monitor scour. The objective of this section is to present each of the scour instrumentation, how they work, where they can be used, along with the advantages and limitations.

### 4.1.1 Fixed Instrumentation

The fixed instrumentation was developed, tested, and evaluated under National Cooperative Highway Research Program (NCHRP) project 21-3. This project duration ran from 1989 to 1996 and was split into three phases. Phase 1 was the development of scour monitoring

instrumentation with initial testing and cost analysis. Phase 2 was to test the instrumentation in the laboratory and field. Phase 3 consisted of the completion of field-testing and documentation. The results of project 21-3 were published under NCHRP Report 396. 397A, and 397B by the Transportation Research Board in 1997.

The first fixed instrumentation to be discussed is the sliding magnetic collar (ETI Inc., scour tracker model SMC-3). The sliding magnetic collar is a low-cost scour sensor developed to monitor smaller bridges with less severe scour and where more expensive monitoring instrumentation would not be feasible. This measuring device consists of sensors and instruments supported by a vertical member such as a pipe, which is driven into the streambed at a scour critical location (Figure 4-1). A magnetic sliding collar is placed around the pipe and moves freely downward as scour progresses. Sensors run inside the pipe that can detect the location of the sliding collar using magnetic tracing. The signal runs to a datalogger, which records the location of the collar. The datalogger is connected to a remote computer through a phone line and modem. This enables the datalogger to be remotely activated and scour data to be automatically recorded and transmitted to the computer. For engineers concerned about the instrumentations affecting the depth of scour, experiments have determined that the sliding collar does not increase or decrease the scour at the installed location.

The advantages of the magnetic sliding collar include that it is a simple mechanical device and not affected by flowing debris. The limitations include that the installation of the buried pipe is difficult and may cause damage to the sensors (since installation procedures require that the pipe be hammered or vibrated into the ground). In addition since the pipe is supported by the streambed, severe scour might cause the sliding collar to fail since the pipe length will be unsupported. Furthermore, the sliding collar only moves downward and therefore

only records the maximum scour for the largest storm but not scour for multiple storms. In addition the sliding collar only records scour at 6 in intervals as explained in section 3.4.2.3. Table 4-1 and 4-2 present the applicability of the magnetic sliding collar to different parts of the bridge and types of soil. More information on installation, operation, and fabrication of the magnetic sliding collar can be found in NCHRP Report 397B. This instrument has been mounted near the middle pier and the upstream abutment of Kaelepulu Bridge in the present study.

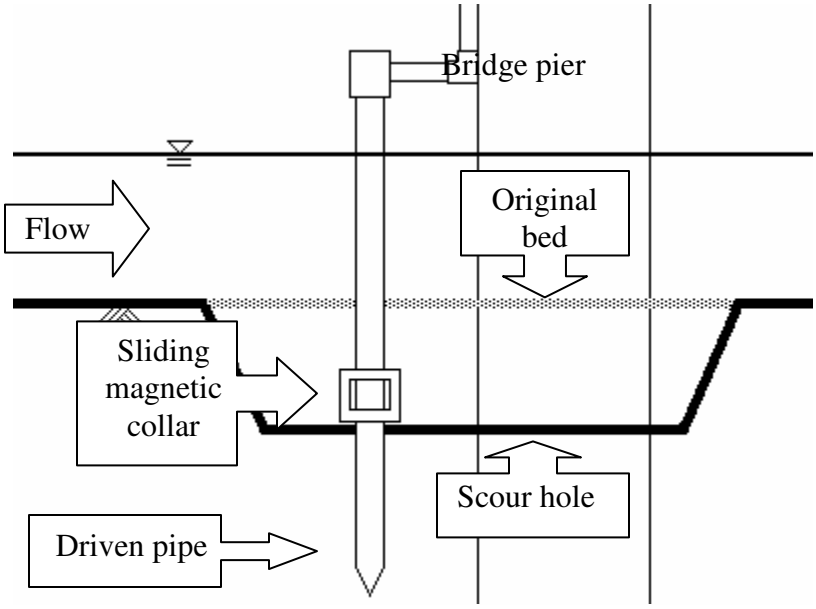


**Figure 4-1:** Magnetic sliding collar

**Table 4-1:** Applicability of scour measuring devices for pier and abutment geometry (Lagasse, et. al, 1997)

| Device Type | Piers | | | Abutments | |
|---|---|---|---|---|---|
| | Spread Footing | Sloping Column | Vertical Column | Vertical | Spill-Through |
| Magnetic Sliding Collar | Yes | Possible | Yes | Yes | Yes |
| Active Sonar | Possible | Yes | Yes | Yes | Possible |

**Table 4-2:** Applicability of scour measuring devices for geomorphic conditions (Lagasse, et. al, 1997)

| Device Type | Streambed Characteristics | | | Remarks/Warrants |
|---|---|---|---|---|
| | Sand Bed | Cobble Boulder | Silt/Clay Cohesive | |
| Magnetic Sliding Collar | Yes | Large bed material may preclude installation | Cohesive bed material may preclude installation | May require predrilling in coarse or cohesive bed streams. May require diver support in deeper water |
| Active Sonar | Yes | Yes | Yes | Ice and debris pose significant problems |

The second fixed instrumentation device to be discussed is the active sonar scour monitor (ETI Inc., scour tracker model AS-3). The active sonar monitor is suited for large bridges with deep water and no debris problems. Sonar measurement is based on the elapsed time that an acoustic pulse takes to travel from a generating transducer to the streambed and back (FHWA, 1998). Since the velocity of sound propagation in water is known (by calibration of the sonar instrumentation), the elapsed time can be converted to distance. The transducers are connected to a datalogger mounted on the bridge superstructure, which records the depth from the transducer to the streambed. Similar to the sliding magnetic collar, the active sonar monitor is connected to a remote computer through a phone line and modem.

The main advantages of the sonar scour tracker are that it can be used in deep water and provide a dynamic record of scour over time. The limitations include that the sonar cannot record data when it is above the water surface or too close to the streambed. In addition, the transducer must be positioned so that it does not record the bridge footing instead of the streambed. Also debris in the stream can give false sonar readings or block the sonar signal. Furthermore, there is a ±1-foot range of accuracy in the readings depending on the temperature and salinity of the water. Table 4-1 and 4-2 display the applicability of the active sonar monitor to parts of the bridge and types of soil. More information about installation, operation, and fabrication of the active sonar scour monitor is found in NCHRP Report 397A. This instrument has been mounted on Kahaluu Bridge on one of the center piers on the upstream Kaneohe section. Figure 4-2 displays a sketch of the active sonar tracker.

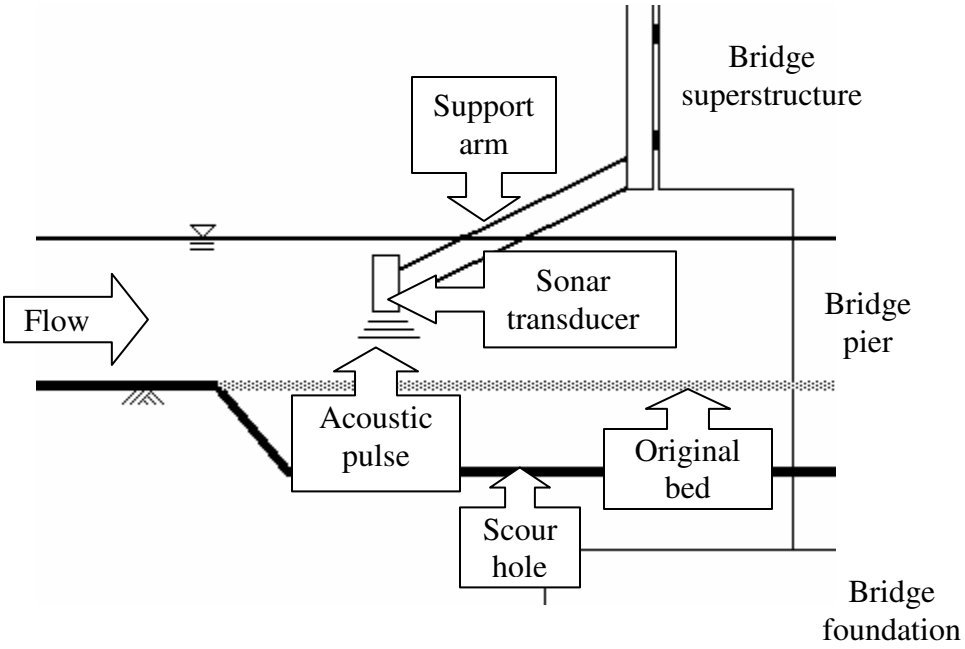


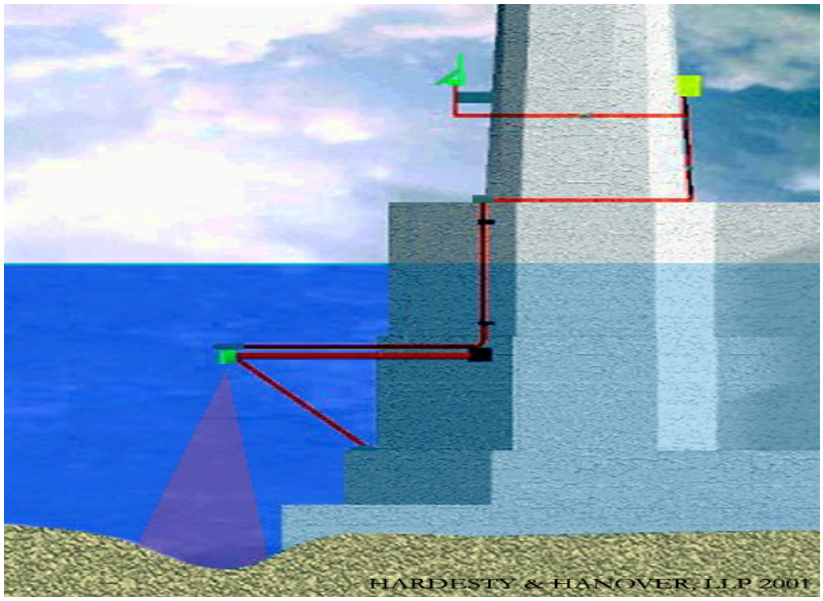


**Figure 4-2:** Active sonar scour monitor (ETI, Inc)

### 4.1.2 Portable Instrumentation

The first portable scour instrumentation is the portable sonar tracker, which works under the same physical principle as the fixed active scour monitor. A portable sonar device consists of a transducer connected to display, which reveals the water depth on a convenient LCD screen (Figure 4-3). The transducer is attached to a floating foam device, which is pulled on the surface of the water manually from a boat or on a bridge. The advantages of a portable scour tracker are that complete scour mapping of the bridge cross-section can be obtained, it is simple to use, accurate, and easily deployed. The limitations are that the floating foam device can be difficult to use under high flow conditions and the portable sonar can only be operated from low bridges because of restrictions on the cord length. In addition there is ±1-foot range of accuracy in the readings depending on the temperature and salinity of the water. This instrument was used to measure the scour depth at Kahaluu Bridge and Kaelepulu Bridge.

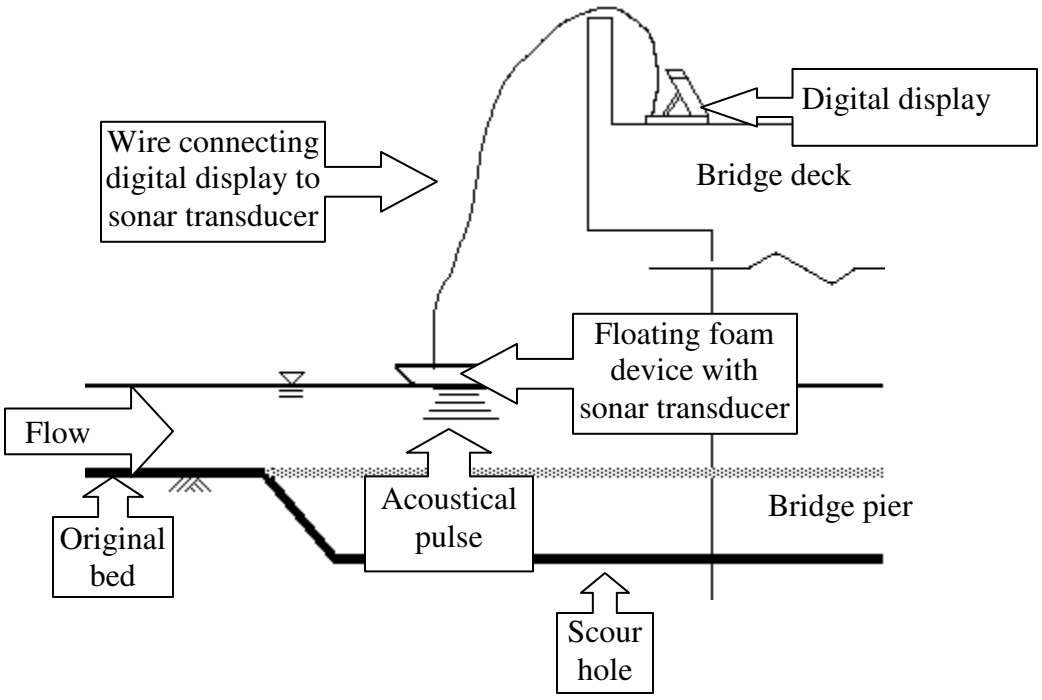


**Figure 4-3:** Portable sonar scour tracker

The last scour-monitoring instrument reviewed is the sounding reel (Figure 4-4), which consists of a digital suspension cable with a heavy weight fastened to the end. The cable is lowered from a bridge (using an USGS bridge board) or boat into the stream until the heavy weight hits the streambed. The scour depth is determined by measuring the amount of cable submerged in the stream. The cable is lowered manually or by using a cable reel, which contains an odometer for measuring the amount of cable deployed. This instrument is not suitable under heavy flow conditions since the flow rate might deflect the cable, resulting in an incorrect reading.

The sounding reel is also equipped with a Price meter, which measures the velocity of the stream. The Price meter is attached to the weight and is lowered by the digital suspension cable running from the sounding reel. The digital suspension cable has wires inside that transmit the data from the Price meter to the digital flow indicator, which conveniently displays the stream velocity. The Price meter consists of 6 “bucket wheels” which rotate around a pivot. The Price meter works by recording the number of revolutions the “bucket wheels” complete over time. For example if the streamflow causes 40 revolutions of the Price meter in 40 seconds, the stream velocity is 2.23 ft/s.

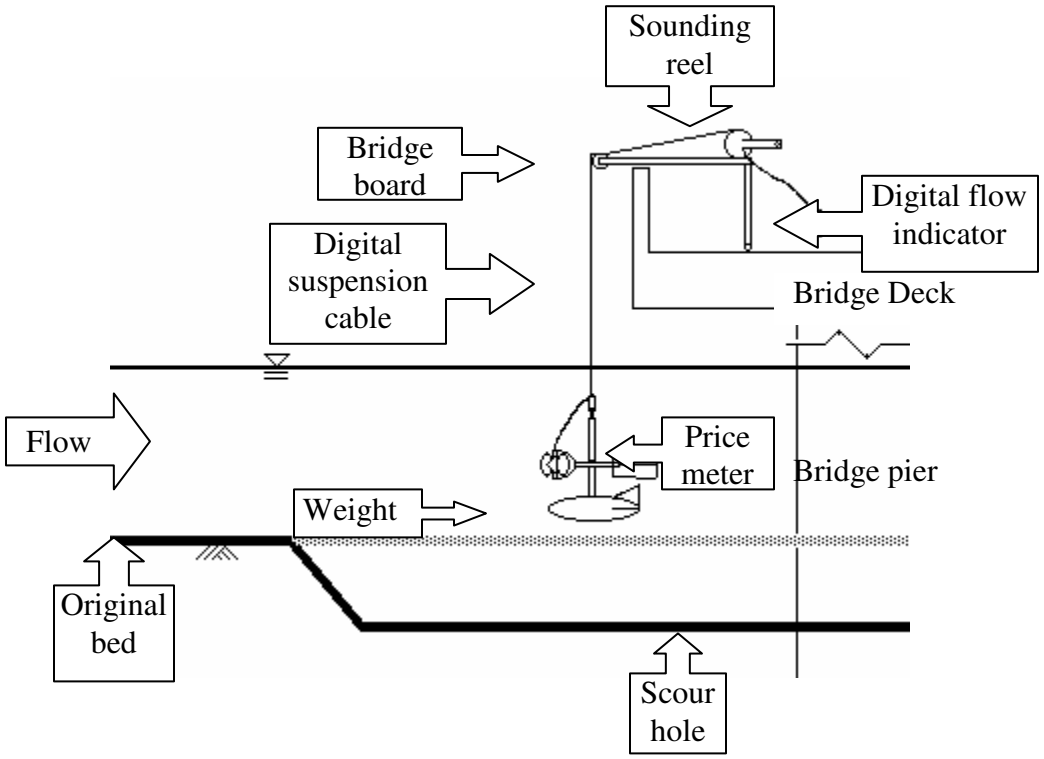


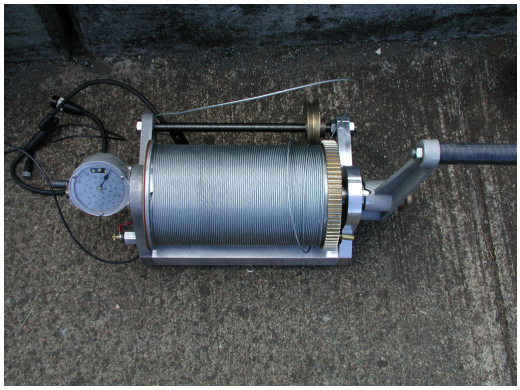

**Figure 4-4:** Sounding reel and Price velocity meter

## 4.2 Installation and Performance of Fixed Scour Measuring Devices

This section presents the research group's actual observations of the scour monitoring instrumentation. The prior sections were taken from manuals and workshops while this section describes the actual installation, calibration, and monitoring procedures undertaken by the author of this thesis for the instrumentation. The end of this section summarizes the authors' observations and presents recommendations for future studies.

### 4.2.1 Installation and Testing

The sliding magnetic collar was installed at Kaelepulu Bridge. A 10 ft long 1.5 in diameter aluminum support mast was mounted on the bridge parapet by two 10-inch long unistrut brackets and ½ in anchor bolts. The datalogger is enclosed in an electronic enclosure box, which protects the logger from vandals and the environment. The electronics enclosure box is connected to the upper portion of the support mast by unistrut pipe clamps. A solar panel orientated towards the sun (Figure 4-7), was attached to the lower portion of the support mast by unistrut pipe clamps. Flexible conduits connect the wires from the solar panel and the fixed instrumentation to the electronic enclosure box.

Prior to installation, the proposed site at Kaelepulu Bridge was probed by driving a steel rod into the streambed to determine if there is any obstruction that may damage the sliding collar and sensors during the hammering process. No obstructions were present and a drilling crew from GeoLabs installed the support masts (2 in diameter stainless steel pipe) using a drill and hammer mounted on a tripod. The collar was slid on the support mast and held in place by a rope so the collar would not be buried during the hammering process. Cables from the support mast run through 2 in and ¾ in PVC conduits and connect to the datalogger. The support mast was

installed at the center pier and abutment both at the upstream section of the bridge. See Appendix H for detailed drawings and pictures of the magnetic sliding collar installation on Kaelepulu Bridge. The following photos show the installation at the Kaelepulu site.

**Figure 4-5:** Installation of the magnetic sliding collars at Kaelepulu Bridge

**Figure 4-6:** The magnetic sliding collars at the middle pier and abutment at Kaelepulu Bridge

For Kahaluu Bridge, we installed the fixed active sonar monitor system. The pier transducer was extended and lowered into the water away from the bridge foundation and supported by a steel frame that is anchor bolted to the bridge pier. A 1 in PVC conduit was mounted on the bridge parapet connecting the wires from the transducer to the electronic enclosure box. Finally, the phone line was run from a telephone line through a ¾ in PVC conduit mounted on the bridge parapet to the electronic enclosure box. See Appendix I for detailed drawings and pictures of the installation of the active sonar monitor on Kahaluu Bridge. The datalogger, sonar panel, and phone line were connected to the bridge girder in the same manner as on the Kaelepulu Bridge. The installation is shown in the following photos.

**Figure 4-7:** Installation of the active sonar sensor at Kahaluu Bridge

**Figure 4-8:** The installed active sonar sensor at Kahaluu Bridge

After installation, the fixed scour measurement instrumentations was calibrated and tested for accuracy. The calibration consisted of surveying the Kaelepulu and Kahaluu Bridge for the elevations of the transducer and sliding collars then setting the datalogger program to those elevations. Surveying was needed to establish a reference measurement to base the depth of scour on. The testing consists of two steps, the first step was to test the wiring and phone connection and the second step was to verify the reading of the fixed instrumentation. To test the wiring, a call was placed to the datalogger, if the scour measurements recorded a large scour measurement such as -212.5 ft then the wiring is incorrect. The scour measurement readings from fixed instrumentation were verified by using the portable scour instrumentation.

### 4.2.2 Scour Monitoring

The scour monitoring consists of monitoring by fixed and portable scour trackers. The fixed instruments record the location of the streambed every 15-minutes during wet season and every 24 hours during dry season. The fixed instruments are connected by modem to a computer in the hydraulics laboratory at UH through the local telephone system. The computer activates the instruments and records the scour measurements remotely.

Everyday at 12:30 pm, the datalogger places a call to a phone number specified by the operator. The phone call leaves a voice message, which gives the measurement of the streambed and the battery voltage. The purpose of this call is to assure the user that the system is working properly. In addition, investigators can place a call any time to the datalogger on the bridge to check if the system is working. If there is a drop of streambed elevation of 2 ft or more, the datalogger automatically calls the operator with a warning so the bridge can be immediately investigated for potential of failure.

The portable scour instruments were used after heavy rains and routinely during the year. Since the fixed instrument can only measure the scour at the location where it was installed, it is important that the other piers and abutments be checked by the portable instrumentation for scour especially after rains and floods. The portable scour instruments can also be used to check the results of the fixed instrumentation and determine the bridge scour at every pier and abutment along the bridge cross-section. Once a month the instrumentation was manually inspected regardless of heavy rains or floods. This is necessary to check for damage due to vandalism and corrosion.

### 4.2.3 Comparison and Discussion

During the period of one year after installation, the portable and fixed scour instrumentation was analyzed for accuracy, installation ease, material cost, maintenance, and durability. Accuracy is checked by comparing the results between the instrumentation. Installation comparison is made from considering the effort involved in the mounting procedures and part fabrication. Material cost is the overall cost of materials used in installing and testing the instrumentation. Maintenance is measured by how frequent and expensive repairs are, since the instrumentation is in a highly corrosive and humid environment. Durability is how well the instrumentation endures damage from boats, debris, and vandals. This analysis will be useful in determining the feasibility for the HDOT to place instrumentation on more bridges in the state.

From personal experience using the scour monitoring devices on bridges in Oahu, the advantages and limitations to using each instrument are noted. These advantages and limitations are in addition to those noted in section 4.1.1 and 4.2.2. The portable sonar monitor, from ETI (assembly shown in Figure 4-3 and Figure 4-9), was tested at both Kaelepulu and Kahaluu Bridge and cost $650. The main advantages of the portable sonar are that it is easy to deploy (no assembly required) and operate (comes with a digital display). The assembly is small (entire assembly can fit in a backpack) and only requires one person to operate and map the bridge streambed. Other advantages include that little maintenance is required since the portable sonar monitor is easy to clean, has no metal in the portion that is exposed to water, and requires no additional parts. Limitations to using the portable sonar monitor include that it is difficult to keep the foam-floating device in an exact location because of the streamflow (as a result measuring scour in an exact location is difficult). In addition the sonar reads the streambed depth from the water surface not from a point with a fixed elevation (bridge), therefore the sonar reading will

vary with the waves. Furthermore the fish finder can not turn off so the battery must be recharged before going to the field. Lastly this particular portable sonar monitor came with no documentation on how to operate the fish finder.

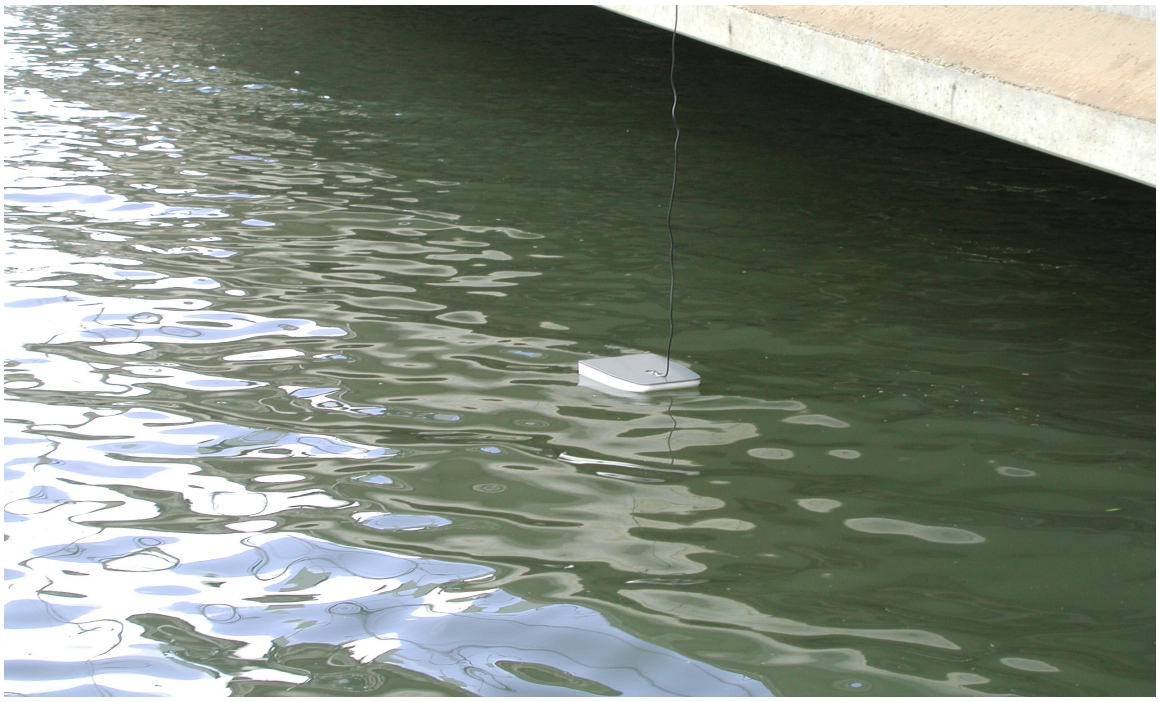

**Figure 4-9:** Portable sonar monitor at Kahaluu Bridge

The sounding reel, which is from Gurley Precision Instruments and cost $2115, was tested at Kahaluu Bridge (the sounding reel assembly is shown in Figure 4-4 and 4-10). The advantages of the sounding reel include that it can accurately measure scour and velocity in an exact location. The instrumentation is simple to assemble and includes an instruction manual with a parts list. Also no additional parts are required when the assembly is put together (all required parts come with the assembly). In addition the Price meter (instrument that measures water velocity) has other applications such as measuring the velocity in a laboratory flume. Limitations include that the sounding reel is heavy (excess of 60 pounds), therefore two people

are required to set up and operate it. The assembly consists of many costly parts that can easily be lost. The assembly also must be cleaned thoroughly after every use (a few seconds of use may require several minutes in cleaning and maintenance) to prevent corrosion of the reel and Price meter. Finally measuring the depth of scour in soft streambeds is difficult since the weight sinks in soft mud.

**Figure 4-10:** Sounding reel and Price meter at Kahaluu Bridge

The telemetry devices (Figure 4-11) are the equipments common to the fixed instrumentation such as the datalogger, solar panel, electronics enclosure box, phone lines, conduits, and mounting devices. The following two paragraphs discuss the advantages and limitations of the telemetry portions of the fixed instrumentations. The advantages include that the pieces needed to mount the electronics enclosure box and solar panel are inexpensive and commercially available. The instrumentation comes with documentation, which presents

instructions on how to mount and operate the telemetry devices. The datalogger requires no programming since the suppliers, ETI, programmed the datalogger for each bridge prior to shipping. Consequently the only procedure needed is to connect the wires and phone line to the electronics enclosure box. The instrumentation arrives with computer software designed to connect a remote computer to the datalogger over the phone line.

**Figure 4-11:** Telemetry devices at Kaelepulu Bridge

Limitations experienced when using the telemetry devices include that the modem settings are difficult to establish (the modem settings are necessary to connect a remote computer to the datalogger). The fixed instrumentation comes with many pieces that are subject to corrosion and algae growth, therefore frequent maintenance and inspection is required. The most annoying disadvantage with the telemetry instrumentation is that the datalogger does not always respond over the phone lines. For example if one should call the datalogger and hears a busy

signal, the result is that the voltage (should be above 13 volts) is low and inspection is needed to check the connections to the battery and the solar panel's alignment toward the sun. If the datalogger does not answer (only ringing is heard) then the datalogger or the phone line is damaged and needs to be inspected and/or repaired. If the datalogger answers the phone call and reports an incorrect reading the resulting faults may include that the line connecting the fixed instrumentation to the datalogger are damaged, not connected properly, or the instrumentation is damaged. The final disadvantage is due to the result of vandalism, where damaged conduit and pulled-out wiring are the most common problems. To prevent vandalism the conduits and telemetry devices should be out of sight, however this will increase the cost of installation and maintenance because it will be difficult to access the installation area.

The magnetic sliding collar assembly (Figure 4-1, 4-6, and 4-11), from ETI, costs $12,492 and includes three sliding collars, three support masts, conduits, datalogger and an electronic enclosure box. The advantages of the magnetic sliding collar, observed at Kaelepulu Bridge, include that the sliding collar can be installed at any location (only restricted by the contractor limitations and the hardness of the ground). Material costs are low since installation only requires the parts that come with the instrumentation in addition to commercially available conduits and mounting devices. Also marine growth does not affect the sliding collar results when installed in a coastal area. The main limitation to the magnetic sliding collar is that the installation requires an experienced contractor to install the support mast without damaging the sensors inside. Another limitation is that the support mast sticks out of the sand at certain locations, which may become a safety issue or subject to vandalism. The electronics enclosure box and locking mechanism is made from metal and may corrode, as a result regular inspections

are necessary. Lastly if one decides to remove the magnetic sliding collars and reinstall them on another bridge, an experienced contractor is needed to pull the support mast from the streambed.

The active sonar monitor assembly (Figure 4-2, 4-8) from ETI costs $8579 and includes three sonar transducers, a digital display, a datalogger, and an electronics enclosure box. The advantages of the active sonar monitor include that the device does not need an experienced crew to install. In addition little wiring is involved since only one wire runs from the transducer to the electronics enclosure box. Another advantage is the accuracy since it acts like the portable sonar fixed at a certain elevation, therefore the depth of scour is easily determined. In addition the electronics enclosure box is constructed from plastic to resist corrosion. Furthermore the sonar assembly can be easily removed from one bridge and installed at another bridge.

Observed limitations include the sonar transducer must be held underwater and away from the foundation at all times. This requires an experienced fabricator to build a hanging support arm for the transducer, which will increase the cost for extra materials and labor (cost the university over $800 in material cost for the support arm). The transducer assembly can damage passing boats if proper warning devices are not installed. Lastly marine growth can grow on the transducers and block the signal although the specifications say that the transducer can work through ½" of growth. Consequently routine maintenance is required to grind off the marine growth if the transducer is installed in a marine environment.

As stated in sections 4.1.1 and 4.1.2, the active sonar scour monitor and the portable sonar scour tracker have an accuracy of ±1 ft. Using the sounding reel to test the results of the sonar trackers showed that the sonar trackers have an error of a few inches under normal flow

conditions at Kahaluu Bridge. The readings of the sonar trackers should be verified often with the sounding reel to check for accuracy and obtain a range of error. If the error range is found to be minimal then the results of the sonar trackers can be used in the formation of Hawaii based scour equations. With the ±1 ft accuracy, the sonar tracker is satisfactory for bridge failure warning purposes.

From the preceding paragraphs each of the scour monitoring devices has its positive and negative aspects. For instance the portable sonar monitor is easy to use but the accuracy suffers since readings vary with wave height. The sounding reel gives accurate depth and velocity measurements in an exact area, but is heavy and requires two people to operate. The sliding magnetic collar is not affected by marine growth but is difficult to install and remove. The fixed sonar gives constant depth measurements and is relatively easy to move from bridge to bridge but expensive fabrication and constant maintenance is required. Each instrument has it uses for instance the portable sonar can be used for quick rough measurements such as finding scour locations. The sounding reel can be used after floods to record depth of scour. The magnetic collars can be installed at smaller non-major bridges and scour critical bridges where water does not flow year round. Finally the sonar monitor can be used on large bridges with year round flow where crews can easy mount and maintain the instrumentation.

### 4.2.4 Observed Damage at Scour Instrumentation during Storms

Two serious storms passed through the islands at the end of 2003 and the beginning of 2004. The first storm passed through on December 7$^{th}$ 2003, and the second January 2$^{nd}$ 2004. The fixed instrumentation suffered little damage to the heavy rains on December 7$^{th}$, but suffered serious damage due to the January 2$^{nd}$ storm.

On November 29th thru December 8th 2003, heavy rainfall swept across Oahu with the peak on December 7th. About 3 to 10 inches of rain fell on Kailua between November 29th and December 7th. According to Hawaii NWS (National Weather Service) provisional rainfall reports for December 7th, no rainfall was recorded at NWS Hydronet Automated Rain Gage network rain gage station at Olomana Fire Station (HI24) while 1.49 in was recorded at Maunawili (HI22). No movement of the abutment or pier magnetic collar was recorded and site investigations revealed no damage to the sliding magnetic collars and datalogger.

At Kahaluu watershed, Waihee Pump (HI30) and Ahiumanu Loop (HI16) rain gage stations recorded 7.54 in and 3.33 in respectively during December 7th, but the combinations of vandals and algae growth prevented the sonar scour monitor from recording the scour. This is unfortunate since the storm system dumped 22.49 inches of rain on the nearby rain station Ahiumanu Loop between the end of November and beginning of December.

At the start of the New Year, a second storm system moved across the state with the peak on January 2nd 2004. At Kahaluu, Waihee pump rain gage recorded 5.44 inches and Ahiumanu Loop rain gage recorded 6.26 inches over a 24-hour period. Before the New Year storm the instrumentation at Kahaluu Bridge was damaged by vandals. The steel support mast, which the datalogger is attached to, was bent to almost a 70-degree angle (Figure 4-12). Wiring was tampered with and fireworks were stuffed into the datalogger openings. Fortunately the datalogger still can receive calls and record measurements. Unfortunately the combinations of vandals and algae growth on the transducer prevented the sonar scour monitor from recording accurate scour measurements during the flood event at Kahaluu Bridge.

**Figure 4-12:** Damage at Kahaluu Bridge after New Years storm due to vandals

At Kailua 6.6 inches of rain was recorded at Maunawili and 4.72 inches at Olomana rain gage stations. The flow from the rain caused the streambed at Kaelepulu Bridge to be scoured away exposing the conduit connecting the abutment sliding magnetic collar to the datalogger. Previously the conduit was buried 1 to 2 ft below the streambed (Figure 4-13) to prevent tampering from vandals. One week later vandals damaged the exposed conduit probably by standing on it until the conduit cracked thus exposing the wires (Figure 4-13). Earlier in 2003 the decision was made to bury the conduit beneath the streambed since before then the conduit was above the streambed and visible to the naked eye. Once visible, vandals stepped on and damaged the conduit according to eyewitness accounts.

**Figure 4-13:** Damage at Kaelepulu Bridge after New Years storm due to vandals

### 4.2.5 Future Study

Future projects in scour monitoring instrumentation should include the use of a wireless phone connection. A wireless connection would be advantageous since it will save in labor and materials cost during installation (since a phone line must run from the telephone pole to the datalogger). Some bridges may lie in areas where there are no phone lines nearby. The instrumentation might also be installed on larger bridges with high flow rates, especially bridges on the neighbor islands. This would present a better analysis on installation, accuracy, and performance of the fixed instrumentation, since most scour critical bridges on Oahu have low flow rates or none at all most times of the year. The portable instrumentation would also benefit from being tested in deeper waters with higher flow rates.

# CHAPTER 5 COMPARISON BETWEEN MEASURED AND PREDICTED SCOUR DEPTH DURING THE JANUARY 2004 FLOOD

After the scour monitoring instrumentation systems were installed at Kahaluu Bridge and Kaelepulu Bridge, two major storm systems passed through the state. The first storm peaked on December 7th, 2003 and the second storm peaked on January 2nd, 2004. The objective of this chapter is to simulate the January 2nd storm over Kaelepulu Bridge using HEC-18 and HEC-RAS and compare the simulation results to the actual recorded scour depth. This comparison can help us to evaluate the accuracy and validity of the HEC-18 equations for predicting bridge scour.

## 5.1 January 2nd 2004 Storm

As described in the previous chapter, magnetic sliding collars were installed on Kaelepulu Bridge and sonar sensors were installed on Kahaluu Bridge. The data collected from the fixed scour instrumentation include the elevation of the magnetic sliding collars at Kaelepulu Bridge and the distance from the sonar transducer to the streambed at Kahaluu Bridge (See Masaki 2004 Appendix Section G.1 and G.2). The starting surveyed elevations of the sliding collar at Kaelepulu Bridge on March 29th, 2003, were -0.1 ft at the abutment and -3.3 ft at the pier.

Over the project duration the data logger recorded missing and erroneous data from the fixed scour instrumentation. The cause was due to damaged scour measuring devices from the environment and vandals. Frequent repairs were required which accounted for the missing magnetic sliding collar elevations in March 2003, missing sonar readings from mid July to

September 2003, and the erroneous sonar readings from September till 2004. For example the sliding magnetic collar was first installed in May 2002 but frequent vandalism required the sliding collar to be repaired multiple times with the final survey done on March 29th, 2003.

At the start of the New Year, a second storm system moved across the state with the peak on January 2nd 2004. In the Kailua area, 6.6 in of rain was recorded at NWS Hydronet Automated Rain Gage network rain gage stations at Maunawili (HI22) and 4.72 in at Olomana (HI24). From the storm the Kaelepulu Datalogger reported SMC movements at both the abutment and pier on January 2nd. The abutment SMC first moved between 6:30-pm and 6:50-pm from elevation 0.1 ft to –0.37 ft. At 11:20-pm to 11:35-pm the abutment SMC further dropped to an elevation of –1.37 ft for a total scour of 1.5 ft during the January 2nd storm. The pier SMC first moved between 12:05-pm and 6:05-pm where the SMC dropped from its original elevation of –3.3 ft to –3.8 ft. Then at 6:35-pm the pier SMC dropped to an elevation of –4.3 ft for a total movement during the January 2nd storm of 1 ft (total scour). Onsite investigations revealed evidence of the scour and no visible damage to the SMC or datalogger that would result in erroneous measurements.

## 5.2 Simulation of the January 2nd Storm over Kaelepulu Watershed

When heavy rainfall such as the January 2nd storm occurs and causes changes in the scour readings then the scour equations can be examined for their validity. This can be accomplished by obtaining the 15-minute rainfall recorded of the storm from NCDC or NWS rain gage networks. With the rainfall data, the storm can be simulated over the watershed using the Muskingum Method of hydrologic river routing to find the flow rate at the bridge. From the stage sensors mounted on the bridge, the stream surface elevation during the storm can be

determined. Now all the variables needed to calculate the depth of contraction and local scour are available and the HEC-18 equations can be compared and analyzed with the recorded scour depths. Fortunately scour readings and 15-miunte rainfall records are available for the January 2nd storm at Kaelepulu Bridge at the NWS Hawaii Website at http://www.prh.noaa.gov/hnl/hydro /hydronet/hydronet-data.php.

### 5.2.1 Muskingum River Routing

The process used to simulate the January 2nd storm over the Kailua area is known as hydrologic river routing using the Muskingum Method. River routing is a way to predict the outflow of a flood as it moves down a river. The basic Muskingum routing equation is shown in equation 5-1:

$$O_2 = C_o I_2 + C_1 I_1 + C_2 O_1 \tag{5-1}$$

$$C_0 = -\frac{K(1-C_2)}{\Delta t} + 1 \tag{5-2}$$

$$C_1 = \frac{K(1-C_2)}{\Delta t} - C_2 \tag{5-3}$$

$$C_2 = e\text{^}(-\frac{\Delta t}{K}) \tag{5-4}$$

$$C_0 + C_1 + C_2 = 1$$

where:

$O_1$ = Outflow rate for time interval 1

$O_2$ = Outflow rate for time interval 2

$I_1$ = Inflow rate for time interval 1

$I_2$ = Inflow rate for time interval 2

$C_0$ = Muskingum coefficient

$C_1$ = Muskingum coefficient

$C_2$ = Muskingum coefficient

$\Delta t$ = Time increment

K = Muskingum storage constant

Variables $I_1$, $I_2$, and $\Delta t$ are known from available rainfall data (converted into flow). The known data is lined into rows for each time increment. Variable $O_1$ is from the previous time increment while $O_2$ is the flow rate from the current time increment that is to be solved for using equation 5-1. At the next time increment $O_2$ becomes $O_1$ and $I_2$ becomes $I_1$. For the first time increment (start of recorded rainfall) $I_1$ and $O_1$ equals 0. At the completion of equation 5-1 for all time increments, an outflow hydrograph can be constructed at the downstream point.

### 5.2.2 Simulation Input Parameters

A map of Kaelepulu Watershed is shown in Figure 5-1. Local consulting firm Park Engineering (ParEn Inc.) delineated the watershed boundaries in their report to the City and County of Honolulu called "Kaelepulu Stream Drainage Study" dated 1993. In addition the map displays the location of Olomana Fire Station where the rainfall for the January 2$^{nd}$ storm was recorded. Although the rain gage is located outside the boundary of the watershed, this study assumes that the rainfall recorded at this gage would be recorded if the rain gage were in any location within the watershed. Another rain gage is located within the watershed boundaries at Kailua Fire Station but the 15-minute rainfall recorded for the January 2$^{nd}$ storm at this gage has not been published yet.

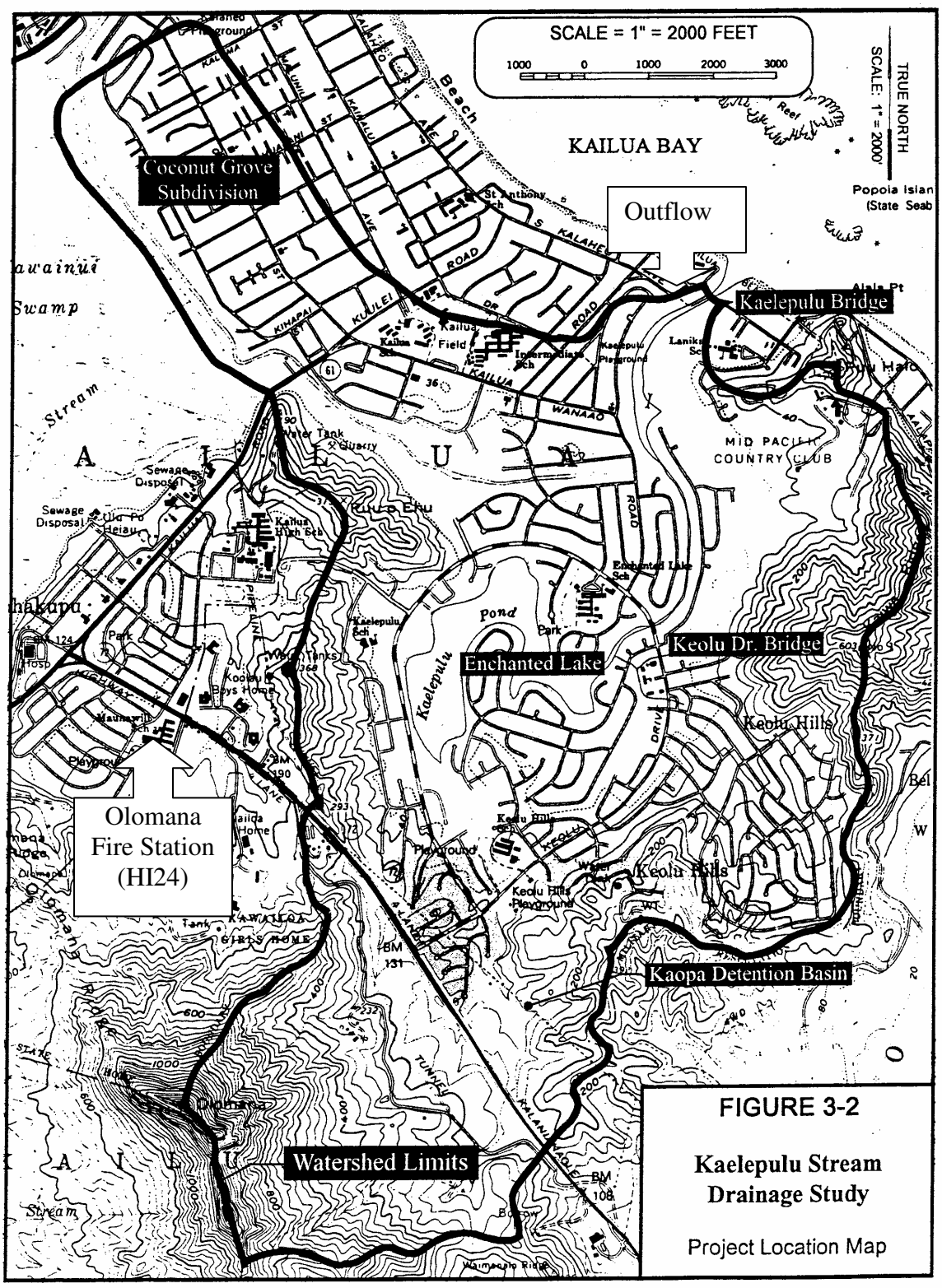


**Figure 5-1:** Kaelepulu Stream Watershed (ParEn Inc, 1993)

The first step in the Muskingum Routing procedure is to obtain the 15-min rainfall data and convert the values to runoff flow. For example at 4:00 pm on January 2nd, 0.1 in was recorded for an interval of 15-minutes at Olomana Fire Station. The average rainfall is 0.1 in/15 minutes or 0.1 in*(4.3 square miles)/15 minutes over the entire watershed. Converting this to cubic feet per second gives 1110.80 cfs in runoff.

The next step is to solve the Muskingum coefficients ($K_1$, K, $C_0$, $C_1$, and $C_2$). The variable K is obtained from the plot of watershed area versus recession constant $K_1$ for windward watersheds on Oahu developed by I-Pai Wu (1969) from his regression analysis and hydrograph study of watershed variables on Oahu. From Figure 5-1 with the watershed area of 4.3 $mi^2$, $K_1$=1.27 hours therefore K=1.18 hours, then from equations 5-2 to 5-4, we found that $C_0 = 0.099$, $C_1 = 0.092$, $C_2 = 0.808$. Using these variables with $\Delta T = 0.15$ hours (15 minutes) and equation 5-1, the direct runoff hydrograph can be constructed.

The final step is to account for runoff losses due to the water infiltration of the soil. This is determined from the engineering properties of the watershed soil types found in Soil Survey Maps published by the Soil Conservation Service (now National Resources Conservation Service, abbreviated NRCS in short) in 1969. An effective runoff value of 60% was used in this watershed based on a prior study by Edmond Cheng, who performed hydrological analysis of the neighboring Makawao Watershed, which has similar soil types as Kaelepulu Watershed. Cheng determined the effective runoff coefficient for Makawao would be 55% (Cheng, 1992). Therefore a 60% effective runoff value was used for Kaelepulu Watershed. This would be a conservative value for Kaelepulu since the area is more urbanized than Makawao watershed.

### 5.2.3 Discussion of the Muskingum Simulation Results

From the Muskingum routing simulation results the runoff hydrograph was plotted over the magnetic sliding collar elevation movements recorded during the January 2nd storm on the same graph (Figures 5-2 and 5-3). In the plots the Muskingum simulation results are read from the left y-axis while the SMC elevation is read from the right y-axis. Figure 5-2 shows that the SMC began to drop in elevation due to scour at the rising portion of the hydrograph and that the biggest drop occurred at the peak of the hydrograph when the flow was about 918 cfs at 6:15pm. This validates the Muskingum routing simulation since the biggest drop/time occurred between 6:05 pm and 6:35 pm when the SMC dropped 0.5 ft at the simulated hydrograph peak flow.

Figure 5-3 presents the Muskingum routing simulated hydrograph flow versus the SMC elevations at the abutment. A 0.5 ft drop occurred between 6:35 pm and 6:50 pm while a 1 ft drop occurred between 11:20 pm and 11:35 pm. The plot of the SMC elevations at the abutment does not match up with the Muskingum routing simulation hydrograph since the largest drop did not occur at the hydrograph peak. This discrepancy is explained if one studies how the SMC operates. As the depth of scour increases, the SMC slides down a fixed pole, which has magnetic actuated switches every 0.5 ft. When the SMC triggers the magnetic switch, the electronics enclosure records the elevation of the switch. Hence the SMC only measures scour 0.5 ft at a time and there is no sudden drop in SMC elevations even though Figure 5-3 shows a sudden 1 ft drop between 11:20 pm and 11:35 pm. Since the SMC only records scour elevations in 0.5 ft intervals, the 0.5 ft interval magnetic switch between -0.371 ft and -1.371 ft was never recorded. In addition since the SMC records scour at 6-inch intervals, a scour of 1 in above the 6-inch switch would be recorded at the elevation of the prior 6-inch switch while 5 in below the 6-inch

switch would be recorded at the elevation of that switch. Factoring this in, there is a possibility that the biggest drop elevation occurred near the peak of the hydrograph.

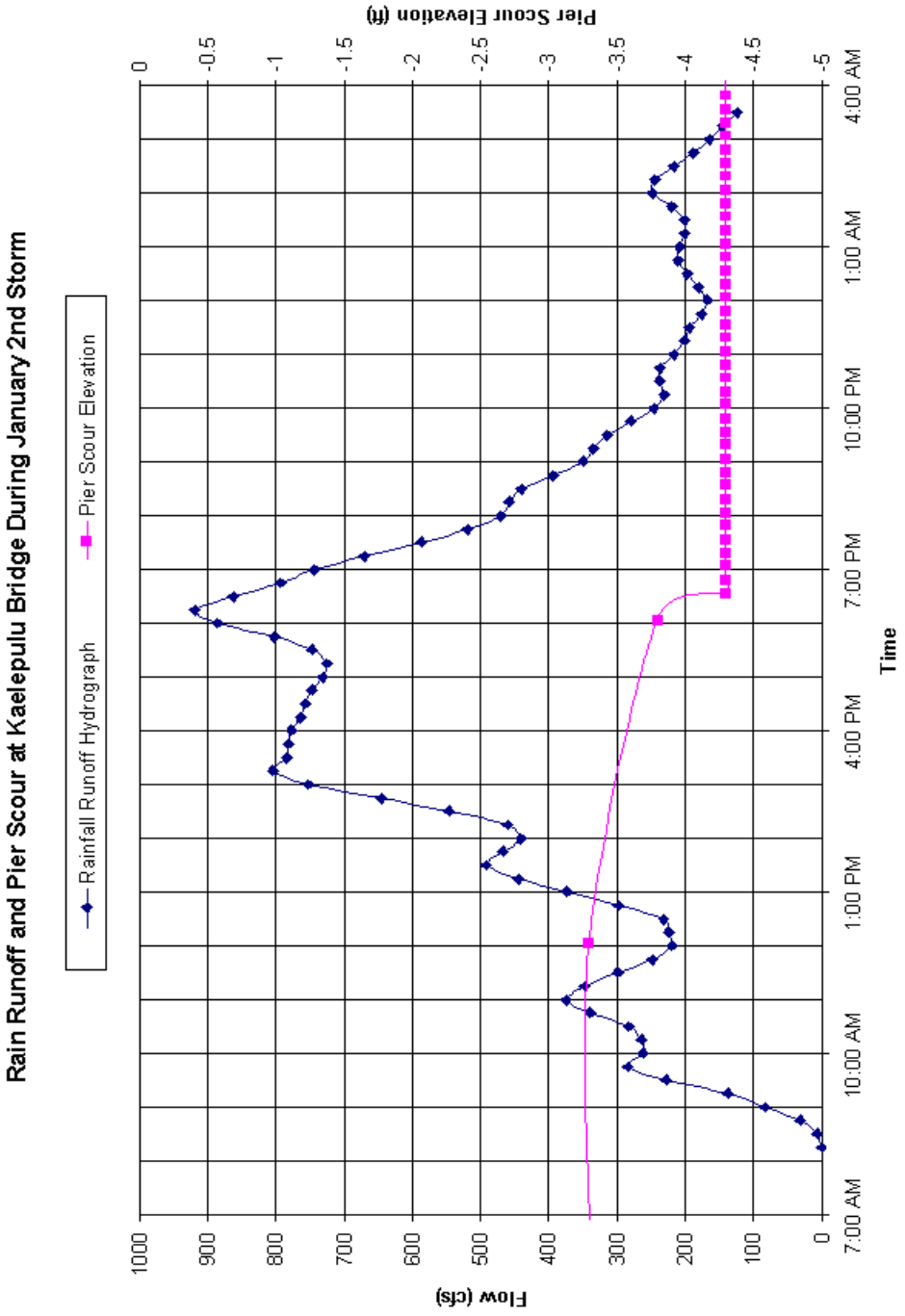


**Figure 5-2:** January 2nd simulation and scour results at Kaelepulu Bridge Pier

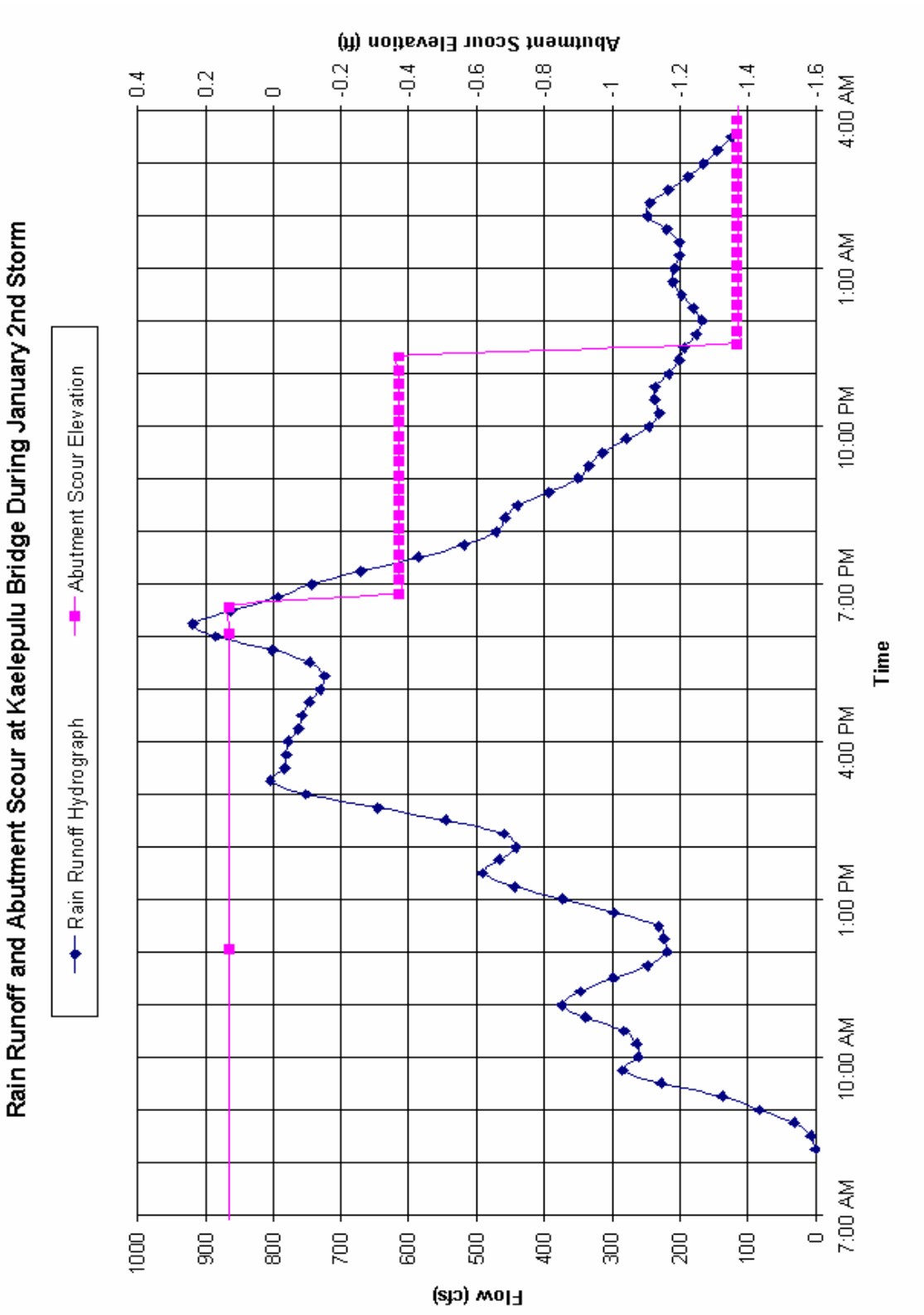


**Figure 5-3:** January 2nd simulation and scour results at Kaelepulu Bridge Abutment

## 5.3 HEC-RAS Scour Results Using Muskingum Simulated Hydrograph

Using the results of the Muskingum simulated hydrograph, we were able to simulate the January 2nd scour analysis of Kaelepulu Bridge using HEC-RAS. Input parameters included the simulated peak hydrograph flow of 918 cfs and the water surface elevation at the bridge of 2.6 ft (elevation recorded by a stage sensor at the time of peak flow). The starting streambed surface elevation was assumed to be of 0.129 ft (the abutment SMC elevation prior to January 2nd) and that the elevation was uniform across the width of the streambed. To obtain an accurate comparison, the field conditions on January 2nd were modeled in HEC-RAS. The field conditions include the sand plugging of the flow area near the bridge abutment and pier sections. The sand covers approximately 40-50 feet of flow area through Kaelepulu Bridge. In addition 6 ft wide and 3 ft deep scour holes were added to each sharp-faced pier (Figure 5-4), since from numerous site visits to Kaelepulu Bridge, scour holes were noticed at each of the sharp-faced piers approximately 3 to 4-ft deep. The remaining HEC-RAS input parameters are similar to that of Section 3.2.1.1.

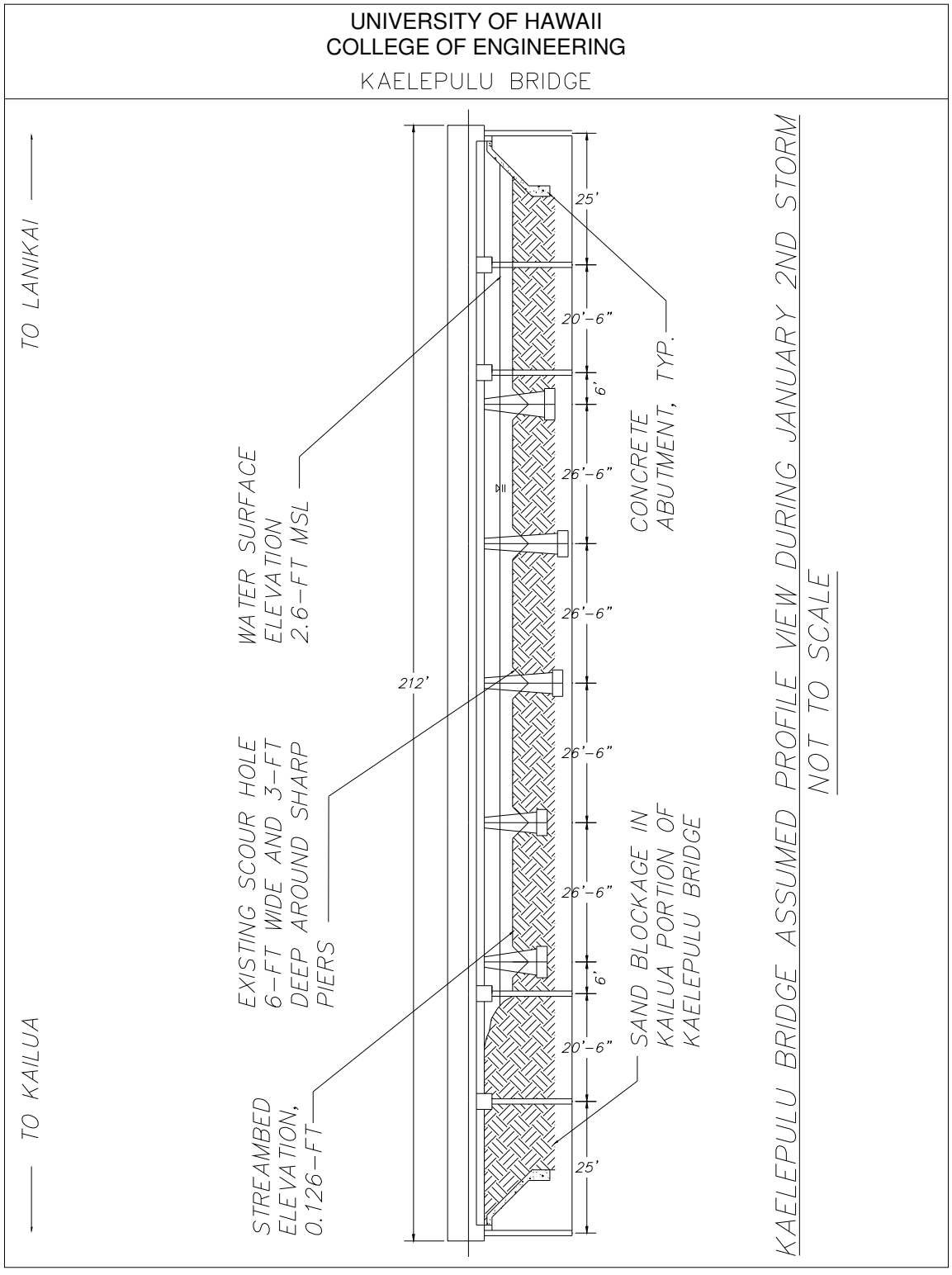


**Figure 5-4:** Profile of Kaelepulu Bridge before January 2nd storm

The result of this HEC-RAS analysis is shown below:

```
Hydraulic Design Data
Contraction Scour
Input Data
  Average Depth (ft):                 2.82
  Approach Velocity (ft/s):           1.65
  Br Average Depth (ft):              2.79
  BR Opening Flow (cfs):              918.00
  BR Top WD (ft):                     141.02
  Grain Size D50 (mm):                0.19
  Approach Flow (cfs):                918.00
  Approach Top WD (ft):               196.72
  K1 Coefficient:                     0.590
Results
  Scour Depth Ys (ft):                0.64
  Critical Velocity (ft/s):           1.14
  Equation:                           Live

Pier Scour
  All piers have the same scour depth
Input Data
  Pier Shape:                         Sharp nose
  Pier Width (ft):                    3.00
  Grain Size D50 (mm):                0.19000
  Depth Upstream (ft):                4.05
  Velocity Upstream (ft/s):           2.00
  K1 Nose Shape:                      1.00
  Pier Angle:                         25.00
  Pier Length (ft):                   33.00
  K2 Angle Coef:                      3.00
  K3 Bed Cond Coef:                   1.10
  Grain Size D90 (mm):                0.49000
  K4 Armouring Coef:                  1.00
  Set K1 value to 1.0 because angle > 5 degrees
Results
  Scour Depth Ys (ft):                10.39
  Froude #:                           0.17
  Equation:                           CSU equation

Combined Scour Depths

  Pier Scour + Contraction Scour (ft):
       Channel:       11.03
```

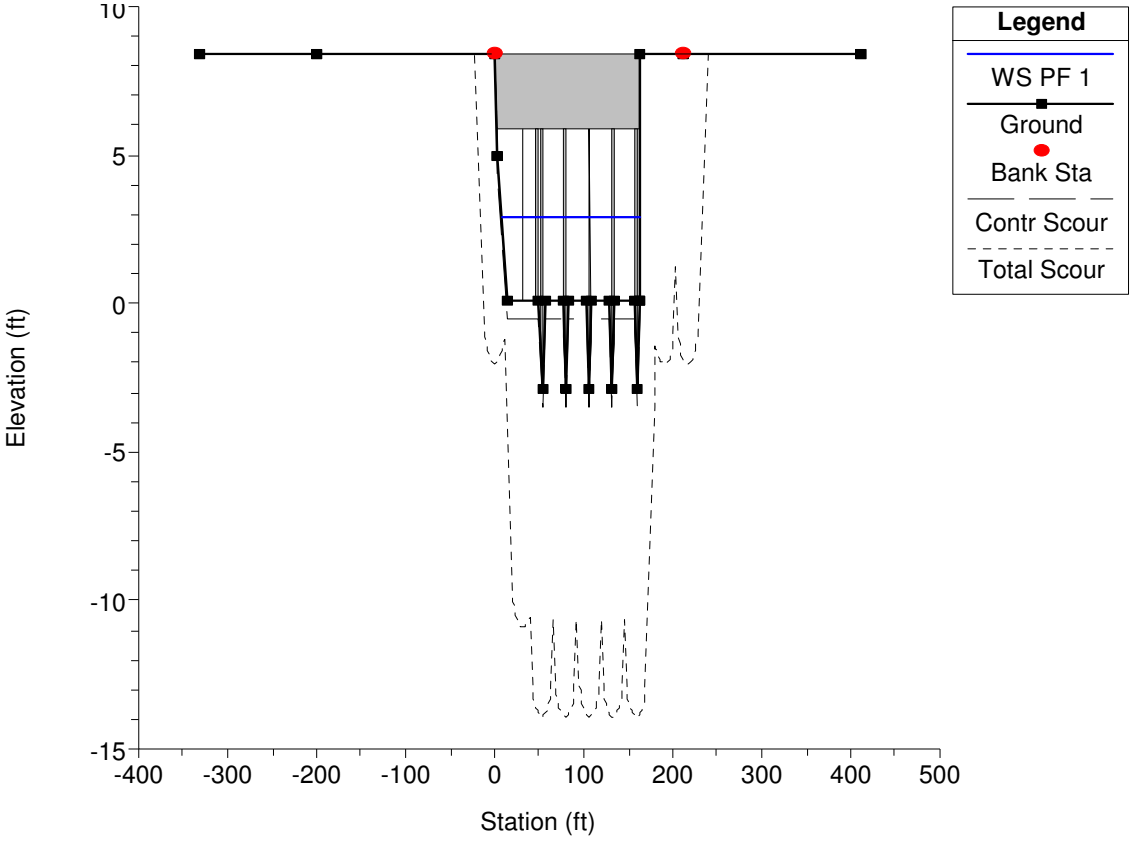


**Figure 5-5:** Simulated scour at Kaelepulu Bridge during the January 2nd storm

The scour information from Figure 5-5 and the Hydraulic Design Data shown above was compared to the actual SMC scour data from the January 2nd storm. HEC-RAS simulation computed scour near the abutment to be –7.89 ft MSL while the abutment SMC recorded a scour hole depth elevation of –1.371 ft MSL. For pier scour, HEC-RAS used the sharp-faced piers aligned 25 degrees to the flow. Using HEC-RAS, the scour hole elevation near the middle pier was found to be -13.89 ft MSL, which is more than the actual recorded scour elevation depth of -4.3 ft MSL at the pier.

From this information we can see that the scour equations from FHWA HEC-18 overestimated the total scour at the pier and near the abutment. This overestimation is due to the fact that at this bridge site, hard coral rocks exists at a shallow depth (<7 ft) and can greatly limit

the scour depth during a flood. In the simulation, this actual condition cannot be considered based on existing scour equations. Another factor for the overestimation is due to the geometric properties of the bridge since the HEC-18 pier scour equations heavily relies on factors as pier width, length, and pier alignment to the flow. The difference in scour depths can be also be traced to other errors such as the routing process that may have affected the flow rate.

## 5.4 Discussions

From available scour readings and on-sight investigations, the largest magnitude of scour for the bridge occurred at the pier. Over the duration of the project, both the abutment and pier SMC moved. The pier SMC started at a survey elevation of –3.3 ft that was an existing local scour hole caused by the normal flow of Kaelepulu Stream and the tides of the ocean. During the heavy rains over the New Year, the pier scour hole further deepened by 1 ft. and the abutment SMC moved about 1.5 ft during heavy rainfall therefore. Similarly to Kaelepulu Bridge, Kahaluu Bridge experienced scour at the pier over the duration of the project. Kahaluu watershed did not experience any heavy rainfall when the change in scour depth occurred which may be caused by the tidal effect.

In addition to local and contraction scour there is also long term streambed elevation changes known as aggradations and degradation. The standard HDOT practice for long-term streambed changes is to compare the present streambed elevation with the streambed elevation listed on the bridge plans. If the present streambed elevation is greater than the elevation listed on the bridge plans then aggradation occurs and long-term elevation changes are not considered in the scour analysis. If the present streambed elevation is lower than the elevation listed on the bridge plans then degradation occurs and long-term elevation changes are factored in the scour

analysis. For bridges across a tidal inlet, they may also experience seasonal streambed elevation change due to sand build-up induced by tidal action. For Kaelepulu Bridge the streambed elevation on the bridge plans is at –4 ft while the surveyed streambed elevation was at 0.1 ft in this project. As stated earlier in this report most times during the year sand fills the mouth of Kaelepulu stream and the water does not reach Kailua Bay. Normally flow does not occur except when the City and County periodically dredges the stream mouth. The streambed elevation of Kahaluu Bridge from the HDOT plans is –6.5 ft and the streambed depth at the time of surveying is –5.7 ft. For these two bridges aggradation at the streambed occurs and the seasonal change in streambed elevation effect of scour is ignored.

From the simulation of the January 2nd storms using the Muskingum Routing Method a hydrograph was developed with a peak flow of 918 cfs at 6:15-pm. This peak corresponds to the biggest recorded drop on the measured pier SMC movement of 0.5 ft in 15-minutes that verifies the results of the simulation. The flow rate was then used in a HEC-RAS simulation, which produced a scour elevation depth of –7.89 ft MSL near the abutment, and a scour elevation of -13.89 ft MSL near the pier as compared to the actual recorded scour hole elevation of -4.3 ft MSL near the middle pier and -1.371 ft MSL at the near abutment. The total predicted measured depth of scour was 8.02-ft near the abutment (+0.129 starting elevation and –7.89 ending elevation) and 11.03-ft at the pier (-2.871 starting elevation due to 3 ft deep existing scour holes and –13.89 ending elevation) as compared to –1.5 ft near the abutment and –1 ft at the pier. As noted earlier, the SMC only measured the streambed elevation in 6-in intervals thus possessing a potential error of ±0.5 ft. During the January 2nd storm the abutment SMC recorded elevation drop of 1.5 ft, factoring the error into account the SMC elevation drop could be in the range from 1.0 ft to 2.0 ft.

**Table 5-1:** Comparison between measured and predicted scour depth at Kaelepulu Bridge due to the January 2nd, 2004 flood

| | predicted scour depth (ft) | Recorded scour depth (ft) |
|---|---|---|
| pier | 11.03 | $1.0 \pm 0.5$ |
| abutment | 8.02 | $1.5 \pm 0.5$ |

The significant discrepancy between the measured and predicted pier scour depth show that the HEC-18 scour equations may overestimate the local scour at the piers and the abutment by a large margin. The HEC-18 equations may need to be modified to improve its accuracy by considering non-uniform streambed material through further experimental and field studies.

# CHAPTER 6 SUMMARY AND CONCLUSION

In this research project, a combined hydrological, computational and field monitoring study was carried out to investigate the problem of bridge scour on Oahu Island in Hawaii. The following sections summarize the specific tasks performed and results obtained:

1. Statistical analysis of updated rainfall data (up to 2002 during the project period) for selected watersheds on Oahu was performed. By comparing the current results with the results based on older rainfall records to the 1970s, it was found that rainfall maps of Oahu published in 1984 (DLNR R-73) show little deviation from the updated (as updated as 2002) frequency analysis of 8 rainfall records from gages across Oahu for storm durations of 10 years, 50 years, 100 years 24-hour rainfall in the present study. However, updated rainfall maps for the entire state are needed since the neighbor islands rely on maps published in 1962 (Department of Commerce TP-43) as the 1983 study did not include the neighbor islands. The present study found that rainfall values from the TP-43 rainfall maps differ from current rainfall analysis by 20-30% for some rain gage stations on Oahu.
2. Streamflow analysis using rational method, City and County of Honolulu Plate 6 Method, USGS Regression Equation Method, and the NCRS TR-55 Method was carried out to predict stream discharge under different flood frequency on Oahu. The predicted values were compared with the results based directly on the streamflow frequency analysis of 9 streamflow records measured by gage stations around Oahu. Findings from this study revealed that the rational method and Plate 6 did not compare well while the USGS Regression method did. This study concludes that the Regression method compared well since the method is based on the frequency analysis of stream gage records. The TR-55

method involves more hydrologic input parameters, which is subjective to whomever is applying it.

3. Analysis to predict 500-year streamflow was performed on the 9 stream gage records by extending the Log-Pearson III curve from 100-years to 500-years. Current FHWA practice assumes the ratio between the 500-year flood flow to the 100-year flood flow to be 1.7. This analysis reports that the average value for the ratio on Oahu is 1.41 slightly smaller than 1.7. However, 1.7 seems to be a conservative upper limit ratio of Oahu streams and can be considered as a satisfactory assumption for Hawaii.
4. Scour analysis of two selected bridges on Oahu, namely, Kahaluu Bridge and Kaelepulu Bridge, was performed using the HEC-RAS computer package. Results of this study determined that Kahaluu Bridge should not fail due to scour during a 100-year flood as Kahaluu Bridge has foundations that extend past the maximum depth of scour. Further investigation is needed for Kaelepulu Bridge since the piers for this bridge are supported on unknown foundations that might be undermined during a flood. In addition, the boring log as well as samples obtained in the present study during drilling at the site showed that the streambed material at Kaelepulu Bridge is complex and non-uniform. Hard coral rocks start to appear at shallow depth. The current existing scour prediction equations mostly assume bed material of fine particles and do not account for the effect of large rocks adequately. As a result, the scour prediction based on the existing equations over-estimates the scour depth at a bridge site such as Kaelepulu Bridge.
5. Sensitivity analysis of 100-year flood scour on the two bridges demonstrated that contraction scour is a small part of the total scour for these bridges. Changing the streambed grain size (i.e., $D_{50}$) by 20% will have no effect on the depth of the contraction scour based on the

existing equations. The foremost portion of total scour is found to be the local scour at piers where the most sensitive variable is the bridge pier alignment to the flow. Findings indicate that if the bridge piers are aligned 1 degree more from the flow then scour can increase by 1 ft.

6. According to boring logs of the scour-critical bridges on Oahu, the streambeds often consist of different layers of soil within a depth that is susceptible to scour during a flood. Current practice is to assume that the entire depth of the streambed consists of the worst soil with the smallest $D_{50}$. This can over-estimate the scour depth greatly. An indirect HEC-RAS analysis based on a new multilayered approach in the present study determined that analyzing the streambed using layers would reduce the depth of contraction scour and save the cost of new bridge construction. More research is needed to develop multilayered approaches for scour prediction for piers for cases with cohesive soils.
7. This study is the first in Hawaii to monitor bridge scour in the field. In this study, two types of state-of-the-art fixed scour sensors with telemetry were installed on two selected bridges on Oahu, specifically, the sliding magnetic collar on Kaelepulu Bridge and the active sonar monitor on Kahaluu Bridge, in order to monitor bridge scour and collect valuable field data during storms and floods. In addition, portable sensors such as the portable sonar monitor (developed from fish-finders) and sounding reel were also tested and evaluated. Table 6-1 below summarizes the main advantages and disadvantages of the instrumentation experienced over the project duration.

**Table 6-1**: Scour monitoring instrumentation advantages and liabilities

| Instrument | Advantage | Disadvantage |
|---|---|---|
| Portable Sonar Monitor | Easy to use and requires little maintenance. | Accuracy suffers since readings vary with wave height. Difficult to keep in an exact location. ±1 foot of accuracy. |
| Sounding Reel | Measures accurate depth and velocity in an exact area | Heavy and requires 2 or more people to operate. Many small parts in the assembly. Needs to be thoroughly cleaned after each use. |
| Magnetic Sliding Collar | Can be installed at any location and less maintenance required than the active sonar monitor. | Difficult to install and remove. Records scour only 6 in at a time. |
| Active Sonar Monitor | Accurate since it performs similar to a portable sonar monitor at a fixed location. | Expensive fabrication and constant maintenance is required. ±1 foot of accuracy. |

8. Movement of the magnetic sliding collar was recorded at Kaelepulu Bridge during the heavy rainfall of January 2nd of 2004. During the 24-hour period 4.72 inches of rain was recorded at nearby rain gage station Olomana Fire Station. The sliding magnetic collar moved 1.5 ft near the abutment and 1 ft near the center pier. The data were recorded based on 15-min intervals and therefore provided a clear and valuable field record of the dynamic development of the scour depth at the bridge during the storm. Muskingum method was used to route the streamflow from the gaging location to the bridge site. The results showed that the recorded maximum scour depth coincided with the peak flow at the bridge verifying that the recorded scour was indeed induced by the storm flow in the stream. The HEC-RAS computer package was then applied to simulate the hydraulics of the stream flow during the January 2nd, 2004 storm at the bridge site and the scour depth was predicted based on the existing empirical

equations. The predicted scour depth is about 11.03 ft compared to the recorded 1 ft at the pier and 8.02-ft compared to the 1.5 ft near the abutment. This result indicates that the current scour predicting equations given in FHWA HEC-18 may over-estimate the scour depth at both a pier and an abutment by a large margin in some cases.

We should mention that even though this study was the first in Hawaii to install sensors to monitor bridge scour, there exist a large amount of field data and prediction results on bridge scour from the US mainland (Jackson 1996, Miller and Wilson 1996, Mueller and Wagner 2005, Zhang et al 2013 among others). For example, the FHWA-RD-03-052 report (Mueller and Wagner 2005) "Field Observations and Evaluations of Streambed Scour at Bridges" includes field data on bridge scour from more than 200 sites and events. Comparison between the measured scour depth and the predicted scour depth was performed in order to evaluate and validate the existing scour equations. The report includes the evaluations of the HEC-18 equations as well as many other equations such as the Arkansas, Froehlich, Inlis-Poona I, Melvill & Sutherland, Mississippi, Shen, simplified Chinese equations and others for predicting pier scour. The results showed that most of the equations tend to over-estimate the scour depth, while the Arkansas equation consistently under-estimates the scour depth. These field data along with the available laboratory data have been very useful in improving the existing equations to make them more accurate. For example, researches have been studying whether a correction factor K4 should be added to the pier scour equation in HEC-18 so that the predicted scour depth can match the field data better.

Hawaii has unique stream and soil characteristics (for example, the Hawaiian sand may be more calcium-based than silicon-based). More field monitoring studies will be needed for collecting valuable field data for validating the HEC-18 equations for streams in Hawaii. The

current existing scour equations can be improved by adding a correction factor to them based on sufficient field data to be collected in Hawaii.

# PART II STUDY ON SAND PLUGGED HIGHWAY CULVERTS

# CHAPTER 7 INTRODUCTION

In a coastal state like Hawaii, the highway culverts near the shoreline are often found to be clogged by sand brought in by ocean tides. The sand blockage reduces the drainage capacity of a culvert and may cause serious highway flooding or "overtopping" by surface runoff during a storm. In addition, it may cause water backup and flooding of the nearby communities. How to mitigate the problem of sand plugged coastal culverts is of great interests to DOT design engineers.

**Figure 7-1:** Typical sand-plugged culverts on Oahu

Mitigation measures should involve two considerations. The first management measure is routine maintenance of a culvert, namely, the culvert is maintained free of debris to facilitate unimpeded surface runoff through a culvert. The second management measure is to assess the size and condition of the existing culvert and determine if the culvert can be self-cleaning of the sand blockage (i.e., sand being flushed out by the flood water naturally) during a storm. If the self-cleaning capacity is evaluated to be inadequate, then we are

interested in examining whether a detention pond can be added to help with opening the blockage in a flood event. Various combinations of the culvert size and the storage capacity of the detention pond may be appropriate to facilitate proper drainage of surface runoff.

To minimize overtopping of roadways for a design storm, the ability to keep drainage culverts clear of debris and/or sand blockage, and also to have an adequate combination of culvert size and detention pond storage capacity for a specific drainage basin are two key criteria for long-term management. In order to establish the management criteria, two tasks are undertaken in this project. The first task is to create a flood routing-based computational scheme. This simulation model considers the design storm, drainage area, detention pond, and culvert size as a system. For predicting whether a sand-blocked culvert may be opened by flood water or it may require manual cleaning, the second task is to build hydraulic models for selected existing culverts on Oahu in the Hydraulic Laboratory at the University of Hawaii at Manoa and perform flow measurement on the models. This study is intended to: (1) report the findings of observed ranges of time for the scaled culvert models to self-open under completely sand-blocked conditions; (2) compare the range of times observed in laboratory to the time for surface runoff overtopping the highway obtained from the simulation models; and (3) provide screening criteria intended to evaluate existing culvert and detention pond storage capacity measured against simulation models to assess likelihood for overtopping.

## 7.1 Technical Background

The northeastern portion of the island of Oahu, commonly known as “Windward” Oahu, is primarily made up of numerous small watersheds, characterized with steep valley walls and

relatively flat coastal regions. The surface runoff of the watershed moves from the steep valley walls toward the ocean. The coastal regions located at the base of the watershed are primarily urbanized with built infrastructure located relatively close to the ocean. Kamehameha Highway, the main arterial highway for Windward Oahu, is located along the "fringe" of the ocean shoreline. Developed urban areas are located inward toward the mountains of Kamehameha Highway, or "mauka" from the highway. The single highway transverses along the shoreline crossing numerous drainage culverts intended to minimize watershed runoff from overtopping the highway.

Many of the drainage culverts along Kamehameha Highway are located within very close proximity to the ocean shore, at generally low topographical elevations. These drainage culverts are continually exposed to ocean conditions and subject to sand and debris generated from the ocean currents and tides. As a result, sand frequently accumulates within the culvert outlet located on the ocean side of the highway during periods of frequent rainstorms. The accumulation of sand and debris in the culvert causes culvert blockage in a relatively short time.

The frequency required to clean and maintain an open culvert along Kamehameha Highway on Windward Oahu is not practically feasible as the large quantity of culverts and the rapid sand accumulation from continual exposure of the culvert to the ocean conditions that overwhelm available manpower from HDOT. To better manage available resources, it is of our and HDOT's interest to investigate whether a sand plugged culvert can self-open during a storm. Specifically, we would like to examine the time required for a completely sand-blocked culvert to self-open as a result of surface runoff (i.e., flood water flow) caused by a specified design storm. If the time required for a completely sand-blocked culvert to self-open is less than the time it takes the flood water to overtop the highway for the design storm, then we can say that

the culvert can self-open and self-clean during the storm. In this case, the frequency of manual cleaning of a culvert can be greatly reduced.

The questions now become (1) how can we predict the time required for the sand to be flushed out from a fully-blocked culvert and (2) how can we determine how long it takes for the flood water to overtop the highway for the same storm? The following section will discuss about the means that will help us to investigate these two questions in order to evaluate whether an existing culvert can self-open and self-clean during a storm.

### 7.2 Laboratory Study and Computer Simulation of Blocked Culverts

In order to investigate whether a completely sand-blocked culvert may be self-opening and self-cleaning for a drainage basin and design storm, we used both laboratory experiments and computer simulations. First, to predict how long it takes for a sand blockage to be flushed out from a clogged culvert, we built scaled models of selected highway culverts and performed flow measurement on these models in the lab. In the experiments, the culver models were filled with sand to simulate the fully-blocked condition. Then a water flow was fed to the blocked culvert model while the time it took the sand blockage to erode and flush out was recorded. This measured time can then be converted to the actual time in the field through the similarity principle based on Froude number in hydraulic modeling.

To predict the required time that surface water would overtop the highway, we applied computer simulations that incorporate the actual culvert size and storage capacity of its detention ponds. Specifically, we applied the POND software package to calculate the time it would take the flood water to overtop the highway by inputing flood hydrograph, culvert shape and size, and detention pond information in the software. After that, we compared the time to open the sand-

blockage with the time to overtop the highway. If the former is shorter than the latter, then we can judge that the culvert can self-open and self-clean during the storm.

### 7. 3 Screening Criteria of Existing Culvert and Detention Pond Storage Capacity

As we know, both the flood peak flow and hydrograph depend on the area of a contributing drainage basin to a culvert. Simulation models developed in this study indicate that a change of the outflow hydrograph from the drainage basin affects the adequacy of an existing combination of culvert size and detention pond storage capacity to accommodate the resulting surface runoff not overtopping the road. Even under open culvert conditions, as the drainage basin is increased for a specified storm, the culvert size or storage capacity of the detention pond may not be able to accommodate the resulting surface runoff. Results of the simulation model confirmed that overtopping of a roadway is not only a function of a culverts status – open or blocked. To minimize overtopping of the roadway, the simulation model requires estimation of the drainage area for a given design storm, and selection of the appropriate combination of culvert size and storage capacity of the detention pond.

In this study, various simulation model runs were performed for various combinations of outflow hydrographs from different drainage areas, culvert sizes, and storage capacity of detention ponds. The results of the various simulation runs are intended for the use as the screening tool to assess the adequacy of existing culverts and detention ponds along Kamehameha Highway on Windward Oahu.

## 7.4 Objectives of the Study

This study attempts to provide two sets of criteria for long-term management policy of existing culverts and detention ponds along Kamehameha Highway on Windward Oahu. The first criterion evaluates whether a completely sand-blocked culvert will be self-opened before the surface runoff from its contributing drainage basin exceeds the storage capacity of the detention pond and thus overtops the roadway. If the self-open time for a blocked culvert is less than the time for the flood water that overtops the roadway, the frequency of maintenance and cleaning of the culvert may then be performed at reduced intervals.

The second criterion is to assess the adequacy of existing culverts and their corresponding detention ponds under no blockage or fully "open" conditions for their respective contributing drainage basins and design storms.

Two specific culverts along Kamehameha Highway on Windward Oahu, namely, the circular pipe culvert in Punaluu and the rectangular box culvert in Hauula, were selected to be examined in this study. Our objective is to use these two culverts as sample culverts to demonstrate our methodology and results. Other culverts can be examined in a similar way.

# CHAPTER 8 FIELD OBSERVATION AND LABORATORY EXPERIMENTS

As mentioned in the previous chapter, two existing culverts – a circular pipe culvert in Punaluu and a rectangular box culvert in Hauula, both in Windward Oahu, were selected to be investigated in this study. This chapter reports our lab experiments and field observations of the two culverts.

## 8.1 Description of the Study Area

A description of the Punaluu and Hauula culverts is presented in this section. Required input parameters for the laboratory models and computer simulations are based on the description here.

The area northeast of the Koolau mountain range is commonly known as "Windward" Oahu, as prevailing winds from the east north east of the island of Oahu frequently pass from the sea over this area. A spectacular line of cliffs on the seaward side of the Koolau Mountain range may be viewed from the coastal areas.

Oahu is composed of two major volcanic mountains, the Koolau Range in the east and the Waianae Range in the west. The two mountain ranges are nearly parallel to each other with a relatively large plain area between the two ranges. Lava flows from the younger Koolau volcano banked against the already-eroded slope of the Waianae Volcano. Both ranges are the eroded remnants of large, elongated shield volcanoes that have lost most of the original shield outlines and are now long narrow ridges shaped largely by erosion. The deposition of alluvium, produced during the erosion of the mountains, formed the Honolulu Plain on the southern flank of the Koolau.

The watersheds of Windward Oahu are generally characterized as "small" watersheds, encompassing less than five square miles. Relatively long narrow valleys extend from the base of the Koolau mountain range and extend toward the sea. The coastal areas of Windward Oahu are predominantly urban and developed, with a single arterial highway winding along the coast.

The eastern portion of the island of Oahu is primarily made up of small watersheds, with steep valley walls and relatively flat coastal regions. The coastal regions are primarily urbanized and relatively close to the ocean. The main highway for the eastern portion of Oahu is located at the "fringe" of the ocean shoreline for much of the area, with urban areas located inward toward the mountains, or "mauka" from the highway.

A small Hawaiian watershed is characterized as relatively small in area, has steep slopes, and high infiltration. Therefore, the numerical model assumes the following:

- Rainfall is uniformly distributed over the watershed in both time and space;
- Infiltration is uniformly distributed over the watershed in both time and space; and
- Rainfall not infiltrated by the watershed is considered surface runoff and entirely collected by the stream channel. This assumes storage within the channel is negligible, conserving the appropriate water balance for drainage basin.

The high rate of infiltration attributed to each drainage basin is conservatively estimated at 40% of the rainfall rate. Constant infiltration capacity of some Hawaiian soil may range from the 0.5 in/hr to greater than 10 in/hr (Wu 1967). Water not infiltrated by the drainage basin, moves from the mountains, down steep side slopes toward the stream channel.

The Punaluu and Hauula drainage areas were selected for study (Figure 8-1 and 8-2) by using GIS software and topological maps. The Punaluu watershed is estimated at 262 acres and the Hauula watershed is estimated at 163.7 acres (Fujioka 2006). The general location and estimated drainage basin area of the Punaluu and Hauula are presented in Figures 8-1 and 8-2, respectively:

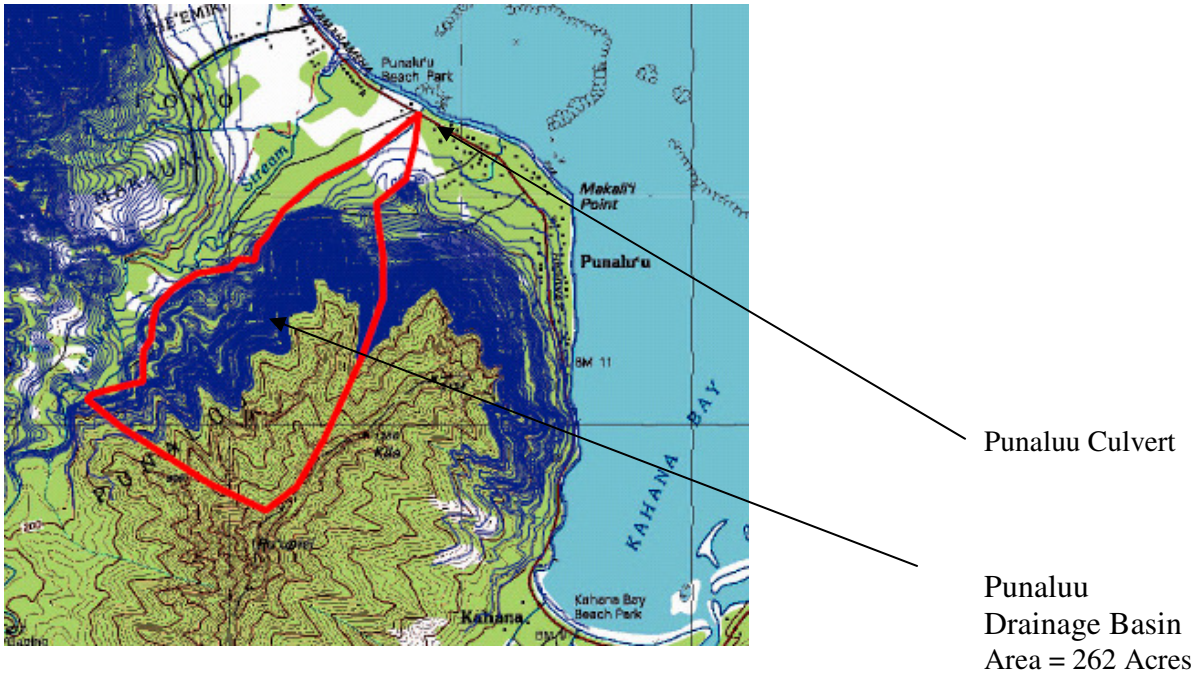


**Figure 8-1:** Contributing drainage basin for the Punaluu 30-inch culvert located at 53-270 Kamehameha Highway, Hauula, HI 96717

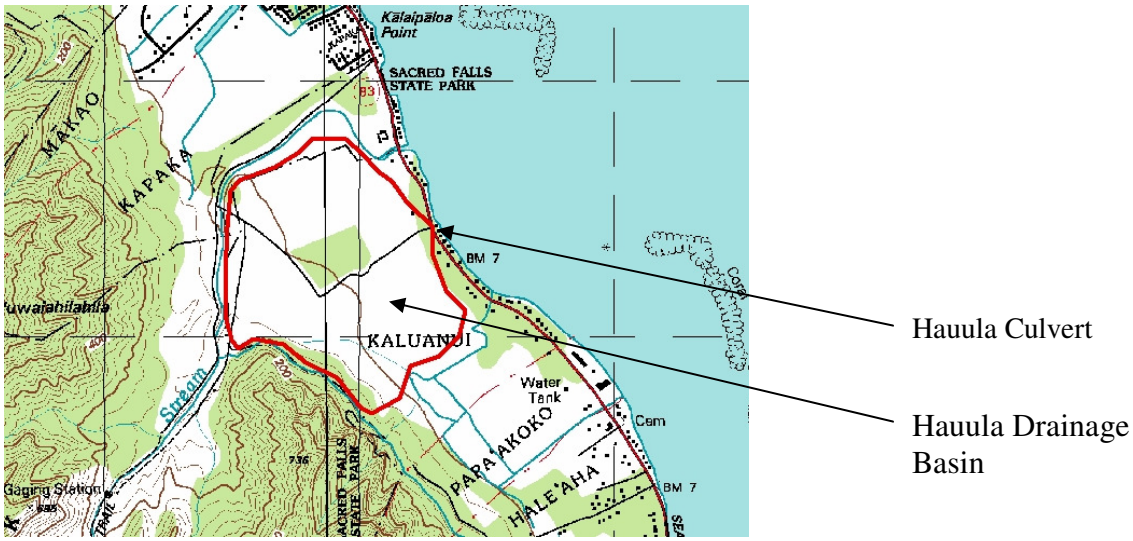


**Figure 8-2:** Contributing drainage basin for the Hauula 6-ft x 8-ft box culvert located at 53-707 Kamehameha Highway, Hauula, HI 96717

## 8.2 Design Storms

The principal rain producing mechanism on Oahu is orographic lifting of tradewinds along the Koolau and Waianae mountain slopes. The prevailing winds from the northeast of the island of Oahu are commonly known as "tradewinds". The direction of the tradewinds is generally perpendicular to the Koolau mountain range, where water moisture from the sea is trapped against the mountain range. Water moisture trapped against the Koolau Mountain range generally attributes the large amount of rainfall experienced on Windward Oahu. (Giambelluca 1984)

Isohyets depicting rainfall duration of 1, 6, and 24 hours for 1, 10, 50 and 100 year return periods for the Island of Oahu are found in the "Rainfall Frequency Study for Oahu, Report No. R-73". The isohyets from this report are based upon rainfall data collected for the island of Oahu over a ten-year period, and interpolated for the various storm frequency and return periods. The rainfall estimates from the isohyets are commonly used for various engineering applications for the Island of Oahu.

Rainfall is distributed equally in time for a given storm duration of a 50-year recurrence interval. The probability a 50-year storm occurs each year is approximately 2 percent. The 50-year recurrence interval for a 1-hour and 6-hour duration storm was selected by HDOT, and based upon the risk tolerance of flooding caused by rainfall (Matsuda 2006). Drainage basins of area less than 200 acres will be subject to 1-hour storm duration, and watersheds with an area greater than 200 acres will utilize the 6-hour duration storm.

Interpolating the isohyets for rainfall intensity for windward Oahu for a recurrence interval of 50-years, it is estimated for a 1-hour storm, three inches of rainfall is uniformly

applied over the watershed. For a 6-hour storm, 7.5 inches of rainfall is uniformly applied over the drainage basin.

### 8.3 The Punaluu and Hauula Culverts

The Punaluu culvert is a 30 in-dia. circular pipe culvert while the Hauula culvert is a 6 ft by 8 ft box culvert. The two culverts are shown in the following photos:

**Figure 8-3:** Punaluu culvert – 30 in-dia. circular pipe

**Figure 8-4:** Hauula culvert – 6 ft by 8 ft rectangular box

From these photos, we can see that during dry season, a coastal culvert can be fully and severed clogged by sand and debris (Figure 8-4). It is important that engineers and researchers investigate the problem sand-plugging of coastal highway culverts and seek engineering solutions to mitigate the problem.

## 8.4 Laboratory Experiments

Hydraulic models of the Punaluu circular culvert and Hauula box culvert were fabricated in the hydraulics laboratory of the University of Hawaii at Manoa. The purpose of the model study is to observe the time for a culvert to self-open under various completely sand blocked conditions. The scaled models were blocked with beach sand, and experiments were conducted to evaluate the time the culvert would open as a function of head water depths. This section describes the rationale of the scaled model, the laboratory experiment, and the results.

### 8.4.1 Laboratory Culvert Model and Dynamic Similitude

The model scale was calculated using the concept of dynamic similitude for open channel flows. Dynamic similitude provides a relationship between the laboratory results and actual conditions expected in the field. For free surface flows the dimensionless parameter in dynamic similitude between the model and prototype is the Froude Number, Fr. By definition:

$$Fr = \frac{V}{\sqrt{gy}} \tag{8-1}$$

where V is the velocity, g is the gravitational constant; and y is the depth of the flow.

Therefore, for free surface flow models, the dynamic similitude between the model and the prototype is:

$$Fr_m = Fr_p$$

$$\text{or, } \frac{V_m}{\sqrt{g * y_m}} = \frac{V_p}{\sqrt{g * y_p}} \tag{8-2}$$

$$\text{or, } \frac{V_m}{\sqrt{y_m}} = \frac{V_p}{\sqrt{y_p}}$$

where, $V_m$ and $V_p$ are model velocity and prototype velocity, respectively; and $y_m$ and $y_p$ are the flow depths in the model and prototype.

$$\text{or, } \frac{V_m}{V_p} = \left(\frac{y_m}{y_p}\right)^{\frac{1}{2}} = L_r^{\frac{1}{2}} \tag{8-3}$$

where the model scale $L_r = \frac{y_m}{y_p}$.

Since $\frac{V_m}{V_p} = \frac{\left(l_m / t_m\right)}{\left(l_p / t_p\right)}$, therefore, $\frac{V_m}{V_p} = L_r\left(\frac{t_p}{t_m}\right)$ (8-4)

where $l_m$ and $l_p$ are length dimensions in model and prototype, respectively. Substituting Eq. (8-3) into Eq. (8-4) yields:

$$t_m = t_p * \sqrt{L_r} \tag{8-5}$$

where $t_m$ = model time for culvert to self-open; and $t_p$ = actual time for the culvert to self-open.

In the experiments, the circular pipe model has a diameter of 6 in while the box culvert model was 9 in by 12 in. This means that for the Punaluu culvert, the model scale Lr is 1/5 and for the Hauula box culvert, the model scale Lr is 1/8.

### 8.4.2 Description of Laboratory Experiment

The culverts were "packed" with beach sand to simulate a complete blockage. The sand was placed in the model culvert with various compaction efforts. A constant volume of sand was placed in the model culvert for all experimental trials. The slope of the culverts was placed at 0 % for both the 9-inch by 12-inch model box culvert and 6-in model circular culvert. The sand was placed in the middle of the length of the model culvert, simulating actual conditions along the coast of Windward Oahu.

The inlet of the model culverts was connected to a water tank, with the outlet open to free flowing conditions. The water tank was filled with water to a prescribed level simulating elevation head of water in a detention pond. The water tank and a sluice gate controlled the culvert outflow.

Once the model culverts were packed with sand and the water tank was filled to the prescribed levels, the sluice gate was opened. The time for the culvert to self-open was defined as the time between the opened sluice gate and collapse of sand column in the barrel. It was observed that the model culvert is self-opened quickly after the incipient sand movement occurs.

### 8.4.3 Experiments on the Rectangular Box Culvert Model

A constant volume of 1.875 $ft^3$ of beach sand was placed in the model of the box culvert. Sand was centered over a 2.5-ft length of the model culvert. For each experimental run, the sand was weighed on a scale prior to compacting in the culvert, and a representative grab sample of

the sand was collected. The sample of sand was weighed and placed in a drying oven, and reweighed to estimate soil moisture content. Various weight of sand was placed in the culvert. The sand in the culvert was "compacted" with various compaction efforts for each trial run.

Since $L_r$ = ⅛ for the box culvert model, water level in the water tank was filled to 3.0 inches above the crown of the model culvert to simulate a prototype of 2.0-ft maximum allowable water elevation above the crown of the culvert in Hauula. Once the water level was reached, the sluice gate was lifted immediately and the culvert's to self-open condition was timed. Once the sand in the culvert started to liquefy and quickly collapsed, the time was then recorded. The timing from the initial sand movement to completely clear the culvert is very short under the constant water head in the tank. The laboratory experimental trials were digitally videotaped and presented in the appendix.

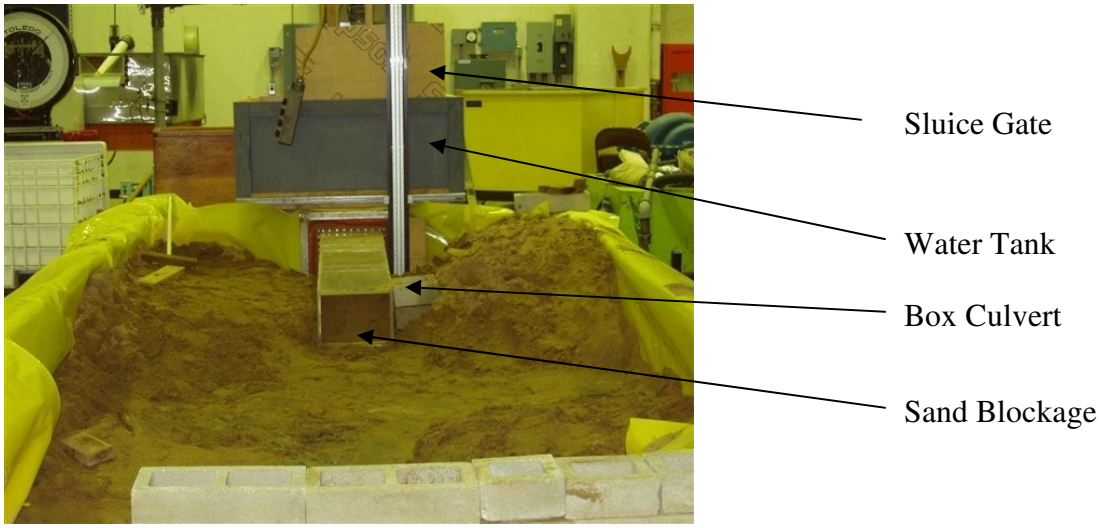


**Figure 8-5:** Photograph of model box culvert experiment for Hauula culvert

### 8.4.4 Experiments on the Circular Culvert Model

Sand was placed in the middle of the model circular culvert over a 2-ft length. For each experimental trail run, the sand was weighed on a scale prior to placing in the culvert. The sand in the culvert was "compacted" with various compaction efforts similar to actions described in Section 8.4.3.

Since $L_r$=1/5 for this model, water level in the water tank was filled to 8.4 inches above the crown of the model culvert to simulate a prototype of 3.5-ft maximum allowable water elevation above the crown of the 30-inch culvert in Punaluu.

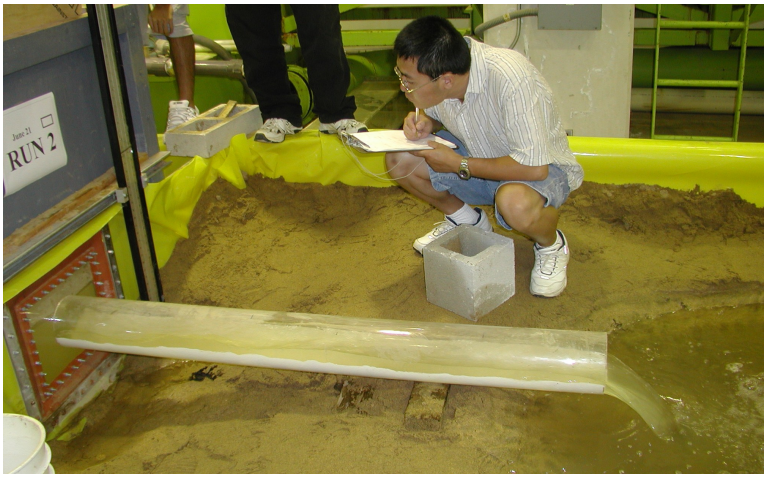


**Figure 8-6:** Photographs of model circular culvert experiment for Punaluu culvert

### 8.4.5 Results of the Laboratory Experiments

Summary results of the laboratory experiments are tabulated in Tables 8-1 and 8-2.

**Table 8-1: Summary of Laboratory Results for the 9-inch by 12-inch Box Culvert Model**

| Trial No. | Sand Weight (lbs) | Moisture Content (%) | Time to Self-Open |
|---|---|---|---|
| 1 | 214 | 8.64 | 8 minutes 36 |
| 2 | 205 | 19.98 | 1 minute 20 s |
| 3 | 196 | 4.02 | 3 minutes 20 s |
| 4 | 203 | 3.31 | 15 seconds |

**Table 8-2: Summary of Laboratory Results for the 6-inch Circular Culvert Model**

| Trial No. | Sand Weight (lbs) | Time to Self-Open |
|---|---|---|
| 1 | 40 | 3 minutes13 seconds |
| 2 | 34 | almost immediately |
| 3 | 46 | almost immediately |
| 4 | 38 | almost immediately |
| 5 | 42 | 4 minutes 5 seconds |

Laboratory observations from model study of both the box culvert as well as the circular culvert indicate that the time for the culvert to open varies as a function of the soil moisture and the degree of "compactness" of the sand in the model culvert. The time for the model box culvert to self-open ranged from 15 seconds to 8 minutes 39 seconds. The time for the circular culvert to self-open ranged from instantaneous to 4 minutes and 5 seconds.

The observed range of 15 seconds to 8 minutes 36 seconds for the model box culvert to self-open appear to be attributed to the moisture content of the sand and compaction effort in placing the sand in the model barrel. It was observed in Trial 1 which has the longest time to self-open (Table 8-1). The compaction effort for this trial was the greatest, with compaction occurring in 8-inch intervals, while compaction effort in Trial 3 occurred in 12-14 inch intervals. Soil moisture may also play a role, as indicated in Table 8-1, as Trial 2 and Trial 4 had a large disparity of moisture contents for a similar compaction effort of 12-14 inches intervals.

# CHAPTER 9 NUMERICAL MODELING AND SIMULATION

The computer simulation model developed in this study is a flood routing-based computational scheme, which considers design storm, drainage area, detention pond and culvert size as an interactive system.

As indicated in Figure 9-1, for the drainage area, a direct runoff hydrograph may be synthesized under a given design storm. This synthesized direct runoff hydrograph from the defined drainage area is actually the inflow hydrograph to the detention pond. The dynamic routing of the inflow hydrograph through the detention pond and culvert system will result in a outflow hydrograph. This routing process is carried off by using PondPak (Bentley, 2005).

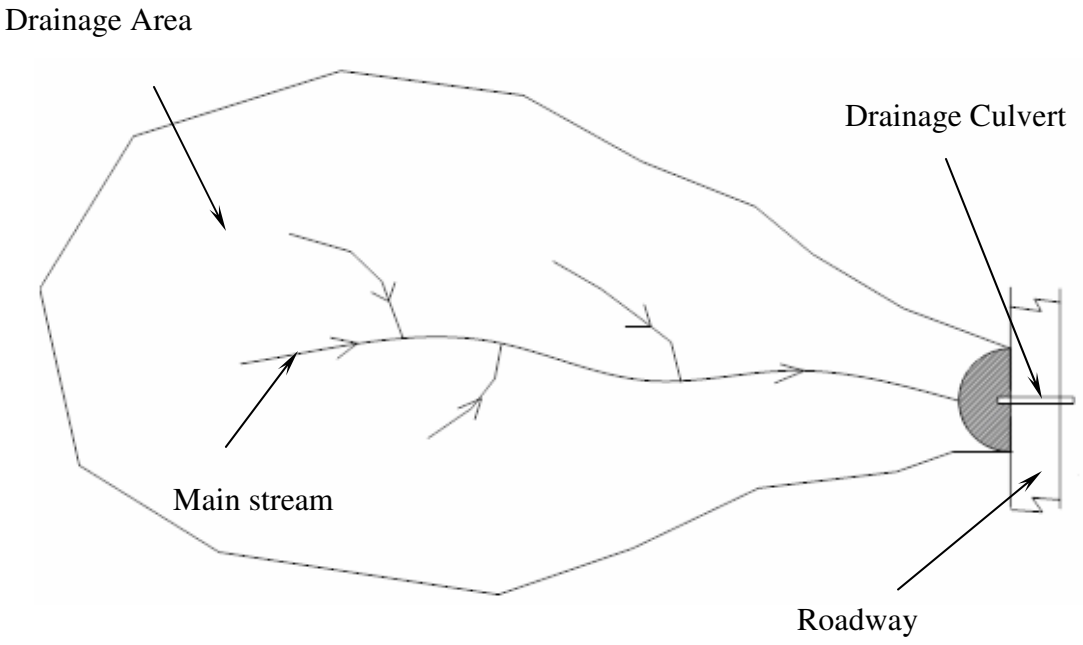


**Figure 9-1:** Conceptual Simulation Model – Plan View

## 9.1 Design Storm

In accordance with HDOT's Design Criteria for Highway Drainage, this study uses a one-hour 50-year rainstorms or six-hour 50-year rainstorms for drainage areas less than 200 acres or drainage areas equal to or greater than 200 acres, respectively.

### 9.1.1 Synthesizing Direct Runoff Hydrograph

Direct runoff from a drainage basin may be simulated by the Nash-Muskingum method if one assumes that:

1. Inflow to the basin is a known design rain storm; and
2. The drainage basin storage can be represented by one or more reservoir type storage.

#### 9.1.1.1 Nash-Muskingum Method

The Nash-Muskingum method is used to compute direct runoff of the drainage basin given the area, rainfall intensity for a 50-year recurrence interval, and the recession constant. The direct runoff hydrograph from the drainage basin is the inflow hydrograph to the detention pond. The outflow hydrograph of the drainage basin is calculated by the following relationship:

$$O_2 = C_o I_2 + C_1 I_1 + C_2 I_2 \tag{9-1}$$

where

$O_2$, $O_1$ are the outflow rates for time intervals 2 and 1 respectively;

$I_2$, $I_1$ are the inflow rates for time intervals 2 and 1 respectively; and

$C_0$, $C_1$, and $C_2$ are:

$$C_2 = e^{-\left(dt/K\right)}$$

$$C_1 = \left(\frac{K}{dt}\right) * \left(1 - C_2\right) - C_2$$

$$C_0 = -\left(\frac{K}{dt}\right) * \left(1 - C_2\right) + 1$$

The Muskingum coefficient, K, is considered as a function of recession constant, $K_1$, of a watershed (Wu, 1969).

#### 9.1.1.2 Development of Recession Constant For Windward Oahu

The Hawaiian small watershed is generally characterized as a watershed relatively small in size, steep side slopes, and high capacity of rainfall infiltration (Wu 1969). During periods of intense rain (or when the rainfall is no longer infiltrated by the watershed), the steep side slopes of the watershed and the small physical area yield a short time of concentration within the watershed. The relatively short time of concentration indicates a short time to reach a peak discharge for a watershed.

The small Hawaiian watershed is characterized by the following parameters: area of the watershed, length of the mainstream, the average slope of the main stream, height of the watershed, and the estimated time of concentration attributed to the watershed. Eight watersheds located on the windward area of Oahu were evaluated. Estimated values for each of the characteristics for Windward Oahu watersheds are presented in the following table:

**Table 9-1: Watershed Characteristics on Windward Oahu**

| Watershed No. | Watershed Area (acres) | Length of Main Stream (ft) | Average Slope of Main Stream (%) | Height of Watershed (ft) | Estimated Time of Concentration (hr) |
|---|---|---|---|---|---|
| 2540 | 1,306 | 14,360 | 4.43 | 2,540 | 0.40 |
| 2739 | 2,803 | 25,480 | 1.15 | 2,782 | 0.75 |
| 2750 | 621 | 5,594 | 11.80 | 2,128 | 0.14 |
| 2830 | 179 | 1,438 | 23.00 | 2,222 | 0.03 |
| 2838 | 198 | 2,250 | 19.70 | 2,069 | 0.05 |
| 2840 | 595 | 4,875 | 11.40 | 2,377 | 0.19 |
| 2910 | 634 | 3,750 | 6.92 | 2,500 | 0.09 |
| 2965 | 2,394 | 21,700 | 2.73 | 2,630 | 0.63 |

The recession constant, $K_1$, may be interpreted as the as the travel time of the flood wave from the upstream end to the downstream end of the channel reach. Therefore, $K_1$, accounts for the translation (or concentration) portion of the routing. (Ponce 1969)

The recession constant, $K_1$, is a constant or coefficient of an assumed linear storage model of recession flow, S = KQ, where S is the surface-water storage and Q is the outflow. The recession constant, $K_1$, is a theoretical value in which more than one linear relationship may exist within the watershed. The recession flow of Hawaiian small watersheds is largely influenced by surface runoff, and the first part of the recession is used to determine the recession constant designated as $K_1$ (Wu 1969).

Statistical software, BMDP2R – Stepwise Regression (Statistical, 2001), was used to estimate the first part of the recession, $K_1$, associated with windward Oahu. BMDP2R computes the coefficients of the independent variable (predictors) of a multiple linear regression in a stepwise manner by entering or removing variables one at a time from a list of potential predictors (Dixon 1983). The first part of the recession, $K_1$, was established as the dependent variable. Independent variables (predictors) were quantitative characteristics of the watershed,

watershed area, length of the main stream, average slope of the main stream, and height of the watershed.

Eight watersheds were used in the development of the recession constant for windward Oahu, as these watersheds contained a complete data set for each watershed. BMDP2R does not include incomplete data sets in estimating the dependent parameter with independent variables.

Forward stepping of the multiple regression analysis of all independent variables yields the first step of estimating $K_1$ as dependent variable is a function of the watershed area. $K_1$ estimated as follows:

$$K_1 = 0.2957 + 0.000367 * \text{Area (in acres)} \quad (9\text{-}2)$$

The $K_1$ estimate above had an R-squared value of 0.8597, and an F-distribution value of 36.77. The F-distribution value of 36.77 was compared against the F-distribution table value at the 5% significance level of 5.99, with 1 degree of freedom in the numerator and 6 degrees of freedom in the denominator.

Another variable was added to the multiple regression analysis. The recession constant as a function of the both watershed area and slope was estimated as follows:

$$K_1 = -0.1339 + 0.000531 * \text{Area (in acres)} + 0.0247 * \text{Slope} \quad (9\text{-}3)$$

The $K_1$ estimate above had an R-square value of 0.9324, and an F-distribution value of 34.46. The F-distribution value of 34.66 was compared against the F-distribution table value at the 5% significance level of 5.79, with 2 degrees of freedom in the numerator and 5 degrees of freedom in the denominator.

Eq. (9-2) was considered the appropriate equation to estimate $K_1$ as a function of the watershed area. Eq. (9-3) is considered acceptable, as the F-distribution value of 34.66 is significantly larger than 5.79, however, the F-distribution value of Eq. (9-3) is slightly less than

the F-distribution value associated with Eq. (9-2). Multiple R-square values increased as more predictor values were added, the F-distribution values decreased as predictor values were added. The decrease in the F-distribution value is statistically more significant than the increase of the multiple R-square values. Eq. (9-2) is in agreement of the findings of a study where $K_1$ values for Hawaiian watersheds using multiple correlation of predictor values "indicate that drainage area alone is the most significant factor to the recession constant" (Wu,1969). To estimate the Muskingum coefficient, K, (Wu, 1969)

$$K = 0.67\, t_r \tag{9-4}$$

where $t_r$ is defined as the time from the peak rate to the end of the triangular hydrograph (Wu, 1969), and

$$t_r = 1.38 K_1 \tag{9-5}$$

Substituting Eq. (9-5) into Eq.(9-4) yields

$$K = 0.9246 K_1 \tag{9-6}$$

### 9.1.2 Design Storms

As mentioned in section 8.2, interpolating the isohyets for rainfall intensity for windward Oahu for a recurrence interval of 50-years, it is estimated for a 1-hour storm, three inches of rainfall is uniformly applied over the watershed. For a 6-hour storm (Figure 9-2), 7.5 inches of rainfall is uniformly applied over the drainage basin.

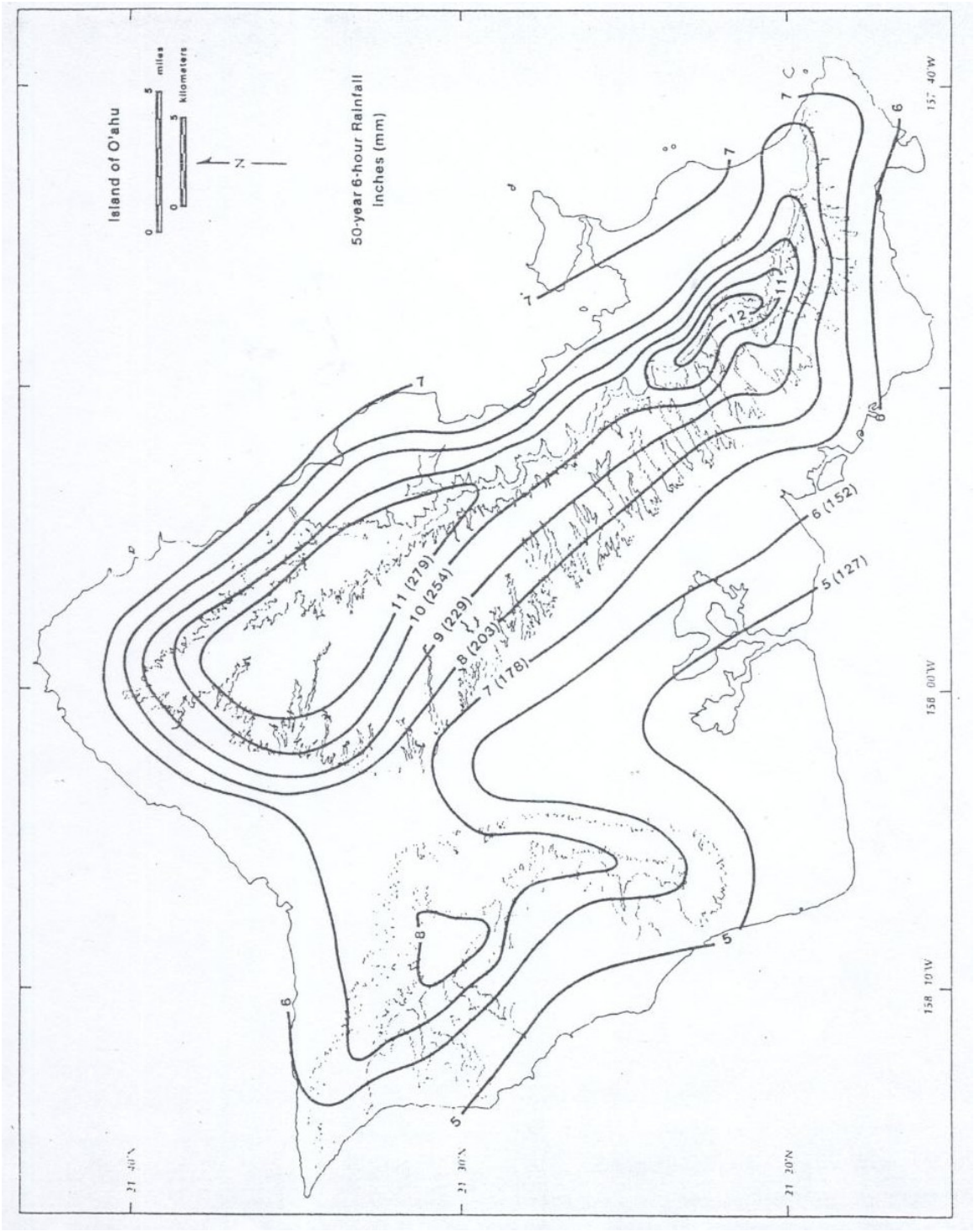


**Figure 9-2:** Map of 50-yr 6-hr rainfall, Oahu, Hawaii.

### 9.1.3 Muskingum Coefficient

The Muskingum Coefficient, K, is a function of $K_1$ (Eq. 9-6). The time interval (dt) was established as 0.1 hours, or six minutes. The watershed inflow is calculated as effective rainfall. Effective rainfall is the rainfall less drainage basin infiltration of 40%, divided by the time interval over the drainage basin area. A sample calculation of the outflow from the drainage basin, or the inflow hydrograph to the detention pond is presented below for the Punaluu drainage basin with an area of 262-acres, using a 6-hour 50-year design storm:

**Punaluu Detention Pond Inflow Hydrograph Calculation**

Design Storm and Drainage Basin

Given Storm Parameters

Return Period: 50 Years

Rainfall Duration: 6 hours

Estimated Total Precipitation: 7.5 inches

Drainage Basin Characteristics

Drainage Area: 262-acres

Drainage basin infiltration: 40%

Determining Recession Coefficient $K_1$

$$K_1 = 0.2957 + 0.00367 * \text{area (acres)}$$
$$K_1 = 0.2957 + 0.00367 * 262$$
$$K_1 = 0.3919$$

Calculating Muskingum K

$$K = 0.9254 * K_1$$
$$K = 0.9254 * 0.3919$$
$$K = 0.3626$$

Calculating the drainage basin inflow for each time interval of 0.1 hours in cubic feet per second for the six-hour storm duration.

Drainage Basin Inflow

For each time interval of 0.1 hours

$$\frac{7.5\text{ in}}{6\text{ hours}} = 1.25\frac{\text{in}}{\text{hour}} * 0.1\text{hour} = 0.125\text{in}$$

$$\frac{262\text{acres}\left(\frac{43{,}560\text{ft}^2}{\text{acre}}\right) * 0.125\text{in}\left(\frac{1\text{ft}}{12\text{in}}\right) * (100\% - 40\%)}{0.1\text{hr}\left(\frac{3600\text{sec}}{1\text{hr}}\right)} = 198.14\text{cfs}$$

Determining the coefficients $C_0$, $C_1$ and $C_2$ for Eq. (9-1) :

$$C_2 = e^{-\left(0.1/0.3626\right)} = 0.7590$$
$$C_1 = \left(\frac{0.3626}{0.1}\right) * (1 - 0.7590) - 0.7590 = 0.1150$$
$$C_0 = -\left(\frac{0.3626}{0.1}\right) * (1 - .7590) + 1 = 0.1260$$

Therefore

$$O_2 = 0.1260I_2 + 0.1150I_1 + 0.7590I_2$$

Sample calculation of the first hour of the detention basin outflow hydrograph is presented in Table 9-2.

**Table 9-2: Outflow Hydrograph from Punaluu Drainage Basin for the first hour**

| Time (hours) | Drainage Basin Inflow (cfs) | Drainage Basin Outflow (cfs) |
|---|---|---|
| 0 | 0 | 0 |
| 0.1 | 198.138 | 24.97280 |
| 0.2 | 198.138 | 66.70759 |
| 0.3 | 198.138 | 98.38380 |
| 0.4 | 198.138 | 122.42565 |
| 0.5 | 198.138 | 140.67312 |
| 0.6 | 198.138 | 154.52274 |
| 0.7 | 198.138 | 165.03442 |
| 0.8 | 198.138 | 173.01267 |
| 0.9 | 198.138 | 179.06806 |
| 1 | 198.138 | 183.66402 |

## 9.2 Detention Ponds

The existing detention ponds for the Punaluu and Hauula culverts were surveyed by the project team. The maximum water surface elevation is the height corresponding to the maximum storage value of a detention pond. The maximum height is considered as the top of the road surface, and is the physical limitation of the simulation model. The surveyed elevation versus storage volumes are presented in Table 9-3.

**Table 9-3: Surveyed Punaluu and Hauula Detention Ponds**

| Punaluu | | Hauula | |
|---|---|---|---|
| Elevation (ft) MSL | Storage Volume (ac-ft) | Elevation (ft) MSL | Storage Volume (ac-ft) |
| 6.00 | 0.000 | 7.00 | 0.000 |
| 7.00 | 0.009 | 8.00 | 0.001 |
| 8.00 | 0.021 | 9.00 | 0.002 |
| 9.00 | 0.035 | 10.00 | 0.006 |
| 10.00 | 0.051 | 11.00 | 0.007 |
| 11.00 | 0.072 | 12.00 | 0.018 |
| 12.00 | 0.086 | 13.00 | 0.030 |
| | | 14.00 | 0.041 |
| | | 15.00 | 0.053 |

### 9.3 Culvert Parameters

The invert of the drainage culvert was placed at the elevation of the detention basin where storage volume is equal to zero. The culvert extends from the detention basin a minimum slope of 0.5% toward the outlet of the culvert. The typical culvert length is at 40-feet, and the invert at the outlet of the culvert is placed 0.2 feet below the invert at the entrance.

Culvert hydraulics in the simulation model is based upon inlet control. The inlet end may be unsubmerged or submerged in relation to the surface water in the detention pond, however, water at the outlet end flows freely. Since control is at the upstream end in inlet control, only the headwater and inlet configuration affect culvert performance (USDOT 2001). The simulation model developed for Punaluu and Hauula examined flow of water through the culverts under inlet control only. Inlet control is anticipated to cause the quickest rise of surface runoff elevation in the detention pond with respect to time.

Inlet design coefficients as a function of the type of material and inlet configuration are integral to culvert flow under inlet control. For the rectangular box culvert, a rectangular box with 0° wingwall flares was used as the inlet parameters of the numerical model. For the circular culvert, a circular concrete with a square edge and headwall was used as inlet parameters in the simulation model.

### 9.4 Simulation Model Runs for Punaluu and Hauula Culvert Systems

One series of numerical model runs was performed for the circular culvert at Punaluu and another for the rectangular box culvert at Hauula, respectively. Each model runs were executed to examine two different culvert scenarios. The first culvert scenario attempts to estimate the time for the surface runoff to reach the maximum surface water elevation of the detention pond

under sand blocked conditions, where the culvert blockage is nearly complete. The second culvert scenario attempts to model surface water elevation of the detention pond under "open" culvert conditions.

### 9.5 Results and Discussions of Simulated Output for Sand Blocked Conditions

The simulation model for the circular culvert in Punaluu under sand blocked conditions predicted surface runoff would overtop the road in approximately 0.100 hours or 6 minutes. The simulated result for the rectangular box culvert in Hauula under sand blocked conditions in approximately 0.07 hours or 4.2 minutes.

### 9.6 Results and Discussions of Simulated Output for Open Conditions

The simulation runs for both the Hauula and Punaluu drainage systems were executed under open culvert conditions, where flood flows were not impeded. The Punaluu simulated results indicated the existing 30-inch circular culvert and detention pond capacity of 0.086 ac-ft (Table 9-3) are inadequate to accommodate the surface runoff from a 262-acre drainage basin and 6-hour 50-year design storm.

On the other hand, the model result for Hauula indicated that the 6-ft by 8-ft box culvert and detention pond capacity of 0.053 ac-ft (Table 9-3) are adequate to accommodate surface runoff from a 163.7-acre drainage basin and a 1-hour 50-year design storm. The peak discharge and its surface water elevation from the Hauula pond-culvert system were 280.22cfs and 5.74 ft, respectively. It is noteworthy that the 280.22 cfs peak discharge from the 6-ft by 8-ft barrel is almost identical to its peak flow, 280.46 cfs. This result suggests that routing through this small 0.053 ac-ft detention pond may not be necessary.

# CHAPTER 10 CRITERIA FOR CULVERT MANAGEMENT

The establishment of management criteria for culverts along the windward coast of Oahu is based upon a generalized simulation model. A version of the simulation model specifically applicable to Punaluu and Hauula culvert systems is described in the previous chapter 9.

This chapter defines the generalized simulation model, its components and required parameters. Applications of this model are presented. The generalized simulation model begins at the watershed. The outflow from the drainage basin is obtained by applying the Nash-Muskingum method as described in Chapter 9. This direct runoff hydrograph is actually the inflow hydrograph to the detention pond. The various combinations of detention pond capacities and culvert sizes are used to estimate the floods routed through the systems. Figure 9-1 exhibits the overall conceptual design of the drainage basin, detention pond, and culvert. Figures 10-1 and 10-2 describe a typical detention pond and culvert system for use in the simulation model.

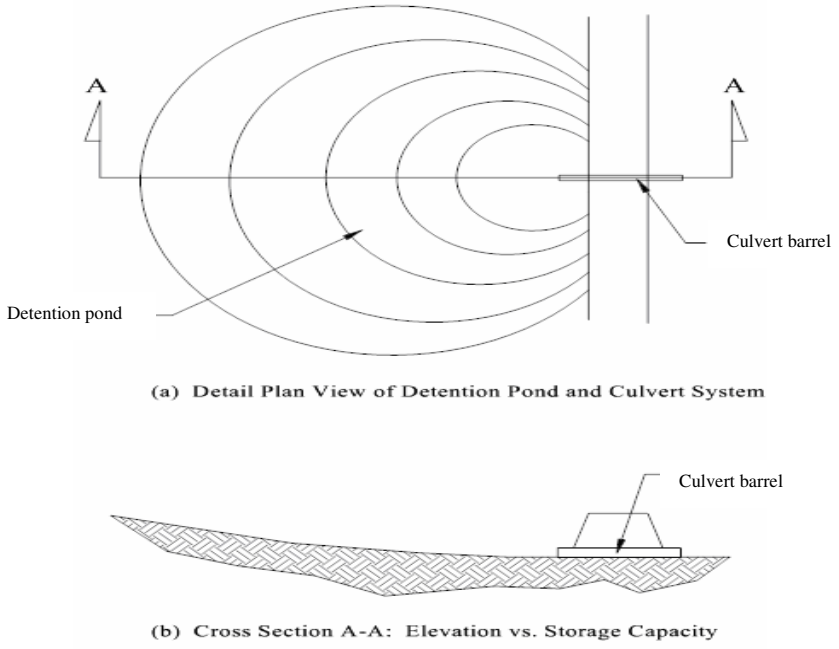


**Figure 10-1:** Schematic diagram of detention pond-culvert system

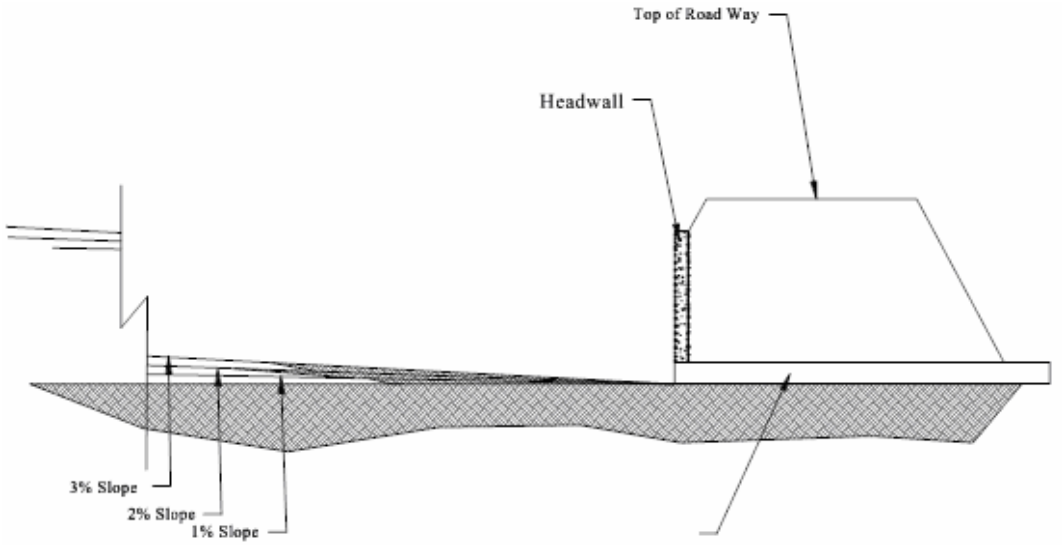


**Figure 10-2:** Details of a culvert

### 10.1 Simulation Model Parameters

This section defines the necessary parameters required for the generalized simulation model. These parameters are the inflow hydrograph, the detention basin, and culvert type and sizes.

#### 10.1.1 Inflow Hydrograph Rationale and Assumptions

The inflow hydrograph used in the generalized simulation model is actually the time-dependent outflow from the drainage basin for a given design storm. The direct runoff hydrograph from the drainage basin is calculated in the same manner presented in Chapter 9. The assumptions regarding the drainage basin characteristics presented in Chapter 9 also apply in this chapter.

A 6-hour or 1-hour design storm for a 50-year recurrence interval is selected as a function of the size of the drainage area. For drainage areas less than 200 acres, the 50-year 1-hour design

storm is assigned, which is estimated about 3-inches along the coast on Windward Oahu. For drainage basin areas greater than 200 acres, the 50-year 6-hour design storm is assigned, which is estimated about 7.5 inches at the study area.

In this study, drainage areas less than 200 acres, the area considered ranged from 25 acres to 200 acres with an increment of 25 acres. Drainage areas used are limited to 500 acres. For areas between 200 and 300 acres, the increment is 25 acres. For drainage basin areas between 300 and 500 acres, the increment is 50 acres.

### 10.1.2 Detention Pond Rationale and Assumptions

Three different conceptual detention ponds were considered in this study (Figure 10-2). An average slope of 1%, 2% or 3% of a detention basin was used to estimate the storage capacity prior to flood routing process through a culvert. As indicated in Figure 10-1, the detention basin is assumed to be half of a cylindrical cone (through the conic method), where the center of the cone is the projection of the culvert, headwall, and roadway. The average slope represents the slope of the right cone.

The selection of 1%, 2%, and 3% average slope was based upon physical observations of the coastal areas along windward Oahu. General topography of the coastal areas along windward Oahu is relatively "flat" with little elevation change. Therefore, the creation of a detention pond where side slopes in excess of 3% is most unlikely along the coastal Windward Oahu. A detention pond in excess of a 3% gradient would more than likely create a meaningful detention pond since it is assumed that the maximum depth of the detention pond is measured from the culvert invert (Figure 10-2).

### 10.1.3 Culvert Rationale and Assumptions

Two structural types of drainage culverts with rectangular and circular cross-sections were studied. The single box culvert of various sizes ranging from 2-ft by 2-ft to 10-ft by 12-ft were used. Box culvert dimensions were taken from The State of Hawaii Standard Details for Public Works Construction (State of Hawaii, 1984). Circular pipe was based upon standard sizes for reinforced concrete pipe, ranging from 24-inches to 108-inches (Lindeburg, 2001). A box culvert in excess of 10-feet in height or a circular pipe in excess of 108-inches would no longer be considered a "culvert" and surface runoff would require the use of a "bridge" to adequately address the proper cross drainage.

The inlet design coefficients and parameters used in the Hauula and Punaluu culverts described in Chapter 8 also were used in the generalized simulation model here. Inlet control of the culvert was adopted in the simulation model since inlet control is anticipated to cause the quickest rise of flood water in the detention pond.

### 10.1.4 Determination of Maximum Headwater Elevation

To comply with HDOT's design criteria for Highway Drainage, two different cases of headwater (HW) are investigated. The first maximum allowable headwater elevation, $H_1$, is equal to 1.2*D above the inlet barrel invert (Figure 4-3(a), D=vertical dimension of the barrel). Therefore, for a 6-ft high box culvert, the maximum headwater elevation is 7.2-ft measured at the invert of the culvert.

The second maximum allowable headwater elevation, $H_2$, is equal to 3-ft plus D (Figure 10-3(b)). Therefore, for a 6-ft high box culvert, the maximum headwater elevation is 9-ft above the invert of the culvert.

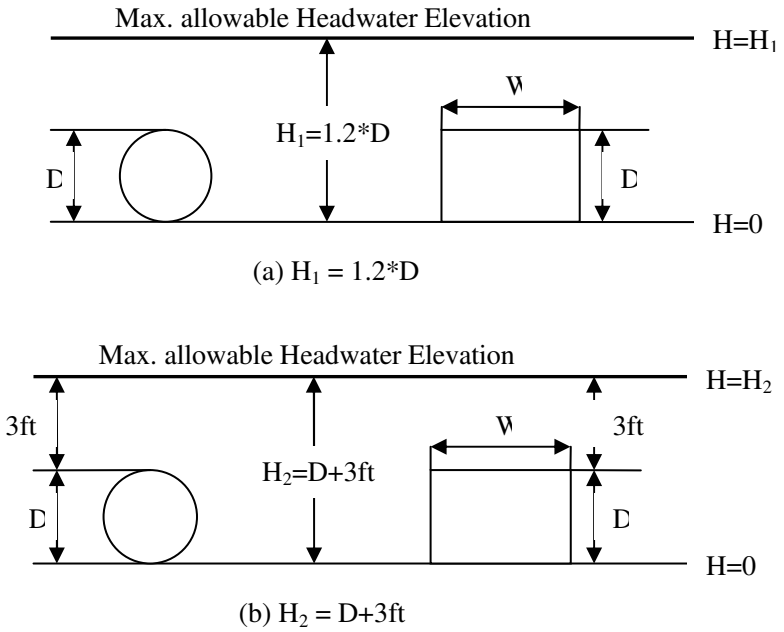


**Figure 10-3:** Definition of Maximum Allowable Headwater (HW) Elevation

## 10.2 Simulated Model Results and Discussions

As indicated in Figure 10-4, a total of 12 model runs were performed. Forty different sizes of box culverts and fifteen different sizes of circular pipe culverts were modeled for each of the three different conceptual detention ponds under 17 different inflow hydrograph scenarios. A block diagram of model runs in presented in Figure 10-4.

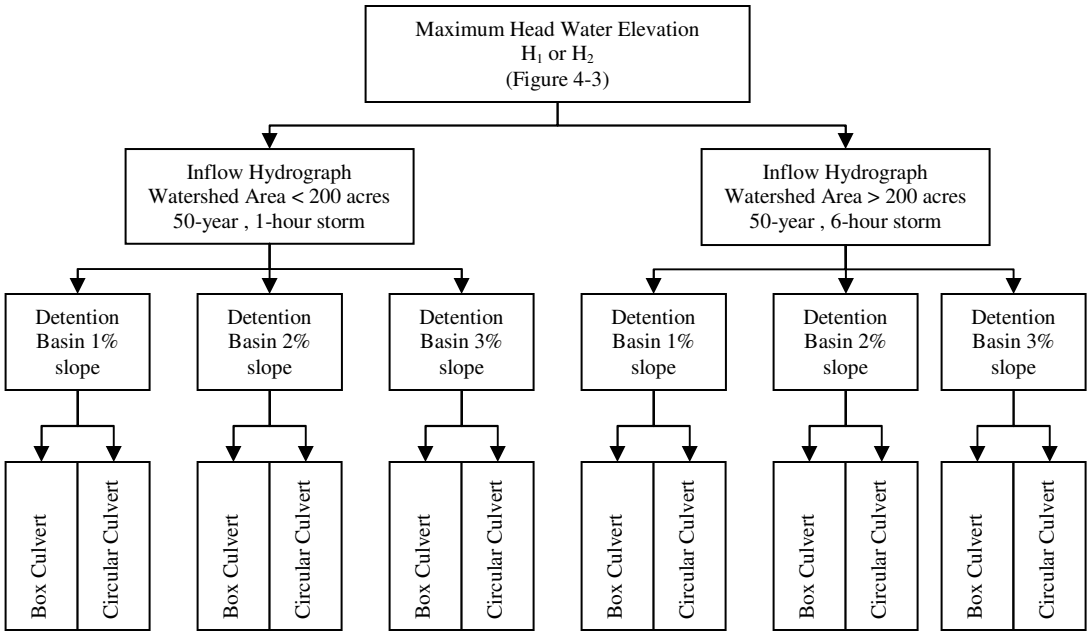


**Figure 10-4:** Block diagram of model runs

The detailed results are presented in Appendix D in Kamaka (2006). As an example, in this report, we present the results for the Hauula 6-ft by 8-ft box culvert in Table 10-1. The storage capacity for its existing detention pond is 0.053 ac-ft and its inflow produced drainage area is 162.7 acres. The same size box culvert, with a drainage basin of 175 acres, and a 3% slope detention pond is summarized as Table 10-1.

**Table 10-1: Table Values for Headwater Elevation $H_1$=1.2D, Inflow Hydrograph <200 acres, 3% average slope detention pond, 6-ft by 8-ft box culvert**

| | | | 175 Acres | | | | | |
|---|---|---|---|---|---|---|---|---|
| Box Culvert Size | | | Time to Max Headwater (hr) | | Detention Pond | | | |
| Hgt (ft) (D) | Wdt (ft) (W) | Max. Headwtr (ft) ($H_1$) | Closed BC $t_p$(hr) (1) | Open Qpeak $t_p$(hr) (2) | Qpeak (cfs) (3) | Max WSEL (ft) (4) | Min Vol (ac-ft) (5) | Min Area (ac) (6) |
| 6 | 6 | 7.20 | 0.47 | 1.10 | 261.44 | 6.85 | 4.295 | 1.88 |
| 6 | 7 | 7.20 | 0.47 | 1.07 | 271.69 | 6.35 | 3.417 | 1.61 |
| 6 | 8 | 7.20 | 0.47 | 1.05 | 278.77 | 5.92 | 2.764 | 1.40 |
| 6 | 10 | 7.20 | 0.47 | 1.03 | 287.19 | 5.21 | 1.891 | 1.09 |
| 6 | 12 | 7.20 | 0.47 | 1.02 | 291.45 | 4.67 | 1.363 | 0.88 |

Notes:
D,W: Height and Width of a box culvert, respectively
$H_1$: Defined in Figure 4-3
Col. (1): Time to reach the maximum allowable HW elevation, when culvert is completely blocked, for a given detention pond with inflow generated from a given area of a drainage basin
Col. (2): Time to reach the peak discharge specified in Col. (3), when the culvert is fully open, in a specified detention pond
Col. (3): Peak discharge for a fully open culvert
Col (4): Maximum water surface elevation when the peak discharge in Col. (3) is reached
Col. (5): The volume of the detention pond for the time and peak discharge specified in Col. (2) and Col. (3)
Col. (6): The detention pond surface area for volume specified in Col. (5)

For a 163-acre drainage basin, the system response may be conservatively estimated with 175 acres condition in the Table 10-1. As indicated in Table 10-1, a detention pond with an average gradient of 3% requires a minimum of storage capacity of volume of 2.764 ac-ft, and yield a maximum surface water elevation of 5.92 ft above the culvert invert, if the box culvert is fully open. Therefore, the highway will not be overtopped. However, the completely blocked

culvert would take approximately 0.47 hours (Col.1), or 28 minutes and 12 seconds, to open before overtopping occurs at a maximum allowable headwater elevation of 7.2 ft.

The range of observed time in the laboratory for the Hauula model box culvert to self-open is between 15 seconds and 8 minutes and 36 seconds (Table 8-1). Converting the model time, $t_m$, to prototype time, $t_p$:

From Eq. 8-5, $t_m = t_p * \sqrt{L_r}$

Therefore: $t_p = (L_r)^{-1/2} * t_m$ (10-1)

Since $L_r$ = ⅛ for the Hauula model culvert, time for the prototype, $t_p$,

$$t_p = \left(\frac{1}{8}\right)^{-1/2} * t_m$$

And 8 minutes and 36 seconds is equal to 0.1433 hours, the projected self-opening is estimated:

$$t_p = \frac{t_m}{0.3536} = \frac{0.1433\text{hr}}{0.3536} = 0.405\text{hr} \quad (10\text{-}2)$$

Eq. (10.2) implies that if the 6-ft by 8-ft box culvert at Hauula is completely blocked, it will self-open before the detention pond is overtopped, provided the minimum storage capacity of the pond is 2.764 ac-ft. However, the existing storage capacity at the Hauula culvert system is 0.053 ac-ft, therefore, under the 1-hour 50-year design storm the highway will be overtopped. Furthermore, as presented in Chapter 9, the peak discharge and its surface elevation for the Hauula box culvert system under fully open conditions, were 280.22 cfs and 5.74-ft respectively. The corresponding values in Table 10-1 are 278.77 cfs and 5.92-ft. This example illustrates the effectiveness of the simulated results.

# CHAPTER 11 DISCUSSIONS, SUMMARY AND CONLUSION

The existing culvert and drainage pond at Punaluu appear inadequate to handle surface runoff from the drainage area, since the likelihood that many of the culverts and detention ponds may have been installed over 50 years ago when Kamehameha Highway was constructed. As a result of the age of the Highway, design documentation for the culverts and detention ponds are not readily available for examination. It is not feasible to examine all the design parameters of the existing detention ponds and culverts intended to calculate the direct runoff from a drainage area. Therefore, the surface runoff froma contributing drainage area for a given design storm can be estimated by means of the Nash-Muskingum Method described in Chapter 9. In addition, rainfall data used in this study were published in 1984, and may not have been available when the original culvert and detention pond were designed or selected.

Once the culvert is installed, and the roadway completed, it is not likely the culvert size will change as watershed characteristics may change with time. Changes to watershed characteristics may be attributed to changes of land use, where the natural drainage area may be replaced by additional urbanization, thereby diminishing the watershed's infiltration capacity for rainfall and increasing the surface runoff. The generalized simulation model does not account for different land use scenarios within a given watershed. For instance, the simulation model is incapable of recognizing the difference between urban land-use and preservation land.

Constant water pressure, or the maximum water surface level were used, in the model study in determining the time for a culvert to self-open. This approach is not completely accurate in simulating the actual conditions. Actual conditions of the water level in the self-opening of a completely blocked culvert are a dynamic problem. It is possible that the culvert would start to

self clear during the gradual build up of the water surface level in the culvert and detention pond system. Therefore, more time would be available for self-clearing in real conditions. Laboratory results provide the most conservative estimate for culverts self-opening.

Nevertheless, the methodologies developed in this study may provide an invaluable tool to accomplish the two criteria described in this project: "To evaluate whether a completely sand-blocked culvert may be self-opened before the surface runoff from its contributing drainage basin exceeds the storage capacity of the detention pond; and to assess the adequacy of existing culverts and their corresponding detention ponds under fully open conditions for their respective contributing drainage basins and design storms." For example, the Punaluu 30-inch circular culvert system has a 262-acre drainage basin and a detention pond with 0.083 ac-ft storage capacity (Table 9-3). Results from this study (Kamaka 2006 Appendix D) showed a minimum size of 48-inch circular culvert would be needed for not overtopping the highway. Furthermore, we obtained the results that implied that a 30-inch circular culvert is only capable of draining the inflow produced from a 25-acre drainage basin with a 2.0 ac-ft detention pond for a 1-hour 50-year design storm.

To summarize this study, a generalized simulation model has been demonstrated in establishing the management criteria for clearing and maintenance of culverts along the Kamehameha Highway throughout Windward Oahu.

It is recommended that a survey of the drainage basins on Windward Oahu be conducted to: (1) Identify different type of land uses within a watershed; and (2) Estimates the approximate quantity of area attributed to each land use type.

This type of survey may be performed using a USGS topographical map which outlines different types of land use. The area of different types of land use may be estimated with the aid of a GIS software.

It is also recommended that a field survey be conducted to identify the quantity, type, and sizes of drainage culverts along Kamehameha Highway. A survey should also be performed to estimate the storage volume of the culvert's corresponding detention pond. A formal survey for a screening effort is not necessary, and a rough estimate of the storage volume versus elevation is acceptable. The survey should also describe the type of culvert and headwall configurations.

## REFERENCES

### (related to bridge scour)


Arneson, L. A., Zevenbergen, L. W., Lagasse, P. F., & Clopper, P. E. (2012). "Evalutaing scour at bridges", Federal Highway Administration, HEC-18, 5th Edition. Washington D.C.

Briaud, J. L., Chen, H. C., Kwak, K. W., Han, S. W., and Ting, F. C. K., (2001). "Multiflood and multilayer method for scour rate prediction at bridge piers." *Journal of Geotechnical and Geoenvironmental Engineering*, ASCE, Vol. 127, Number 2, 114-125.

Briaud, J. L., Ting, F. C. K., Chen, H. C., Gudavalli, R., Perugu, S., and Wei, G. (1999). "SRICOS: prediction of scour rate in cohesive soils at bridge piers." *Journal of Geotechnical and Geoenvironmental Engineering*, ASCE, Vol. 125, Number 4, 237-246.

Cheng, E. D., (1992) "A forensic engineering study of a flood control levee swamp system." *Proceedings INTERPRAEVENT 1992, Protection of Habitat Against Floods and Debris Flows*, Berne, Switzerland, 187-196.

City and County of Honolulu, (2000), "Rules relating to storm drainage standards." City and County of Honolulu Department of Planning and Permitting, Honolulu, HI.

Das, B. M., (1998). *Principles of geotechnical engineering*. PWS Publishing Company, Boston, Massachusetts.

Environmental Modeling Research Laboratory, (1999) *Watershed modeling system version 6.1. tutorial*. Brigham Young University, Utah.

ETI Instrument Systems Inc, (2001), "Scour tracker AS-3 active sonar scour monitor." Scour Measurement Systems, Fort Collins, Colorado.

ETI Instrument Systems Inc, (2001), "Scour tracker SMC-3 sliding magnetic collar." Scour Measurement Systems, Fort Collins, Colorado.

FEMA (2002). “Flood insurance study City and County of Honolulu volume 1 of 4.” Volume 1, Federal Emergency Management Agency, Washington, D.C.

FEMA (2002). “Flood insurance study City and County of Honolulu volume 3 of 4.” Volume 3, Federal Emergency Management Agency, Washington, D.C.

FHWA (2002). “Countermeasure design for bridge scour and stream instability.” Report No. FHWA NHI 02-060, Federal Highway Administration, Washington, D.C.

FHWA “Hydrological analysis and design with WMS.” Federal Highways Administration, Washington, D.C.

FHWA (1998). “Scour monitoring and instrumentation.” Report No. FHWA-SA-96-036, Federal Highways Administration, Washington, D.C.

Garbrecht, J., and Martz, L. W., (1999). “TOPAZ an automated digital landscape analysis tool for topographic evaluation, drainage identification, watershed segmentation, and subcatchment parameterization.” Rep.# GRL 99-1, USDA, Agricultural Research Service, El Reno, Oklahoma.

Giambelluca, T. W., Lau, L. S., Fok, Y., and Schroeder, T. A. (1984). “Rainfall frequency study for Oahu.” Report R-73, State of Hawaii Department of Land and Natural Resources, Honolulu, HI.

Grace, R. A. (1998). *Descriptive statistics and regression models for civil, environmental, and ocean engineers*. Ocean Sci-Tech Publications, Honolulu, Hawaii.

Haan, C. T. (1977). *Statistical methods in hydrology*. Iowa State University Press, Ames, Iowa.

Hill, B. R., Taogoshi, R. I., Fontaine, R. A., and Teeters, P. C. (2000). “Water resources data Hawaii and other pacific areas water year 1999.” Water-Data Report HI-99-1, U.S. Geological Survey, Washington D.C.

Jackson, K. S. (1996). "Evaluation of bridge scour data at selected sites in Ohio". Columbus, OH: US Geologic Survey Water Resources Investigation Report 97-4182.

Jones, J. S., Sheppard, D. M., (2000). "Scour at wide bridges." http://www.tfhrc.gov//structur /hydrlcs/pdf/7.pdf, Federal Highways Division Turner-Fairbanks Highway Research Center.

Lagasse, P. F., Richardson, E. V., Schall, J. D., and Price, G. R., (1997). "Instrumentation for measuring scour at bridge piers and abutments." National Cooperative Highway Research Program Report 396, Transportation Research Board, Washington D.C.

MaCuen, R. H., Johnson, P. A., and Ragan, R. M. (2002). "Highway hydrology hydraulic design series number 2, second edition." Report No. FHWA-NHI-02-001 HDS-2, Federal Highway Administration, Washington, D.C.

Masaki, Gavin. (2004) "Scour Monitoring and Prediction for Selected Highway Bridges on Oahu." Master's Thesis, Department of Civil and Environmental Engineering, University of Hawaii at Manoa, Honolulu, Hawaii, USA.

Masaki, G., Teng, M.H., Cheng, E.D.H. and Matsuda, C. (2005) "A validation study of the empirical bridge scour equations", *Proceedings of the 2005 Joint ASME/ASCE/SES Conference on Mechanics and Materials (McMat-2005),* Baton Rouge, Louisiana, USA.

Miller, R. L., & Wilson, J. T. (1996). "Evaluation of scour at selected bridge sites in Indiana." Indianapolis, IN: US Geologic Survey Water Resources Invesigation Report 95-4259.

Mueller, D.S. and Wagner, C.R. (2005). "Field observations and evaluations of streambed scour at bridges", FHWA-RD-03-052, Federal Highway Administration, Washington, D.C.

Minami, M. (2000). *Using arc map*, Environmental Systems Research Institute, Davis, California.

NRCS (1986). “Urban hydrology for small watersheds.” National Resources Conservation Service Technical Release No. 55, Second Edition, U.S. Department of Agriculture, Washington, D.C.

ParEn, Inc, (1993), “Kaelepulu Stream Drainage Study.” Division of Engineering, Department of Public Works, City and County of Honolulu.

Richardson, E. V., and Davis, S. R. (2001). “Hydraulic engineering circular No. 18: evaluating scour at bridges forth edition.” Report No. FHWA NHI-01-001, Federal Highway Administration, Washington, D.C.

Schall, J. D., Price, G. R., Fisher, G. A., Lagasse, P. F., and Richardson, E. V. (1997). “Magnetic sliding collar scour monitor: installation, operation, and fabrication manual.” National Cooperative Highway Research Program Report 397B, Transportation Research Board, Washington D.C.

Schall, J. D., Price, G. R., Fisher, G. A., Lagasse, P. F., and Richardson, E. V. (1997). “Sonar scour monitor: installation, operation, and fabrication manual.” National Cooperative Highway Research Program Report 397A, Transportation Research Board, Washington D.C.

SCS (1981). “Erosion and sediment control: guide for Hawaii.” Soil Conservation Service, Honolulu, HI.

SCS (1972). “Soil survey of islands of Kauai, Oahu, Maui, Molokai, and Lanai, State of Hawaii.” U.S. Department of Agriculture, Washington, D.C.

SCS (1992). “TR-20 computer program for project formulation hydrology.” Soil Conservation Service Technical Release No. 20, U.S. Department of Agriculture, Washington, D.C.

USACOE (1998). *HEC-RAS river analysis system applications guide, version 2.2*. US Army Corps of Engineers Hydrologic Engineering Center, Davis, CA.

USACOE (1998). *HEC-RAS river analysis system user's manual, version 2.2*. US Army Corps of Engineers Hydrologic Engineering Center, Davis, CA.

USACOE (1993). "Hydrologic frequency analysis." Engineering Manual 1110-2-1415, U.S. Army Corps of Engineers, Washington D.C.

USGS (2000). "The national flood-frequency program - methods for estimating flood and frequency in rural areas in Hawaii, island of Oahu, 2000." USGS Fact Sheet 004-00, U.S. Geological Survey, Washington D.C.

U.S. Weather Bureau (1962). "Rainfall frequency atlas of the Hawaiian islands." *Technical Paper No. 43*, U.S. Department of Commerce, Washington, D.C.

Viessman, W., and Lewis G. L. (1996). *Introduction to hydrology forth Edition*, Harper Collins, New York, New York.

Weiss, L. L. (1964). "Ratio of true to fixed-interval maximum rainfall." *Journal of the Hydraulics Division Proceedings of the America Society of Engineers*, ASCE, Vol. 90, 77-82.

Wong, M. F. (1994). "Estimation of magnitude and frequency of floods for streams on the island of Oahu, Hawaii." Water Resources Investigations Report 94-4052, U.S. Geological Survey, Washington D.C.

Wu, I-Pai (1967). "Hydrological data and peak discharge determination of small Hawaiian watersheds: Island of Oahu." Water Resources Report Technical Paper 15, Water Resources Research Center, University of Hawai'i at Manoa, Honolulu, Hawaii.

Wu, I-Pai (1969). “Hydrograph study and peak discharge determination of Hawaiian small watersheds: Island of Oahu..” Water Resources Report Technical Paper 30, Water Resources Research Center, University of Hawai'i at Manoa, Honolulu, Hawaii.

Zhang, G., Hsu, S.A., Guo, T., Zhao, X., Augustine, A.D. and Zhang, L. (2013). “Evaluation of design methods to determine scour depths for bridge structures”, FHWA/LA.11/491, Louisiana Department of Transportation, Baton Rouge.

## REFERENCES

### (related to highway culvert)


Bentley PondPack 10.0 (2005), computer software, Bentley Systems, Inc..

BMDP New System 02.00 (2001), computer software, Statistical Solutions Ltd..

Dixon, W.J. and Robert Jennrich (1983). *13.2 Stepwise Regression*. BMDP Statistical Software. University of California Press.

Giambelluca, Thomas W, et. al. (1984) "Rainfall Frequency Study for Oahu", prepared by the University of Hawaii Water Research Center. State of Hawaii, Department of Land and Natural Resources, Division of Water and Land Development: US Army Corps of Engineers, Honolulu District.

Fujioka, Matt, Personal Conversation and Notes, September 28, 2006.

Kamaka, M. (2006) "Coastal highway culvert management criteria for Windward Oahu", MS Plan B Report, Department of Civil and Environmental Engineering, University of Hawaii at Manoa, Honolulu, Hawaii, USA.

Kamaka, M., Cheng, E. D-H., Teng, M. H. and Matsuda, C. (2007) "Analytical and hydraulic model study of highway culverts sand blockages", In *Proceedings of the Thirteenth International Conference on Computational Methods and Experimental Measurements,* July 2-4, 2007, Prague, Czech Republic.

Lindeburgh, Michael R. (2001) "Civil Engineering Reference Manual for the PE Exam", 8th Edition. Belmont California: Professional Publications, Inc.

Matsuda, Curtis, Personal Conversation and Notes, June 16 and August 16, 2006.

Ponce, Victor Miguel. (1989) "Engineering Hydrology, Principles and Practices." Prentice Hall, New Jersey.

State of Hawaii (1984). "Standard Details for Public Works Construction". (Honolulu: State of Hawaii, September 1984)

United States Department of Transportation (USDOT) (2001) Federal Highway Administration. "Hydraulic Design of Highway Culverts". Publication No. FHWA-NHI-01-020.

Wu, I-Pai. (1967). "Hydrological Data and Peak Discharge Determination of Small Hawaiian Watersheds: Island of Oahu", Water Resources Research Center, University of Hawaii at Manoa.

Wu, I-Pai. (1969). "Hydrograph Study and Peak Discharge Determination of Hawaiian Small Watersheds: Island of Oahu", Water Resources Research Center, University of Hawaii at Manoa.